

Aus der Abteilung Genvektoren des Helmholtz Zentrum München  
Vorstand: Prof. Dr. Wolfgang Hammerschmidt

*The influence of deregulated CD30  
signaling and  $\gamma$ -herpesviral infection on the  
development of B cell lymphoma*

Dissertation  
zum Erwerb des Doktorgrades der Naturwissenschaften  
an der Medizinischen Fakultät der  
Ludwig-Maximilians-Universität zu München

vorgelegt von  
Stefanie Alexandra Sperling

aus  
Gera

Jahr  
2020

MIT GENEHMIGUNG DER MEDIZINISCHEN FAKULTÄT  
DER UNIVERSITÄT MÜNCHEN

Berichterstatter: PD. Dr. Ursula Zimmer-Strobl

Mitberichterstatter: PD. Dr. Barbara Adler

Mitbetreuung durch: Prof. Dr. Heiko Adler

Dekan: Prof. Dr. Reinhard Hickel

Tag der mündlichen Prüfung: 27.01.2020

# Contents

<b>Contents</b>	<b>I</b>
<b>List of Figures</b>	<b>V</b>
<b>List of Tables</b>	<b>VII</b>
<b>List of abbreviations</b>	<b>VIII</b>
<b>1 Abstract</b>	<b>1</b>
<b>2 Zusammenfassung</b>	<b>3</b>
<b>3 Introduction</b>	<b>5</b>
3.1 B cells . . . . .	5
3.1.1 Development . . . . .	5
3.1.2 The role of B1 cells . . . . .	6
3.1.3 Immune response . . . . .	7
3.2 B cell lymphoma . . . . .	9
3.2.1 Cellular origin of B cell lymphomas . . . . .	10
3.2.2 Transforming events . . . . .	10
3.2.3 CD30 <sup>+</sup> B cell lymphoma . . . . .	12
3.3 CD30 . . . . .	13
3.3.1 Signaling . . . . .	13
3.3.2 Function . . . . .	14
3.4 MHV-68 . . . . .	15
3.4.1 Biology . . . . .	15
3.4.2 $\gamma$ -Herpesviruses in disease . . . . .	16
3.5 The LMP1/CD30flSTOP mouse strain . . . . .	17
<b>4 Aim</b>	<b>18</b>
<b>5 Results</b>	<b>19</b>
5.1 CD30 expression on murine B cells . . . . .	19
5.2 Chronic CD30 signaling drives plasma cell differentiation . . . . .	21
5.2.1 Chronic CD30 signaling drives plasma cell differentiation <i>in vitro</i> . . . . .	22
5.2.2 Chronic CD30 signaling drives plasma cell differentiation upon T-cell independent immunization . . . . .	31
5.2.3 LMP1/CD30 expression drives plasma cell differentiation in germinal center B cells . . . . .	33

5.3	Influence of MHV-68 infection on the development of CD30 positive lymphomas . . . . .	42
5.3.1	Cloning of the reporter virus MHV-68-NGFR . . . . .	42
5.3.2	Viral infection of the LMP1/CD30//C $\gamma$ 1-cre mice results in the deletion of the STOP-cassette . . . . .	45
5.3.3	Virus infection leads to a germinal center reaction in LMP1/CD30//C $\gamma$ 1-cre mice . . . . .	48
5.3.4	The virus infection further drives the expansion of LMP1/CD30 expressing B1 and plasma cells . . . . .	50
5.3.5	NGFR positive B cells are found in different sub-populations . . . . .	51
5.3.6	Ongoing virus infection in LMP1/CD30//C $\gamma$ 1-cre mice leads to the expansion of B1a and B1b cell populations . . . . .	53
5.3.7	Aged mice . . . . .	59
5.3.7.1	Viral infection leads to an additive effect in CD30 driven lymphoma development . . . . .	59
5.3.7.2	CD30 signaling leads to the expansion of B and T cells in aged mice . . . . .	60
5.3.7.3	CD30 signaling leads to higher numbers of virus infected B cells . . . . .	64
5.3.7.4	CD30 signaling leads to a further expansion of the B1a and B1b cell populations in aged mice . . . . .	65
5.3.7.5	Virus infection and chronic CD30 signaling induce development of exhausted CD8 <sup>+</sup> memory T cells . . . . .	68
5.3.7.6	Expansion of CD30 expressing cells correlates with increasing splenic weight in aged mice . . . . .	70
5.3.8	Lymphoma characterization . . . . .	70
5.4	Infection of mice with MHV-68-LMP1wt virus leads to its elimination . . . . .	80
5.4.1	MHV-68-LMP1wt infection leads to a terminated splenic GC reaction in mice . . . . .	82
5.4.2	MHV-68-LMP1wt showed impaired lytic replication in the lungs of infected mice and no reactivation <i>ex vivo</i> . . . . .	84
5.4.3	LMP1wt infected B cells obtain survival signals <i>in vitro</i> . . . . .	87
5.4.4	T cells reveal a stronger response to LMP1wt infected B cells . . . . .	88
5.4.5	MHV-68-LMP1wt infected B cells cannot be rescued in TCR $\beta\delta$ KO mice . . . . .	90
5.4.6	NK cells contribute to the clearance of MHV-68-LMP1wt infected B cells . . . . .	92

6.1	LMP1/CD30 expressing cells are encouraged to plasma cell differentiation .	96
6.2	Herpesviral infection amplifies the lymphoma development in LMP1/CD30//C $\gamma$ 1-cre mice . . . . .	98
6.3	Active LMP1 signaling hampers the latency establishment in mice . . . . .	106
<b>7</b>	<b>Material</b>	<b>108</b>
7.1	Mouse strains . . . . .	108
<b>8</b>	<b>Methods</b>	<b>109</b>
8.1	Molecular biology . . . . .	109
8.1.1	DNA isolation . . . . .	109
8.1.1.1	Genomic DNA isolation from tissue . . . . .	109
8.1.1.2	Genomic DNA isolation from whole splenocyte pellets . . . . .	110
8.1.2	Mouse genotyping . . . . .	110
8.1.3	Agarose gel electrophoresis of DNA . . . . .	110
8.1.4	Southern Blot . . . . .	110
8.2	Mouse related assays . . . . .	113
8.2.1	Preparation of murine lymphocytes . . . . .	113
8.2.2	Isolation of B cells, T cells and B cell sub-populations . . . . .	114
8.2.3	Preparation of serum . . . . .	114
8.2.4	ELISA (enzyme-linked immunosorbent assay) . . . . .	114
8.2.5	ELISpot (enzyme-linked immunospot assay) . . . . .	115
8.2.6	Flow cytometry . . . . .	116
8.3	Cell culture . . . . .	116
8.4	Immunohistochemistry and immunofluorescence . . . . .	117
8.5	Western Blot . . . . .	118
8.6	Immunization, infection and depletion . . . . .	119
8.7	Virological assays . . . . .	121
8.7.1	Virus stock production . . . . .	121
8.7.2	Plaque assay . . . . .	121
8.7.3	Generation of recombinant virus . . . . .	122
8.7.4	<i>Ex vivo</i> reactivation assay . . . . .	123
8.7.5	Viral infection of B cells <i>in vitro</i> . . . . .	123
8.8	Statistics . . . . .	123
	<b>References</b>	<b>124</b>
<b>9</b>	<b>Supplement</b>	<b>S139</b>
9.1	Supplement data . . . . .	S139
9.2	Curriculum Vitae . . . . .	S141

9.3	Eidesstattliche Erklärung . . . . .	S143
9.4	Erklärung . . . . .	S143
9.5	Danksagung . . . . .	S144

## List of Figures

1	CD30 expression <i>in vivo</i> and <i>in vitro</i> . . . . .	21
2	Differentiation into plasmablasts unstimulated and upon CD40 stimulation	22
3	Differentiation into plasmablasts upon LPS stimulation . . . . .	23
4	Proliferation of B and CD43 <sup>lo</sup> B cells . . . . .	24
5	Plasmablast differentiation of B1 and B2 cells . . . . .	26
6	Differentiation of B2 cells upon CD40 stimulation . . . . .	28
7	Differentiation of B2 cells upon CD40 stimulation . . . . .	29
8	Isotype switching of FoBs . . . . .	31
9	NP specific ASCs and antibodies in serum, SP, and BM . . . . .	32
10	GC B cells in the PP . . . . .	33
11	Reporter expression upon NP-CGG immunization . . . . .	34
12	Histology of GC . . . . .	35
13	GC and NP <sup>+</sup> upon NP-CGG immunization . . . . .	36
14	Distribution of NP <sup>+</sup> , GC B cells, and reporter <sup>+</sup> cells . . . . .	37
15	Differentiation into PC and CD43 <sup>+</sup> , CD23 <sup>low</sup> cells upon NP-CGG immunization . . . . .	38
16	NP specific ASCs and antibodies in the SP and the serum upon NP-CGG immunization . . . . .	39
17	Distribution of DZ and LZ . . . . .	40
18	IRF4 <sup>+</sup> cells in the GC . . . . .	41
19	IgG1 <sup>+</sup> B cells upon NP-CGG immunization . . . . .	41
20	Cloning and characterization of MHV-68-NGFR . . . . .	44
21	Reporter expression upon NP-CGG immunization and viral infection . . . . .	46
22	B and T cell numbers upon NP-CGG immunization and viral infection . . . . .	47
23	NGFR <sup>+</sup> cells in SP and PerC . . . . .	48
24	GC B cells upon NP-CGG immunization and viral infection . . . . .	49
25	Phenotype of reporter expressing cells . . . . .	50
26	Characterization of NGFR <sup>+</sup> cells . . . . .	52
27	B and T cell numbers in the spleen after 2 months . . . . .	53
28	B and T cell numbers in the PerC after 2 months . . . . .	54
29	Reporter expression after 2 months . . . . .	54
30	NGFR <sup>+</sup> cells after 2 months . . . . .	55
31	GC B cells after 2 months . . . . .	56
32	Phenotype of reporter <sup>+</sup> cells after 2 months . . . . .	57
33	Characterization of B1 sub-populations of reporter <sup>+</sup> cells . . . . .	58
34	Reporter <sup>+</sup> memory B cells after 2 months . . . . .	58
35	Tumor incidence in aged mice . . . . .	60

36	Splenic cell numbers of aged mice . . . . .	61
37	Cell numbers in the PerC of aged mice . . . . .	62
38	Reporter expression in aged mice . . . . .	62
39	Time course of reporter expression . . . . .	63
40	NGFR <sup>+</sup> cells in aged mice . . . . .	65
41	Phenotype of reporter <sup>+</sup> cells in aged mice . . . . .	66
42	PC differentiation in aged mice . . . . .	67
43	Memory B cells in aged mice . . . . .	68
44	Characterization of T cells of aged mice . . . . .	69
45	Correlation of splenic weight, reporter expression, and CD19 <sup>+</sup> B cells . . .	70
46	Lymphoma characterization . . . . .	72
47	Phenotype of lymphoma . . . . .	74
48	CD79 $\beta$ expression of lymphoma . . . . .	75
49	CD95 expression of lymphoma . . . . .	76
50	HE staining of splenic sections of aged mice . . . . .	77
51	Immunohistochemistry staining of lymphoma sample . . . . .	78
52	Histology of reporter expression of aged mice . . . . .	80
53	Cloning and characterization of MHV-68-LMP1wt . . . . .	81
54	GC reaction upon infection with MHV-68-LMP1wt . . . . .	83
55	Histology of GC upon MHV-68-LMP1wt infection . . . . .	84
56	Characterization of MHV-68-LMP1wt infection <i>ex vivo</i> . . . . .	86
57	Genomic load in the PerC upon MHV-68-LMP1wt infection . . . . .	87
58	Cell survival and proliferation of MHV-68-LMP1wt infected B cell <i>in vitro</i>	88
59	IFN $\gamma$ ELISpot . . . . .	90
60	TCR $\beta\delta$ KO mice infection with MHV-68-LMP1wt virus . . . . .	92
61	NK cell activation of TCR $\beta\delta$ KO mice . . . . .	93
62	Viral infection of NK cell depleted TCR $\beta\delta$ KO mice . . . . .	95
S1	Sorting strategy of B1 and B2 cells . . . . .	S139
S2	Southern blot analysis . . . . .	S140
S3	Histogram of KLRG1 and TIM3 . . . . .	S140
S4	pCDH-SFFV-hspCas9-T2A-NGFR . . . . .	S141

## List of Tables

1	PCR Primer . . . . .	111
2	PCR reaction mixtures . . . . .	112
3	PCR programmes . . . . .	112
4	Histology antibodies . . . . .	118
5	Antibodies for western blot . . . . .	119

## List of abbreviations

<b>ABC</b>	activated B-cell like
<b>AID</b>	activation induced cytidine deaminase
<b>ALCL</b>	anaplastic large cell lymphoma
<b>ASC</b>	antibody secreting cells
<b>BAC</b>	bacterial artificial chromosome
<b>BAFF</b>	B cell activating factor
<b>Bcl6</b>	B-cell lymphoma 6 protein
<b>BCM</b>	B cell medium
<b>BCR</b>	B cell receptor
<b>BL</b>	Burkitt Lymphoma
<b>Blimp-1</b>	PR domain zinc finger protein 1
<b>BM</b>	bone marrow
<b>BSA</b>	Bovine serum albumin
<b>CAR</b>	coxsackievirus adenovirus receptor
<b>CB</b>	centroblasts
<b>CC</b>	centrocytes
<b>CCR7</b>	C-C chemokine receptor 7
<b>CD30L</b>	CD30 ligand
<b>CFSE</b>	Carboxyfluorescein succinimidyl ester
<b>cHL</b>	classical Hodgkin lymphoma
<b>CGG</b>	Chicken Gamma Globulin
<b>CPE</b>	cytopathic effect
<b>CSR</b>	class switch recombination
<b>ctrl</b>	control
<b>CXCR5</b>	C-X-C chemokine receptor type 5
<b>CXCR4</b>	C-X-C chemokine receptor type 4
<b>d</b>	day
<b>DLBCL</b>	diffuse large B cell lymphoma
<b>DZ</b>	dark zone
<b>EBER</b>	Epstein-Barr virus-encoded small RNAs
<b>EBNA</b>	Epstein-Barr nuclear antigens
<b>EBV</b>	Epstein Barr Virus
<b>ELISA</b>	Enzyme-linked Immunosorbent Assay
<b>ELISpot</b>	Enzyme Linked Immuno Spot Assay
<b>ERK</b>	extracellular signal-regulated kinases
<b>FACS</b>	flow cytometry
<b>FCS</b>	fetal calf serum

<b>FDC</b>	follicular dendritic cells
<b>GC</b>	germinal center
<b>FL</b>	Follicular lymphoma
<b>FoB</b>	follicular B cells
<b>HL</b>	Hodgkin lymphoma
<b>HRS</b>	Hodgkin and Reed/Sternberg cells
<b>HSC</b>	hematopoietic stem cell
<b>IKK</b>	I $\kappa$ B kinase
<b>IFN</b>	Interferon
<b>i.n.</b>	intranasally
<b>i.p.</b>	intraperitoneally
<b>Irf4</b>	Interferon regulatory factor 4
<b>JNK</b>	c-Jun N-terminal kinase
<b>KSHV</b>	Kaposi's sarcoma-associated herpesvirus
<b>LCL</b>	lymphoblastoid cell lines
<b>LN</b>	lymph node
<b>LMP</b>	latent membrane proteins
<b>LP</b>	Leader protein
<b>LPS</b>	Lipopolysaccharide
<b>LZ</b>	light zone
<b>MACS</b>	magnetic cell separation
<b>MALT</b>	mucosa-associated lymphoid tissue
<b>MAPK</b>	mitogen activated protein kinase
<b>MFI</b>	median fluorescence intensity
<b>MHV-68</b>	murine gamma-herpesvirus 68
<b>MOI</b>	multiplicity of infection
<b>MZB</b>	marginal zone B cells
<b>NGFR</b>	nerve growth factor receptor
<b>n.i.</b>	untouched
<b>NLPHL</b>	nodular lymphocyte predominant form
<b>NP</b>	(4-hydroxy-3-nitrophenyl)acetyl
<b>Orf</b>	open reading frame
<b>Pax5</b>	Paired box protein 5
<b>PB</b>	plasmablasts
<b>PC</b>	plasma cells
<b>PEL</b>	primary effusion lymphoma
<b>PerC</b>	peritoneal cavity
<b>p.i.</b>	post infection
<b>p.im.</b>	post immunization

<b>PP</b>	Peyer's patches
<b>rpm</b>	rounds per minute
<b>sCD30</b>	soluble CD30
<b>SHM</b>	somatic hypermutation
<b>SP</b>	spleen
<b>TACI</b>	transmembrane activator and CAML interactor
<b>TCR</b>	T cell receptor
<b>TD</b>	T cell dependent
<b>TF</b>	transcription factors
<b>TI</b>	T cell independent
<b>TLR</b>	Toll like receptor
<b>TNF</b>	tumor necrosis factor
<b>TRAF</b>	TNFR-associated factor
<b>w/o</b>	without
<b>wt</b>	wild type

# 1 Abstract

CD30 is only expressed on a few activated B and T cells. Until now, the small amount of these cells limited the ways of investigations. Several B cell lymphomas, like Hodgkin lymphomas and diffuse large B cell lymphomas, express the CD30 receptor and are often associated with herpesviral infections. However so far, the contribution of CD30 signaling and herpesviral infections to lymphomagenesis remained largely unknown.

In order to address the physiological and patho-physiological function of CD30 in B cells, a transgenic mouse line expressing conditionally a constitutively active CD30 (LMP1/CD30) was generated by my predecessor Petra Fiedler. She could show that the activation of LMP1/CD30 in all B cells by CD19cre resulted in the expansion of the B1 cell and plasma cell population in the spleen and in the peritoneal cavity. I analyzed this phenotype further and could show that the expanded B1 cells are intermixed with plasmablasts and plasma cells. My data provided evidence that the expansion of B1 cells and plasmablasts occurs during T cell independent immune responses. Moreover, B2 cells, with a chronic CD30 signaling, differentiated towards this B1-like population upon CD40 stimulation *in vitro*. Analysis of the signaling pathways which may be responsible for this phenotype, revealed increased pSTAT3 and pSTAT6 levels, and a stronger nuclear translocation of p65 and Interferon regulatory factor 4 (Irf4) upon CD40 stimulation *in vitro*. These data suggest that the expanded B1-like cell population in LMP1/CD30 mice is generated upon activation of B1 and B2 cells. Together with Petra Fiedler, I could show that aged LMP1/CD30 mice develop pre-germinal center B cell lymphomas with a plasmablastic phenotype. These results proofed for the first time that deregulated CD30 signaling has an oncogenic potential in B cells.

Most of CD30<sup>+</sup> B cell lymphomas derive from germinal center or post-germinal center B cells. Since LMP1/CD30 mice displayed a block in the germinal center reaction, these mice were insufficient to study the function of deregulated CD30 signaling in germinal center B cells. To induce a deregulated CD30 signaling in germinal center B cells, we crossed the LMP1/CD30 mouse strain with a C $\gamma$ 1-cre mouse strain. Immunization of these mice resulted in elevated numbers of IRF4<sup>+</sup> plasmablasts and plasma cells, indicating that constitutive CD30 signaling also drives plasma cell differentiation in GC B cells. Next, we studied whether the deregulated CD30-expression in germinal center cells results in lymphoma development and whether herpesviral infections further increases lymphomagenesis. Since EBV does not infect murine B cells, we used instead the murine herpesvirus MHV-68. To detect the infected cells, a reporter virus expressing NGFR was constructed (MHV-68-NGFR). The infection with MHV-68-NGFR induced a germinal center reaction with germinal center B cells positive for NGFR and was therefore suited to study the cooperative effect of deregulated CD30 signaling and herpesviral infections in germinal center B cells. A significantly higher incidence of lymphomas was developed in

the infected LMP1/CD30//C $\gamma$ 1-cre mice in comparison to the immunized mice, suggesting a synergistic effect of a  $\gamma$ -herpesviral infection and chronic CD30 signaling in germinal center B cells regarding lymphomagenesis. The lymphomas of both groups displayed a B1-like or plasmablasts phenotype. IRF4 was upregulated in all lymphomas whereas PR domain zinc finger protein 1 (Blimp-1) was rather downregulated. These data indicated that lymphomas arise from plasma cell progenitors which have not upregulated BLIMP-1 yet.

Since most of the EBV<sup>+</sup> CD30<sup>+</sup> lymphomas express the EBV protein LMP1, I evaluated in the third part of the thesis, whether a LMP1-expressing MHV-68 virus further enhances lymphomagenesis in LMP1/CD30-mice. Up to this end, LMP1 was inserted in the MHV-68 genome. Two viruses were generated, MHV-68-LMP1wt and as control, MHV-68-LMP1mut which leads to the expression of LMP1 with a truncated signaling domain. Strikingly, the MHV-68-LMP1wt but not the MHV-68-LMP1mut infected cells were eliminated upon infection of wildtype mice. We could demonstrate that the elimination of the infected cells was partly but not exclusively evoked by T cells and NK cells. Although, this MHV-68 LMP1 virus was not suited to study its impact on B cell lymphomagenesis, it is an interesting tool to investigate why LMP1 signaling induces such a strong immune response in context with a MHV-68 infection.

## 2 Zusammenfassung

CD30 wird nur von wenigen aktivierten B und T Zellen exprimiert. Die geringe Anzahl dieser Zellen erschwerte bisher die Funktionsanalyse von CD30. Des Weiteren wird CD30 von verschiedenen B Zell Lymphomen, wie dem Hodgkin Lymphom und dem diffusen großzelligen B Zellymphom, stark exprimiert. Dabei treten diese Lymphome häufig mit  $\gamma$ -herpesviralen Infektionen auf. Bisher war nicht bekannt, ob und welchen Einfluss das CD30 Signal und die herpesvirale Infektion auf die Lymphomentstehung haben.

Um die physiologische und pathophysiologische Funktionsweise von CD30 aufklären zu können, wurde zunächst das transgene Mausmodell entwickelt, welches zu einem konditionalen, konstitutiv-aktiven CD30 Signal (LMP1/CD30) führt. Dieses Mausmodell wurde von meiner Vorgängerin Petra Fiedler generiert. Sie konnte zeigen, dass die Aktivierung von LMP1/CD30 in allen B Zellen durch die Kreuzung mit CD19cre zu einer Expansion von B1 Zellen und der Plasmazellpopulation in der Milz und im Peritoneum führt. Ich analysierte diesen Phänotyp weiter und konnte zeigen, dass die expandierte Population sowohl aus B1 Zellen, Plasmablasten aber auch Plasmazellen bestand. Meine Daten bewiesen, dass die Expansion dieser Zellen durch eine T Zell unabhängige Immunantwort hervorgerufen wird. Weiterhin zeigten die B2 Zellen dieser Mäuse eine verstärkte Differenzierung zu dieser B1-zellähnlichen Population nach CD40 Stimulation. Die Analyse der Signalwege, welche für den Phänotyp verantwortlich sein könnten, wiesen eine erhöhte Phosphorylierung von STAT3 und STAT6, sowie verstärkte nukleäre Translokation von p65 und IRF4 nach CD40 Stimulation *in vitro* auf. Diesen Daten weisen darauf hin, dass die expandierte B1-ähnliche Population in LMP1/CD30 Mäusen durch Aktivierung von B1 und B2 Zellen generiert wird. Zusammen mit Petra Fiedler konnte ich zeigen, dass gealterte LMP1/CD30 Mäuse Prä-Keimzentrums-B-Zellymphome mit einem Plasmablasten Phänotyp entwickeln. Diese Ergebnisse zeigten zum ersten Mal, dass dereguliertes CD30 Signal ein onkogenes Potential in B Zellen hat. Jedoch handelt es sich bei den meisten CD30<sup>+</sup> B-Zellymphomen um Keimzentrums-oder Post-Keimzentrums-B Zellen. Da LMP1/CD30 Mäuse keine Keimzentrumsreaktion nach Immunisierung zeigen, waren sie zur Funktionsanalyse von dereguliertem CD30 Signal in Keimzentrum B Zellen ungeeignet. Aus diesem Grund kreuzten wir LMP1/CD30 Mäuse mit C $\gamma$ 1-cre Mäusen, um dereguliertes CD30 Signal in Keimzentrums-B-Zellen zu induzieren. Die Immunisierung dieser Mäuse führte zu einer erhöhten Anzahl von IRF<sup>+</sup> Plasmablasten und Plasmazellen. Das weist darauf hin, dass konstitutives CD30 Signal die Plasmazelldifferenzierung auch in Keimzentrums-B-Zellen treibt. Nachfolgend analysierten wir, ob die Expression von LMP1/CD30 in Keimzentrums-B-Zellen zur Lymphomentstehung führt und, ob eine zusätzliche herpesvirale Infektion diese weiter ansteigen lässt. Da EBV keine murinen B Zellen infiziert, verwendeten wir stattdessen MHV-68, einen murinen  $\gamma$ -Herpesvirus. Dieser wurde als NGFR exprimierender Reportervirus kloniert. Da die In-

fektion mit dem Reportervirus zu NGFR exprimierenden Keimzentrums-B-Zellen führte, stellte er sich als geeignet zur Bearbeitung der Fragestellung heraus. Die virusinfizierten LMP1/CD30//C $\gamma$ 1-cre Mäuse entwickelten signifikant mehr Lymphome als die immunisierten. Dies implizierte einen eindeutigen synergistischen Effekt zwischen Virusinfektion und dereguliertem CD30 Signal in Keimzentrums-B-Zellen hinsichtlich der Lymphomentstehung. Die Lymphome zeigten einen B1 Zell/Plasmablasten-ähnlichen Phänotyp. IRF4 war in allen Lymphomen hochreguliert, wohingegen BLIMP-1 eher runterreguliert war. Dies weist daraufhin, dass die Lymphome aus Plasmazellvorläufern entstehen, welche BLIMP-1 bisher nicht hochreguliert haben.

Da die meisten EBV<sup>+</sup>, CD30<sup>+</sup> Lymphome das EBV Protein LMP1 exprimieren, bestimmte ich im dritten Teil der Arbeit, ob ein LMP1 exprimierender MHV-68 zur gesteigerten Lymphomentstehung in LMP1/CD30 Mäusen führt. Dafür wurde LMP1 in zwei Varianten in das MHV-68 Genom integriert. Zum einen MHV-68-LMP1wt und als Kontrolle, MHV-68-LMP1mut, welcher zur Expression von LMP1 mit trunkierten Signaldomänen führt. Nach der Infektion von Wildtyp Mäusen wurden MHV-68-LMP1wt infizierte Zellen, jedoch nicht die MHV-68-LMP1mut infizierten Zellen, eliminiert. Wir konnten zeigen, dass T Zellen und NK Zellen teilweise, aber nicht ausschließlich, für diesen Vorgang verantwortlich sind. Obwohl MHV-68-LMP1wt nicht geeignet ist, um seinen Einfluss auf die B Zell Lymphomentwicklung zu untersuchen, ist es ein gutes Hilfsmittel, um herauszufinden, aus welchem Grund das LMP1 Signal ein solche starke Immunantwort während einer MHV-68 Infektion hervorruft.

## 3 Introduction

Every year, 20 new cases of lymphomas per 100.000 people occur in the western world [Küppers, 2005]. Despite similar amounts of B and T cells in the human body, most of the lymphomas derive from B cells. In order to generate a broad repertoire of diverse antibodies, B cells undergo several differentiation processes which makes them vulnerable for malignant transformation [Murphy et al., 2012]. There are more than 15 different types of B cell lymphomas distinguished by the World Health Organization [Küppers, 2005]. These lymphomas originate from B cells at various differentiation stages where they are somehow "frozen". Besides the physiological mechanisms which are exploited by malignant transformation, also  $\gamma$ -herpesviral infections seem to be involved in these processes. Some of the B cell lymphomas contain to a high extent Epstein Barr Virus (EBV) and Kaposi's sarcoma-associated herpesvirus (KSHV) which are implicated in the pathogenesis of these lymphomas [Küppers, 2005].

### 3.1 B cells

#### 3.1.1 Development

Both, B and T lymphocytes originate from the same progenitor cell, the common lymphoid progenitor which arises by differentiation from the pluripotent hematopoietic stem cell (HSC). The common cell progenitor is situated in the bone marrow (BM) but only B cells derive from this site whereas T cells mature in the thymus. But unlike T cells, B cells also undergo further maturation in this site. The micro-environment provided by the BM is crucial for this differentiation process of B cells. Mainly, stromal cells contribute through direct cell contact over adhesion molecules and ligands and by secreting chemokines and cytokines which induce proliferation and differentiation of the B cell progenitors [Tsuneto et al., 2014]. The common lymphoid progenitor gives rise to the early pro-B cell. This is the first stage of B cell commitment which differentiates afterwards through the following phases called late pro-B cell, large pre-, small pre-, and immature B cell. During this process, the B cells start to rearrange and to express their immunoglobulin genes. The light chain and the heavy chain are encoded in different gene segments. The light chains are assembled from V and the J segments, the heavy chain includes an additional D segment. From all segments, several copies are present but only one is chosen during recombination of the final chains. First, the heavy chain undergoes VDJ recombination and afterwards the pre-B cell receptor is formed, followed by the VJ recombination of the light chain. After successful recombination of the heavy and light chain, membrane bound IgM is expressed on the immature B cells [Murphy et al., 2012].

The specificity of the B cell receptor (BCR) is characterized by a high diversity. The first set of the diverse repertoire is generated during the V(D)J recombination in the B cell de-

velopment. Rag1 and Rag2 are recombination-activating enzymes and build the enzyme complex V(D)J-recombinase which is essential for the V(D)J-recombination. During the recombination process, for every gene segment one copy is randomly chosen which results in the great diversity of the BCR. Additionally, the enzyme terminal deoxynucleotidyl transferase introduces random nucleotides to the single strand DNA ends which occur after hairpin cleavage. This ends up with a B cell repertoire which recognizes  $5 \times 10^{13}$  antigens in human. The immature B cell leaves the BM and migrates towards the spleen. There, it undergoes three transitional stages (T1-T3) and differentiates either towards marginal zone B cells (MZB) or follicular B cells (FoB). The strength of the BCR signaling, canonical NF- $\kappa$ B signaling downstream of B cell activating factor (BAFF) receptor, and an active Notch signaling are crucial players in mediating the cell fate decision into one of the two phenotypes in the periphery [Pillai and Cariappa, 2009].

Besides MZB and FoB which are called B2 cells, B1 cells belong to the B cell populations. The model of the "layered immune system hypothesis" suggests B1 and B2 cells as two different emerging lineages [Herzenberg and Herzenberg, 1989]. B1 cells are proposed to emerge earlier during the embryonal development of the murine embryo in the yolk sack and the fetal liver. After birth, B2 cells are generated in the BM. After migrating to the spleen, B1 cells also undergo the three transitional stages which differ in terms of regulation from the B2 cell transitional cells [Montecino-Rodriguez and Dorshkind, 2011]. In the pleural and peritoneal cavities, the B1 cell gains either the B1a or the B1b cell phenotype [Montecino-Rodriguez and Dorshkind, 2012]. The development of B1a cells depends on CD19 signaling. In contrast, an overexpression of CD19 leads to impaired B1b cell development [Haas et al., 2005]. Further, the survival and proliferation of B1 cells which were generated from the transitional stage rely upon strong BCR and canonical NF $\kappa$ B signaling. But, B1 cells are independent from BAFF and alternative NF $\kappa$ B signaling. These signaling pathways are necessary for the development of MZB and FoB [Montecino-Rodriguez and Dorshkind, 2012]. A few weeks after birth, the development of B1 cells is abandoned and the population is maintained mainly by self-renewal [Baumgarth, 2016].

### 3.1.2 The role of B1 cells

The B1 cells play a main role in this thesis. For this reason, this chapter explains the function of B1 cells in more detail. Besides the developmental differences, B1 and B2 also vary in tissue distribution and receptivity, and response towards antigens and mitogens [Baumgarth, 2016]. Unlike B2 cells, B1 cells undergo self-renewal in the periphery and are probably replaced by cells from the adult BM to a very limited extent [Kreslavsky et al., 2018]. The expression of CD5 divides the B1 cell population in CD5<sup>+</sup> B1a and CD5<sup>low</sup> B1b cells. CD5 is a membrane glycoprotein which is also expressed on T cells. Its role on B1 cells is to prevent uncontrolled self-reactivity and

to inhibit BCR signaling [Dalloul, 2009]. B1 cells produce natural antibodies which are generated independent of the presence of an exogenous antigen. By regulating B cell development and selection as well as clearing of self-antigens, they prevent auto-reactivity [Savage et al., 2017]. Further, they avert as primary response towards bacterial and viral infections like *Streptococcus pneumoniae* and *Salmonella thyphi* as well as the influenza virus [Baumgarth, 2016]. The natural antibodies which are secreted by the B1 cells are mainly of IgM and, to a lesser extent of, class-switched isotype, IgG3. The differentiation towards natural IgG3 antibody secreting cells (ASC) has been shown to be BLIMP-1 independent in some cases [Savage et al., 2017]. The highest frequencies of B1 cells are found in the peritoneal cavity (PerC), other major niches are the spleen and the BM [Hayakawa et al., 1986, Baumgarth, 2016]. The functions of the B1 cells differ depending on the site they reside. In the spleen, B1 cells mostly show effector functions through IgM and cytokine secretion, however, B1 cells from the PerC seem to provide a natural memory compartment and migrate upon innate signals like IL5, IL10, and type-I Interferon (IFN) into the spleen in order to differentiate to ASC [Baumgarth, 2016]. Nevertheless, adoptive transfer of adult-derived PerC B1 cells into newborn mice leads to colonization of all known niches like the spleen, BM and other body cavities [Lalor et al., 1989, Choi et al., 2012, Förster and Rajewsky, 1987]. Additional data reveal a dependency of tissue location for the gene expression profile of isolated B1 cells [Stoermann et al., 2007]. Further, B1 cells of the PerC are characterized by  $\beta$ -2 integrin CD11b expression and a continuous circulation. CD11b gets lost after arrival of B1 cells into the secondary lymphoid organs but is necessary for the effective homing in the lymph node (LN) and the spleen [Waffarn et al., 2015]. Peritoneal B1 cells can also differentiate towards intestinal IgA ASC. The Peyer's patches (PP) and mesenteric LN with constitutively active GC reaction are the source of these plasma cells (PC). The differentiation of intestinal IgA ASC can be proceeded in a T cell independent (TI) or T cell dependent (TD) manner [Bunker et al., 2015]. Isolated lymphoid follicles which belong also to the gut-associated mucosa mainly support the TI differentiation of IgA ASC [LORENZ and NEWBERRY, 2004, Bunker and Bendelac, 2018]. Up to 40% of the secreted serum IgA originates from B1 cells [Mora and von Andrian, 2008].

### 3.1.3 Immune response

B1 and B2 cells differ not only in their development but also in the repertoire of antigens they respond to. B1 cells react mainly towards TI antigen whereas B2 cells respond upon TD antigen encounter. An exception are the MZB which belong to the B2 cells but work also as a first line defense against penetrating pathogens like the B1 cells [Balázs et al., 2002]. The TI antigens are further divided into class 1 and 2 antigens. Lipopolysaccharide (LPS) and bacterial DNA belong to the TI1-antigens and cause polyclonal activation which induces, regardless of the B cell specificity, proliferation and

differentiation through signaling over the Toll like receptor (TLR) [Murphy et al., 2012]. Penetrating capsulated pathogens belong to the TI2-antigens. If the highly repetitive structures, like found in bacterial capsular polysaccharides, crosslink a critical number of BCRs, mature B cells can differentiate to IgM secreting plasmablasts (PB). This happens without the help of T cells and therefore represents a rapid response against capsulated bacteria. However, dendritic cells, which provide membrane bound signaling molecules and release BAFF, support proliferation and class switch towards IgG3. BAFF is a cytokine which belongs to the tumor necrosis factor (TNF)-family and interacts with transmembrane activator and CAML interactor (TACI) and the BAFF receptor on B cells. Only mature B cells can be activated by TI2 antigens, whereas TI1 antigens can also activate immature B cells. The encounter with a TI1 antigen does not lead to the development of memory cells [Murphy et al., 2012].

Another class of antigens are TD antigens. These antigens which evoke a germinal center (GC) reaction are mainly recognized by FoB [MacLennan, 1994]. In order to obtain signals from T cells, B cells need to present the antigen in a specific manner. Upon antigen recognition by the BCR, the BCR-antigen complex is internalized. The antigen gets processed into antigenic peptides and is loaded onto a major histocompatibility complex (MHC)-class II molecule. The MHC-class II-peptide complex is transferred onto the B cell surface and interacts with the T cells [Yuseff et al., 2013]. The encounter with an antigen induces the upregulation of C-C chemokine receptor 7 (CCR7) in B cells and C-X-C chemokine receptor type 5 (CXCR5) in T cells. Due to the secreted chemokines CXCL13 and CCL21, the cells migrate towards the border of the T and B cell zone. At this site, they start excessive proliferation and form a GC. The GC is divided into two zones called the dark zone (DZ) and the light zone (LZ). In the DZ, the B cells are named centroblasts. These cells express C-X-C chemokine receptor type 4 (CXCR4) which keeps them into this densely packed site where they undergo several rounds of proliferation. Targeted mutations in the immunoglobulin V regions are introduced by the enzyme activation induced cytidine deaminase (AID) [Muramatsu et al., 2000]. This process is called somatic hypermutation (SHM) [Murphy et al., 2012]. The downregulation of CXCR4 and the upregulation of CXCR5 leads them into the LZ. Here, the follicular dendritic cells (FDC) and the T follicular helper cells control the affinity of the BCR. If the B cell is able to bind the antigen, it achieves signals from the FDC and the T follicular helper cells which leads partly to the migration back into the DZ [Victora and Nussenzweig, 2012]. There it goes through further rounds of proliferation and SHM known as the cyclic reentry model. The avidity and affinity of the antigen binding of the B cells is controlled by T cells. B cells with successful mutated BCR receive survival and proliferation signals which induce the differentiation towards either PC or memory B cells. Besides SHM, GC B cells also undergo class switch recombination. This is mediated by the cytokine release and CD40 interaction of mainly CD4<sup>+</sup> T helper cells.

The change of the isotype of the heavy chain changes the effector function of the released antibody and increases its versatility. After escape from the GC, PC migrate to different body cavities also depending on their isotype [Murphy et al., 2012, Kräutler et al., 2017]. Memory B cells persist as recirculating cells in the organism and are positioned nearby antigen drainage, for example the splenic marginal zone, the mucosal epithelium of the tonsil and the BM [Tangye and Tarlinton, 2009]. Memory B cells are long lived cells, with surface immunoglobulin expression, no antibody secretion, and a very slow proliferation rate. In contrast, the life span of PC depends on the site they are residing, they only express intracellular immunoglobulin and secrete high amounts of antibodies. Short-lived PC are located in the extra follicular sites like the spleen or the medullary chords of the LN. Long-lived PC are situated in the BM and the gut-associated lymphoid tissues [Brynjolfsson et al., 2018]. Upon secondary immune response, memory B cells can efficiently present low amounts of antigen towards T cells and either differentiate rapidly into PC or re-enter with other B cells the GC reaction [Victora and Nussenzweig, 2012]. Also, they produce high amounts of specific antibodies. The mechanisms which control the differentiation to either one of the phenotypes upon GC reaction still need to be investigated [Kräutler et al., 2017].

But the regulation network of the different transcription factors (TF) is broadly established. B-cell lymphoma 6 protein (Bcl6) is highly expressed during the GC reaction and acts as transcriptional repressor. Thereby, it prevents terminal B cell differentiation by repressing TFs like BLIMP-1. Additionally, it leads to proliferation of GC B cells and facilitates tolerance of high rates of SHM [Cattoretti et al., 2006]. BACH2 induces the expression of *Aicda* which is necessary for class switch recombination and SHM. Paired box protein 5 (Pax5) represses *Xbp1* and has an essential role in preserving the GC phenotype [Nera et al., 2006]. Also, IRF4 is expressed in low levels which also induces *Bcl6* and *Aicda* expression. If GC B cells are committed to the PC phenotype, high levels of IRF4 are expressed which leads to expression of BLIMP-1 and repression of BCL6. BLIMP-1 in turn also represses *Bcl6* and *Pax5* [Nutt et al., 2015]. This allows the expression of XBP1, another master regulator of PC differentiation [De Silva et al., 2016]. Memory B cells remain positive for BACH2 and PAX5 expression [Nutt et al., 2015].

### 3.2 B cell lymphoma

In order to provide this wide range of diverse specific antibodies, the BCR undergoes different processes during development and upon antigen encounter as described in chapter 3.1.1 and 3.1.3. These cascades used to establish antibody diversification in B cells make them vulnerable for malignant transformation. Therefore, it is not surprising that 95% of lymphomas originate from B cells and only 5% from T cells [Campo et al., 2011].

### 3.2.1 Cellular origin of B cell lymphomas

The subtypes of lymphomas originate from distinct stages of the B cell differentiation process. They were characterized depending on the presence or absence of mutations in the immunoglobulin variable region and by gene expression profiles. The splenic follicle consists of different regions characterized by the composition of specific cell types. The marginal zone surrounds the B cell follicle and is dominated by the MZB. Extra nodal mucosa-associated lymphoid tissue (MALT) lymphomas and nodal marginal-zone B-cell lymphomas originate probably from the marginal zone and consist of FoB and MZB with unmutated variable V region genes. Therefore, it is assumed that these lymphomas derive from naive B cells which are in the differentiation process towards MZB. The mantle zone borders the GC and contains naive B cells expressing the surface marker CD5. The mantle cell lymphomas probably originate from this cell type but 20-30% of the lymphoma cells contain mutated V regions hinting to cells which passed the GC [Shaffer et al., 2012]. Also, chronic lymphocytic leukemia arises from CD5<sup>+</sup> B cells which are characterized by either unmutated or mutated variable heavy chain mutations. Therefore, they evolve either from SHM unexperienced cells or from cells which underwent the GC reaction, respectively [Kipps et al., 2017]. Follicular lymphoma (FL), classical Hodgkin lymphoma (cHL), Burkitt Lymphoma (BL) and the GC B cell-like subtype of the diffuse large B cell lymphoma (DLBCL) derive from GC B cells [Küppers, 2005]. Post-germinal center PB are the origin of the activated B-cell like (ABC) subtype of DLBCL [Matsumoto et al., 1996, Shaffer et al., 2000]. In most cases, post-transplant lymphomas which often derive in patients with an organ transplant, are composed of antigen-selected, GC B cells. The cells of the primary effusion lymphoma (PEL) reveal distinct cellular origins and can either come from naive, GC, or post-germinal center B cells which is also influenced by the presence or absence of an EBV infection [Hamoudi et al., 2004].

### 3.2.2 Transforming events

The transforming events during B cell maturation and differentiation processes can cause oncogenic mutations. The engagement of one of the Ig loci and a proto-oncogene are found in many types of B cell lymphomas. Due to the translocation, the proto-oncogene is positioned under the control of the active Ig locus. Now, the expression of the proto-oncogene is deregulated and constitutive active. These events can occur during V(D)J recombination in the early B cell development in the BM but mostly during the GC reaction while SHM process or class-switch recombination take place [Küppers, 2005]. There are three different kinds of breakpoints in the Ig locus. The first is adjacent to the Ig heavy chain J-region or next to the joining region of the Ig heavy chain D-region and J-region. This can be found in the FL which is associated with a Bcl2-IgH translocati-

tion. Other translocations are by-products of SHM because they are present within or nearby of somatically mutated rearranged V(D)J- genes. During class switch recombination, DNA breaks are introduced in the IgH constant switch regions. These breakpoints characterize the third type of translocations. Examples for IgH translocations are *BCL2* found in the FL, *MYC* in the BL and *cyclin D1* in the mantle cell lymphoma [Chesi, 1996, Johnson et al., 2009, Gostissa et al., 2009]. During SHM, mutations are introduced in the immunoglobulin variable regions of the BCR through substitution, deletion, or insertions of single base pairs. In lymphomas, aberrant SHM leads to mutations in genes in addition to the V genes. For example, the DLBCL displays mutations in proto-oncogenes like *PIM1*, *MYC*, *RhoH/TTF*, and *PAX5* [Pasqualucci et al., 2001]. The characteristic mutation pattern in these genes is similar to SHM in the V-gene region. However, normal GC B cells do not display mutations in these loci [Pasqualucci et al., 2001].

One of the most common targets influenced by translocation, amplification, and mutation occurring in the lymphomas are genes encoding for TFs. *BCL6*, *IRF4* and *BLIMP-1* which are important TFs during the GC reaction belong to the main targets in this process. Therefore, the following section explains several mutations in these TFs leading to lymphoma development (see: 3.1.3). The master regulator of the GC reaction, *BCL6* is often deregulated in B cell lymphomas. For example, in DLBCL and FL, the promoter region of *BCL6* is replaced by constitutive active heterologous regulatory regions leading to an impaired downregulation of *BCL6* in these lymphomas [Ye et al., 1993]. This in turn leads to a block in PC differentiation, increased proliferation, and a block of the DNA repair mechanisms [Shaffer et al., 2000, Phan et al., 2005]. Multiple myeloma and ABC DLBCL reveal a high expression of *IRF4* [Alizadeh et al., 2000]. The active  $\text{NF}\kappa\text{B}$  pathway in these lymphomas mediates directly the expression of *IRF4* which plays a key role in PC differentiation by transactivating *PRDM1* and repressing *BCL6* [Saito et al., 2007]. The difference between multiple myeloma and the ABC DLBCL is the differentiation stage of the lymphoma cells. The cells of multiple myeloma have a PC phenotype displaying the full gene expression profile of mature PC, the cells of the ABC DLBCL have a plasmablastic phenotype caused by the inactivation of *PRDM1* [Pasqualucci et al., 2006].

In order to avoid cell death, lymphoid malignancies are often characterized by a constitutively active  $\text{NF}\kappa\text{B}$  signaling.  $\text{NF}\kappa\text{B}$  signaling promotes survival in different kinds of cell types and gets transiently activated via receptors like BCR, CD40, CD30, and diverse TLRs. Among others, ABC DLBCL, cHL, gastric MALT lymphoma, and multiple myeloma are associated with constitutively active  $\text{NF}\kappa\text{B}$  signaling. The  $\text{I}\kappa\text{B}$  kinase (IKK) complex consisting of  $\alpha$ ,  $\beta$ ,  $\gamma$  (NEMO) subunits is applied in the classical pathway and requires phosphorylation of  $\text{IKK}\beta$  and ubiquitination of  $\text{IKK}\gamma$ . Upon activation,  $\text{IKK}\beta$  phosphorylates  $\text{I}\kappa\text{B}\alpha$  which leads to its ubiquitination and degradation.  $\text{I}\kappa\text{B}\alpha$  is an inhibitor of the heterodimers p50/p65 and p50/cRel, preventing them to shuttle into the

nucleus. Due to degradation of  $I\kappa B\alpha$ , the heterodimers migrate into the nucleus and activate the transcription of target genes. In contrast, the alternative pathway relies on the IKK complex consisting of two  $IKK\alpha$  subunits which get activated by the kinase NIK. The activated  $IKK\alpha$  complex phosphorylates p100 causing proteolytic processing into the  $NF\kappa B$  subunit p52. This subunit migrates together with RelB towards the nucleus, activating transcription by binding to the DNA [Shaffer et al., 2012]. The stabilization of NIK is the main cause for constitutive active  $NF\kappa B$  pathway in multiple myeloma. This is either achieved through mutations causing loss of function in *TRAF3* or with gain-of-function-mutations inducing overexpression of *NIK*, *CD40*, or *LT $\beta$ R*. Chronic BCR signaling which is induced through gain-of-function-mutations in *CD79A/B* result in constitutively active  $NF\kappa B$  signaling in ABC DLBCL. Additionally, inactivation of A20 which is a negative regulator of the  $NF\kappa B$  pathway contribute to the steady active  $NF\kappa B$  pathway in this B cell lymphoma [Nagel et al., 2014].

### 3.2.3 CD30<sup>+</sup> B cell lymphoma

CD30 is highly expressed in Hodgkin lymphoma (HL) and anaplastic large cell lymphoma (ALCL) but also found on cells of the PEL and DLBCL, especially in EBV positive cases. The HL is subdivided into the cHL which amounts to 95% of all cases and the nodular lymphocyte predominant form (NLPHL). The hallmark of the cHL are the Hodgkin and Reed/Sternberg cells (HRS). HRS cells derive from GC B cells, have downregulated the most B cell specific genes, and display clonally rearranged and somatically mutated Ig heavy- and light-chain genes. The HRS cells are surrounded by various different cell types. The most frequent ones are the T cells. Different kind of T cells are attracted through chemokine release of the HRS cells and are arranged in a rosette like structure around these cells. Genetic lesions in HRS cells lead to constitutively active  $NF\kappa B$ , JAK/STAT, and PI3K/Akt pathways [Küppers, 2012]. CD30 is also expressed on non HL like the DLBCL. These subsets reveal partly EBV infection. EBV<sup>+</sup> DLBCL show more frequently a CD30 expression than EBV<sup>-</sup> cases. EBV<sup>+</sup>, CD30<sup>+</sup> DLBCL cases are often accompanied with advanced age. The pathological analysis of the EBV<sup>+</sup> DLBCL of the elderly displays strong polymorphisms and varies from large B-cell like, Hodgkin lymphoma-like, and polymorphic lymphoproliferative disorder-like. The B cells display an activated B cell phenotype. The surrounding cells are mostly composed of small lymphocytes and PC. Further, this lymphoma displays an involvement of the canonical and alternative  $NF\kappa B$  pathways, concomitantly or independent of one another [Ramachandiran et al., 2015]. Thereby, the EBV infection seems to have an additional impact in activating these pathways [Montes-Moreno et al., 2012]. CD30<sup>+</sup> DLBCL cases seem to have a preferable outcome than CD30 negative cases. However, the combination of CD30 expression and EBV infection resulted in significantly poorer clinical survival and outcome in comparison to CD30<sup>+</sup>, EBV<sup>-</sup> and CD30<sup>-</sup>, EBV<sup>+</sup> cases [Hu et al., 2013]

### 3.3 CD30

Lymphomas which are positive for CD30 expression reveal this CD30 expression in almost all lymphoma cells [Montes-Moreno et al., 2015]. Under physiological conditions, the expression of CD30 is restricted to a few activated T and B cells [Dürkop et al., 1997]. Despite the high incidence of CD30<sup>+</sup> lymphomas, the role of CD30 in B cells is still not fully understood. It is a member of the TNF-receptor superfamily and characterized as a marker for different kinds of B cell lymphomas [Younes and Aggarwall, 2003, Klein et al., 2003, Bhatt et al., 2013]. Further, the use of CD30 as prognostic value to determine the clinical outcome of the lymphoma is still unclear. But in DLBCL, it could be shown that CD30<sup>+</sup> cases are characterized by more B symptoms, and stronger BM involvement than the CD30<sup>-</sup> cases [Hao et al., 2015]. The CD30 protein undergoes different maturation stages during biosynthesis. The precursor protein with a size of 84 kDa is processed by high mannose N-linked glycosylation to a 90 kDa precursor. This precursor migrates in the endoplasmic reticulum and the Golgi complex and gets further processed through addition of sialic acids, O-linked glycosylation and the conversion of N-linked glycosylation to a complex type. The result is a 120 kDa mature transmembrane protein [Nawrocki et al., 1988, Froese et al., 1987]. The soluble CD30 (sCD30) is produced by cleavage of the extracellular domain of CD30 through membrane-anchored metalloprotease [Hansen et al., 2000, Josimovic-Alasevic et al., 1989]. The sCD30, which is found in high concentrations in the serum of patients with CD30<sup>+</sup> malignancies, has a size of 85 kDa. The CD30 ligand (CD30L) has a size of 40 kDa and is found on activated T and B cells, macrophages, and dendritic cells [Marín and García, 2017, Hendrickson et al., 2007].

#### 3.3.1 Signaling

The interaction of CD30 with CD30L leads to activation through receptor trimerization which is a common feature of all TNFRs [Smith et al., 1994]. The C-terminal domain of CD30 reveals significant homologies to TNF receptors I, II, CD27 and CD40 [Smith et al., 1993]. Similar to the other TNF-receptors, the intracellular domain of CD30 possesses no intrinsic enzymatic domain. The members of the TNFR-associated factor (TRAF) family and various TRAF-binding proteins are the only mediator of signal transduction [Schneider and Hübinger, 2002]. TRAF 1, 2, 3 and 5 bind one of the two different intracellular binding sites of CD30 [Boucher et al., 1997, Lee et al., 1996]. These two intracellular domains activate differentially the canonical and alternative NF $\kappa$ B pathway in human lymphocytes [Buchan and Al-Shamkhani, 2012]. Additionally, CD30 induces signaling through the mitogen activated protein kinase (MAPK) pathway. This leads to different anti-apoptotic and pro-survival signaling. Further, there seems to be a positive feedback loop between the MAPK/extracellular signal-regulated kinases (ERK) pathway and the nuclear transcription factor JunB which promotes cell survival but also

CD30 expression [van der Weyden et al., 2017].

### 3.3.2 Function

Little is known about the function of CD30. The knowledge which derived from different lymphoma cell lines is contradictory. Studies which used the monoclonal antibody Ki-1 to activate CD30 signaling reported decreased proliferation and increased apoptosis in ALCL whereas cells lines derived from HL remained unaffected [Hirsch et al., 2008]. Analysis of the gene expression profile of both cell lines revealed strong differences in these two cell lines upon CD30 stimulation. This study revealed only a response in cell lines from ALCL and not from HL. Further, Hirsch et al. show that ALCL cell lines respond with activation of caspases and NF $\kappa$ B-mediated survival upon CD30 stimulation [Hirsch et al., 2008]. It is assumed that the ability to activate the NF $\kappa$ B signaling governs the outcome in these cells [Mir et al., 2000]. Another hypothesis is that the outcome upon activation of CD30 signaling depends on the activation of different regions on the cytoplasmic tail of CD30. As shown in different kind of lymphoma cell lines, the signaling mechanism are also accompanied with paracrine, juxtacrine, and autocrine regulatory loops between CD30L and CD30 expressing cells [Hsu and Hsu, 2000]. Therefore, the microenvironment is critical in order to predict the influence of CD30 signaling.

In the immune system, CD30 acts as co-stimulatory molecule together with the CD3/T cell receptor (TCR) complex in T cells. Knock out mouse models reveal a role of CD30 during regulation of memory T cells [Muta and Podack, 2013]. Additionally, without CD30, the capacity of sustaining GC responses is impaired and the memory antibody response is reduced [PODACK et al., 2002, Gaspal et al., 2005]. Further, the interaction of CD30-CD30L is involved in the negative selection process of autoreactive T cells in the thymus [Chiarle et al., 1999, Gilfillan et al., 1998, Amakawa et al., 1996]. However, the active CD30 signaling on human Th0, Th1, and Th2 also results in increased proliferation rates and cytokine production [Del Prete et al., 1995, Tarkowski, 2003]. Murine B cells which encounter CD30 stimulation combined with either IL4 or IL5, react with proliferation and enhanced antibody production and secretion [Shanebeck et al., 1995]. *In vitro* studies with human B cells revealed impeded CD40L induced class switch. Besides, it was shown that CD30L expressing human B cells receive inhibitory signals from CD30<sup>+</sup> T cells which can result in hampered class switch and reduced production of IgA, IgG and IgE. This process is accomplished by the so called reverse signaling [Kennedy et al., 2006].

## 3.4 MHV-68

### 3.4.1 Biology

The two known human gammaherpesviruses EBV and KSHV have a high association with different B cell lymphomas like DLBCL and PEL, respectively. A known murine virus which also belongs to the subfamily of *Gammaherpesvirinae* is the murine gamma-herpesvirus 68 (MHV-68). The *Gammaherpesvirinae* are further assigned to the family of *Herpesviridae*. This family is ancient, widely distributed, and has a large double-stranded DNA genome. The *Herpesviridae* are characterized by four main biological properties. They share a large pool of enzymes which are associated with the nucleic acid metabolism, DNA synthesis, and processing of proteins [Fields et al., 2007]. In the nucleus, the viral DNA synthesis and capsid assembly takes place. However, the final processing of the virion occurs in the cytoplasm. Further, the production of the progeny virus leads always to the destruction of the infected cell. Finally, the herpesviruses are able to persist in a phase of latency in their natural hosts. While doing this, the viral genome remains as closed circular molecule and just a few viral genes are expressed. This stage is reversible, meaning the viruses preserve the ability to replicate and can cause a disease in the lytic phase upon reactivation. All herpesviruses stay latent in a specific cell subset. But this subset varies and depends on the virus. Gammaherpesviruses remain latent mainly in lymphoid tissue, especially in B cells [Fields et al., 2007]. This subfamily is partly associated with lymphoproliferative diseases and lymphomas but also non-lymphoid malignancies. It is assumed that the DLBCL in elderly is caused by a defective immune surveillance of EBV infected B cells [Montes-Moreno et al., 2012]. In cHL, all EBV positive cases carry BCR with crippled mutations which preclude their functional expression. Since B cell cannot survive without a BCR, the EBV infection is a precondition for these cells to survive and undergo malignant transformation. Otherwise, these cells would undergo apoptosis. Further, EBV intervenes with epigenetic and transcriptional processes which leads to growth and survival independent of transforming mutations [Shannon-Lowe et al., 2017]. MHV-68 was first isolated from voles in Slovakia [Blaskovic et al., 1980, Nash et al., 2001]. It infects laboratory mice and a variety of tissue culture cell lines [Blaskovic et al., 1980, Virgin et al., 1997]. In mice, the virus establishes a lifelong latent infection in B cells, macrophages and splenic dendritic cells. The natural infection route is unknown but it is assumed to be over the respiratory tract. A frequently applied technique in the laboratories, intranasal inoculation, leads to a lytic replication in the lung accompanied by infection of alveolar epithelial cells. After the peak of viral titers is reached at day (d) 7, the infection spreads to distal organs like the spleen with the help of B cells. The acute phase of virus replication in the spleen is cleared between d 14-16 post infection (p.i.). In the early phase of latency, between d 16-18, around 1 of 100 splenocytes carry the virus. Also during this time, different sub-populations of B cells are found to be infected. These

are naive (sIgD<sup>+</sup>) B cells, GC (PNA<sup>+</sup>, CD95<sup>+</sup>) B cells, and isotype switched memory B cells. However, upon three months p.i., the number of infected naive B cells diminishes constantly. Now, a steady level of 1 among 10.000 cells is infected which are mainly composed of isotype-switched memory B cells [Barton et al., 2011]. Without B cells, latency in macrophages can only be established if the virus is applied intraperitoneally (i.p.). Only in particular immune-compromised mice, infection with MHV-68 leads to lymphoma development [Nash et al., 2001].

### 3.4.2 $\gamma$ -Herpesviruses in disease

EBV and KSHV belong to two different subgroups of the  $\gamma$ -Herpesviruses. EBV is assigned to the lymphocryptoviruses and KSHV to the rhadinoviruses. EBV is found in almost all cases of endemic BL and partly in PEL and HL. The *in vitro* infection of B cells with EBV leads to immortalized proliferating lymphoblastoid cell lines (LCL) [Toplin et al., 1966]. LCL express two groups of viral antigens: six nuclear antigens declared as Epstein-Barr nuclear antigens (EBNA) and three membrane proteins cited as latent membrane proteins (LMP). LMP1, known as an oncogene, is one of these and is essential, but alone not sufficient for immortalization of B cells. It belongs to the TNF-receptor superfamily, needs no ligand for active signaling due to self-oligimerization in the plasma membrane, and its functions resemble a constitutively active CD40 receptor [Klein et al., 1999]. The signaling domain of LMP1 consists of two effector sites called CTAR1 and CTAR2 interacting with TRAF. CTAR1 induces the non canonical NF $\kappa$ B pathway and CTAR2 is necessary to activate c-Jun N-terminal kinase (JNK) and the canonical NF $\kappa$ B pathway [Kieser and Sterz, 2015].

The cellular counterpart of LMP1 is CD40 which is expressed for example on the surface of B cells. The interaction is performed with CD40L expressing T cells. Active CD40 signaling in B cells induces the initiation of the GC reaction. Further in the LZ of the GC, CD40L bearing T cells participating in the positive selection process of centrocytes. In contrast to *in-vitro* derived LCL, the expression profile of EBV-infected cells *in vivo* is much more restricted. These profiles depend on the differentiation profile of the affected B cell and are categorized in three stages of latency. At the different latency stages, distinct sets of genes are expressed. EBV can adopt all three stages in B cells. After infection of a naive B cell, EBV accesses the latency stage III. There it expresses EBNA 3A, 3B, 3C, and Leader protein (LP), LMP1 and LMP2a+b and Epstein-Barr virus-encoded small RNAs (EBER)1+2. This leads to the transformation of the B cell into a proliferating blast. Afterwards, EBV restricts the expression profile to latency stage II or the so called default programme. Here, EBNA 1, LMP1, LMP2a+b and the EBERs are expressed which induces the B cell to differentiate into a memory B cell. The latency stage I, which follows, comprises only the expression of the EBERs and EBNA 1.

KSHV is present in almost all cases of Kaposi's sarcoma, and it is associated with the

development of PEL. Until now, infection of B cells with KSHV did not lead to immortalization *in-vitro*. KSHV lacks clear homologs of EBV genes which lead to transformation of B cells. As KSHV, also MHV-68 belongs to the group of rhadinoviruses. Several similarities among MHV-68, KSHV and EBV proof MHV-68 as a good model to study the biology of  $\gamma$ -herpesviruses in mice. Various genes like v-cyclin, vBcl-2, vGPCR, LANA, and RTA which are involved in latency establishment and reactivation, are well conserved between primate and rodent viruses [Gauld et al., 2013]. Also, studying the unique gene products of herpesviruses revealed conservation of key functions [Damania et al., 2000]. Finally, all  $\gamma$ -herpesviruses are lymphotropic and share the same strategy of persisting in their hosts [Barton et al., 2011]. The highly conserved innate and adaptive immune response between mice and human appoint MHV-68 as a good model for studying the nature of  $\gamma$ -herpesvirus infections.

### 3.5 The LMP1/CD30<sup>fSTOP</sup> mouse strain

The low number of CD30 expressing cells in human and mice complicates the task of studying the effect of CD30. Further, as described above, some human B cell lymphomas highly express CD30, and the role of CD30 in these diseases is still unknown. For these reasons, Petra Fiedler in the lab of Dr. Zimmer-Strobl developed the LMP1/CD30<sup>fSTOP</sup> mouse strain. Here, the fusion gene LMP1/CD30 consists of the transmembrane domain of the viral protein LMP1 and the cytoplasmic domain of murine CD30. Due to the self-oligomerization of LMP1, the CD30 ligand is not needed to induce CD30 signaling. Instead, a chronic signaling is established in the respective cell in which the fusion gene is expressed. The transgene was inserted into the Rosa26 locus under the control of the endogenous Rosa26 promoter. The fusion gene is preceded by a loxP site flanked STOP-cassette ensuring a cre-dependent expression of LMP1/CD30. An IRES-hCD2 (internal ribosomal entry site-human CD2) cassette was inserted downstream of LMP1/CD30. The inserted hCD2 is truncated. This enables monitoring the LMP1/CD30 expression in any given cell by surface staining for hCD2.

In previous work, the LMP1/CD30 strain was crossed to the CD19cre strain in order to achieve a B cell specific LMP1/CD30 expression. These mice developed already with eight weeks a mild splenomegaly evoked by significant higher B cell numbers. Nevertheless, the splenic follicle structure of these mice displayed a normal organization regarding B and T cell zone. In contrast, the B cell sub-populations displayed a significant increased CD43<sup>+</sup>, CD23<sup>low</sup>, IgM<sup>+</sup>, IgD<sup>low</sup> population resembling a B1 cell population. Additionally, the PC population in BM and spleen was enhanced, accompanied by higher IgM, IgG2a, IgG3 and IgA serum titers. Immunization with the TD antigen (4-hydroxy-3-nitrophenyl)acetyl (NP)-Chicken Gamma Globulin (CGG) led to significant reduced GC and significant reduced IgG1 PC. Finally, the LMP1/CD30 mice developed in 80% of aged mice a mono-

or oligoclonal lymphoma with B cells consisting only of the expanded CD43<sup>+</sup>, CD23<sup>low</sup> cells [Sperling et al., 2019].

## 4 Aim

CD30 was first identified 1982 with a monoclonal antibody obtained by using a HL derived cell line [Schwab et al., 1982]. Afterwards, CD30, a transmembrane glycoprotein receptor, was cloned, characterized as a 120kD protein, and assigned to the tumor necrosis factor receptor superfamily [van der Weyden et al., 2017]. The variable expression on normal cells in comparison to malignant cells on different hematopoietic lymphomas raised the question of the pathogenic mechanisms of CD30 upregulation and its interference in the process towards lymphoma development. The restricted expression of CD30 on specific malignant cells resulted in the attempt to use it as therapeutic target for lymphoma therapy. However, the knowledge about the function of CD30 is restricted so far. To study the physiological and pathophysiological function of CD30, Petra Fiedler generated a transgenic mouse line LMP1/CD30 which allows for conditional expression of a constitutive active CD30 receptor in the targeted cells. The loxP flanked STOP-cassette enables a cre-recombinase dependent expression. Petra Fiedler crossed the LMP/CD30 line to the CD19cre mouse line and analyzed the influence of the LMP1/CD30 expression in all B cells. Thereby, she detected an expanded population with a B1 like phenotype and a block of the GC reaction in the LMP1/CD30//CD19cre mice upon TD immunization. My aims were the following:

### **AIM 1: Elucidate the role of chronic CD30 signaling in B1 and B2 cells.**

The LMP1/CD30 expression resulted in more B1 and PC in these transgenic mice. Here, we will characterize the expanded B1-like population further and analyze its response towards *in vitro* stimulation. Also, LMP1/CD30 expressing B2 cells will be investigated upon stimulation regarding differentiation and signaling pathways. Further, TI immunization of LMP1/CD30 mice should illuminate the role of CD30 signaling during the immune response. Additionally, we will cross LMP1/CD30 mice with C $\gamma$ 1-cre mice to induce deregulated CD30 signaling in GC B cells upon TD immunization. Following, the role of CD30 during the GC reaction and its impact regarding the cell fate decision of B cells will be investigated.

### **AIM 2: Analyze the lymphoma development of LMP1/CD30//C $\gamma$ 1-cre mice upon TD immunization and herpesviral infection.**

LMP1/CD30//CD19cre do not develop GC upon TD immunization. In order to model

GC derived CD30<sup>+</sup> human lymphoma, LMP1/CD30//C $\gamma$ 1-cre mice will be adopted. The infection with MHV-68, a murine  $\gamma$ -herpesvirus, will be used to study the contribution of herpesviral infection in B cell lymphoma development. Infected cells will be examined by cloning a nerve growth factor receptor (NGFR) expressing MHV-68. Two groups of either immunized or infected LMP1/CD30//C $\gamma$ 1-cre mice will be compared and analyzed. Thereby, we will elucidate the impact of deregulated CD30 signaling in GC B cells regarding lymphomagenesis alone and combined with the  $\gamma$ -herpesviral infection. The mice will be analyzed after 2 weeks, 2 months and after becoming ill in order to follow the influence of deregulated CD30 signaling and the virus infection over time.

**AIM 3: Investigation of the additional effect of LMP1 during MHV-68 infection.**

LMP1 plays an important role in the malignant transformation of B cells during an EBV infection. Genetically engineered mouse models, analyzed already the expression of LMP1 in B cells which revealed its oncogenic potential [Wirtz et al., 2016, Zhang et al., 2012, Kulwichit et al., 1998]. However so far, no model which induces the LMP1 expression upon viral infection was established. Therefore, we aimed to use MHV-68 as a tool to express LMP1 in a herpesviral context in murine cells. Since MHV-68 does not express a homologue of LMP1, two recombinant MHV-68 viruses will be cloned. One virus will contain LMP1wt and the other LMP1mut, a LMP1 with truncated signaling domain which will serve as control. We will investigate the influence of MHV-68-LMP1 in GC and non-GC cells. Further, we will analyze the impact of the LMP1 expression in viral infected B cells regarding lymphoma development *in vivo* (knowing that MHV-68 alone is not capable to induce lymphomagenesis in wild type (wt) mice). Here, we will infect LMP1/CD30 mice with the two viruses.

## 5 Results

### 5.1 CD30 expression on murine B cells

Until now, little is known about the expression of CD30 under physiological conditions. Therefore, we analyzed the expression patterns of CD30 in B cells *ex vivo* and *in vitro* under different conditions.

First, the B cell sub-populations of the spleen and the PerC were analyzed for their CD30 expression by flow cytometry (FACS). The B1 cells expressed more CD30 than the B2 cells in the PerC. Additionally, B1a cells were slightly higher in the CD30 staining in comparison to B1b cells. A similar constellation with a slight reduced distinctness was found in the sub-populations of the spleen (Figure 1A). Second, since CD30 is expressed mainly

on activated T and B cells [Dürkop et al., 1997], the question was if CD30 upregulation differs under certain stimulating agents. Isolated splenic B cells reacted upon CD40/IgM stimulation with the highest upregulation of CD30 after 3 d (Figure 1B) compared to LPS, CD40, or IgM stimulation (data not shown). The expression of CD86 was used as positive control for B cell activation. The cooperative effect between BCR engagement and CD40 signaling regarding B cell activation, which was published recently, effects also the CD30 expression [Haxhinasto et al., 2002, Bishop et al., 1995].

Due to the higher CD30 expression of naive B1 cells in comparison to B2 cells *in vivo*, the question arose if B1 cells display a stronger upregulation of CD30 upon stimulation. For this, B1 and B2 cells were sorted and cultivated with CD40/IgM stimulation and analyzed for their CD30 expression. Both subtypes displayed an upregulation of CD30 after 1 d. Nevertheless, the staining for CD30 of B1 cells proofed a higher upregulation in comparison to B2 cells (Figure 1C).

Analysis of *in silico* data of Shi et al. revealed a role of CD30 during murine PC differentiation [Shi et al., 2015, Sperling et al., 2019]. The same could be shown upon investigation of data derived from human PC [Jourdan et al., 2011, Sperling et al., 2019]. Therefore, we immunized mice to induce PC differentiation in B cells. Indeed, developed PB characterized by a positive staining for IRF4 revealed a higher CD30 expression in comparison to IRF4<sup>-</sup> B cells (Figure 1D). This is concurrent with the co-expression of IRF4 and CD30 in human tonsil sections [Cattoretti et al., 2006]. In summary, CD30 is upregulated in PB and in B1 cells which additionally reveal a stronger upregulation of CD30 upon stimulation than B2 cells.

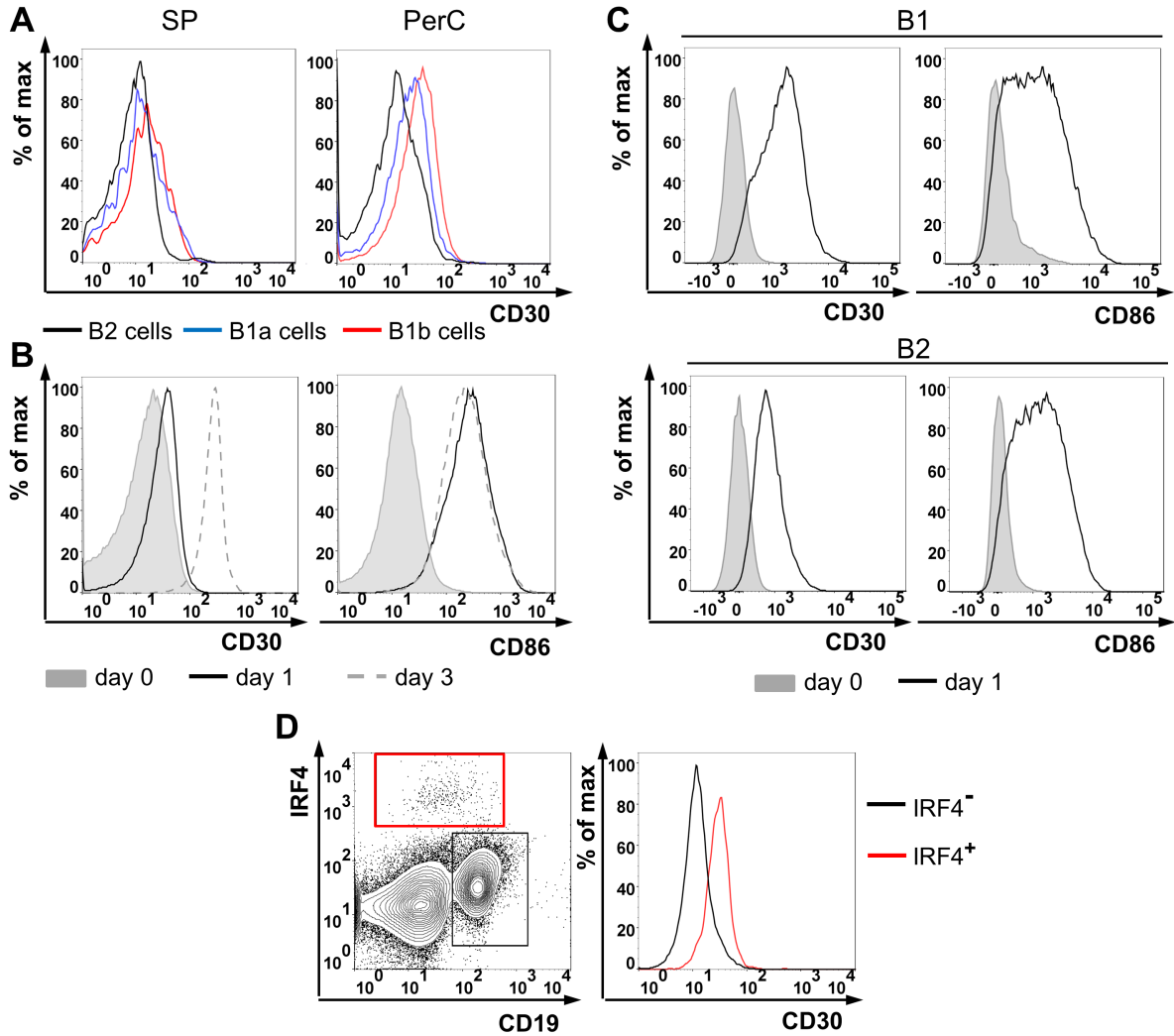


**Figure 1:** (A): Isolated lymphocytes of the peritoneal cavity (PerC) and the spleen (SP) of wildtype (wt) mice were stained for B2 (CD19<sup>+</sup>, B220<sup>+</sup>, CD5<sup>lo</sup>), B1a (CD19<sup>+</sup>, B220<sup>lo</sup>, CD5<sup>+</sup>), and B1b (CD19<sup>+</sup>, B220<sup>lo</sup>, CD5<sup>lo</sup>) and determined for their level of CD30 via flow cytometry (FACS), n=3; (B): B cells were isolated from splenocytes with the Pan-B cell isolation kit and cultivated for three days (d) with CD40 and IgM stimulation and analyzed for their CD30 and CD86 expression via FACS, n=3; (C): B cells were isolated from the SP with the Pan-B cell isolation kit and then sorted for B1 (CD19<sup>+</sup>, CD43<sup>+</sup>, CD23<sup>lo</sup>) and B2 (CD19<sup>+</sup>, CD43<sup>lo</sup>, CD23<sup>+</sup>) cells. Cells were cultivated for 1 d with CD40 and IgM stimulation and CD30 and CD86 expression was determined with FACS; (D): Wt mice were immunized with NP-LPS intraperitoneally (i.p.), at d 3 post infection (p.i.) after intracellular IRF4 staining, splenocytes were analyzed with FACS, n=3. The experiment was performed in cooperation with Markus Lechner from the laboratory of Dr. Zimmer-Strobl.

## 5.2 Chronic CD30 signaling drives plasma cell differentiation

In the following analysis, we used heterozygous BALB/c LMP1/CD30<sup>STOPfl</sup>//CD19cre mice designated LMP1/CD30 thereafter, and as control either CD19cre or wt BALB/c mice.

The previous work of Petra Fiedler displayed already higher PC numbers and an enriched

B1 like population with higher BLIMP-1 expression in LMP1/CD30 mice [Sperling et al., 2019]. Also, the co-expression of IRF4 and CD30 hints to a role of CD30 during PC differentiation. Therefore, the aim was to investigate the role of CD30 during PC differentiation further after *in vitro* stimulation and immunization.

### 5.2.1 Chronic CD30 signaling drives plasma cell differentiation *in vitro*

Isolated B cells of LMP1/CD30 and control mice were kept in culture for 5 d without stimulation, CD40, or LPS stimulation. The cells were analyzed for PB differentiation after 1, 3, and 5 d via FACS. Surprisingly, even without further stimulation, B cells of LMP1/CD30 mice differentiated towards PB (CD138<sup>+</sup>, B220<sup>lo</sup>) (Figure 2). Also, the CD40 stimulation which normally does not support PB differentiation led to significant higher percentages of PB among these cells (Figure 2).

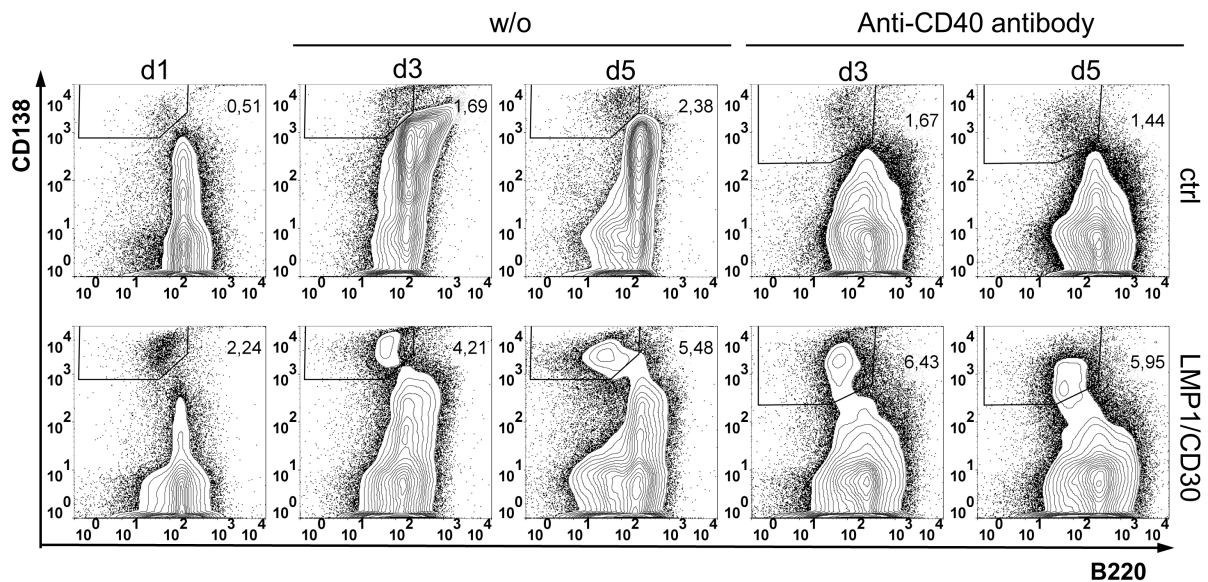


**Figure 2:** B cells of control (ctrl) and LMP1/CD30 mice were isolated with the Pan-B cell kit, cultivated for 5 d either without (w/o) stimulation or with an agonistic anti-CD40 antibody, the percentages of PB (TO-PRO3<sup>-</sup>, CD138<sup>+</sup>, B220<sup>lo</sup>) were determined with FACS at d 1, 3, and 5, shown is one representative experiment, n=3.

Additionally, the B cells of LMP1/CD30 mice stimulated with LPS differentiated to a higher extent towards PB than control B cells (Figure 3A, 3B). Due to the reduced CD138 expression of LMP1/CD30 expressing PB after LPS stimulation, we also checked for further markers. Nevertheless, CD22 was downregulated and TACI was upregulated, proving them as proper PB (Figure 3A). Further, the IgM titers of the supernatant of the cultivated B cells confirmed the differentiation towards ASC and reflect the percentage of developed PB (Figure 3C). The unstimulated LMP1/CD30 B cells secreted significant more antibodies in comparison to unstimulated control mice. But still, the LPS stimulated LMP1/CD30 B cells produced significant more than the unstimulated LMP1/CD30 B

cells.

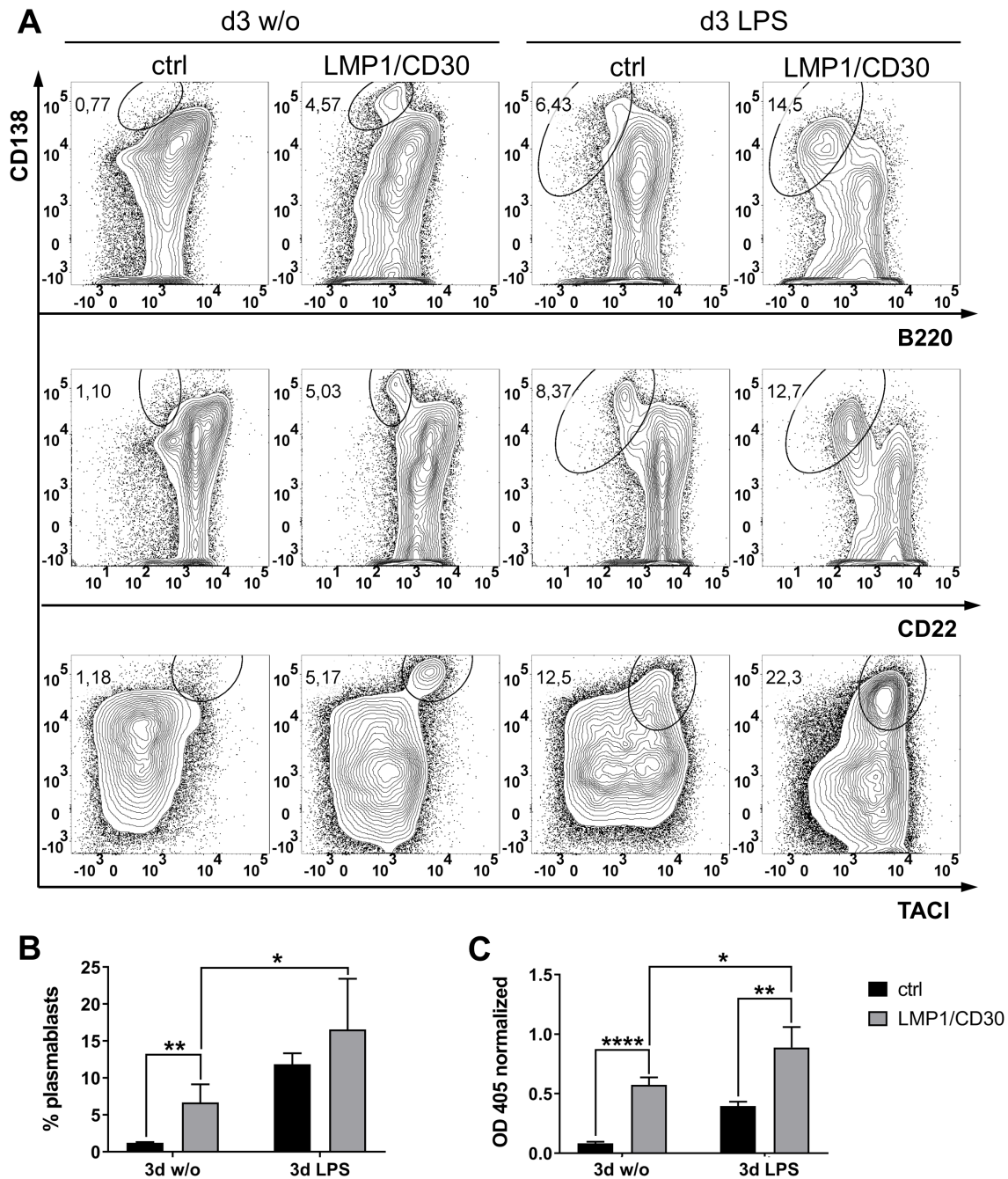


**Figure 3:** (A): B cells of ctrl and LMP1/CD30 mice were isolated with the Pan-B cell kit, cultivated for 3 d either w/o stimulation or with LPS, the percentages of plasmablasts (PB) (TO-PRO3<sup>-</sup>, CD138<sup>+</sup>/B220<sup>lo</sup> or CD138<sup>+</sup>/CD22<sup>lo</sup> or CD138<sup>+</sup>/TACI<sup>+</sup>) were determined with FACS, n=3; (B): The percentages of PB (TO-PRO3<sup>-</sup>, CD138<sup>+</sup>, TACI<sup>+</sup>) are shown in the graph at d 3; (C): The graph shows the amount of the IgM antibodies in the supernatant after cultivation for 3 d w/o or with LPS stimulation which were determined by Enzyme-linked Immunosorbent Assay (ELISA).

Usually PB differentiation is correlated with proliferation. In order to determine these, Carboxyfluorescein succinimidyl ester (CFSE) staining was used. Notably, a certain per-

centage of PB of LMP1/CD30 did not lose the CFSE staining after LPS stimulation even after 5 d of cultivation indicating that they developed to PC without cell division (Figure 4). It is known that some splenic B1 cells are able to differentiate without further proliferation towards PB [Yang et al., 2007]. To investigate whether the B1 cells are responsible for the phenotype, CD43<sup>+</sup> B1 cells were depleted. Using the remaining B cells for the same LPS experiment showed that all PB displayed a reduction of the CFSE staining which means they proliferated (Figure 4). Therefore, the source of the undivided PB were most likely CD43<sup>+</sup> cells in the LMP1/CD30 mice. This might indicate that the CD43<sup>+</sup> B cell population of LMP1/CD30 contains precursors of PB which are able to differentiate without further proliferation towards PB *in vitro*.

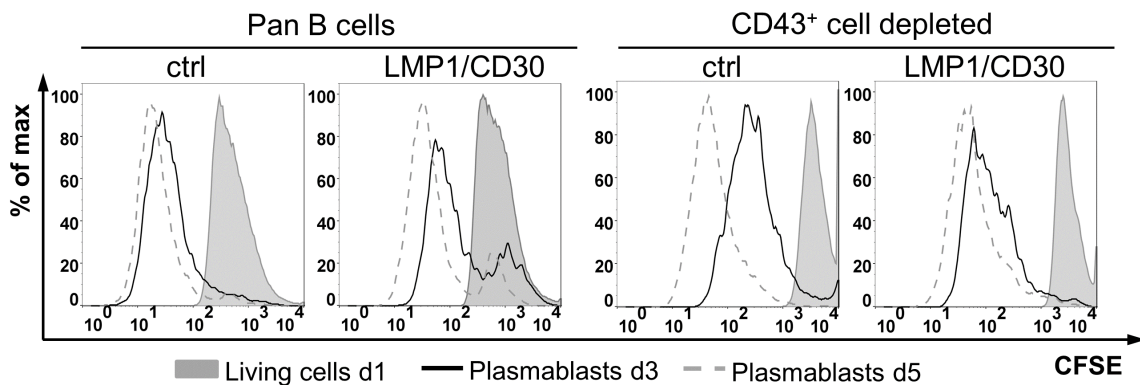


**Figure 4:** B cells of ctrl and LMP1/CD30 mice were isolated with the Pan-B cell kit or the CD43 depletion kit, stained with CFSE and cultivated for 5 d with LPS, displayed are the CFSE histograms of living cells at d 1 and of PB (TO-PRO3<sup>-</sup>, CD138<sup>+</sup>, B220<sup>lo</sup>) at d 3 and 5, shown is one representative example, n=3.

For this reason, we compared now the percentages of CD138<sup>+</sup> PB in the CD43<sup>+</sup>, CD23<sup>lo</sup> and in the CD43<sup>lo</sup>, CD23<sup>+</sup> cell population of LMP1/CD30 and control mice. Here, we found that the CD43<sup>+</sup>, CD23<sup>lo</sup> population of both genotypes contained more PB than the corresponding B2 cells. But additionally, the CD43<sup>+</sup>, CD23<sup>lo</sup> population of LMP1/CD30 mice contained significant higher percentages of PC than the same population of control mice (Figure 5A). To add, the CD43<sup>+</sup>, CD23<sup>lo</sup> cells of LMP1/CD30 mice displayed a significant higher IRF4 median fluorescence intensity (MFI) than the population of the control mice, whereas the B2 cells revealed only a slight increased level (Figure 5B). Further, a larger percentage of the CD43<sup>+</sup>, CD23<sup>low</sup> population of LMP1/CD30 mice expressed high levels of TACI, known as being upregulated in PB, in comparison to the related control population (Figure 5C) [Pracht et al., 2017].

To study whether the B1 cells are responsible for the spontaneous PB differentiation, we compared sorted B1 and B2 cells with regard to PB differentiation *in vitro* without stimulation for 3 d. This experiment designated the CD43<sup>+</sup>, CD23<sup>lo</sup> cells of LMP1/CD30 mice as source for the developed PB (Figure 5D). Almost 5% of PB arose in the B1 cell

population of these mice compared to almost 2% in the B2 cell population. To rule out the high amounts of CD138<sup>+</sup>, B220<sup>lo</sup> cells in this population as cause for these PB, we sorted again only for CD138<sup>lo</sup>, CD43<sup>+</sup>, CD23<sup>lo</sup> cells (Suppl. 1). Still, a significant higher percentage of these LMP1/CD30 expressing cells differentiated after 3 d without stimulation towards PB in comparison to control B1 cells (Figure 5E). This indicates that CD30 signaling drives PC differentiation in B1 cells without further stimulation.

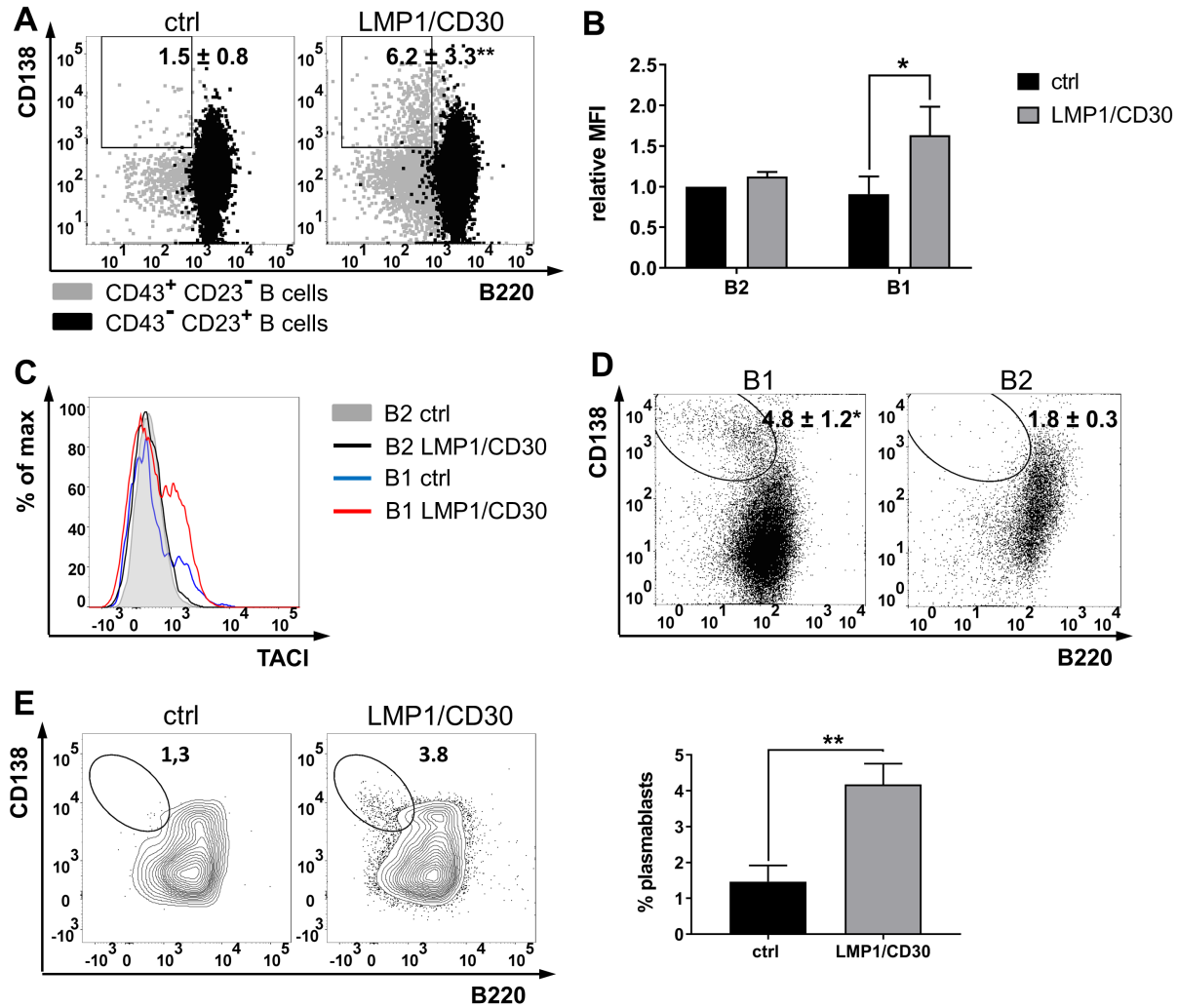


**Figure 5:** (A): These FACS plots show the CD138 and B220 staining as an overlay of splenic B1 (CD19<sup>+</sup>, CD43<sup>+</sup>, CD23<sup>lo</sup>) and B2 (CD19<sup>+</sup>, CD43<sup>+</sup>, CD23<sup>lo</sup>) cells of ctrl and LMP1/CD30 mice, the numbers show the percentages of PB (CD138<sup>+</sup>, B220<sup>lo</sup>) within the B1 cell population; (B): The graph shows the relative median fluorescence intensity (MFI) of IRF4 of splenic B1 (CD19<sup>+</sup>, CD43<sup>+</sup>, CD23<sup>lo</sup>) and B2 (CD19<sup>+</sup>, CD43<sup>lo</sup>, CD23<sup>+</sup>) cells, the MFI was normalized to the MFI of ctrl B2 cells which was set to 1, n=3; (C): The histogram shows the TACI expression as an overlay of splenic B1 and B2 cells of ctrl and LMP1/CD30 mice, one representative example is displayed, n=5; (D): B cells of LMP1/CD30 mice were isolated with the Pan B cell kit and sorted for B1 (CD19<sup>+</sup>, CD43<sup>+</sup>, CD23<sup>lo</sup>) and B2 cells (CD19<sup>+</sup>, CD43<sup>lo</sup>, CD23<sup>+</sup>), the cells were cultivated for 3 d w/o stimulation and analyzed for the percentages of PB (TO-PRO<sup>-</sup>, CD138<sup>+</sup>, B220<sup>lo</sup>) via FACS, the numbers show the mean with SD of the percentages of PB, n=4; (E): B cells of ctrl and LMP1/CD30 mice were isolated from splenocytes with the Pan B cell kit and sorted for B1 cells (CD19<sup>+</sup>, CD43<sup>+</sup>, CD23<sup>lo</sup>) excluding CD138<sup>+</sup> cells. Cells were cultivated w/o stimulation and analyzed for PB differentiation, the FACS plot shows the percentage of PB of one representative experiment, the graph compiles the percentages of all experiments, n=3.

Unlike the CD43<sup>+</sup>, CD23<sup>lo</sup> population of LMP1/CD30 mice, B2 cells did not differentiate towards PB without stimulation. In contrast, CD40 stimulation of LMP1/CD30 expressing B2 cells led to significant higher percentages of PB compared to control cells

(Figure 6A). Additionally, around of 16% B2 cells from LMP1/CD30 mice adopted a CD43<sup>+</sup>, CD23<sup>lo</sup> phenotype which was significant more than in control cells (Figure 6B). This population contained in both genotypes more CD138<sup>+</sup> B cells, expressed higher levels of CXCR4, and lower levels of CD22, being in accordance to a plasmablastic phenotype (Figure 6C+D) [Minnich et al., 2016]. Taken together, CD40 stimulation of LMP1/CD30 expressing B2 cells leads to a CD43<sup>+</sup>, CD23<sup>lo</sup> population composed of PB and their precursors. Therefore, the expanded CD43<sup>+</sup>, CD23<sup>lo</sup> population in LMP1/CD30 mice can be generated by both B1 and activated B2 cells. Further, B2 cells of LMP1/CD30 mice are not able to differentiate spontaneously to PB like LMP1/CD30 expressing B1 cells but display enhanced PB differentiation upon CD40 stimulation in comparison to control B2 cells. Thus, we think that the expanded population is a mixture of B1 cells and PB.

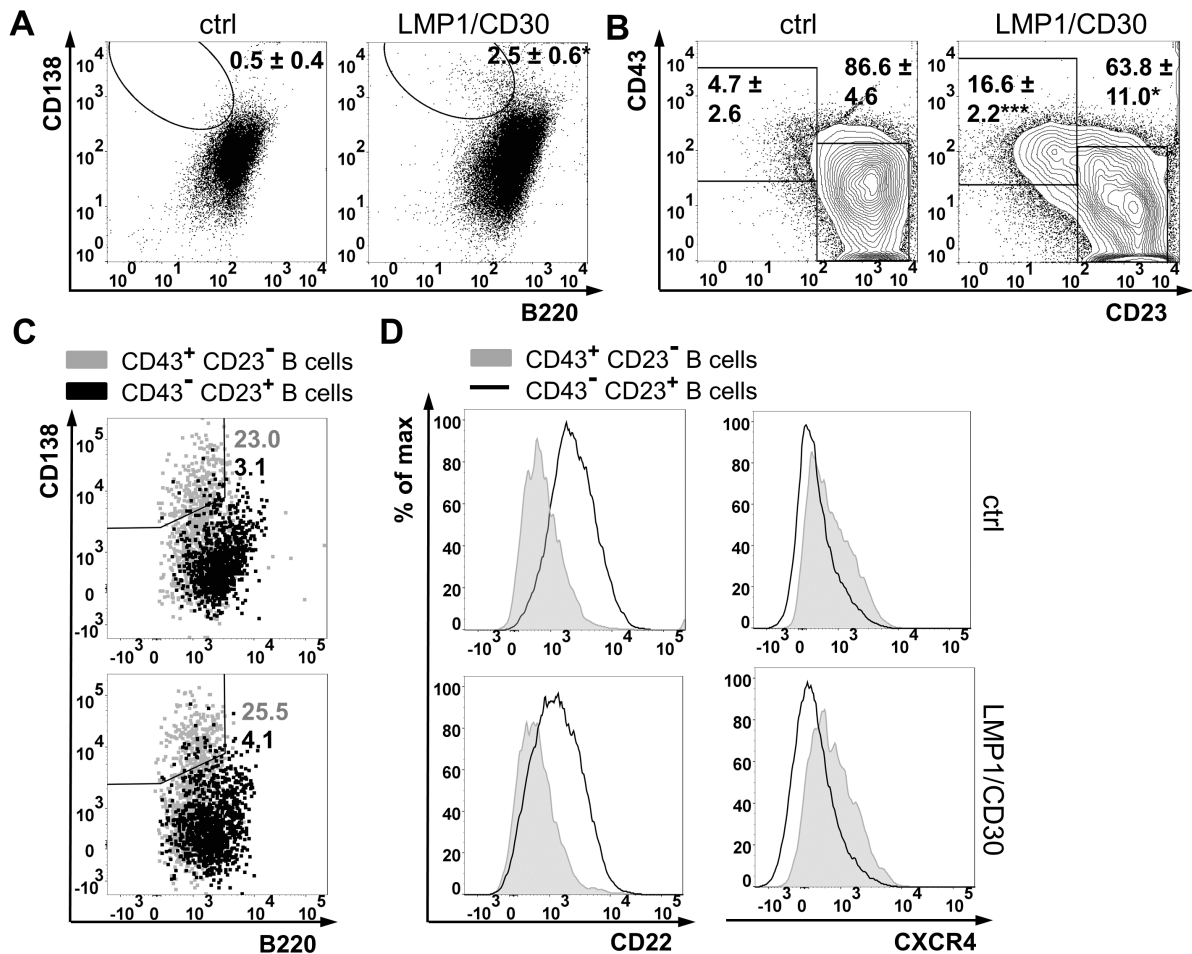


**Figure 6:** (A+B): B cells of ctrl and LMP1/CD30 mice were isolated from splenocytes with the Pan B cell kit, sorted for B2 cells ( $CD19^+$ ,  $CD23^+$ ,  $CD43^{lo}$ ) and cultivated for 3 d with anti-CD40 antibody. Subsequently, they were analyzed for PB and CD43/CD23 expression. Numbers represent the mean and SD of the percentages of the affiliated marked population,  $n=4$ ; (C): This FACS plot shows the CD138/B220 staining of the two populations gated as shown in 6B of ctrl and LMP1/CD30 mice, numbers represent the percentages of the populations of one representative example; (D): These histograms show the CD22 and CXCR4 expression as an overlay of the two populations from 6B,  $n=3$ , one representative example is shown.

Next, we examined the responsible signaling pathways for the enlarged PC differentiation in LMP1/CD30 mice. We found significant higher pSTAT3 and pSTAT6 levels in LMP1/CD30 expressing B2 cells after 10 min and 2 h of CD40 stimulation (Figure 7A). Also, the amounts of p65 and IRF4 were significantly increased in the nucleus of the B2 cells of LMP1/CD30 mice after 10 min of CD40 stimulation in comparison to control B cells (Figure 7B+C). The phosphorylation of STAT3 plays a crucial role in PC differentiation by up-regulating BLIMP-1 and IRF4 is a known  $NF\kappa B$  target [Grumont and Gerondakis, 2000, Reljic et al., 2000, Diehl et al., 2008]. To sum this up, CD30 signaling further increases pSTAT3 and pSTAT6 levels as well as the translocation of p65 into the nucleus upon CD40 stimulation. This in turn drives the upregulation of

IRF4 and BLIMP-1.

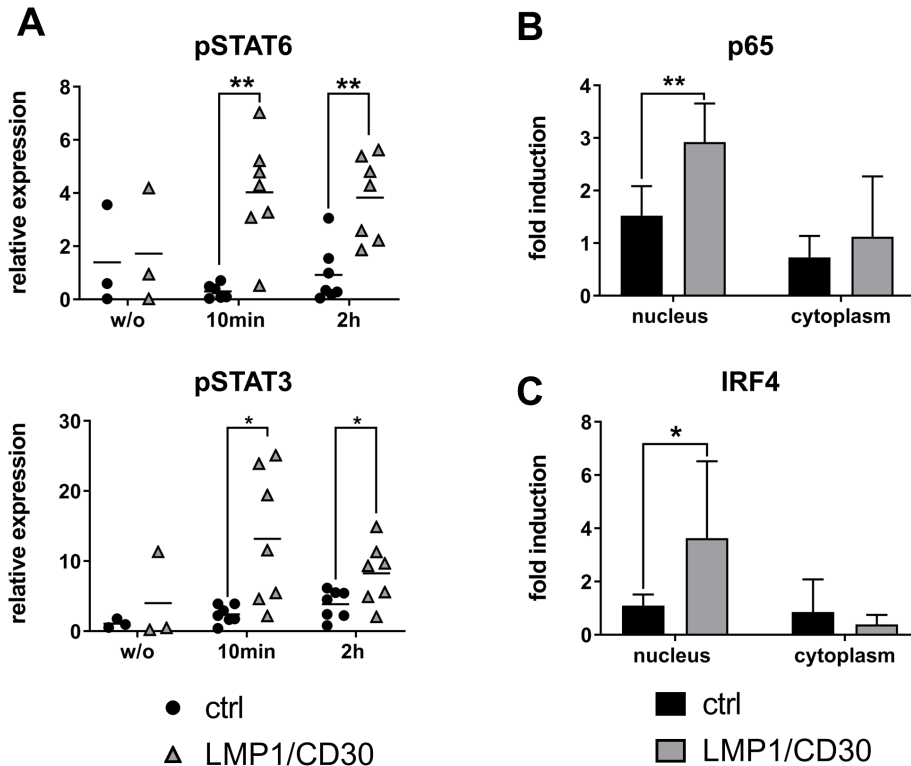


**Figure 7:** B2 cells of ctrl and LMP1/CD30 mice were isolated from splenocytes with the CD43 depletion kit and stimulated with anti-CD40 antibody, (A): Nuclear levels of pSTAT3 and pSTAT6 were determined with WES and normalized to LaminB at the indicated time points; (B+C): Nuclear and cytoplasmic levels of p65 and IRF4 were determined and normalized to  $\alpha\beta$ -Tubulin or LaminB and standardized to their respective value obtained w/o stimulation,  $n \geq 3$ .

During IL4 induced class switch recombination (CSR), pSTAT6 is an essential factor [Linehan et al., 1998]. Therefore, we asked if CD30 signaling might be able to replace CD40 signaling regarding the class switch recombination and proliferation. The encounter with IL4 and anti-CD40 antibody induces class switch recombination of B cells *in vitro* [Cerutti et al., 1998]. For this reason, we sorted FoB (CD21<sup>+</sup>, CD23<sup>+</sup>, CD19<sup>+</sup>) from LMP1/CD30 and control mice and stimulated them with IL-4 alone or in combination with anti-CD40 antibody for 3 and 5 d (Figure 8A). Surprisingly, even with IL-4 alone, around 3% of the LMP1/CD30 expressing FoB switched towards IgG1. The percentage of isotype switched B cells in the control group was below 1% and thus significantly reduced. But compared to the combined stimulation of IL-4/CD40, the number of switched cells was significantly lower in both genotypes (Figure 8B+D). The same was true for the proliferation of the cultivated FoB. The division index of FoB of LMP1/CD30 mice stimulated with IL-4 was significantly higher in comparison to control B cells but still clearly reduced in comparison to the combined stimulation with IL-4/CD40 (Figure 8C).

Also, after stimulation with IL-4 and CD40, the extent of isotype switching and proliferation seemed to be increased in the LMP1/CD30 expressing FoB when compared to control FoB. This means that CD30 signaling alone cannot replace CD40 signaling but might have an additive effect in terms of proliferation and switching. The higher pSTAT6 levels found in the B2 cells of LMP1/CD30 mice were probably responsible for the higher percentage of switched cells. Additionally, the proliferation induced by the combination of constitutive CD30 signaling and IL4 was necessary to enable IgG1 isotype switching [Hasbold et al., 1998]. The higher proliferation might be realized through higher pSTAT3, pSTAT6 and p65 levels upon anti-CD40 antibody encounter.

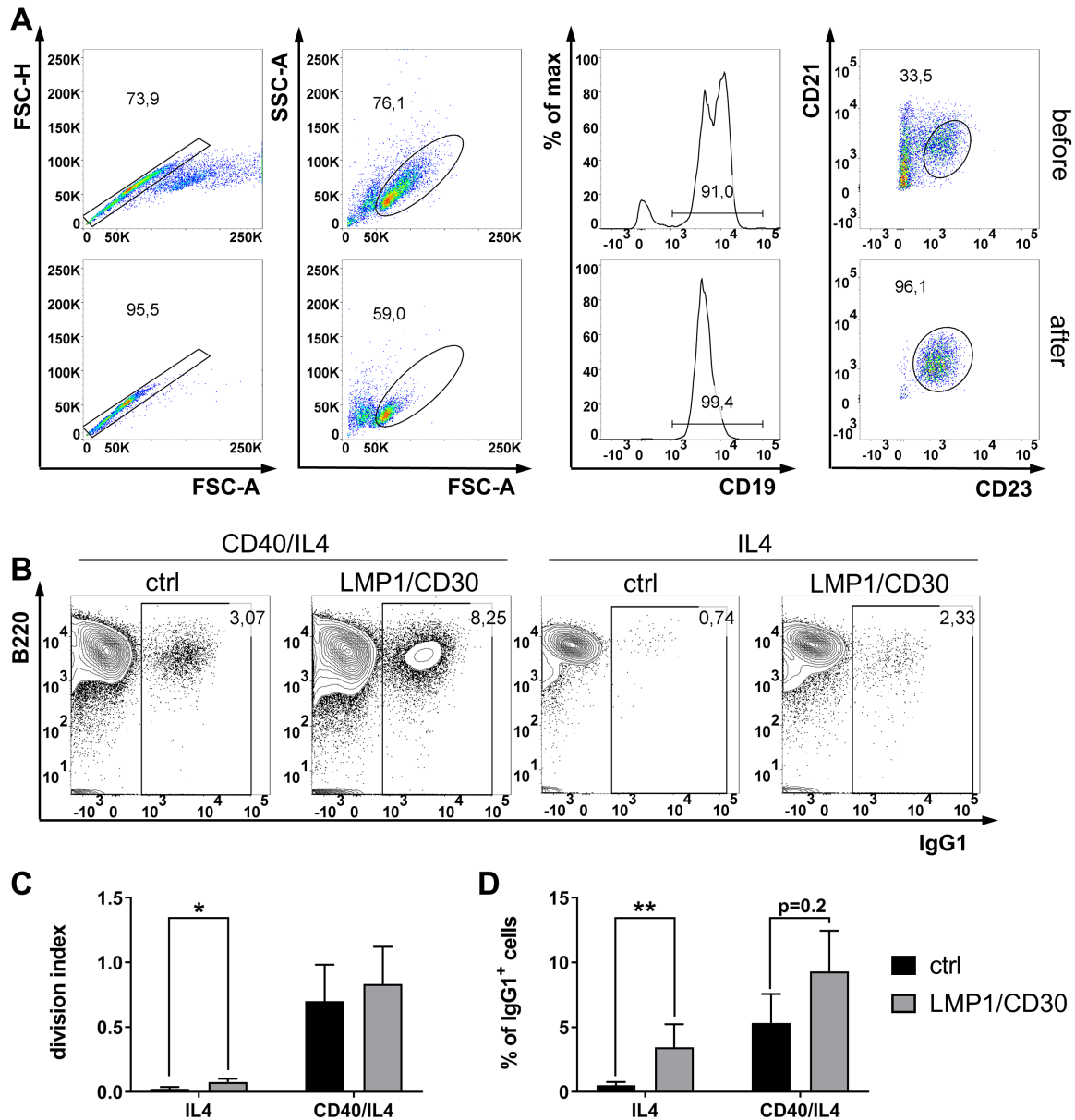


**Figure 8:** (A): Sorting strategy of FoB cells, B cells were isolated with the Pan B cell kit from splenocytes of ctrl and LMP1/CD30 mice and sorted, first doublets were excluded, then the lymphocytes were gated, afterwards CD19<sup>+</sup>, CD23<sup>+</sup>, CD21<sup>mid</sup> were sorted as FoB, after sorting, lymphocytes were gated again and then checked for CD19, CD21, and CD23 expression; (B): Sorted FoB of ctrl and LMP1/CD30 cells were stained with CFSE, cultivated for 5 d in the presence of IL4 alone or in combination with CD40 stimulation, the FACS plots show one representative example of IgG1 switched B cells, the division index (C) and the percentages of IgG1 switched cells (TO-PRO3<sup>-</sup>, B220<sup>+</sup>, IgG1<sup>+</sup>) (D) were determined by FACS and FlowJo. The values are summarized in the graph with mean and SD, n=3.

### 5.2.2 Chronic CD30 signaling drives plasma cell differentiation upon T-cell independent immunization

Given the data of the previous experiments, the question arose if LMP1/CD30 mice respond with a stronger immune response upon antigen administering. Here, we immunized

mice with NP-Ficoll, a TI-2 antigen to which B1 and MZB respond. 14 d post immunization (p.im.), FACS analysis from mice revealed a further expansion of PC and B1a cell population in LMP/CD30 mice in comparison to immunized control mice but also to not immunized LMP/CD30 mice (Figure 9A). Furthermore, the antigen specific IgM and IgG3 secreting PC were significantly increased in the spleen and NP-specific IgM secreting PC in the BM of LMP1/CD30 mice in comparison to the immunized control mice (Figure 9B+C). Also, the serum titers of IgM were significantly higher whereas the IgG3 titers were slightly but not significantly increased in LMP1/CD30 mice (Figure 9D). This leads to the conclusion that immunization with NP-Ficoll results in an increased immune response with further expansion of B1 cells and PC in mice with a chronic CD30 signaling in B cells.

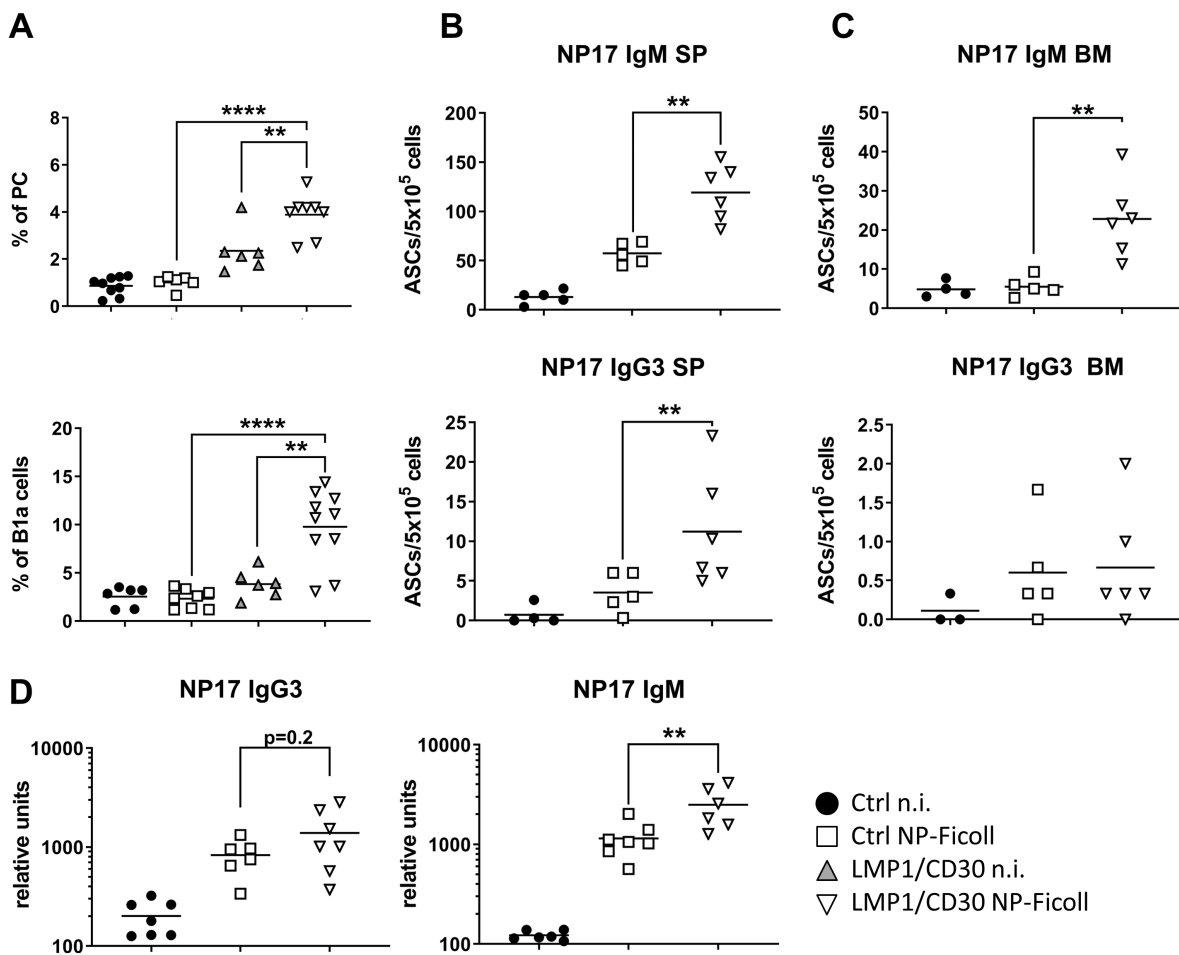


**Figure 9:** Ctrl and LMP1/CD30 mice were immunized with NP-Ficoll and analyzed after 14 d, (A): The graphs show the percentages of PC (Gr1<sup>-</sup>, Thy1.2<sup>-</sup>, Mac1<sup>-</sup>, CD138<sup>+</sup>, B220<sup>lo</sup>) (upper diagram) and B1a cells (CD19<sup>+</sup>, CD5<sup>+</sup>, B220<sup>lo</sup>) (lower diagram) of untouched (n.i.) and immunized mice in the SP; (B+C): The graphs show the number of low affinity IgM and IgG3 secreting PC of immunized mice among splenocytes and bone marrow (BM) cells which were determined by ELISpot; (D): The graphs show the amount of IgM and IgG3 antibodies in the serum. Every dot in the graphs represent the value of one mouse, the mean is represented by the bar.

### 5.2.3 LMP1/CD30 expression drives plasma cell differentiation in germinal center B cells

The induction of a GC reaction by NP-CGG administration led to a block in the GC establishment in LMP1/CD30 mice which was shown by Petra Fiedler [Sperling et al., 2019]. In order to analyze the influence on the GC reaction further, we wanted to study the permanent GC found in the PP. PP are secondary lymphoid tissue in the mucous membrane of the small intestine. Due to steady encounter with antigens through viral and bacterial influx by nutrition and by the microbiome, PP maintain continual GC [Reboldi and Cyster, 2016]. In the PP, we discovered significantly reduced percentages of GC B cells in LMP1/CD30 mice in the PP compared to control mice (Figure 10A). If we predated the B cells of LMP1/CD30 mice for hCD2, the difference between control and LMP1/CD30 mice was even more prominent (Figure 10B). To add on this, the deletion efficiency of the floxed-STOP-cassette in all B cells was at around 96%. In contrast, the deletion efficiency in GC B cells of the spleen amounted to 75% and in the PP around 60% indicating a counter selection of LMP1/CD30 expressing GC B cells (Figure 10C).

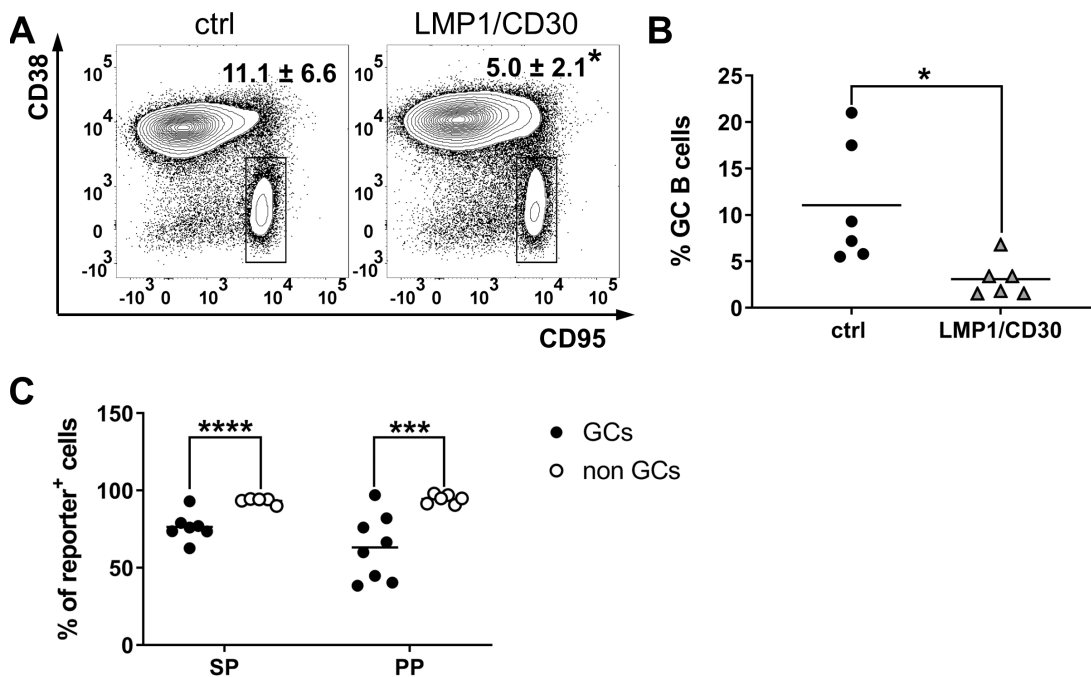


**Figure 10:** (A): The germinal center (GC) B cells (CD19<sup>+</sup>, CD38<sup>lo</sup>, CD95<sup>+</sup>) of the peyers patches (PP) of ctrl and LMP1/CD30 mice were analyzed and shown as a FACS plot; (B): The percentages of GC B cells (CD19<sup>+</sup>, CD38<sup>lo</sup>, CD95<sup>+</sup>, hCD2<sup>+</sup> (LMP1/CD30 only)) of PP of ctrl and LMP1/CD30 mice were analyzed and shown as graph which displays the percentages of all analyzed samples; (C): This graph shows the deletion efficiency of GC and non GC cells of LMP1/CD30 mice analyzed by staining for the reporter hCD2 in the SP and the PP. Every dot represents the value of one mouse, the bar represents the mean of the percentages.

In order to be able to study the role of the CD30 signaling in the GC B cells, we crossed the LMP1/CD30<sup>StopFl</sup> mice with C $\gamma$ 1-cre mice, named LMP1/CD30//C $\gamma$ 1-cre hereafter. In the C $\gamma$ 1-cre strain, a cre-coding sequence is inserted into the C $\gamma$ 1 locus. Cells with a GC cell fate have a sterile transcription of this gene locus which is independent of the expressed isotype upon CSR. This results in the deletion of the STOP-cassette only in GC B cells followed by the LMP1/CD30 expression in these cells [Casola et al., 2006]. As control mice, we used R26/CAG-CAR $\Delta$ 1<sup>StopF</sup> mice crossed with C $\gamma$ 1-cre mice. The GC B cells of these mice express a truncated version of the human coxsackievirus adenovirus receptor (CAR) upon cre mediated recombination [Heger et al., 2015]. These mice are entitled as CAR//C $\gamma$ 1-cre. CAR//C $\gamma$ 1-cre and LMP1/CD30//C $\gamma$ 1-cre mice were immunized with NP-CGG, this resulted in the deletion of the STOP-cassette and in the expression of the transgenes, CAR and LMP1/CD30 or hCD2, respectively. The LMP1/CD30//C $\gamma$ 1-cre mice developed more reporter<sup>+</sup>, CD19<sup>+</sup> cells than control mice after NP-CGG immunization at d 5 and 14 (Figure 11).

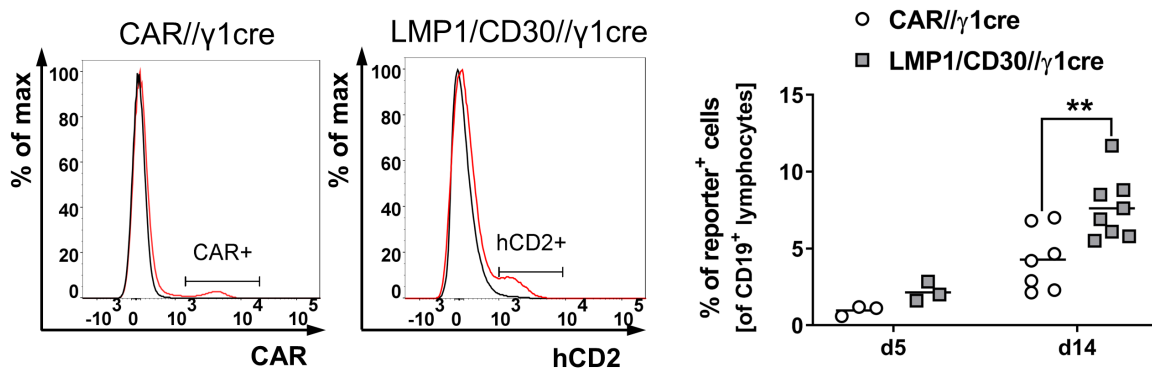


**Figure 11:** The histograms (left panel) show the gating strategy of the reporter expression, the threshold was determined by hCD2 and CAR staining of CAR//C $\gamma$ 1-cre and LMP1/CD30//C $\gamma$ 1-cre mice, respectively. CAR-expression in CAR//C $\gamma$ 1-cre (black line: LMP1/CD30//C $\gamma$ 1-cre; red line CAR//C $\gamma$ 1-cre). hCD2-expression in LMP1/CD30//C $\gamma$ 1-cre mice (black line: CAR//C $\gamma$ 1-cre; red line: LMP1/CD30//C $\gamma$ 1-cre). The diagram (right panel) shows the percentages of reporter<sup>+</sup> cells among the CD19<sup>+</sup> lymphocytes after NP-CGG immunization in the SP of LMP1/CD30//C $\gamma$ 1-cre and CAR//C $\gamma$ 1-cre mice, the bar represents the mean of the percentages.

In contrast to LMP1/CD30 mice, GC of LMP1/CD30//C $\gamma$ 1-cre mice were clearly visible and correctly placed in the follicle upon NP-CGG immunization (Figure 12).

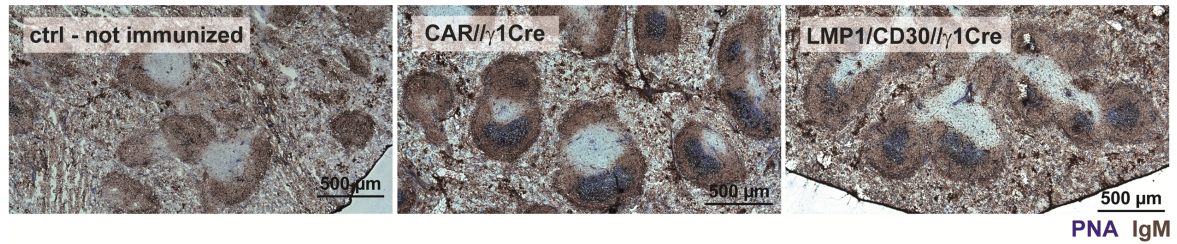


**Figure 12:** The pictures show representative splenic sections of NP-CGG immunized LMP1/CD30//C $\gamma$ 1-cre and CAR//C $\gamma$ 1-cre. The sections were stained for PNA (blue) and IgM (brown) 14 d p.im..

But compared to control mice, the percentages of reporter<sup>+</sup> GC were significantly reduced at d 5 and still slightly reduced 14 d p.im. (Figure 13A). Also, the percentages of the NP<sup>+</sup>, reporter<sup>+</sup> GC were decreased in the LMP1/CD30//C $\gamma$ 1-cre mice in comparison to the CAR//C $\gamma$ 1-cre mice (Figure 13B).

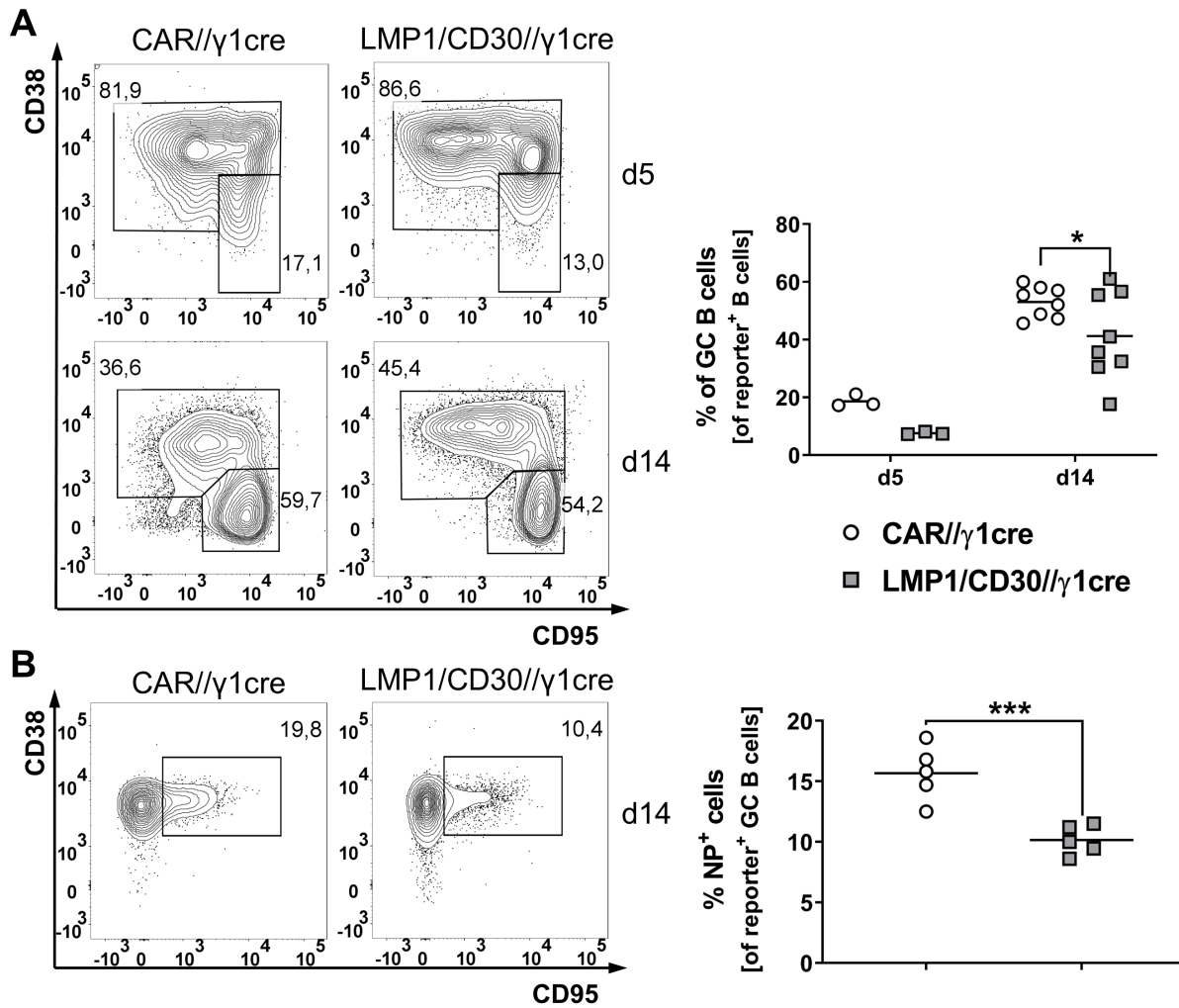


**Figure 13:** LMP1/CD30// $C\gamma$ 1-cre and CAR// $C\gamma$ 1-cre mice were immunized with NP-CGG and analyzed after 5 and 14 d p.i.m.. (A): The FACS plots show the gating strategy of the GC B cells (reporter<sup>+</sup>, CD38<sup>lo</sup>, CD95<sup>+</sup>) (left panel), the graph shows the percentages of splenic GC B cells among all reporter<sup>+</sup> cells (right panel); (B): The FACS plots show the gating strategy (left panel), the graph shows the percentages of NP<sup>+</sup> cells among all reporter<sup>+</sup>, GC cells in the SP (right panel). Every dot in the graphs represent the value of one mouse, the bar represents the mean of the percentages.

However, within the reporter<sup>+</sup> lymphocytes, the percentages of GC B cells and NP<sup>+</sup> cells were comparable between LMP1/CD30// $C\gamma$ 1-cre mice and controls which means that the higher percentages of reporter<sup>+</sup> cells in LMP1/CD30// $C\gamma$ 1-cre were caused by NP<sup>-</sup> non GC B cells (Figure 14).

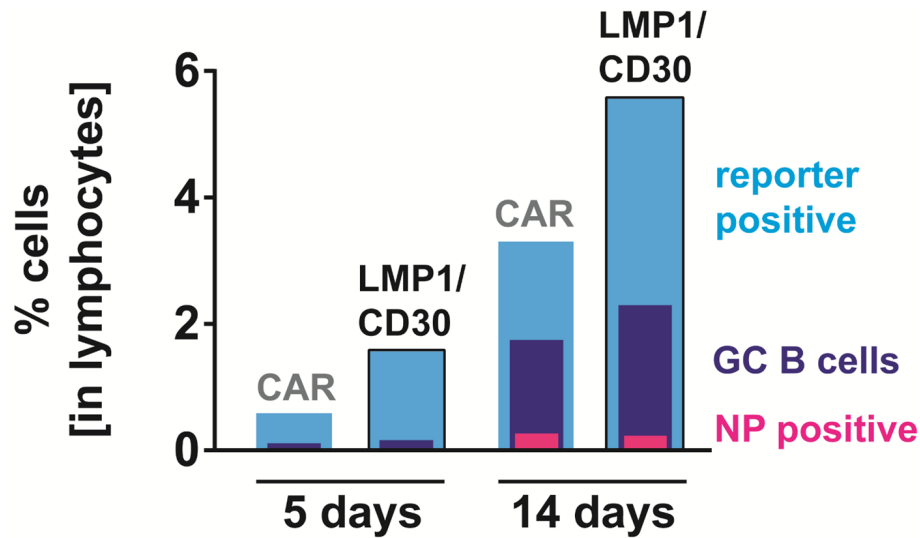


**Figure 14:** The graph shows the percentages of NP<sup>+</sup>, GC B cells and reporter<sup>+</sup> cells among all lymphocytes of LMP1/CD30//C $\gamma$ 1-cre and CAR//C $\gamma$ 1-cre mice 5 and 14 d p.i.m. in the SP.

The induction of the LMP1/CD30 expression only in GC B cells allowed the formation of GC B cells in LMP1/CD30//C $\gamma$ 1-cre mice upon NP-CGG immunization. The percentages of the GC B cells were comparable in both analyzed genotypes. The LMP1/CD30//C $\gamma$ 1-cre mice revealed a higher percentage of reporter<sup>+</sup> cells due to more reporter<sup>+</sup> non GC B cells. The non GC B cells displayed a CD43<sup>+</sup>, CD23<sup>lo</sup> phenotype. The reporter<sup>+</sup> cells of LMP1/CD30 mice revealed higher percentages of CD43<sup>+</sup>, CD23<sup>lo</sup> cells and CD138<sup>+</sup>, B220<sup>lo</sup> cells in comparison to control mice (Figure 15A). All CD138<sup>+</sup>, B220<sup>lo</sup> cells had a CD43<sup>+</sup>, CD23<sup>lo</sup> phenotype and a lower CD19 expression in comparison to CD43<sup>+</sup>, CD23<sup>lo</sup> cells and all reporter<sup>+</sup> B cells (Figure 15B). Still, a certain fraction of the CD43<sup>+</sup>, CD23<sup>lo</sup> population kept CD19 expression, indicating them as deleted B1 cells or PC progenitors (Figure 15B). In summary, the induction of CD30 signaling in the GC B cells led to only slight reduced percentages of reporter<sup>+</sup> GC B cells in comparison to control mice. However, the increased percentage of LMP1/CD30 expressing cells was compiled of CD43<sup>+</sup>, CD23<sup>lo</sup> and PC (CD138<sup>+</sup>, B220<sup>lo</sup>).

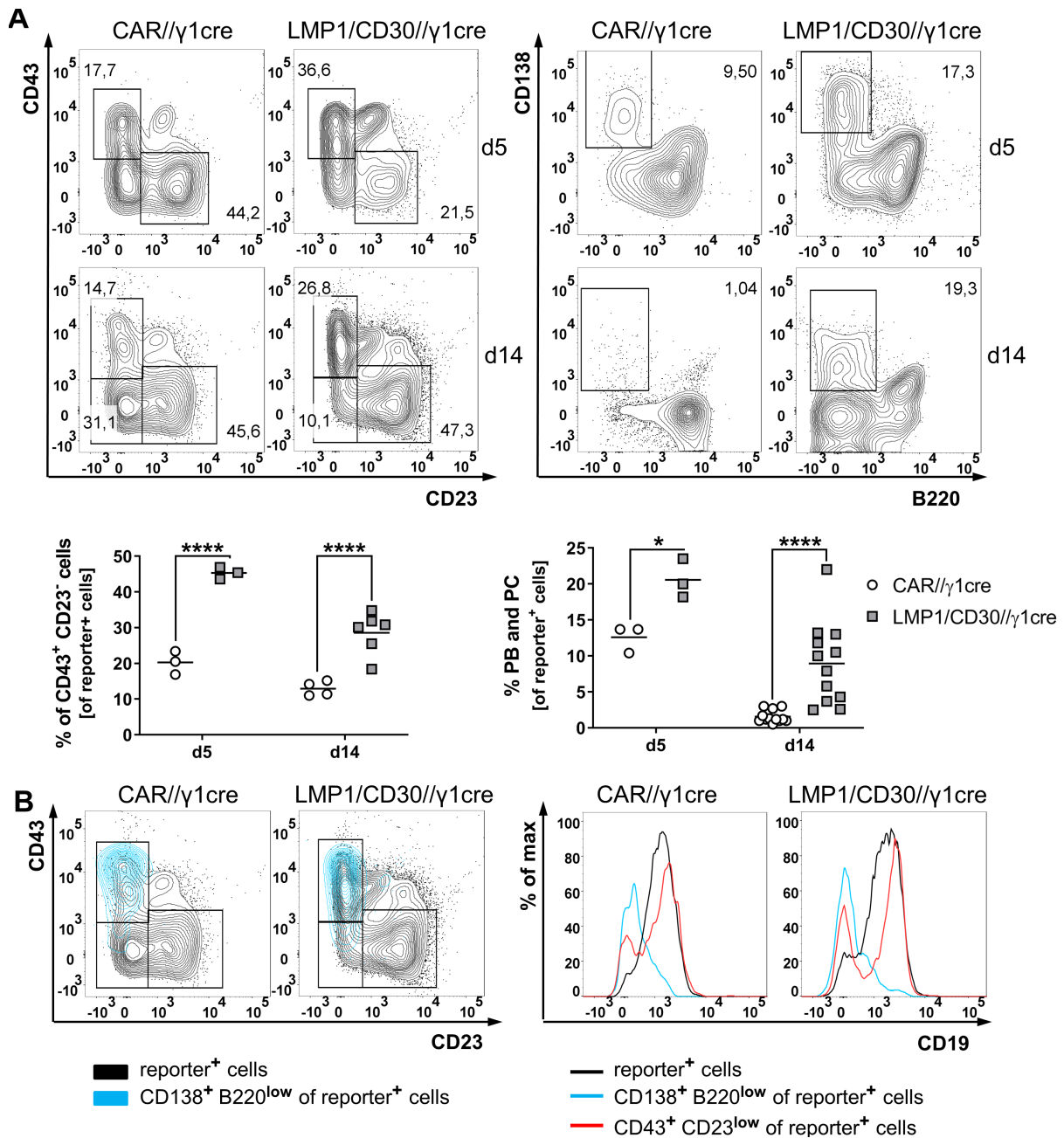


**Figure 15:** LMP1/CD30// $C\gamma 1$ -cre and CAR// $C\gamma 1$ -cre mice were immunized with NP-CGG and analyzed 5 and 14 d p.im. (A): The percentages of CD43<sup>+</sup>, CD23<sup>lo</sup> cells (left panel), and PC/PB (CD138<sup>+</sup>, B220<sup>lo</sup>) (right panel) among the reporter<sup>+</sup> cells were analyzed in the SP, all samples are shown in the graphs below, the FACS plots show the gating strategy, every dot represents the value of one mouse, the bar represents the mean; (B): The FACS plots show an overlay of reporter<sup>+</sup> cells and CD138<sup>+</sup>, B220<sup>lo</sup>, reporter<sup>+</sup> cells of a CD43/CD23 staining from splenocytes (left panel), the histograms show one example of a CD19 staining of the three indicated populations (right panel).

In order to analyze if the higher percentage of PC in the LMP1/CD30// $C\gamma 1$ -cre mice also results in higher percentages of ASCs specific for the given antigen, NP specific ELISA and ELISpots were performed. The immunization of LMP1/CD30// $C\gamma 1$ -cre mice resulted further in higher percentages of NP-specific IgM secreting PC but similar NP-

specific IgG1 secreting PC in comparison to control mice. Serum titers of NP-specific IgM and total IgG1 were enhanced in LMP1/CD30//C $\gamma$ 1-cre mice whereas high affinity NP-specific IgG1 titers were comparable with CAR//C $\gamma$ 1-cre mice. Concluding, LMP1/CD30 expression in GC extends the differentiation towards NP-specific IgM and short lived NP-specific IgG1 secreting PC which may only be detectable through their serum titers at d 14 (Figure 16).

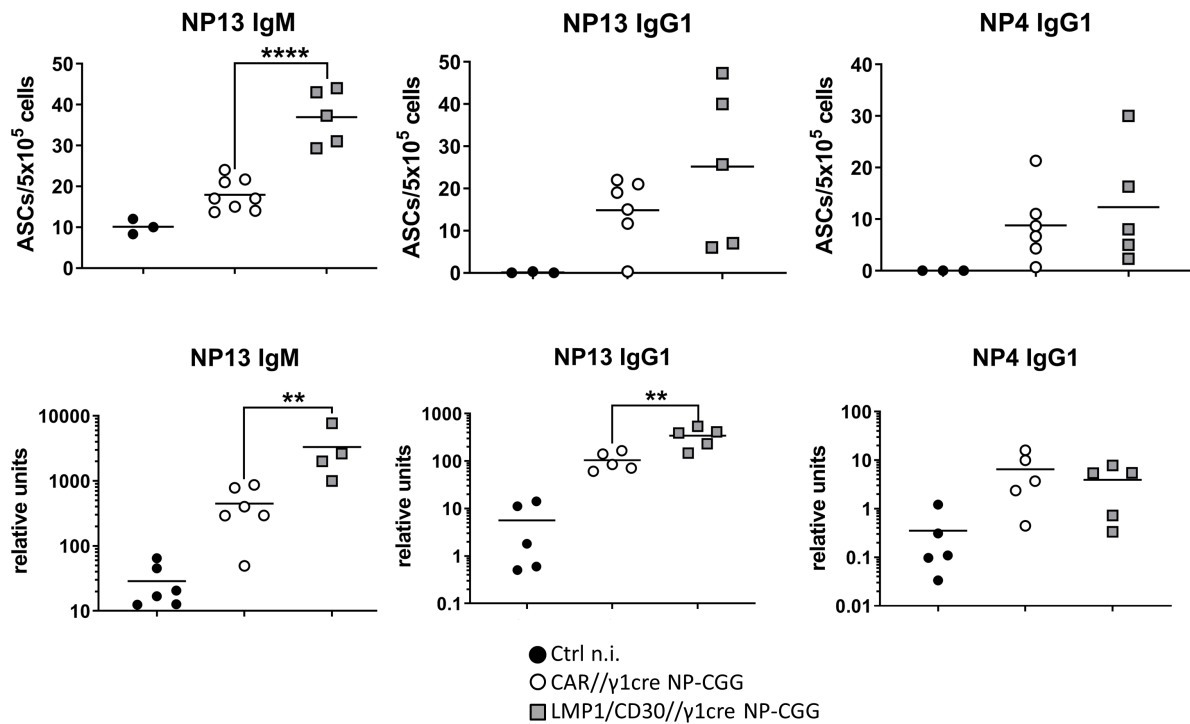


**Figure 16:** The graphs show the amount of total (NP13) IgM, total IgG1, and high affinity (NP4) IgG1 NP-specific antibody secreting splenic cells at d 14 p.i. of LMP1/CD30//C $\gamma$ 1-cre and CAR//C $\gamma$ 1-cre mice. Additionally, the serum titers of NP-specific antibodies are shown in the lower line. Every dot represents the value obtained from one mouse, the bar represents the mean.

Due to the block of GC seen in LMP1/CD30 mice, the question was if the chronic CD30 signaling in the GC influences their organization regarding the percentage of centroblasts and centrocytes. The distribution of both compartments exposed a stronger trend towards centroblasts in the LMP/CD30//C $\gamma$ 1-cre in comparison to control mice (Figure 17A+B) [TARLINTON, 1995].

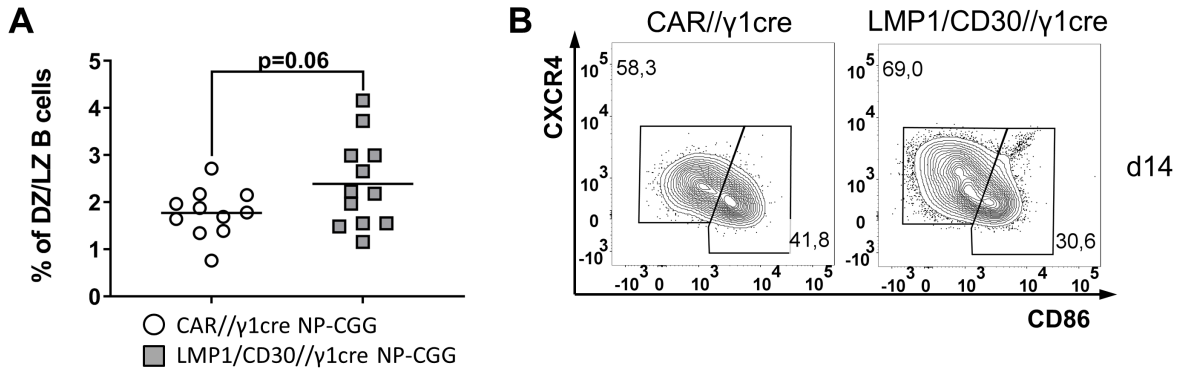


**Figure 17:** (A): The graph shows the distribution of DZ and LZ reporter<sup>+</sup> GC B cells of LMP1/CD30// $C\gamma$ 1-cre and CAR// $C\gamma$ 1-cre mice in the SP, every dot represents the value obtained from one mouse, the mean of the percentages is represented by the bar; the populations were stained and gated for centrocytes (CC) ( $CD86^{lo}$ ,  $CXCR4^{+}$ ) and centroblasts (CB) ( $CD86^{+}$ ,  $CXCR4^{lo}$ ) as indicated in (B).

Due to the strong and fast up-regulation of IRF4 detected *in vitro* after CD40 stimulation in LMP1/CD30 mice, we investigated whether IRF4 is upregulated upon TD immunization in LMP1/CD30 expressing GC B cells, driving the differentiation of PC. Not all LMP1/CD30 expressing cells revealed higher levels of IRF4 but higher percentages of IRF4<sup>+</sup> cells were present in comparison to control mice (Figure 18A). The IRF4<sup>+</sup> cells were mainly localized at the T/B cell border at d 5, hinting their origin either towards early GC [Zhang et al., 2018], or activated pre-GC B cells. The localization at the edge of the GC or follicle at d 14 suggests an exit of the B cells from the GC (Figure 18B). The initiation of PC differentiation seems to be located in the LZ, however, BLIMP-1<sup>+</sup> and IRF4<sup>+</sup> cells are also found in the DZ [Kräutler et al., 2017]. Surprisingly, both the centrocytes and the centroblasts located in the LZ and the DZ, respectively, contained a higher fraction of IRF4<sup>+</sup> cells in LMP1/CD30// $C\gamma$ 1-cre mice in comparison to control mice (Figure 18A). In summary, CD30 signaling seemed to contribute to the up-regulation of IRF4 in B cells of the GC which in turn drives them towards PC. The higher number of PC among the LMP1/CD30 expressing B cells in comparison to control cells supported this hypothesis.

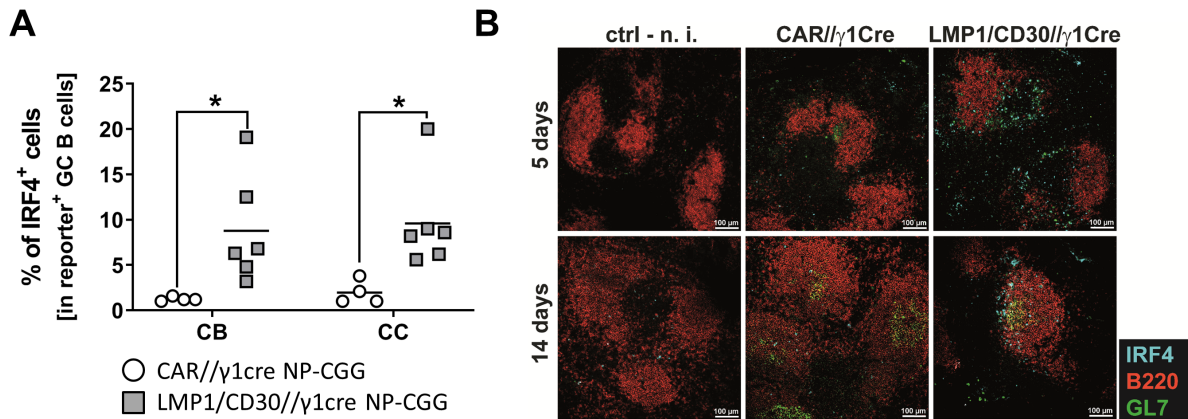


**Figure 18:** (A): The percentages of the IRF4<sup>+</sup> cells of CB and CC of immunized LMP1/CD30// $\gamma$ 1-cre and CAR// $\gamma$ 1-cre mice is shown, every dot represents the value obtained from one mouse, the mean is represented by the bar; (B): Splenic sections of immunized LMP1/CD30// $\gamma$ 1-cre and CAR// $\gamma$ 1-cre mice were stained for IRF4, B220 and GL7 5 and 14 d p.im. The histology was performed together with Markus Lechner in the laboratory from Dr. Zimmer-Strobl.

Besides PC, also memory B cells result from the GC reaction. The B cell population which was positive for IgG1, B220 and CD19 were defined as memory B cells. Therefore, we analyzed the percentages of IgG1<sup>+</sup> B cells in both genotypes. IgG1 is the main isotype of memory B cells. The percentages of IgG1<sup>+</sup> cells were dramatically decreased in the LMP/CD30// $\gamma$ 1-cre mice (Figure 19A+B). Therefore, the increased differentiation towards PC of LMP1/CD30 expressing cells seems to reduce the differentiation towards memory B cells.

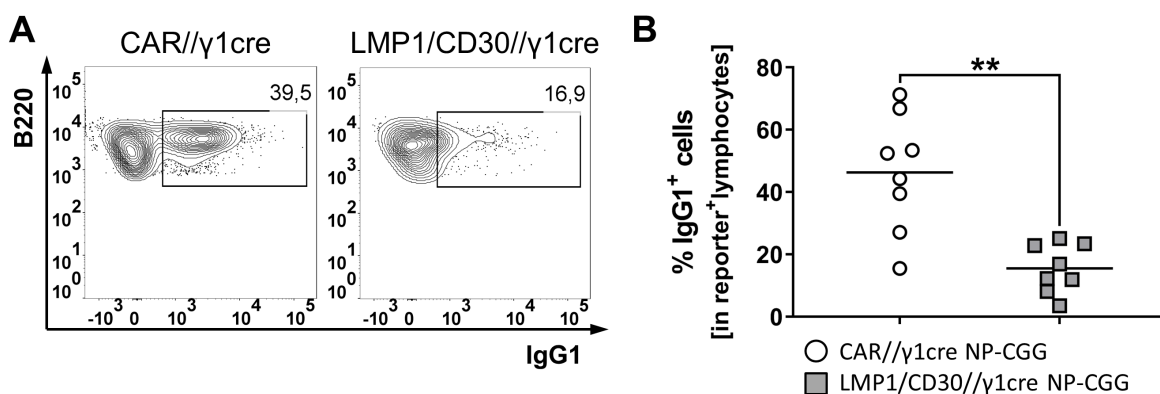


**Figure 19:** (A): The FACS plots illustrate the gating strategy of splenic memory B cells (B220<sup>+</sup>, IgG1<sup>+</sup>) which were pre-gated for reporter<sup>+</sup> and CD19<sup>+</sup> cells; (B): The graph shows the distribution of all analyzed mice regarding their percentages of memory B cells, the mean of the percentages is represented by the bar.

### 5.3 Influence of MHV-68 infection on the development of CD30 positive lymphomas

Petra Fiedler and I could show that around 80% of aged mice developed lymphomas which are reminiscent to DLBCL or FL in histology [Sperling et al., 2019]. This is the first time that we provide evidence for the oncogenic potential of deregulated CD30 signaling in B cells. However, the GC reaction is impaired in these mice. But as described CD30<sup>+</sup> lymphoma derive from germinal or post-GC B cells. Further, HL as well as PEL are associated with EBV and KSHV infection.

This resulted in the questions, whether LMP1/CD30 expression induced in GC B cells leads to lymphoma development and whether an additional  $\gamma$ -herpes-viral infection in combination with the deregulated CD30 signaling generates a further impact during lymphoma development.

To answer these questions, we aged cohorts of LMP1/CD30//C $\gamma$ 1-cre mice after immunization with NP-CGG or infection with MHV-68. Since EBV and KSHV do not infect murine B cells, we instead used the murine  $\gamma$ -herpesvirus MHV-68 in combination with LMP1/CD30//C $\gamma$ 1-cre mice. Further, two cohorts of CAR//C $\gamma$ 1-cre mice, either infected with the MHV-68 or immunized with NP-CGG, served as controls.

#### 5.3.1 Cloning of the reporter virus MHV-68-NGFR

A virus which expresses a detectable reporter enables the tracking of infected cells *ex vivo*. To generate a MHV-68 reporter virus, we introduce the sequence of the human NGFR with a truncated signaling domain into a bacterial artificial chromosome (BAC) containing the complete MHV-68 genome under the control of the SFFV (spleen focus-forming virus) promoter. MHV-68-NGFR was generated by the two-step mutagenesis procedure. Firstly, the sequence for the human truncated NGFR was cloned in a shuttle plasmid between sequences coding for open reading frame (Orf) 27 and Orf29 (Figure 20A). Previously, this locus was used by others and proved to tolerate insertions of foreign sequences [Krug et al., 2007, Collins et al., 2009]. Secondly, the NGFR cassette was inserted by a recombination process into the complete MHV-68 BAC. The parental BAC-derived virus served as control virus. First, the question was if the NGFR infection results in reporter expression in infected cells. Therefore, mouse fibroblast cells (NIH3T3) were infected, stained for NGFR, and analyzed by FACS 3 d p.i.. 44% of NGFR expressing cells could be detected upon infection with the constructed reporter virus (Figure 20B). Thus, the NGFR efficiently marked viral infected murine cells *in vitro*. To study the fitness of the reporter virus, BALB/c mice were infected and splenic cells were analyzed for the number of viral DNA copies per cellular DNA copies. In the spleen and the PerC, the copy numbers were slightly higher after infection with the parental virus in comparison to MHV-68-NGFR virus infected mice (Figure 20C). Further, the number of splenocytes

from which the virus could be reactivated was lower in MHV-68-NGFR infected mice than in mice infected with the parental virus suggesting that the biological activity of the newly generated reporter virus is slightly impaired (Figure 20D). This reduction is often observed after insertion of transgenes into the viral genome. The staining for NGFR revealed 1.6% of NGFR<sup>+</sup> cells among the B cell population in mice infected with MHV-68-NGFR (Figure 20E). This was in line with the infection rate found upon infection with MHV-68 of mice [Barton et al., 2011]. Summing up, MHV-68-NGFR was able to efficiently infect cells *in vitro* and *in vivo*. Further, NGFR<sup>+</sup> cells could be detected upon infection with MHV-68-NGFR. The reached percentages of positive cells were similar to values as published before [Barton et al., 2011].

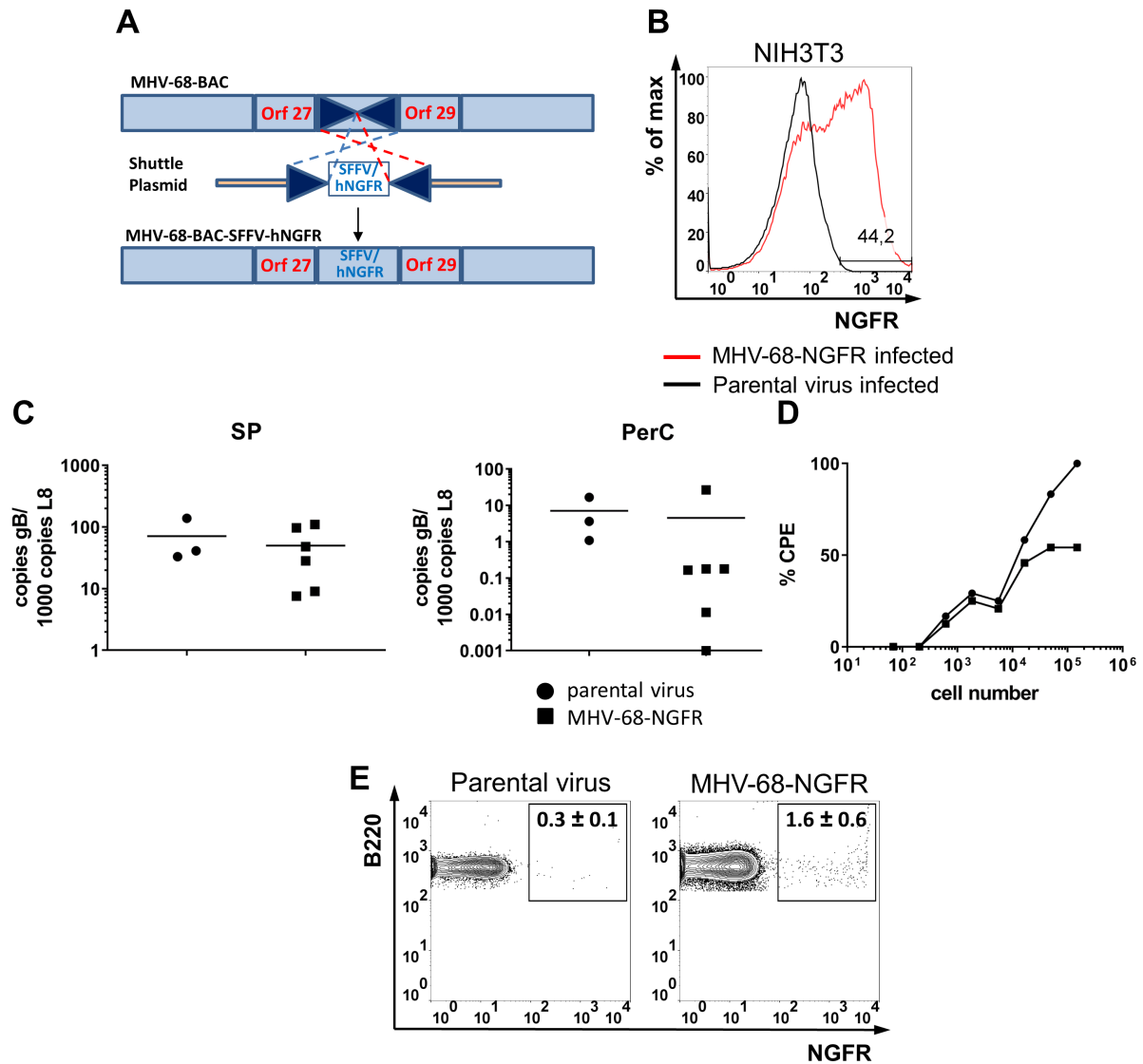


**Figure 20:** Cloning strategy of the MHV-68-NGFR (A): A SFFV-hNGFR cassette was inserted by shuttle mutagenesis in the MHV-68 genome between open reading frame (Orf)27 and 29; (B): FACS histogram of NGFR expression, NIH3T3 were infected with either the MHV-68-NGFR or the parental virus. After 3 d p.i. cells were stained with an anti-hNGFR antibody. The experiment was performed in two independent experiments; (C): Genomic load determined from cells isolated from the SP and PerC; quantitative PCR of the viral gene (gB) and the cellular gene (L8) was performed with DNA of cells isolated from mice infected either with the parental or the MHV-68-NGFR virus. The analysis was performed at d 14 p.i.; (D): The graph shows the results of the reactivation assay comparing parental virus and MHV-68-NGFR infected mice, single splenocyte suspensions were prepared and analyzed in the *ex vivo* reactivation assay for the cytopathic effect (CPE) in every well, splenocytes from three mice were pooled per group, CPE was identified by identification of rounded detached fibroblasts causing a disrupted fibroblast monolayer in the well; (E): NGFR<sup>+</sup> cells which were pregated for B220<sup>+</sup> cells are displayed in a FACS plot. Shown are B cells from BALB/c mice infected with either parental virus or MHV-68-NGFR and analyzed 14 d p.i., n=3, numbers represent the mean and the SD of the percentages.

### 5.3.2 Viral infection of the LMP1/CD30//C $\gamma$ 1-cre mice results in the deletion of the STOP-cassette

As already shown in chapter 3.2, the immunization of LMP1/CD30//C $\gamma$ 1-cre mice with NP-CGG induced the deletion of the STOP-cassette and the generation of LMP1/CD30 expressing GC B cells. The following part focuses on the influence of the herpesviral infection during the GC reaction in combination with the chronic CD30 signaling in these B cells. In order to address this issue, two sets of LMP1/CD30//C $\gamma$ 1-cre mice and CAR//C $\gamma$ 1-cre mice were either immunized with NP-CGG or infected with MHV-68-NGFR and analyzed after 14 d. To test if the infection with the MHV-68-NGFR virus induces the deletion of the STOP-cassette. B cells of LMP1/CD30//C $\gamma$ 1-cre mice and CAR//C $\gamma$ 1-cre mice were stained for hCD2 and CAR, respectively (Figure 21A). Both immunization with NP-CGG and the viral infection led in both analyzed genotypes to the deletion of the STOP-cassette in the spleen and the PerC resulting in the expression of the reporter genes (Figure 21B+C). The percentage of reporter<sup>+</sup> cells was comparable in immunized and infected mice but higher in the LMP1/CD30//C $\gamma$ 1-cre than in the control mice in the spleen (Figure 21B). In the PerC, the percentage of reporter expressing cells was significantly higher in the MHV-68-NGFR infected LMP1/CD30//C $\gamma$ 1-cre mice compared to the immunized mice and their respective control mice (Figure 21C). Therefore, the infection with the MHV-68-NGFR virus resulted in the deletion of the STOP-cassette in LMP1/CD30//C $\gamma$ 1-cre and control mice with the highest reporter expression in the LMP1/CD30//C $\gamma$ 1-cre mice in comparison to the other groups.

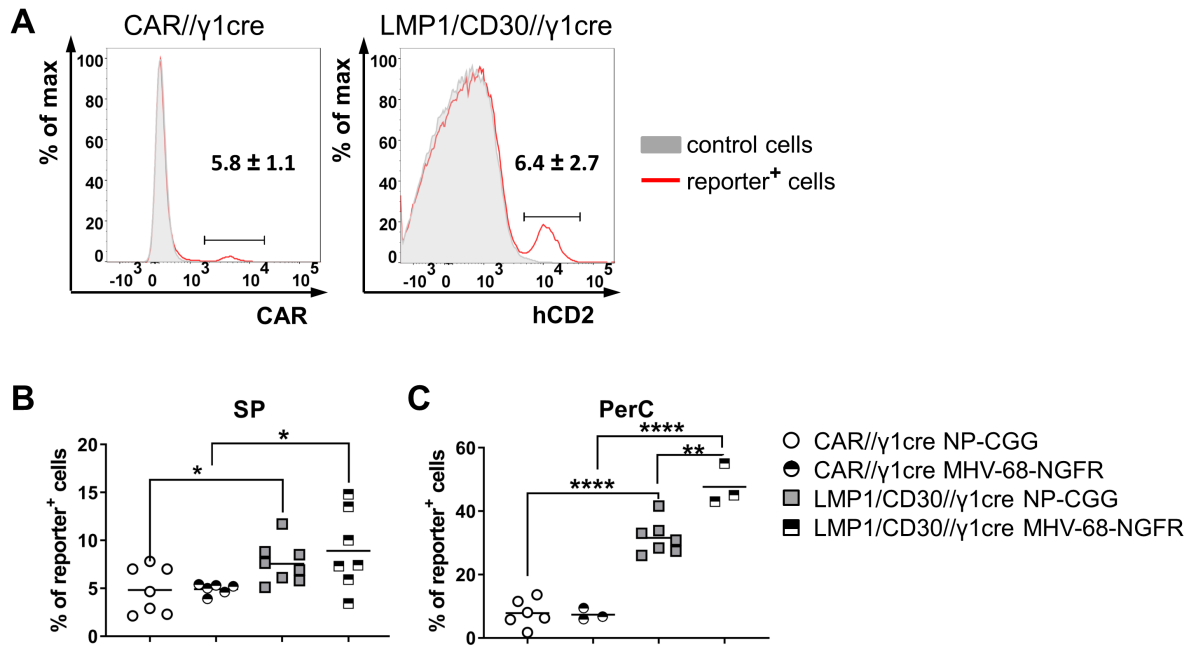


**Figure 21:** LMP1/CD30// $C\gamma$ 1-cre and CAR// $C\gamma$ 1-cre mice were either immunized with NP-CGG or infected with the MHV-68-NGFR virus and analyzed after 14 d. (A): The histograms show the gating strategy of the reporter expression, the threshold was determined by hCD2 and CAR staining of CAR// $C\gamma$ 1-cre and LMP1/CD30// $C\gamma$ 1-cre mice, respectively. CAR-expression in CAR// $C\gamma$ 1-cre (grey histogram: LMP1/CD30// $C\gamma$ 1-cre; red line: CAR// $C\gamma$ 1-cre). hCD2-expression in LMP1/CD30// $C\gamma$ 1-cre mice (grey histogram: CAR// $C\gamma$ 1-cre; red line: LMP1/CD30// $C\gamma$ 1-cre); (B+C): The diagrams show the percentages of all reporter<sup>+</sup> cells among the B cell population in the SP and the PerC. Every dot represents the value obtained from one mouse, the bar represents the mean of the percentages.

The splenic weight of the immunized LMP1/CD30// $C\gamma$ 1-cre and the CAR// $C\gamma$ 1-cre mice was similar at d 14 p.im. but was higher than in unimmunized mice (Figure 22A). The infected mice revealed a further expansion of the splenic weight in comparison to the immunized mice due to higher B and T cell numbers (Figure 22B+C). Additionally, larger numbers of B and T cells were visible in the PerC of infected mice in comparison to the immunized mice (Figure 22D+E). However, both after immunization and infection, B and T cell numbers were comparable between LMP1/CD30// $C\gamma$ 1-cre and the CAR// $C\gamma$ 1-cre mice in spleen and PerC.

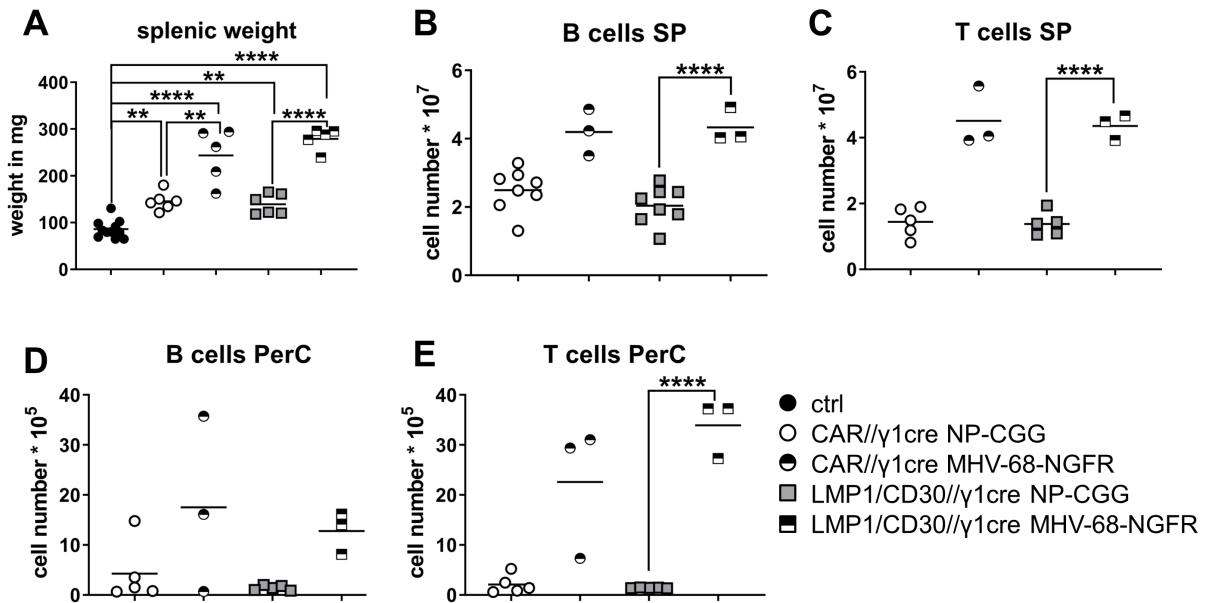


**Figure 22:** LMP1/CD30// $C\gamma$ 1-cre and CAR// $C\gamma$ 1-cre mice were infected with either MHV-68-NGFR or immunized with NP-CGG and analyzed after 14 d, (A): The diagram shows the splenic weight of the indicated mouse groups; (B+D): The graphs display the B cell numbers (CD19<sup>+</sup>) in the SP and the PerC; (C+E): In this graph, T cell numbers (Thy1.2<sup>+</sup>) in the SP and the PerC are indicated. Every dot represents the value obtained from one mouse, the bar represents the mean of the cell numbers.

NGFR<sup>+</sup> cells could be detected within the reporter<sup>+</sup> and reporter<sup>-</sup> B cells indicating that the virus infection does not necessarily induce the deletion of the STOP-cassette both in the LMP1/CD30// $C\gamma$ 1-cre and in the CAR// $C\gamma$ 1-cre mice. The percentages of NGFR<sup>+</sup> were higher in the reporter<sup>+</sup> compartment of the spleen and the PerC (Figure 23A+C). However, calculating the total numbers of NGFR<sup>+</sup> cells revealed a higher number within the reporter<sup>-</sup> B cells in both genotypes due to the higher total numbers of reporter<sup>-</sup> B cells in the spleen (Figure 23B). In the PerC, the total cell numbers were comparable in all subsets besides the outlier of the LMP1/CD30// $C\gamma$ 1-cre mice (Figure 23D).

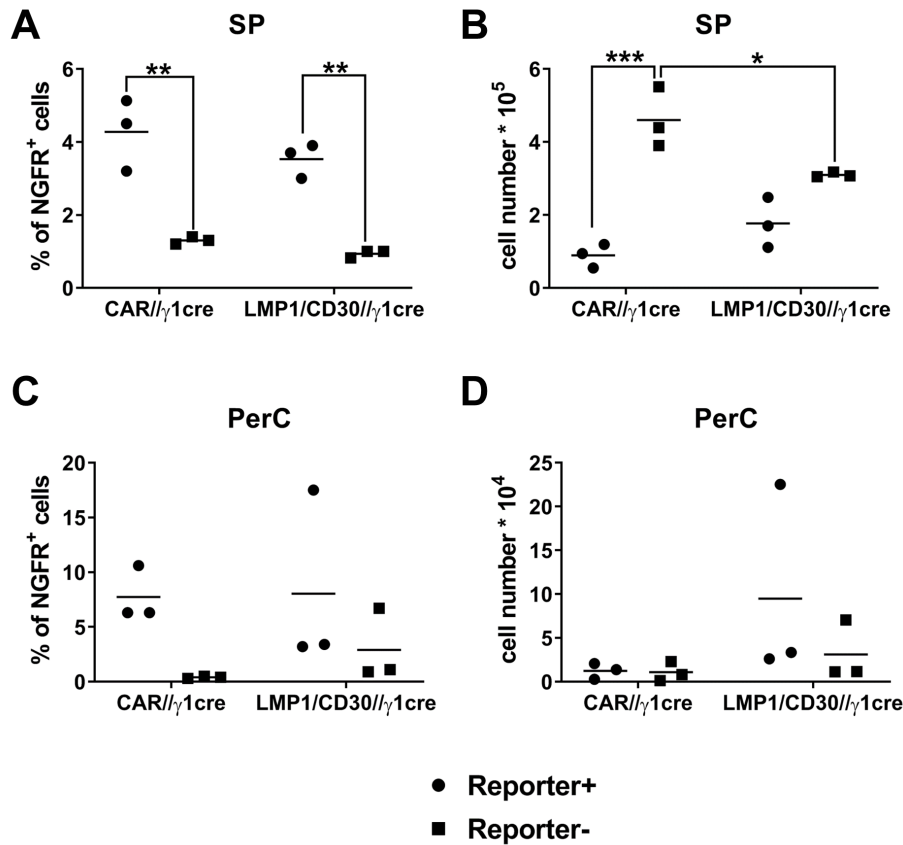


**Figure 23:** LMP1/CD30//C $\gamma$ 1-cre and CAR//C $\gamma$ 1-cre mice were infected with MHV-68-NGFR. After 14 d, NGFR<sup>+</sup> cells were detected by FACS after staining of B cells from the SP and the PerC in the reporter<sup>+</sup> (CAR or hCD2) and the reporter<sup>-</sup> B cells (CD19<sup>+</sup>), (A+B): The diagrams show the percentages and the cell numbers of NGFR<sup>+</sup> cells in the spleen in both genotypes; (C+D): The graphs show the percentages and the cell numbers of the NGFR<sup>+</sup> B cells in the PerC. Every dot represents one mouse, the bar is the mean of the percentages or the cell numbers.

### 5.3.3 Virus infection leads to a germinal center reaction in LMP1/CD30//C $\gamma$ 1-cre mice

Next, I tested if the MHV-68-NGFR infection can generate a GC reaction in LMP1/CD30//C $\gamma$ 1-cre mice. The GC were comparably formed in LMP1/CD30//C $\gamma$ 1-cre and control mice (Figure 24A). However, the percentages of GC B cells were significantly higher in the mice infected with MHV-68-NGFR virus in comparison to the immunized mice (Figure 24A). In accord, total GC B cell numbers were significantly higher in the infected LMP1/CD30//C $\gamma$ 1-cre and CAR//C $\gamma$ 1-cre mice in comparison to the immunized mice (black bars Figure 24B). However, less deleted cells were found within the GC B cell population of infected mice in comparison to immunized mice. Thus, only a small portion of GC B cells expressed the reporter in both genotypes of the infected mouse groups (grey bars Figure 24B). In contrast to the immunized mice, most of the reporter expressing cells of the MHV-68-NGFR infected mice displayed a non GC phenotype (CD38<sup>+</sup>,

CD95<sup>lo</sup>) (Figure 24C+D).

To sum this up, the infection with MHV-68-NGFR induced a GC reaction in LMP1/CD30//C $\gamma$ 1-cre and control mice. The total percentages of GC B cells were higher in infected than in immunized mice, but, the virus infection revealed a reduced deletion efficiency of the STOP-cassette in the GC B cells. The total numbers of reporter expressing GC B cells were comparable after immunization and infection. In comparison to immunized mice, more reporter<sup>+</sup> displayed a non-GC B cell phenotype after infection.

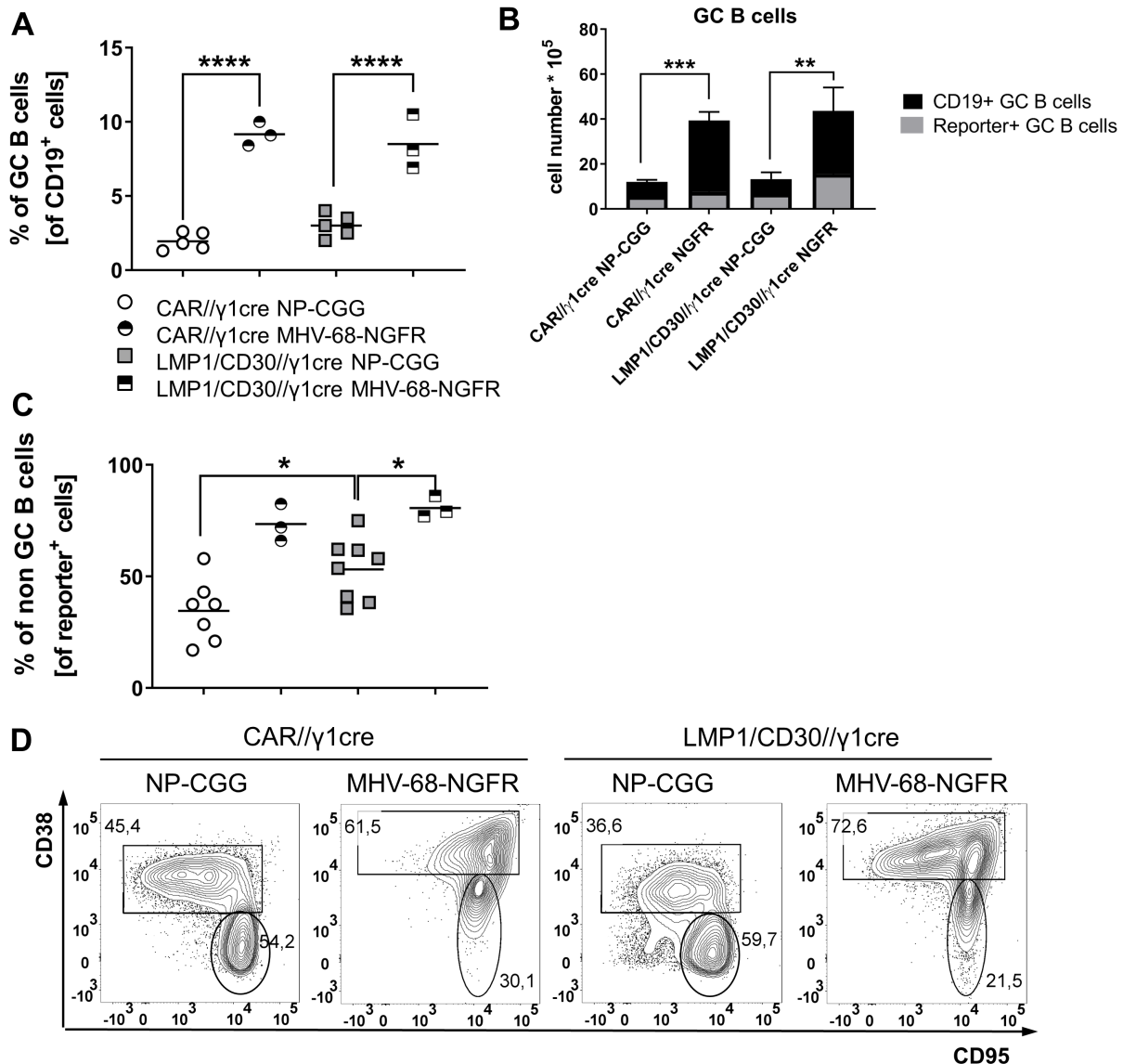


**Figure 24:** (A): The diagram displays the percentages of GC B cells (PNA<sup>+</sup>, CD95<sup>+</sup>) pregated for CD19<sup>+</sup> cells; (B): The diagram shows the cell numbers of splenic GC B cells (PNA<sup>+</sup>, CD95<sup>+</sup>) gated for CD19 (black bars) and of reporter<sup>+</sup> cells within the GC B cells (grey bars),  $n \geq 3$ . Every dot represents the value obtained from one mouse, the bar is the mean of the percentages; (C): The diagram shows the percentages of the reporter<sup>+</sup>, non GC B cells (CD38<sup>+</sup>) of the analyzed mouse groups; (D): The FACS plots show the GC staining of reporter<sup>+</sup> B cells of the indicated genotypes.

### 5.3.4 The virus infection further drives the expansion of LMP1/CD30 expressing B1 and plasma cells

In order to characterize the phenotype of the reporter expressing non GC cells, further staining for B1 cells and PC were performed. PC as well as CD43<sup>+</sup>, CD23<sup>lo</sup> B cells were significantly enriched in LMP1/CD30//Cγ1-cre mice in comparison to CAR//Cγ1-cre mice both after immunization and infection (Figure 25A+B). MHV-68-NGFR infection resulted in a further increase of LMP1/CD30 expressing PC and B1 cells/PB. A similar trend was visible in the PerC of these mice (Figure 25C). Therefore, the viral infection seemed to have an additional effect on the expansion of PC and B1 cells in LMP1/CD30//Cγ1-cre mice.

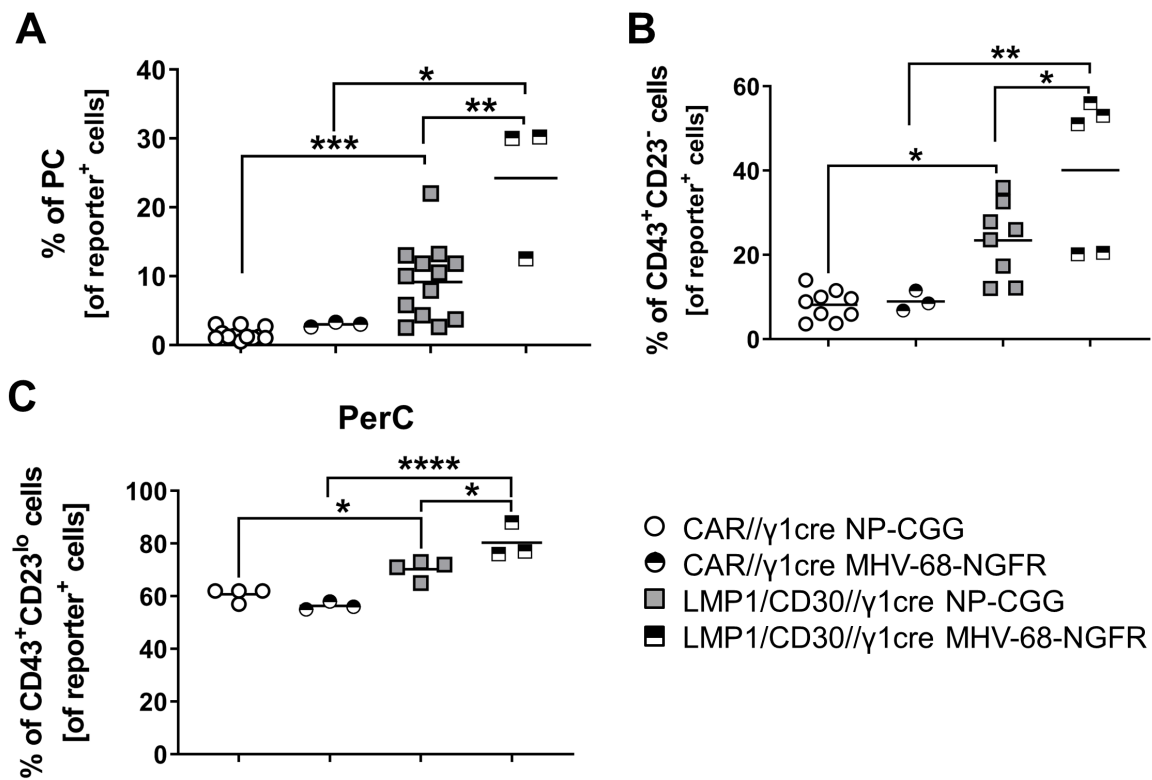


**Figure 25:** (A): Reporter<sup>+</sup> splenocytes were stained with CD138 and B220, the percentages of PC (CD138<sup>+</sup>, B220<sup>lo</sup>) is depicted; (B): Reporter<sup>+</sup>, CD19<sup>+</sup> cells of the spleen were stained with CD43 and CD23, the percentages of reporter<sup>+</sup> B1 cells/PB (CD43<sup>+</sup>, CD23<sup>lo</sup>) is depicted; (C): The diagram shows the percentages of CD43<sup>+</sup>, CD23<sup>lo</sup> pregated for reporter<sup>+</sup>, CD19<sup>+</sup> cells in the PerC. Every dot represents the value obtained from one mouse, the bar represents the mean of the percentages.

### 5.3.5 NGFR positive B cells are found in different sub-populations

During the acute phase of virus infection, B cells of different sub-populations are infected with MHV-68 [Barton et al., 2011]. In order to analyze the phenotype of NGFR<sup>+</sup> B cells, FACS analysis was used. Virus infected B cells were found among all reporter<sup>+</sup> mature B cell populations (Figure 26A). In both the LMP1/CD30//C $\gamma$ 1-cre mice and control mice, the highest percentages of NGFR<sup>+</sup> cells were found in the PC-precursor (CD138<sup>+</sup>, B220<sup>+</sup>). But the percentage was significantly reduced in the LMP1/CD30//C $\gamma$ 1-cre mice compared to the controls. In contrast, NGFR<sup>+</sup> cells were nearly absent in PC in both genotypes. B1 cells of the LMP1/CD30//C $\gamma$ 1-cre mice contained significantly more NGFR<sup>+</sup> cells compared to the cells of the control mice as well as to the other sub-populations. NGFR<sup>+</sup> cells were also detected in the reporter<sup>+</sup> GC B cells. 2 to 3% NGFR<sup>+</sup> cells were identified in the reporter<sup>+</sup> GC B cell population (Figure 26B).

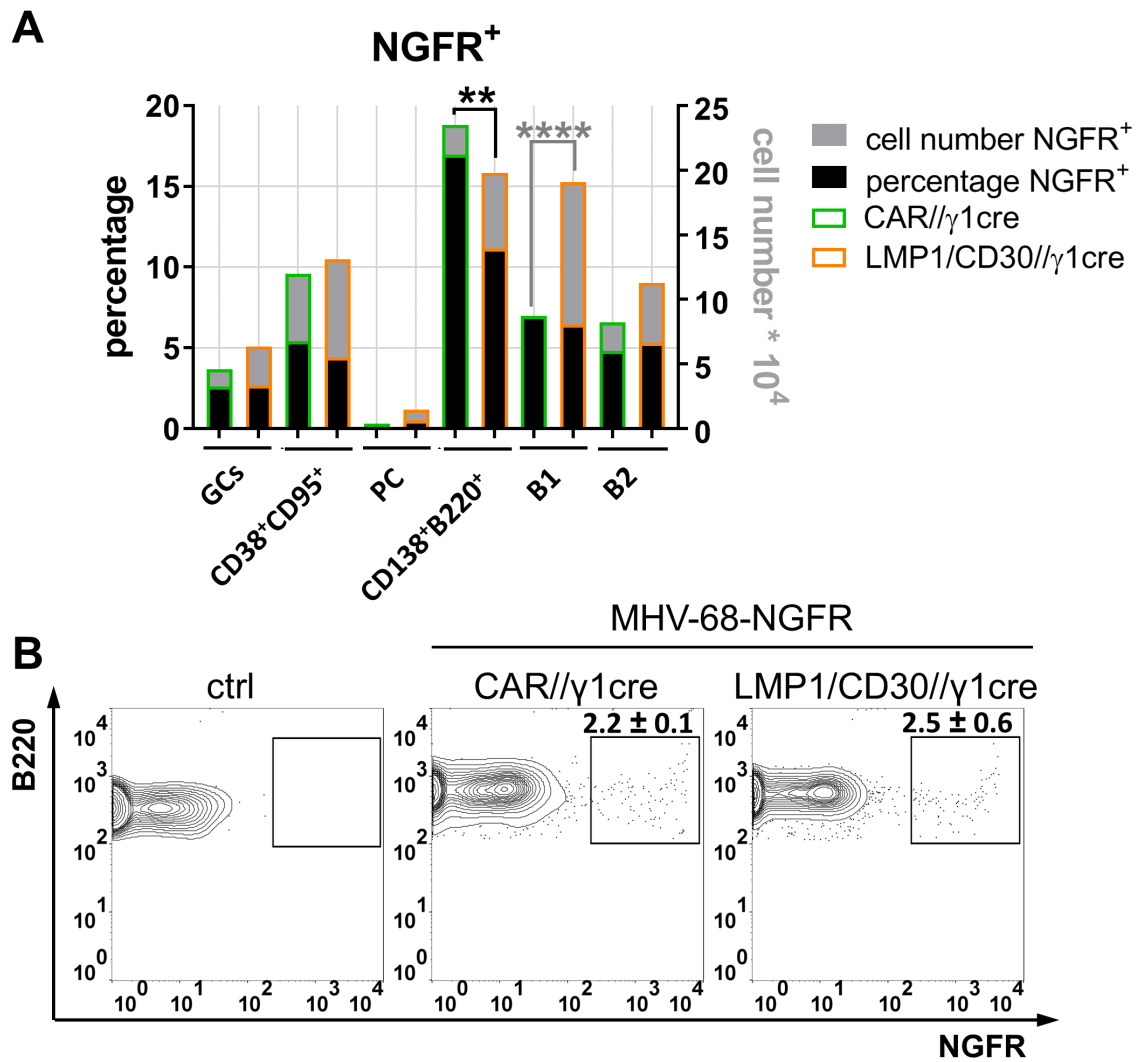


**Figure 26:** (A): The splenic sub-populations from infected LMP1/CD30//C $\gamma$ 1-cre and CAR//C $\gamma$ 1-cre mice indicated in the diagram were analyzed for their cell numbers (grey bars) and the percentages (black bars) of NGFR<sup>+</sup> cells after pre-gating for reporter<sup>+</sup> cells, n=3; (B): The FACS plots show one example of NGFR expression of GC B cells. At d 14 p.i., splenic GC B cells (CD19<sup>+</sup>, reporter<sup>+</sup>, CD95<sup>+</sup>, PNA<sup>+</sup>) of infected LMP1/CD30//C $\gamma$ 1 and CAR//C $\gamma$ 1 mice were stained with anti-hNGFR, n=3.

In summary, the infection with MHV-68-NGFR led to the deletion of the STOP-cassette followed by LMP1/CD30 expressing GC B cells in infected mice. This resulted in similar cell numbers of reporter expressing GC B cells as detected upon immunization. Some of the GC B cells carried the virus, making this mouse model suitable to study the pathogenesis of deregulated CD30 signaling and  $\gamma$ -herpesvirus infection initiated in GC B cells. Additionally, a high percentage of MHV-68-NGFR infected cells could be detected in the PC progenitors (CD138<sup>+</sup>, B220<sup>+</sup>) and in the CD43<sup>+</sup>, CD23<sup>lo</sup> population, whereas the virus was nearly absent in PC.

### 5.3.6 Ongoing virus infection in LMP1/CD30//C $\gamma$ 1-cre mice leads to the expansion of B1a and B1b cell populations

To analyze the long term effect of the virus infection and immunization in LMP1/CD30//C $\gamma$ 1-cre and control mice, we studied the mice after 2 months. Both, after immunization and infection, the splenic weight, B and T cell numbers were higher in LMP1/CD30//C $\gamma$ 1-cre mice mouse groups compared to their respective control mice indicating that LMP1/CD30 expression resulted in the expansion of B cells over time (Figure 27A-C).

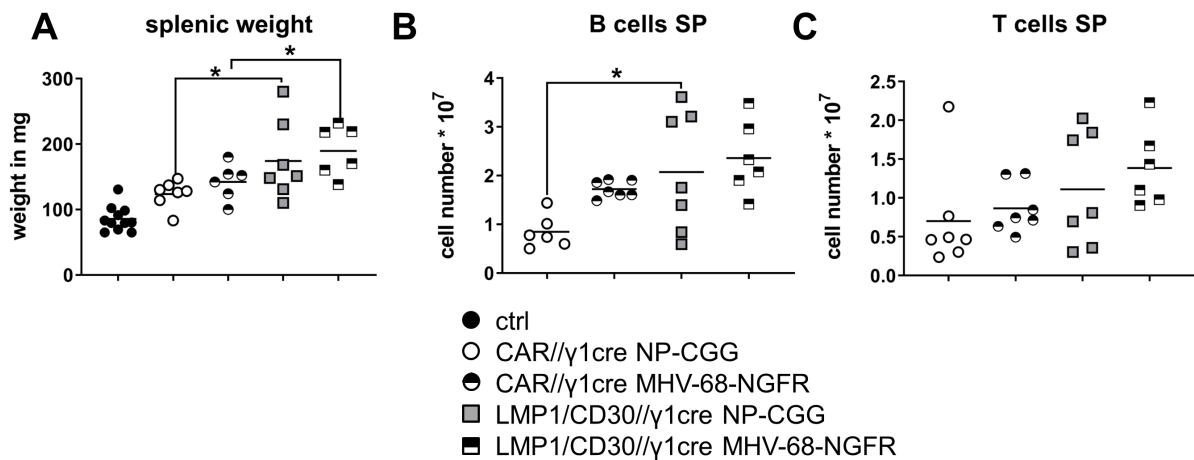


**Figure 27:** LMP1/CD30//C $\gamma$ 1-cre and CAR//C $\gamma$ 1-cre mice were immunized with NP-CGG or infected with the MHV-68-NGFR virus i.p.. After 2 months, the mice were sacrificed and analyzed; (A): This diagram shows the splenic weight of the analyzed mice. The data was obtained in three independent experiments; (B+C): The graphs show the cell numbers of CD19<sup>+</sup> B cells or Thy1.2<sup>+</sup> T cells in the indicated groups in the SP. Every dot represents the value obtained from one mouse, the bar represents the mean of the cell numbers.

In the PerC, the B cell and T cell numbers of the LMP1/CD30//C $\gamma$ 1-cre mice infected with MHV-68-NGFR were higher than in control mice and immunized LMP1/CD30//C $\gamma$ 1-cre mice (Figure 28A+B) suggesting that the virus infection in the LMP1/CD30//C $\gamma$ 1-cre mice led to a further T and B cell expansion in the PerC.

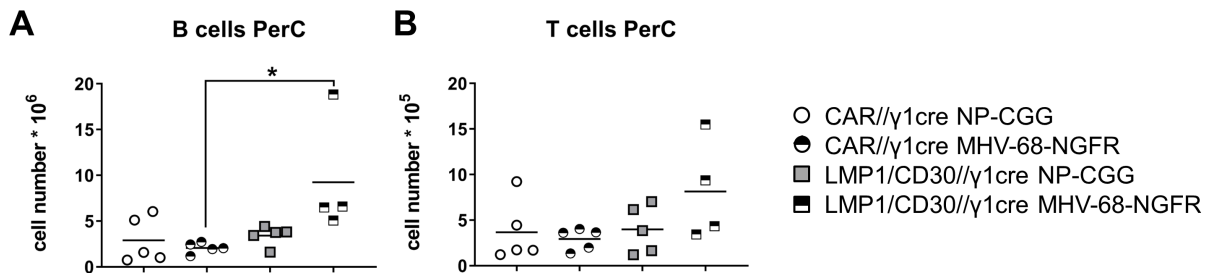


**Figure 28:** (A): This diagram shows the cell numbers of CD19<sup>+</sup> B cells in the PerC of the indicated groups. The cells were isolated by flushing the abdominal cavity; (B): This diagram shows the cell numbers of Thy1.2<sup>+</sup> T cells in the PerC of the indicated groups. Every dot represents the value obtained from one mouse, the bar represents the mean of the cell numbers.

In the spleen and in the PerC, the percentages and the cell numbers of reporter<sup>+</sup> B cells were much higher in the LMP1/CD30//Cγ1-cre mice in comparison to their respective control mice (Figure 29). Strikingly, the percentages of LMP1/CD30 expressing B cells reached 50-80% in the PerC (Figure 29C). Therefore, the reporter<sup>+</sup> cells expanded in the LMP1/CD30//Cγ1-cre mice stronger than in control mice. The MHV-68-NGFR infection seemed to have an additional effect on the increase of LMP1/CD30 expressing B cells in the PerC upon 2 months.

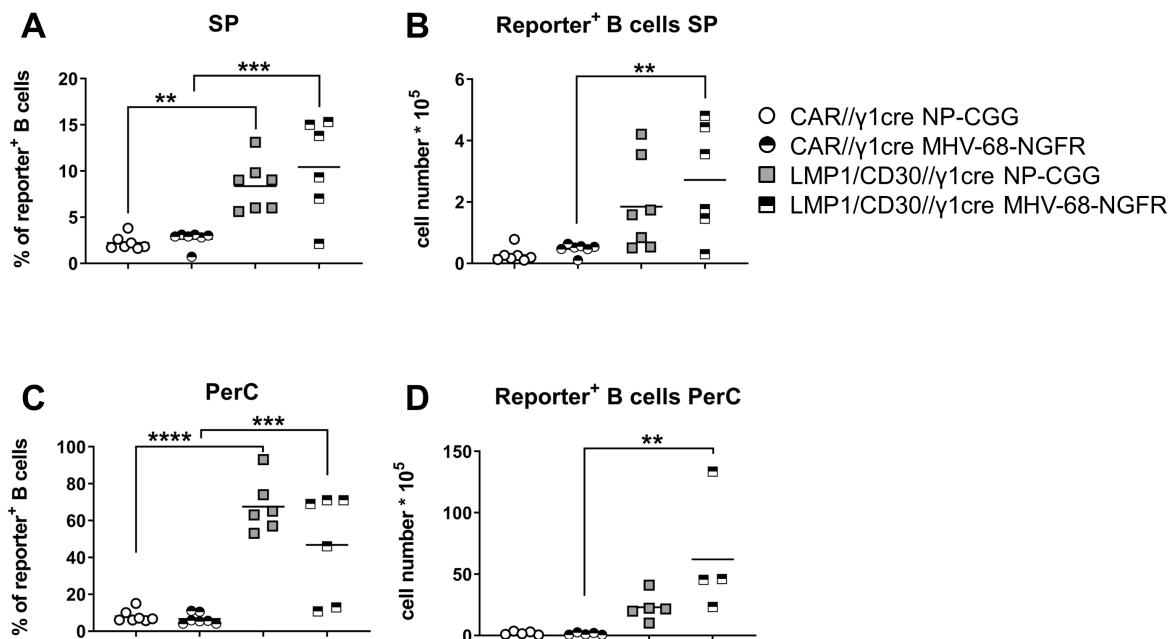


**Figure 29:** (A+B): The diagrams show the cell numbers and the percentages of reporter<sup>+</sup> cells in the SP of the depicted analyzed groups; (C+D): The diagrams show the cell numbers and the percentages of reporter<sup>+</sup> B cells (CD19<sup>+</sup>) in the PerC. Every dot represents the value obtained from one mouse, the bar represents the mean of the percentages or cell numbers.

The percentages of NGFR<sup>+</sup> cells among the reporter expressing cells revealed no difference between CAR and LMP1/CD30//C $\gamma$ 1-cre mice neither in the spleen nor in the PerC (Figure 30A). However, considering the total cell numbers, significantly more NGFR<sup>+</sup> cells were detectable in the spleen and the PerC of the LMP1/CD30//C $\gamma$ 1-cre mice in comparison to control mice (Figure 30B). The expansion of reporter<sup>+</sup> B cells in the LMP1/CD30//C $\gamma$ 1-cre mice resulted in higher total NGFR<sup>+</sup> cell numbers. These data indicate that the herpesviral infection in combination with the deregulated CD30 signaling contributes to the expansion of B cells.

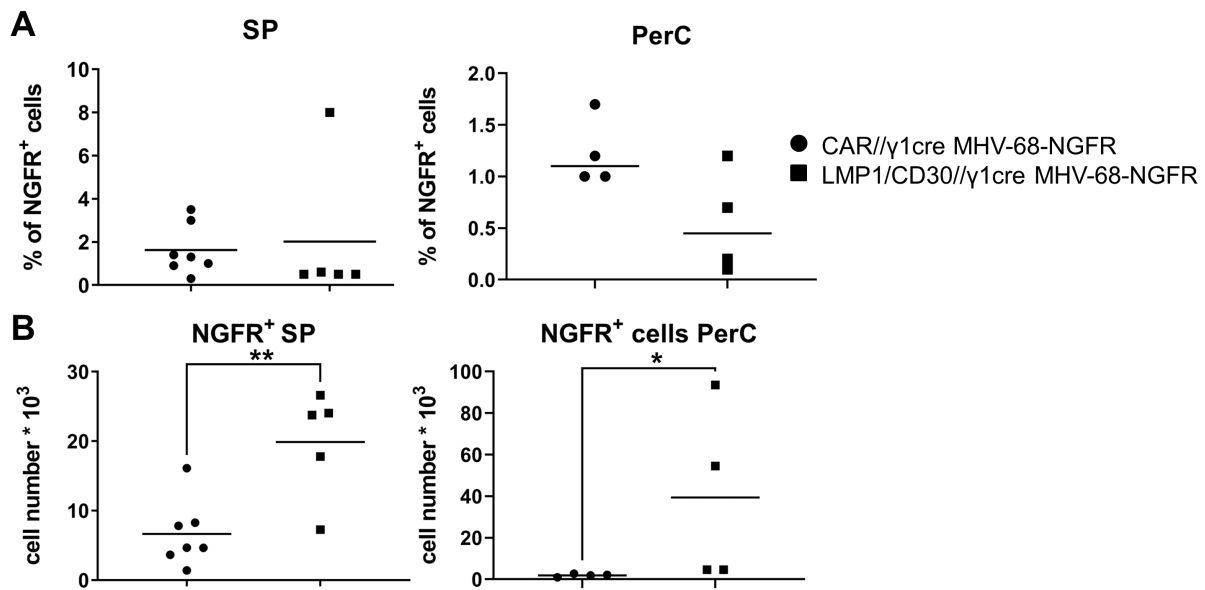


**Figure 30:** (A+B): The diagrams show the percentages and the cell numbers of NGFR<sup>+</sup> cells among the reporter<sup>+</sup> B cells in the SP and the PerC of the infected LMP1/CD30//C $\gamma$ 1-cre and CAR//C $\gamma$ 1-cre mice. Every dot represents the value obtained from one mouse, the bar represents the mean of the percentages or the cell numbers.

Next, I analyzed the phenotype of reporter<sup>+</sup> B cells 2 months after immunization or infection. As expected, the percentages of total GC B cells were lower after 2 months than after 14 d (Figure 31A, see Figure 24A). However, in control mice around 20% of reporter<sup>+</sup> cells still had a GC phenotype (Figure 31B+C). In contrast, only 2% of the LMP1/CD30 expressing cells revealed a GC phenotype. Therefore, the chronic CD30 signaling seemed to block the re-entry into the GC.

Following, we asked, if the expanded reporter<sup>+</sup> B cells in LMP1/CD30//C $\gamma$ 1-cre still have a PC and CD43<sup>+</sup>, CD23<sup>lo</sup> phenotype as displayed after 2 weeks.

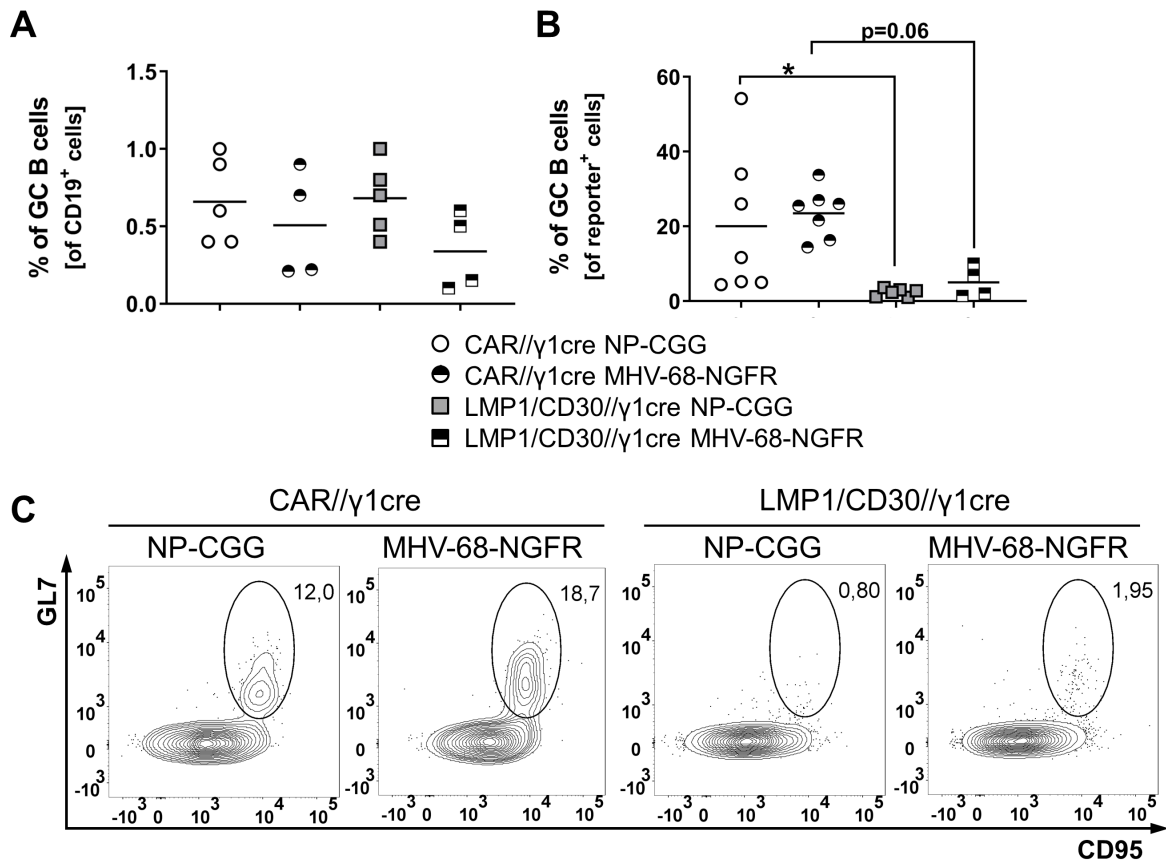


**Figure 31:** The diagram shows the percentages of GC B cells of CD19<sup>+</sup> (A) or of reporter<sup>+</sup> B cells (B). Every dot represents the value obtained from one mouse, the bar represents the mean of the percentages; (C): Reporter<sup>+</sup> cells of the four indicated mouse groups were gated for GC B cells (GL7<sup>+</sup>, CD95<sup>+</sup>) in the SP. Plots were pregated on CD19<sup>+</sup>, reporter<sup>+</sup> cells.

The percentages of the reporter<sup>+</sup> PC and of the CD43<sup>+</sup>, CD23<sup>lo</sup> were significantly higher in the LMP1/CD30//C $\gamma$ 1-cre compared to control mice both upon immunization and infection (Figure 32A-C). There was no clear difference in the percentages of the PC of the LMP1/CD30//C $\gamma$ 1-cre between immunization and infection but after infection the percentage was tendentially a bit lower. However, the percentages of reporter<sup>+</sup>, CD43<sup>+</sup>, CD23<sup>lo</sup> cells were higher in LMP1/CD30//C $\gamma$ 1-cre mice than in controls in the PerC (Figure 32C). The LMP1/CD30 expression resulted in an expanded PC population in the spleen and an increased CD43<sup>+</sup>, CD23<sup>lo</sup> population in the spleen and the PerC. The MHV-68-NGFR infection seemed not to interfere with the PC differentiation after 2 months but contributed to an extended CD43<sup>+</sup>, CD23<sup>lo</sup> population in the PerC.

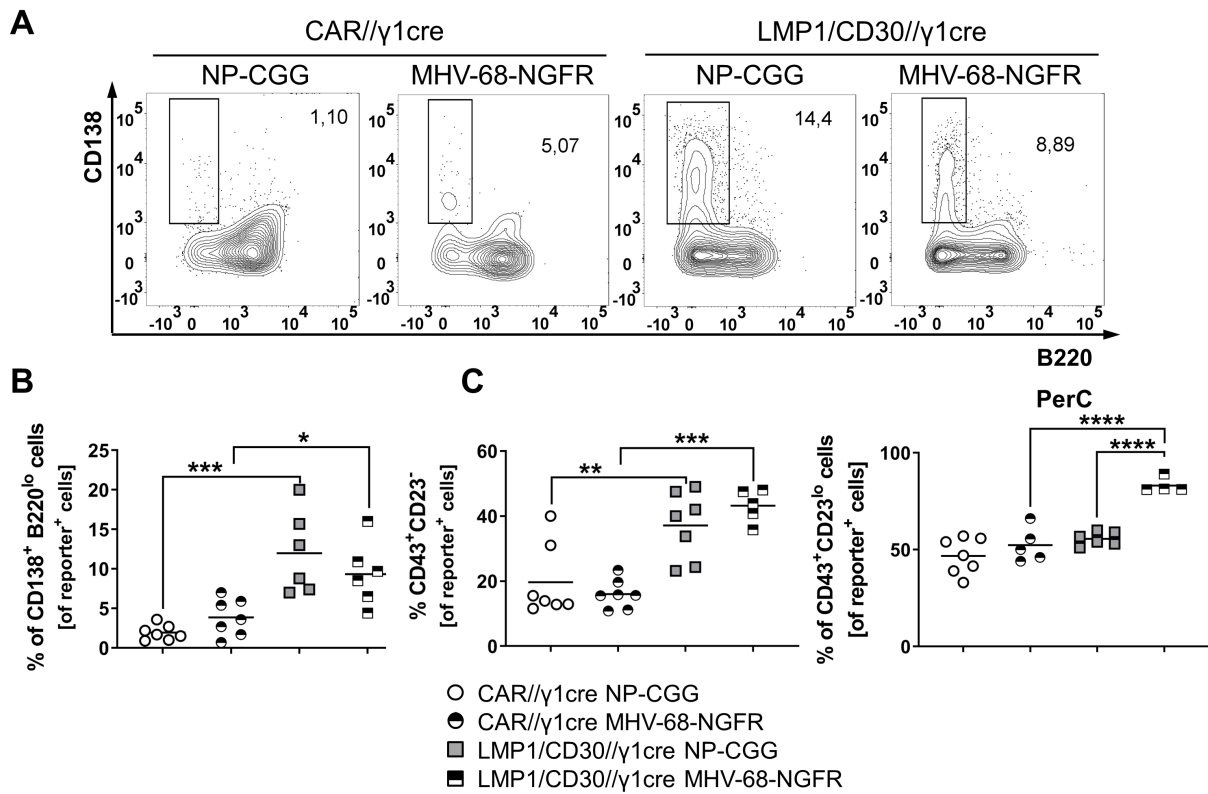


**Figure 32:** (A): Reporter<sup>+</sup> lymphocytes of the four indicated mouse groups were gated for PC (CD138<sup>+</sup>, B220<sup>lo</sup>); (B): The diagram shows the percentages of reporter<sup>+</sup> PC in the spleen of the analyzed mice in the four groups; (C): The graphs show the percentages of reporter<sup>+</sup> B1 cells (CD43<sup>+</sup>, CD23<sup>lo</sup>) of the analyzed mice in the spleen (SP) (middle) and in the PerC (right). Every dot represents the value obtained from one mouse, the bar represents the mean of the percentages.

The B1 cell population, which was characterized as CD43<sup>+</sup>, CD23<sup>lo</sup> so far, is divided into B1a and B1b cells which can be discriminated by CD5 surface expression. To analyze whether B1a and/or B1b cells were expanded in the spleens of LMP1/CD30//C $\gamma$ 1-cre mice in comparison to control mice, we performed further staining (Figure 33). We found that deregulated CD30 expression results in an expansion of both B1a and B1b cells. Moreover, MHV-68-NGFR infection induced an additional increase of B1a cells in comparison to the immunized mice (Figure 33B).

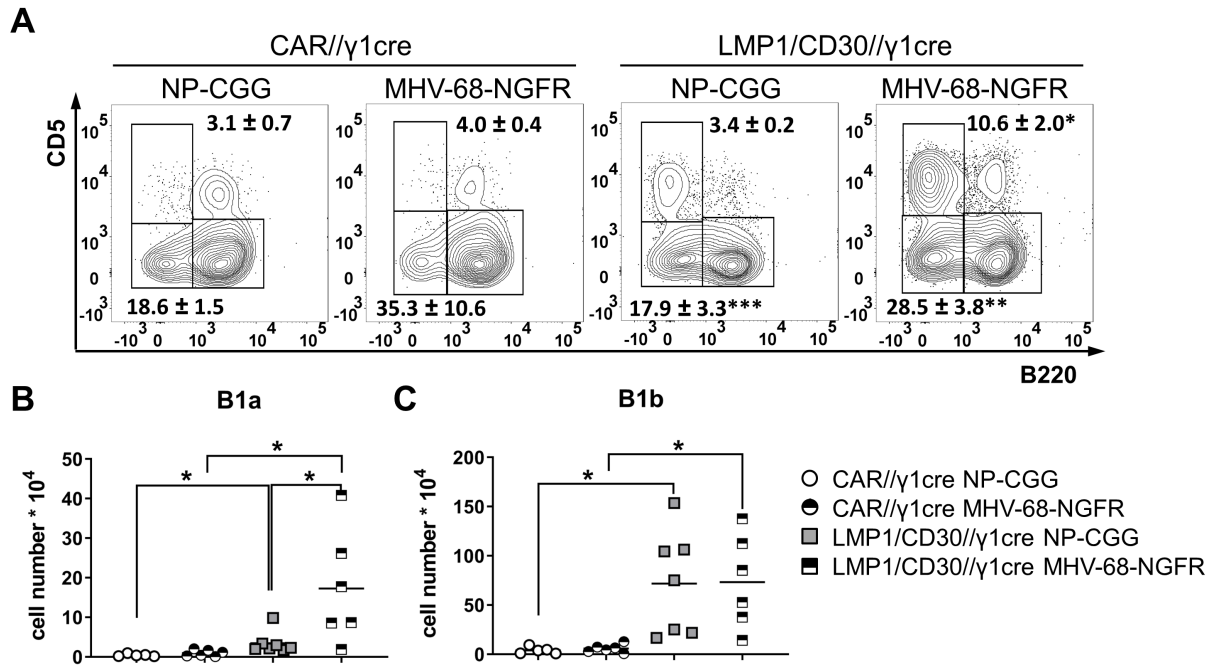


**Figure 33:** (A): The FACS plots show the gating strategy for B1a and B1b cells. Splenic cells were gated for reporter<sup>+</sup> B cells (CD19<sup>+</sup>) and then gated for B1a (CD5<sup>+</sup>, B220<sup>lo</sup>), B1b (CD5<sup>lo</sup>, B220<sup>lo</sup>) and B2 cells (CD5<sup>lo</sup>, B220<sup>+</sup>), the numbers indicate the mean and the SD of the percentages of the B1a or B1b populations, indicated significance are calculated towards the respective control mice,  $n \geq 5$ ; (B+C): The diagrams display the cell numbers of B1a and B1b cells of the indicated mouse groups, gated as indicated in (A). Every dot represents the value obtained from one mouse, the bar represents the mean of the percentages.

The infected as well as the immunized LMP1/CD30// $\gamma$ 1-cre mice displayed significantly lower percentages of IgG1<sup>+</sup> memory B cells compared to their respective controls (Figure 34A). However, the infected mouse groups revealed slightly higher percentages of memory B cells (IgG1<sup>+</sup>) than the immunized groups. Calculating total cell numbers revealed elevated memory B cell numbers in the infected LMP1/CD30// $\gamma$ 1-cre mice compared to their control mice and to the immunized LMP1/CD30// $\gamma$ 1-cre mice (Figure 34B).

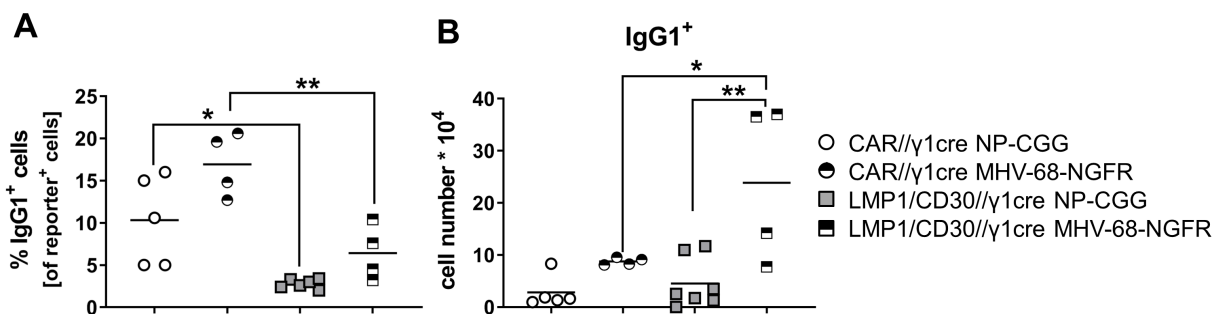


**Figure 34:** (A+B): The graphs show the cell numbers and the percentages of memory B cells (IgG1<sup>+</sup>, CD38<sup>+</sup>, reporter<sup>+</sup>, CD19<sup>+</sup>) in the depicted mouse groups in the SP. Every dot represents the value obtained from one mouse, the bar represents the mean.

In summary, B and T cell numbers were higher in the infected and the immunized LMP1/CD30//C $\gamma$ 1-cre mice in comparison to control mice (see Figure 27B+C). Additionally, the chronic CD30 signaling resulted in an expanded reporter<sup>+</sup> cell population with a B1 cell and a PC phenotype in these mouse cohorts (see Figure 29, Figure 32C). The virus infection in the LMP1/CD30//C $\gamma$ 1-cre mice induced an additional expansion of the B1a cell population when comparing infected and immunized LMP1/CD30//C $\gamma$ 1-cre mice (see Figure 33A+B). Due to the virus infection, the differentiation towards memory B cells was significantly higher in the LMP1/CD30 expressing B cells upon 2 months (see Figure 34B). In contrast, the LMP1/CD30 expressing cells revealed a lower commitment towards a GC phenotype in comparison to control mice reflecting the block of the re-entry of these cells into the GC (see Figure 31).

### 5.3.7 Aged mice

The long term effect of constitutive CD30 signaling induced in GC B cells, alone or in combination with a viral infection, was investigated. The LMP1/CD30//C $\gamma$ 1-cre mice were examined after they developed signs of disease like swollen abdomen, sunken flanks, or accelerated breathing but latest after 18 months. Every LMP1/CD30//C $\gamma$ 1-cre mice was analyzed with a control CAR//C $\gamma$ 1-cre mouse.

#### 5.3.7.1 Viral infection leads to an additive effect in CD30 driven lymphoma development

The next question was whether LMP1/CD30 expression induced in GC B cells leads to lymphomagenesis and whether MHV-68 infection further enhances lymphomagenesis. The CAR//C $\gamma$ 1-cre mouse cohort infected with MHV-68-NGFR was comprised of 12 mice, 2 of them died during the experiment. The CAR//C $\gamma$ 1-cre mouse cohort immunized with NP-CGG consisted of 15 mice, 2 of them could not be used for the experiment. The LMP1/CD30//C $\gamma$ 1-cre mouse cohort infected with MHV-68-NGFR and immunized with NP-CGG started with 13 and 14 mice respectively, in each group one mouse was taken out from experiment. The mice of the four aged cohorts were analyzed for mono- or oligoclonal B cell expansion by southern blot analysis using a radioactive labeled Jh4 probe. Thereby, 5 of 12 of the virus infected LMP1/CD30//C $\gamma$ 1-cre mice and 2 of 13 of the immunized group displayed a mono- or oligoclonal B cell expansion (Figure 35A). The results of the southern blot analysis of the remaining mice is displayed in Supplementary 2. Therefore, the virus infected LMP1/CD30//C $\gamma$ 1-cre mice developed with a significantly higher incidence a lymphoma compared to the immunized ones. Additionally, in two of the virus infected LMP1/CD30//C $\gamma$ 1-cre mice, a strong expansion of lymphocytes in the PerC was noted. These were also tested in the southern blot analysis. In #17, the same clone found in the spleen predominated also the PerC. In contrast, #50 had another

clone growing out to a tumor population in the PerC. However, also both in the infected and the immunized control mouse cohort, one mouse was detected with a mono- or oligoclonal expansion. Further, the incidence of sickness in both LMP1/CD30//C $\gamma$ 1-cre mice was compared (Figure 35B). The MHV-68-NGFR infected LMP1/CD30//C $\gamma$ 1-cre mice displayed a median survival of 14 months, the immunized LMP1/CD30//C $\gamma$ 1-cre mice survived 16 months on average.

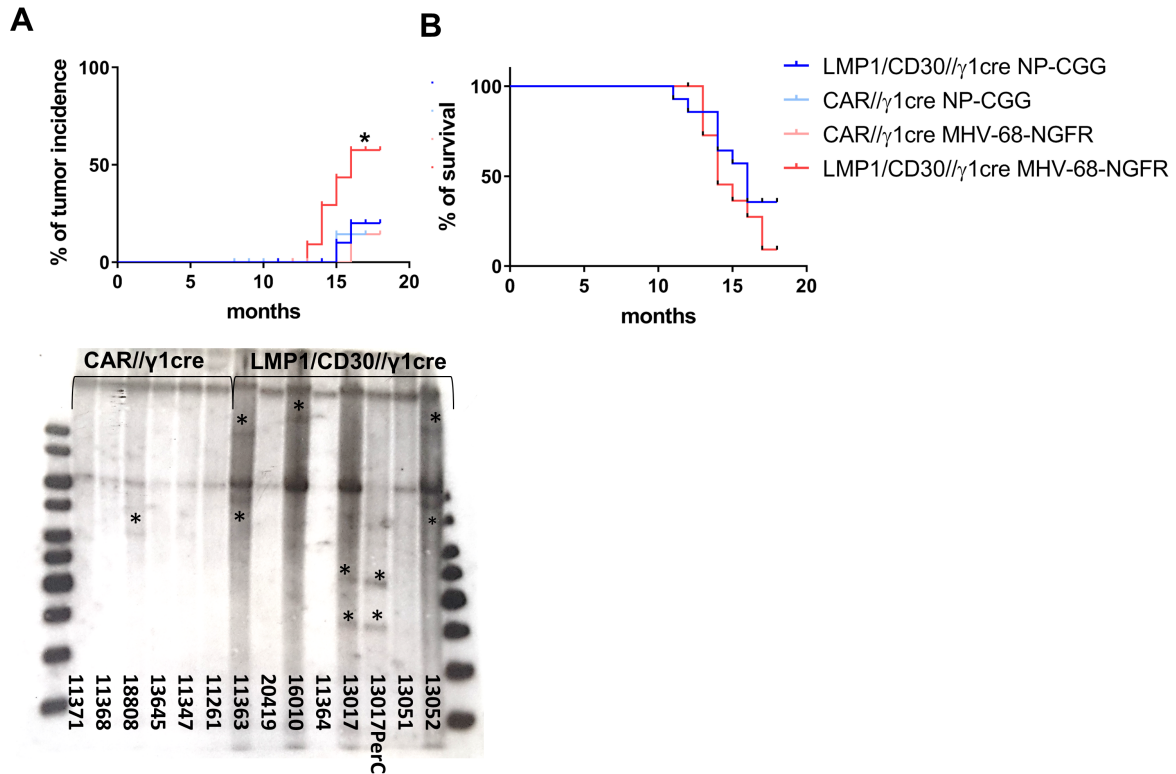


**Figure 35:** (A): The graph shows the tumor incidence of all analyzed mice. The lymphomas were detected by southern blot with a radioactive probe spanning the region between JH4 and E $\mu$  of the IgH locus,  $n \geq 10$ , the lower picture shows one example of a southern blot, the stars indicate additional band besides the germline band at 6 kB; (B): The diagram displays the mice of both LMP/CD30//C $\gamma$ 1-cre mouse cohorts which became sick over the analyzed time,  $n \geq 12$ .

### 5.3.7.2 CD30 signaling leads to the expansion of B and T cells in aged mice

To further determine the phenotype of lymphomas, we analyzed the B cell compartment of aged mice. Both groups of LMP1/CD30//C $\gamma$ 1-cre mice displayed a significantly higher splenic weight than their respective control groups (Figure 36A). Both, the cell numbers and the T cells, were significantly increased in the LMP1/CD30//C $\gamma$ 1-cre in comparison to their respective controls (Figure 36B+D). But only the NP-CGG immunized LMP1/CD30//C $\gamma$ 1-cre developed significantly higher B cell numbers (Figure 36C). The mice with a detected mono- or oligoclonal expansion had in most cases a stronger

splenomegaly and higher splenic cell numbers than mice without clonal expansion. The immunized and infected mice with lymphomas displayed higher T cell numbers than their respective control mice (red icons in Figure 36).

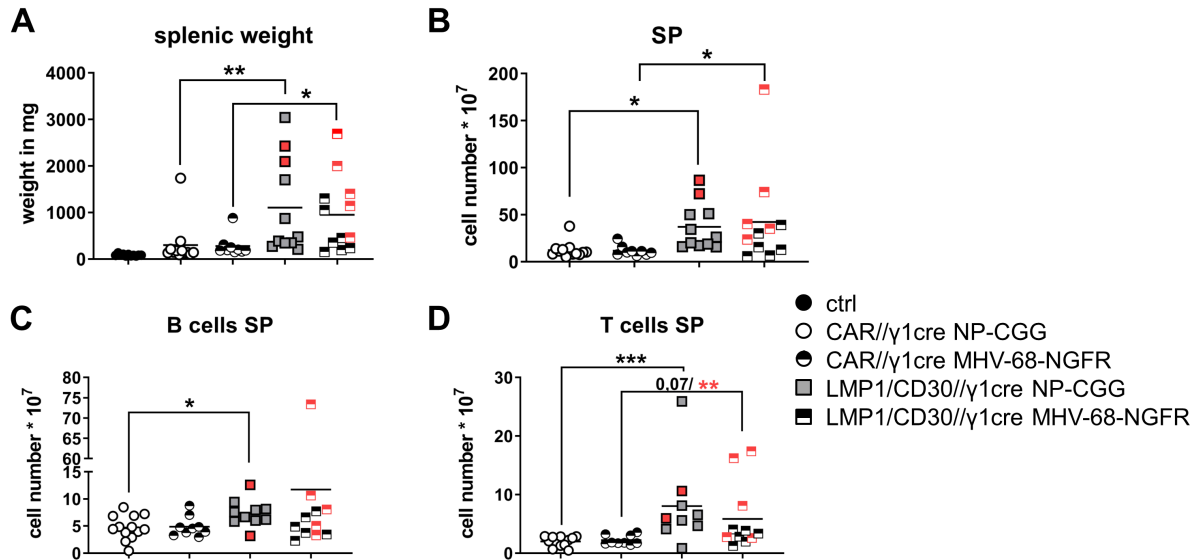


**Figure 36:** Infected and immunized LMP1/CD30// $C\gamma$ 1-cre and CAR// $C\gamma$ 1-cre mice were aged until the LMP1/CD30// $C\gamma$ 1-cre showed signs of sickness. Always one LMP1/CD30// $C\gamma$ 1-cre mouse was analyzed together with a CAR// $C\gamma$ 1-cre control mouse, all red colored dots represent a mouse with a detected mono- or oligoclonal expansion, the red significance was determined by using only the tumor samples. The graphs show the splenic weight (A), total splenic cell numbers (B), total splenic B cell numbers (CD19<sup>+</sup>) (C), and total splenic T cell numbers (Thy1.2<sup>+</sup>) (D) of all analyzed mice in the depicted groups. Every dot represents the value obtained from one mouse, the bar represents the mean.

The cell number of the PerC was slightly higher in infected LMP1/CD30// $C\gamma$ 1-cre mice in comparison to control and the immunized mice (Figure 37A). Additionally, the B and T cell numbers were tendentially increased in these mice (Figure 37B+C). The mice of the infected LMP1/CD30// $C\gamma$ 1-cre mouse group which were detected with a tumor displayed the highest increase of the cell number in the PerC (red points Figure 37C). Among the immunized LMP1/CD30// $C\gamma$ 1-cre mice, the mice with the tumor were not among the mice with the highest cell number.

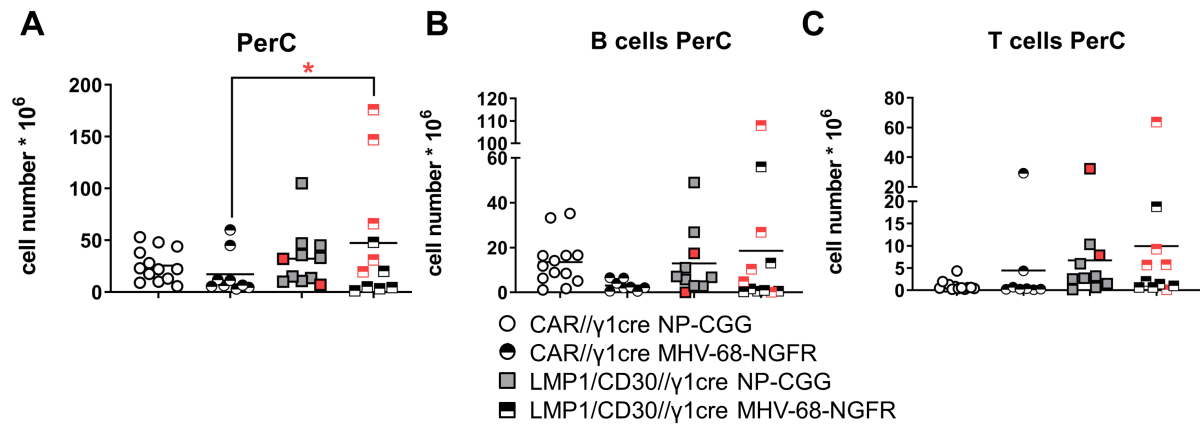


**Figure 37:** The graphs show the total cell numbers (A), the cell numbers of B cells (CD19<sup>+</sup>) (B), and the cell numbers of total T cells (Thy1.2<sup>+</sup>) in the PerC (C) of the PerC of the aged mice. Every dot represents the value obtained from one mouse, the bar represents the mean.

Furthermore, the percentages of the reporter<sup>+</sup> cells were significantly enriched in both groups of LMP1/CD30//Cγ1-cre mice in the spleen as well as in the PerC in comparison to CAR//Cγ1-cre mice (Figure 38). Mice that had developed lymphomas showed in most cases a very high percentage of reporter<sup>+</sup> B cells in the spleen (between 70%-95%). The percentages of cells expressing hCD2 were much higher in the PerC than in the spleen.

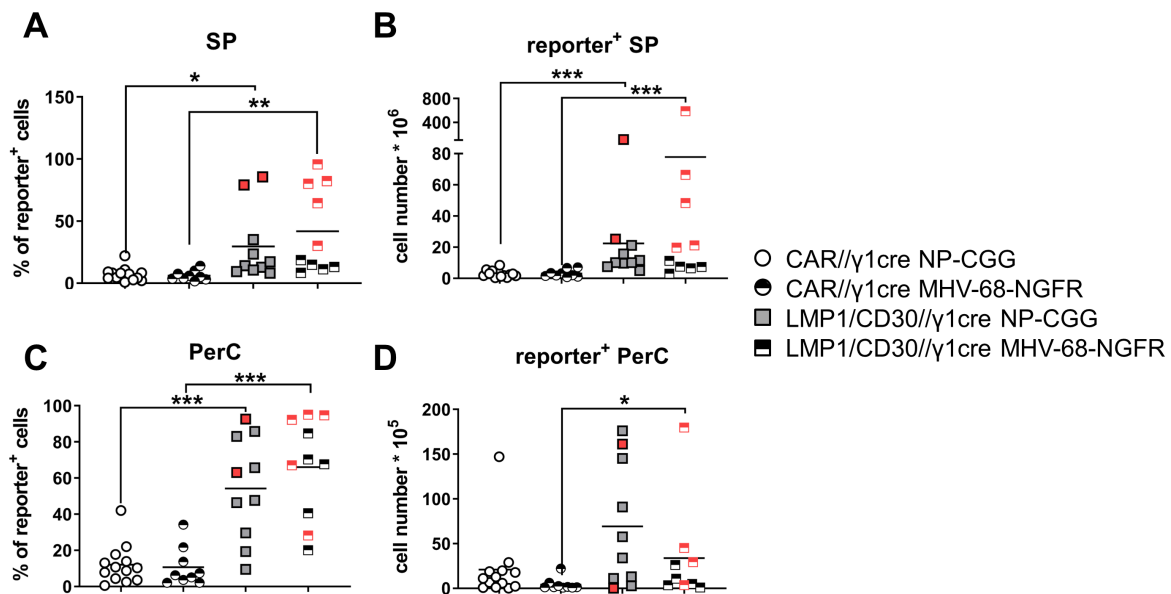


**Figure 38:** (A+B): The graphs show the percentages and the cell numbers of reporter<sup>+</sup> B cells (CD19<sup>+</sup>) in the SP of aged mice; (C+D): The graphs show the percentages and the cell numbers of reporter<sup>+</sup> B cells (CD19<sup>+</sup>) in the PerC of aged mice. Every dot represents the value obtained from one mouse, the bar represents the mean.

To get an overview of the expansion of reporter<sup>+</sup> B cells in the spleen and the PerC

over time, we compiled the percentages of reporter<sup>+</sup> B cells at the analyzed time points in one graph. Additionally, we assembled the cell numbers of reporter<sup>+</sup> cells in the analyzed mouse groups in the spleen and the PerC of different time points. In LMP1/CD30//C $\gamma$ 1-cre mice, the numbers and percentages of reporter<sup>+</sup> cells increased between 2 months and 13 months in the spleen (Figure 39A). The increase of reporter<sup>+</sup> cells was stronger in infected than in immunized mice. The number of reporter<sup>+</sup> cells increased only marginally in control mice. In the PerC, cell numbers of LMP1/CD30-expressing cells increased continuously in immunized LMP1/CD30//C $\gamma$ 1-cre mice. The infected LMP1/CD30//C $\gamma$ 1-cre mice showed already high number of reporter expressing cells after 2 months but afterwards they did not further increase and dropped below the cell numbers of the immunized LMP1/CD30//C $\gamma$ 1-cre mice in the aged cohort (Figure 39B). The percentages of reporter<sup>+</sup> cell in the PerC were very high in both the immunized and infected LMP1/CD30//C $\gamma$ 1-cre mice at each time point reaching between 50% and 70% already after 2 months. The cell numbers and percentages of hCD2<sup>+</sup> cells from infected and immunized LMP1/CD30//C $\gamma$ 1-cre mice were at all time points higher than in the CAR<sup>+</sup> cells of the respective control mice.

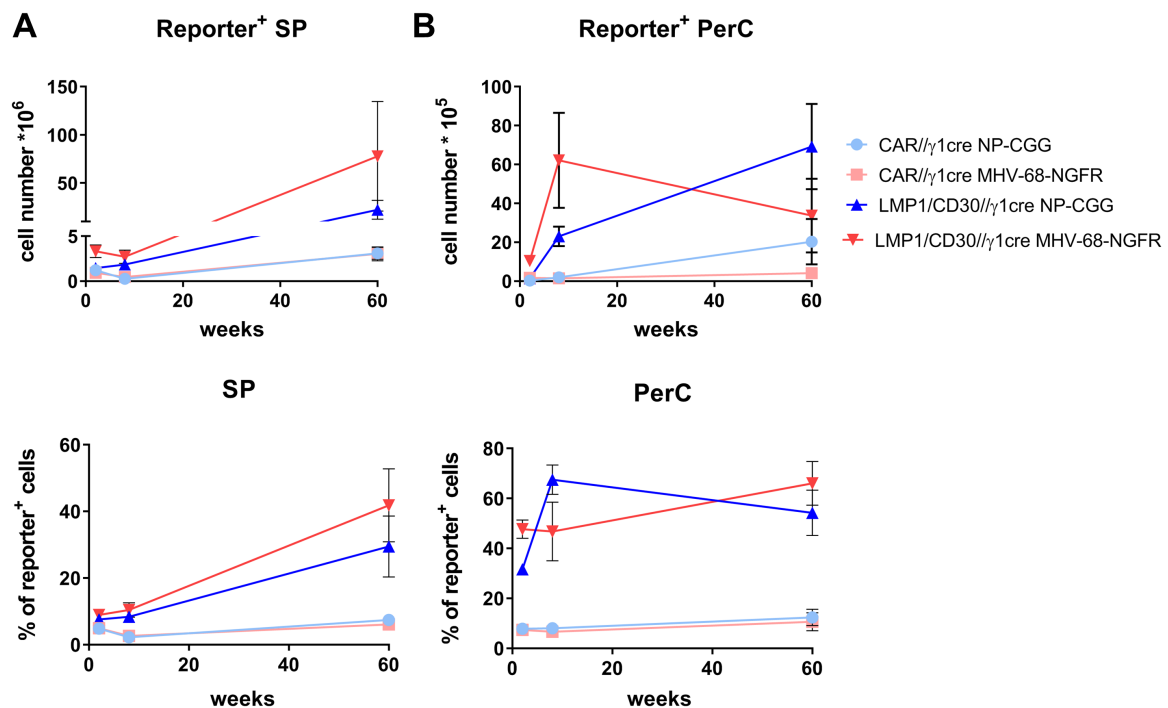


**Figure 39:** The diagrams display the time course of the cell numbers or the percentages of reporter expressing cells in the four indicated mouse groups starting from 2 weeks until completion of the experiment in the SP (A) and the PerC (B).

To sum this up, aged LMP1/CD30//C $\gamma$ 1-cre mice revealed a splenomegaly, increased B and T cell numbers in the spleen and in the PerC. The LMP1/CD30 expressing cells

expanded stronger than CAR expressing cells both in immunized and infected mice. The infected LMP1/CD30//C $\gamma$ 1-cre mice displayed a stronger increase of reporter<sup>+</sup> cells in the spleen in comparison to the immunized mice. In the PerC, the cell numbers of LMP1/CD30 expressing cells of the immunized mice was higher. Most of the mice detected with a clonal expansion were characterized by a stronger splenomegaly in comparison to other aged mice and almost 100% reporter expression among the B cells.

### 5.3.7.3 CD30 signaling leads to higher numbers of virus infected B cells

Next, we analyzed the distribution of the NGFR<sup>+</sup> cells. Notably, the percentages of reporter<sup>+</sup>, NGFR<sup>+</sup> cells were nearly similar in SP, LN, and PerC from LMP1/CD30//C $\gamma$ 1-cre and control mice (Figure 40A). Only in virus infected LMP1/CD30//C $\gamma$ 1-cre mice, the percentages of the NGFR<sup>+</sup> were significantly higher in the spleen than in the PerC. However, the higher percentages of reporter expressing B cells in the spleen and the PerC from LMP1/CD30//C $\gamma$ 1-cre mice in comparison to controls resulted in higher percentages of NGFR<sup>+</sup> cells among all B cells in LMP1/CD30//C $\gamma$ 1-cre mice (Figure 40B grey bars). Also, the total numbers of NGFR<sup>+</sup> cells were significantly higher in the LMP1/CD30//C $\gamma$ 1-cre mice in comparison to the CAR//C $\gamma$ 1-cre mice and increased during aging (Figure 40C+D). The highest number of NGFR<sup>+</sup> cells could be detected in mice with a tumor (Figure 40D, red icons). This means that the chronic CD30 signaling resulted in an expanded population of infected cells in the spleen and the PerC.

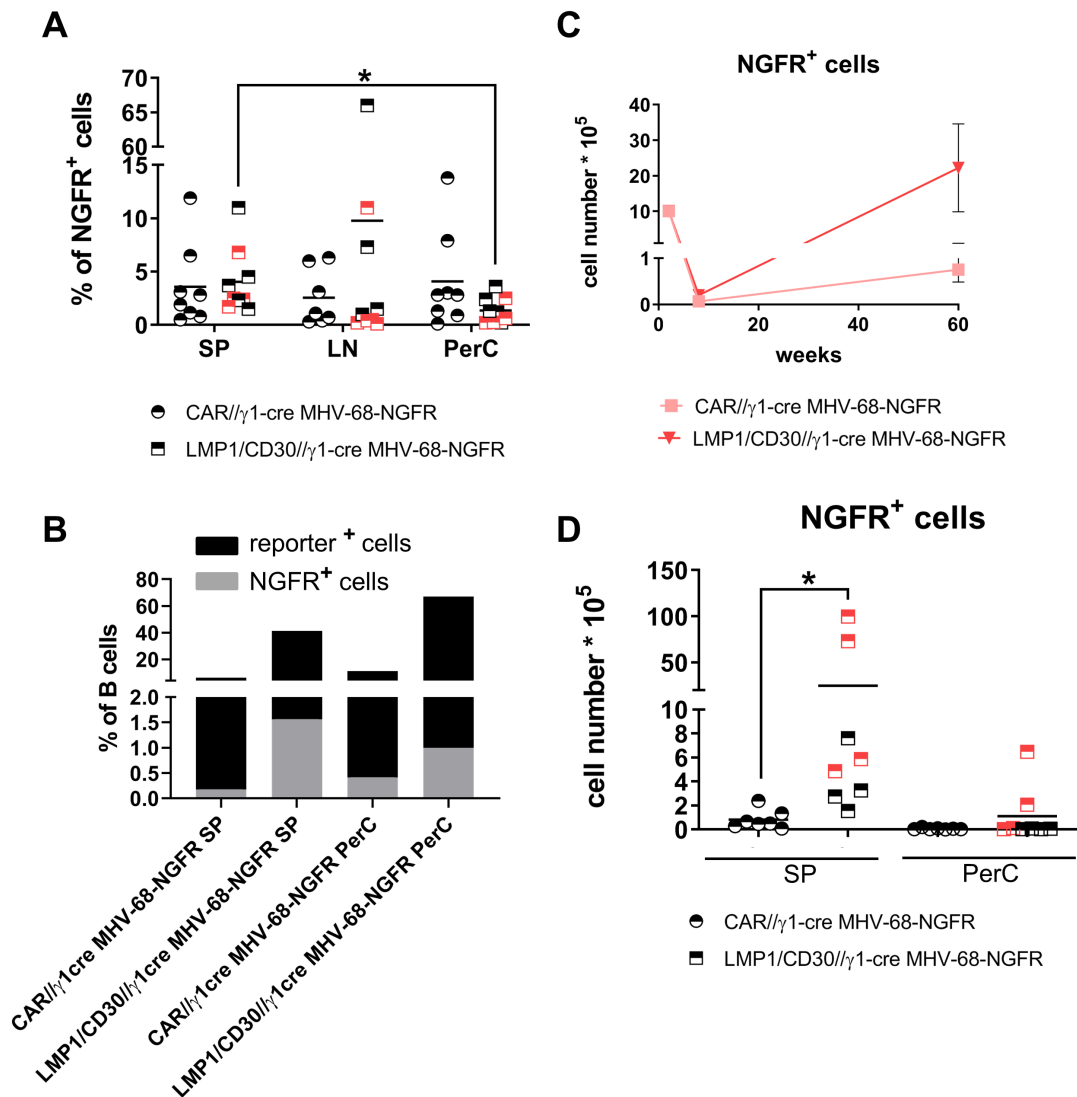


**Figure 40:** (A): The graph shows the percentages of reporter NGFR<sup>+</sup> cells gated for CD19<sup>+</sup>, reporter<sup>+</sup> cells of the infected LMP1/CD30//C $\gamma$ 1-cre and CAR//C $\gamma$ 1-cre mice in the lymph node (LN), spleen (SP), and the PerC; (B): The graph illustrates the percentages of NGFR<sup>+</sup> cells and reporter<sup>+</sup> cells within the B cell population (CD19<sup>+</sup>) in the SP and the PerC of the indicated genotypes. (C) The diagram displays the time course of the cell numbers of NGFR expressing reporter<sup>+</sup> B cells in the indicated mouse groups starting from 2 weeks until termination of the experiment; (D): The graph shows the cell numbers of NGFR<sup>+</sup> cells gated for CD19<sup>+</sup>, reporter<sup>+</sup> cells of the infected LMP1/CD30//C $\gamma$ 1-cre and CAR//C $\gamma$ 1-cre mice in the SP and the PerC.

#### 5.3.7.4 CD30 signaling leads to a further expansion of the B1a and B1b cell populations in aged mice

The reporter expressing B cells were further characterized regarding their surface marker expression. All groups displayed similar percentages of GC B cells among the reporter expressing population (Figure 41A). The B1/PB cell population (CD43<sup>+</sup>, CD23<sup>lo</sup>) was strongly enhanced in both groups of the investigated LMP1/CD30//C $\gamma$ 1-cre mice in com-

parison to controls in the spleen and the PerC (Figure 41B+C). Both, the B1a and the B1b cells, were expanded (Figure 41D+E). All mice detected with a lymphoma revealed a high number of B1b cells (Figure 41E, red icons).

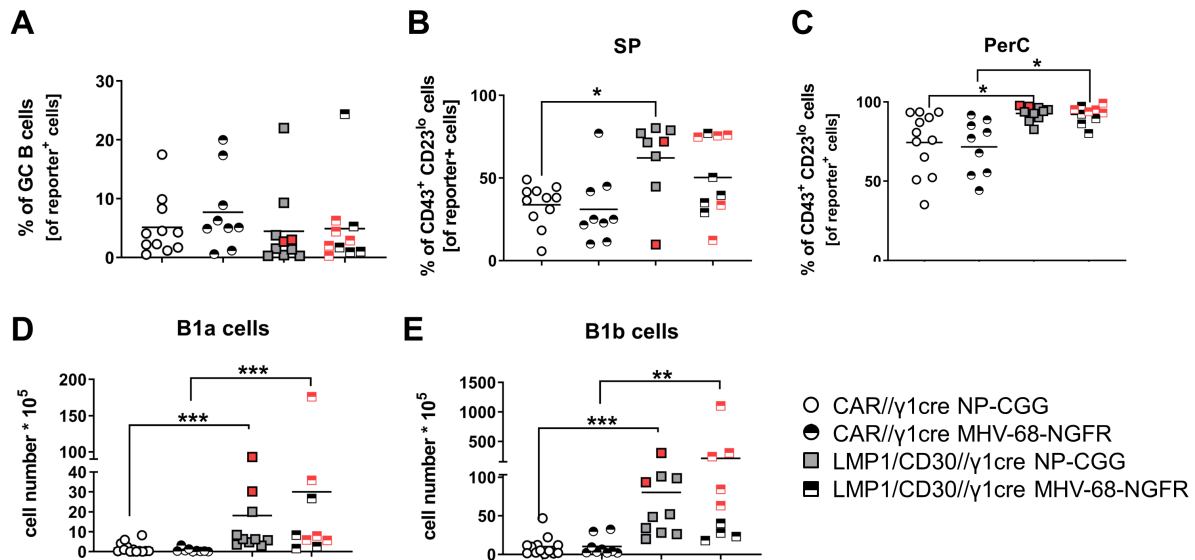


**Figure 41:** (A): The graph illustrates the percentages of GC B cells ( $CD38^{lo}$ ,  $CD95^{+}$ ) of reporter<sup>+</sup> cells in the SP; (B+C): The graphs show the percentages of  $CD43^{+}$ ,  $CD23^{lo}$  B cells pregated for reporter<sup>+</sup>,  $CD19^{+}$  cells of the depicted mouse groups in aged mice in the SP and the PerC; (D+E): The graph shows the cell numbers of B1a ( $CD5^{+}$ ,  $B220^{lo}$ ) and B1b ( $CD5^{lo}$ ,  $B220^{lo}$ ) cells of reporter<sup>+</sup>,  $CD19^{+}$  cells of the aged mice in the SP. Every dot represents the value obtained from one mouse, the bar represents the mean.

The chronic CD30 signaling drove strongly the expansion of PC after 2 weeks and after 2 months after immunization and infection of LMP1/CD30// $C\gamma 1$ -cre mice (Figure 42A, lower diagram). Thus, we also evaluated the PC of these B cells in aged mice. The percentages of PC were not increased in the LMP1/CD30// $C\gamma 1$ -cre mice in comparison to control mice (Figure 42A). The percentages of PC of the infected LMP1/CD30// $C\gamma 1$ -cre mice were even lower in comparison to their respective control mice. Under physiological conditions, BLIMP-1 represents, together with IRF4, the key transcription factor during PC differentiation [Klein et al., 2006]. Further, BLIMP-1 is a known tumor suppressor [Nie et al., 2008]. Thus, we analyzed BLIMP-1 and IRF4 expression in the reporter expressing B cells with FACS analysis. In comparison to naive B cells, the reporter expressing cells of all groups revealed higher BLIMP-1 expression. Nevertheless, immunized LMP1/CD30// $C\gamma 1$ -cre mice displayed decreased BLIMP-1 and IRF4 expression (Figure 42B+C). In the B cells with a mono- or oligoclonal expansion, BLIMP-1 was tendentially downregulated in comparison to the mice free of tumor in the same group and control mice (Figure 42B, red icons), whereas IRF4 levels were comparable between lymphoma

and non-lymphoma mice. These data suggest that LMP1/CD30-expressing lymphoma cells are activated and upregulate IRF4. In comparison to non-lymphoma cells, BLIMP-1 is less upregulated in lymphomas, suggesting that lymphoma cells are attenuated in a (pre)-plasmablastic stage and do not differentiate to PC. This is in accord with our observation that the percentages of PC found in mice with lymphomas were the lowest compared to the whole group (Figure 42A, red icons).

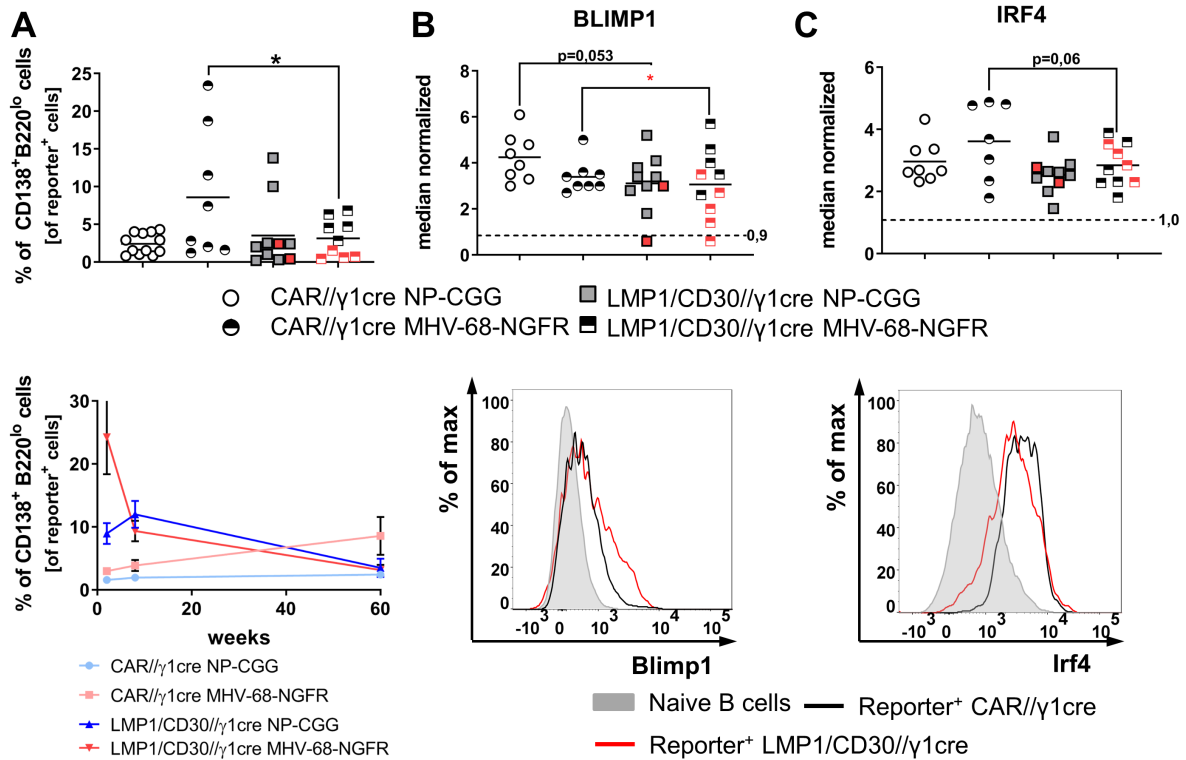


**Figure 42:** (A): The diagram shows the percentages of PC (CD138<sup>+</sup>, B220<sup>lo</sup>) in the depicted mouse groups which were pregenerated for reporter<sup>+</sup> cells in the SP, the lower graph displays the percentages of the PC at the analyzed time points; (B+C): This diagram displays the normalized median of BLIMP-1 (B) and IRF4 (C) of reporter<sup>+</sup> cells in the SP of the illustrated mouse groups, the dotted line represents the median of naive B cells (reporter<sup>-</sup>), the histograms display an example of a BLIMP-1 and IRF4 staining of naive B cells, reporter<sup>+</sup> cells of a CAR//Cγ1-cre, and a LMP1/CD30//Cγ1-cre mouse.

After establishment of latency, MHV-68 is mainly found in isotype switched memory B cells [Barton et al., 2011]. Therefore, we determined the percentages and the cell numbers of memory B cells in all four analyzed mouse cohorts in aged mice. The percentages of memory B cells in the immunized LMP1/CD30//Cγ1-cre mice was decreased in comparison to the control mice and to the infected LMP1/CD30//Cγ1-cre mice (Figure 43A+B). Total cell numbers were higher in the infected LMP1/CD30//Cγ1-cre mice in comparison to the CAR control mice. But the distribution within the infected LMP1/CD30//Cγ1-cre mice was very broad (Figure 43C). Two of the infected mice with a tumor displayed a

strong increase in the percentages of the memory B cells in comparison to the other mice in the cohort. It would be interesting to stain for NGFR<sup>+</sup> memory B cells to determine the virus infection in this population, unfortunately this staining was not performed in this constellation. These data suggest that MHV-68 drives the expansion and transformation of IgG1-memory B cells.

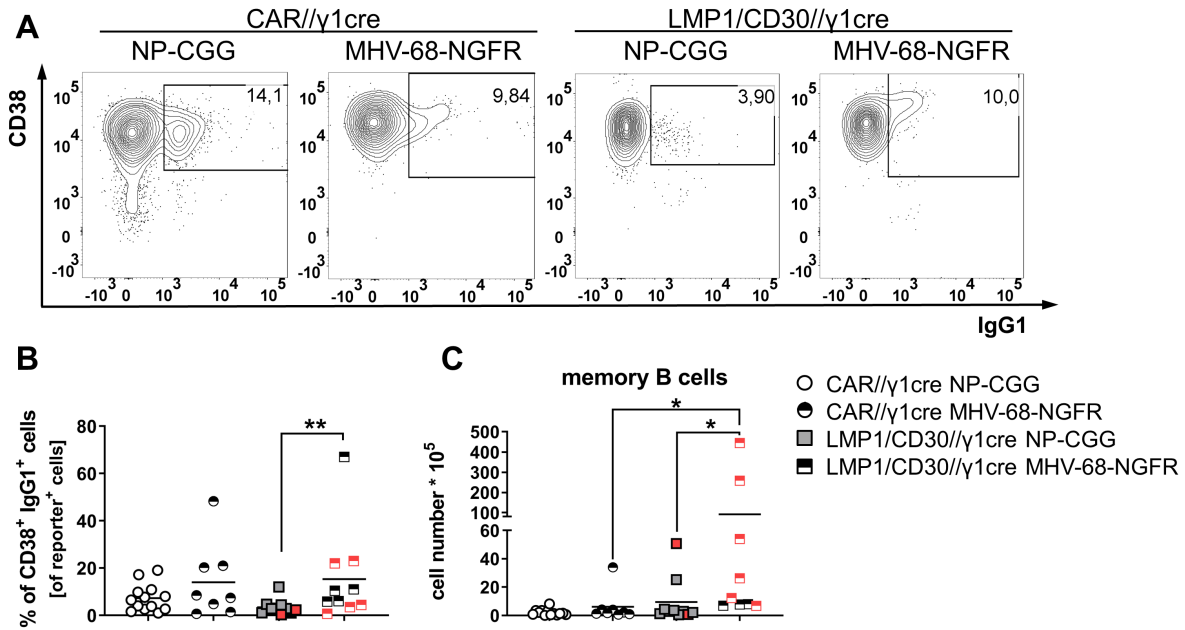


**Figure 43:** (A): The FACS plots illustrate the gating strategy of the IgG1<sup>+</sup> memory B cells (CD19<sup>+</sup>, reporter<sup>+</sup>, CD38<sup>+</sup>, IgG1<sup>+</sup>) in the SP; (B+C): The diagrams show the percentages and the cell numbers of splenic memory B cells in the four analyzed mouse groups. Every dot represents the value obtained from one mouse, the bar represents the mean.

### 5.3.7.5 Virus infection and chronic CD30 signaling induce development of exhausted CD8<sup>+</sup> memory T cells

Due to the expansion of T cells, found in the cohorts of LMP1/CD30//C $\gamma$ 1-cre mice, we further wanted to investigate the T cell sub-populations. Especially CD8<sup>+</sup> T cells play an important role in the host defense against viral infection [Kalia et al., 2013]. Thus, the analysis focused mainly on the CD8<sup>+</sup> T cells. The total numbers of CD4<sup>+</sup> T cells were significantly higher in the immunized and infected LMP1/CD30//C $\gamma$ 1-cre mice in comparison to their respective control mice (Figure 44A). The immunized LMP1/CD30//C $\gamma$ 1-cre mice displayed significantly expanded CD8 T cell numbers in comparison to CAR mice (Figure 44A, right diagram). Two of the infected LMP1/CD30//C $\gamma$ 1-cre mice with a tumor burden revealed elevated CD8<sup>+</sup> T cells compared to the aged mice of this group. Surprisingly, the percentages of the effector CD8<sup>+</sup> T cells (CD62L<sup>lo</sup>, CD44<sup>mid/+</sup>) were significantly higher in the immunized LMP1/CD30//C $\gamma$ 1-cre mice in comparison

to their controls. This difference was not visible in the infected mice (Figure 44C). However, in the infected LMP1/CD30//C $\gamma$ 1-cre mice, memory CD8<sup>+</sup> T cells (CD62L<sup>+</sup>, CD44<sup>+</sup>) were significantly increased in comparison to control mice and to the immunized LMP1/CD30//C $\gamma$ 1-cre mice (Figure 44C, right diagram).

The expanded population of effector and memory T cells hinted towards a stronger T cell activation due to CD30 signaling alone and in combination with the virus infection. To analyze whether this results in T cell exhaustion, different exhaustion markers were studied in CD8<sup>+</sup> T cells. The percentages of Tim3<sup>+</sup> T cells were significantly higher in both cohorts of LMP1/CD30//C $\gamma$ 1-cre mice (Figure 44D). The infected LMP1/CD30//C $\gamma$ 1-cre mice displayed also significantly more KLRG1<sup>+</sup> CD8<sup>+</sup> T cells in comparison to their respective controls. One example of the gating strategy of both markers are displayed in the supplementary 3. The expression pattern of the analyzed exhaustion markers revealed parallel expression of KLRG1 and Tim3. This indicated that the CD30 signaling results in higher percentages of functional exhausted CD8<sup>+</sup> T cells. Surprisingly, the additional virus infection did not amplify this development.

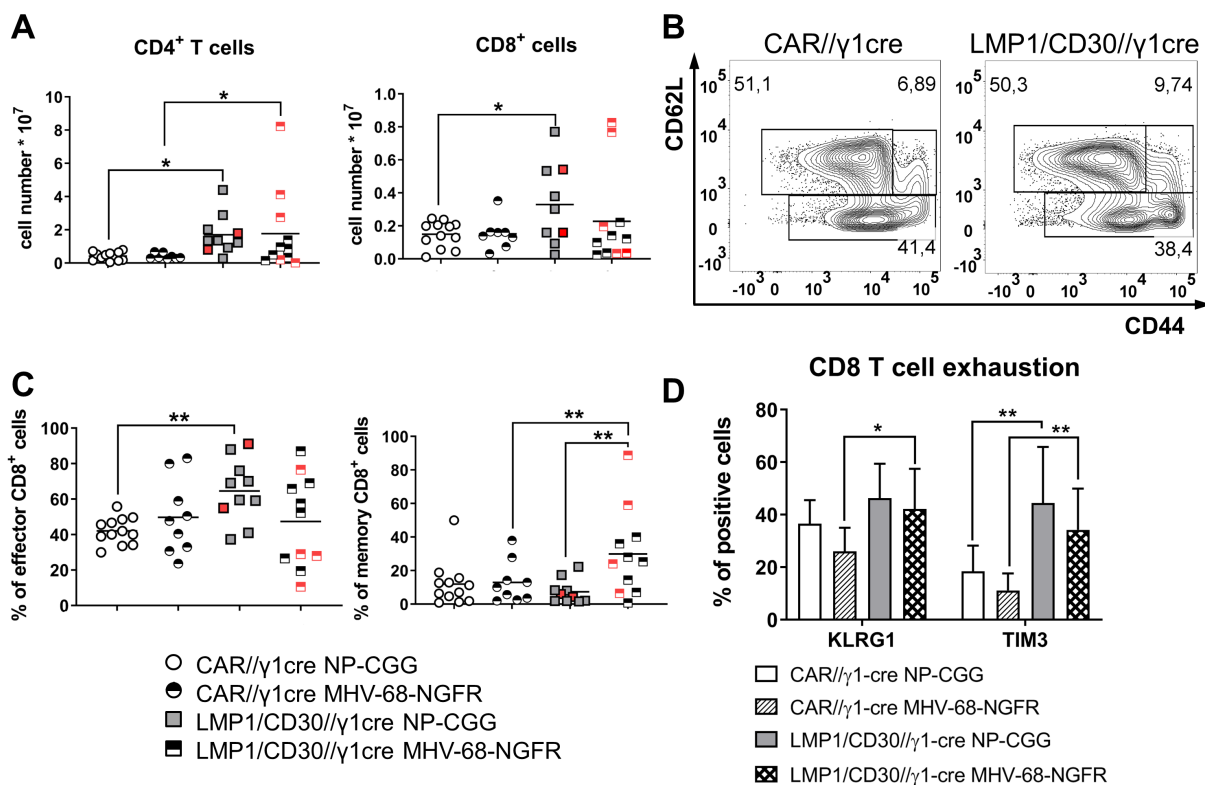


**Figure 44:** (A): The graphs show the cell numbers of CD4<sup>+</sup> and CD8<sup>+</sup> T cells prepared for Thy1.2<sup>+</sup> cells in the SP; (B): The FACS plots show the gating strategy of memory (Thy1.2<sup>+</sup>, CD8<sup>+</sup>, CD44<sup>+</sup>, CD62L<sup>+</sup>) and effector (Thy1.2<sup>+</sup>, CD8<sup>+</sup>, CD44<sup>+</sup>, CD62L<sup>lo</sup>) T cells; (C+D): The diagrams show the percentages of effector and memory CD8<sup>+</sup> T cells of the four analyzed mouse groups in the SP; (D): The graph shows the percentages of exhausted (KLRG1<sup>+</sup>/TIM3<sup>+</sup>) CD8<sup>+</sup> T cells of the analyzed aged mice in the SP.

### 5.3.7.6 Expansion of CD30 expressing cells correlates with increasing splenic weight in aged mice

Of note, there was a strong correlation between splenic weight and the cell number of reporter<sup>+</sup> cells in both LMP1/CD30//C $\gamma$ 1-cre groups (Figure 45A). In contrast, the percentages of CD19<sup>+</sup> B cells declined gradually in number with increasing splenic weight and percentage of reporter<sup>+</sup> cells (Figure 45B). This means more LMP1/CD30 expressing cells resulted in a stronger expansion of non B cells. The red arrows in the diagram represent the mice which were detected with a mono- oligoclonal expansion. Despite their increased percentages of reporter expressing cells among the B cell population, B cells were not the dominating cell population in the spleen of these mice. Therefore, the B cells were not responsible for the splenomegaly.

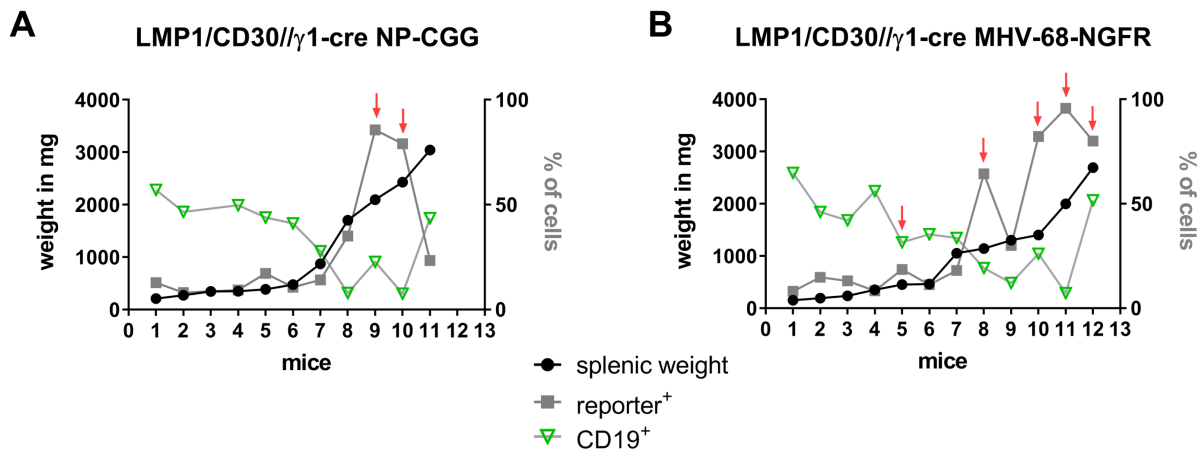


**Figure 45:** (A+B): The graphs show the correlation of splenic weight (left y-axes) and percentages of reporter<sup>+</sup> and CD19<sup>+</sup> cells (right y-axes) of each analyzed NP-CGG immunized and each MHV-68-NGFR infected LMP1/CD30//C $\gamma$ 1-cre mouse in the SP, the red arrows illustrate the mice which were analyzed with a mono- or oligoclonal expansion.

### 5.3.8 Lymphoma characterization

The lymphomas were characterized by a splenomegaly and strongly elevated total splenic cell numbers (see Figure 36, red icons). The percentages of either B or T cells were dramatically increased with one exception in #10. Figure 46 illustrates an overview of all analyzed lymphomas with their corresponding total cell numbers, T and B cell numbers and the reporter<sup>+</sup> cell numbers among the B cells in the spleen and the PerC. The percentages of reporter<sup>+</sup> B cells were in all detected lymphomas higher than 60% despite one exception at #63. Among both LMP1/CD30//C $\gamma$ 1-cre mouse cohorts, the mice detected with the lymphoma revealed the highest total cell numbers in the spleen (see also red icons in Figure 36A+B). Within the lymphoma, the distribution of the analyzed cell populations varied strongly. #10 and #17 did not display an expanded splenic T cell population in comparison to the other groups. #29 and #31, on the other hand, revealed

no increased splenic B cell population. The distribution of cell population in #50 differed in the PerC and the spleen. In the spleen, the B cell population of this mouse dominated, in the PerC, the T cells were strongly expanded. However, #17 displayed a clear enhanced B cell population in the spleen and the PerC. In #17 and #50, in the spleen and the PerC, a mono- or oligoclonal expansion could be detected. #17 revealed the same clone whereas in #50 two different clones could be detected in the spleen and the PerC. This was already reflected in the distribution of the cell populations between spleen and PerC in these two samples.

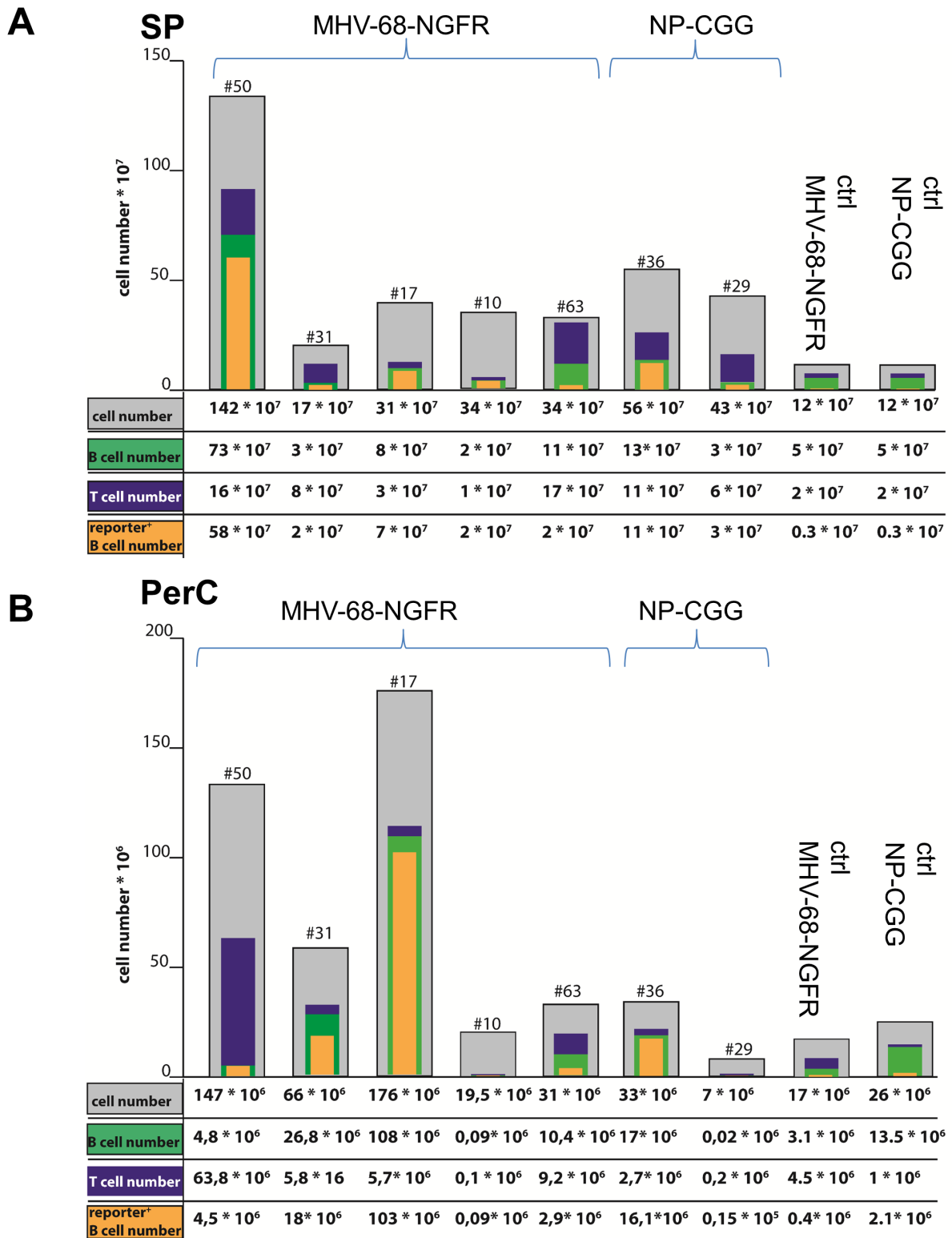


**Figure 46:** (A+B): The graph shows an overview of all analyzed lymphomas from the infected and immunized LMP1/CD30//C $\gamma$ 1-cre mice. The total cell number, T cell numbers (Thy1.2<sup>+</sup>), B cell numbers (CD19<sup>+</sup>), and the reporter<sup>+</sup> cell numbers among the B cell numbers in the SP (A) and the PerC (B) depicted. The table shows the numbers of the cells.

In order to further characterize the tumor population, FACS analyses of surface mark-

ers were performed. Here, all reporter<sup>+</sup> B cells demonstrated a strong expansion of the CD21<sup>lo</sup>, CD23<sup>lo</sup> population. In comparison to the total aged cohort, the mice detected with a lymphoma revealed the highest percentage of CD21<sup>lo</sup>, CD23<sup>lo</sup> cells (Figure 47C, right diagram). Most of the cases were positive for CD43 and low for CD23 but also low in CD5 and B220, hinting to a B1b cell phenotype. Thus, two of the lymphomas were low in all these markers resembling an unknown aberrant B cell population. Also in terms of IgM/IgD surface expression, IgM positive as well as negative cases were represented among the lymphoma incidences (Figure 47A-D). The IgM negative cases might have switched to another isotype e.g. IgG1. Figure 47 illustrates the observed different phenotypes. The sample number above belongs to the depicted FACS plot and the numbers in brackets refer to samples which are similar to the ones shown.

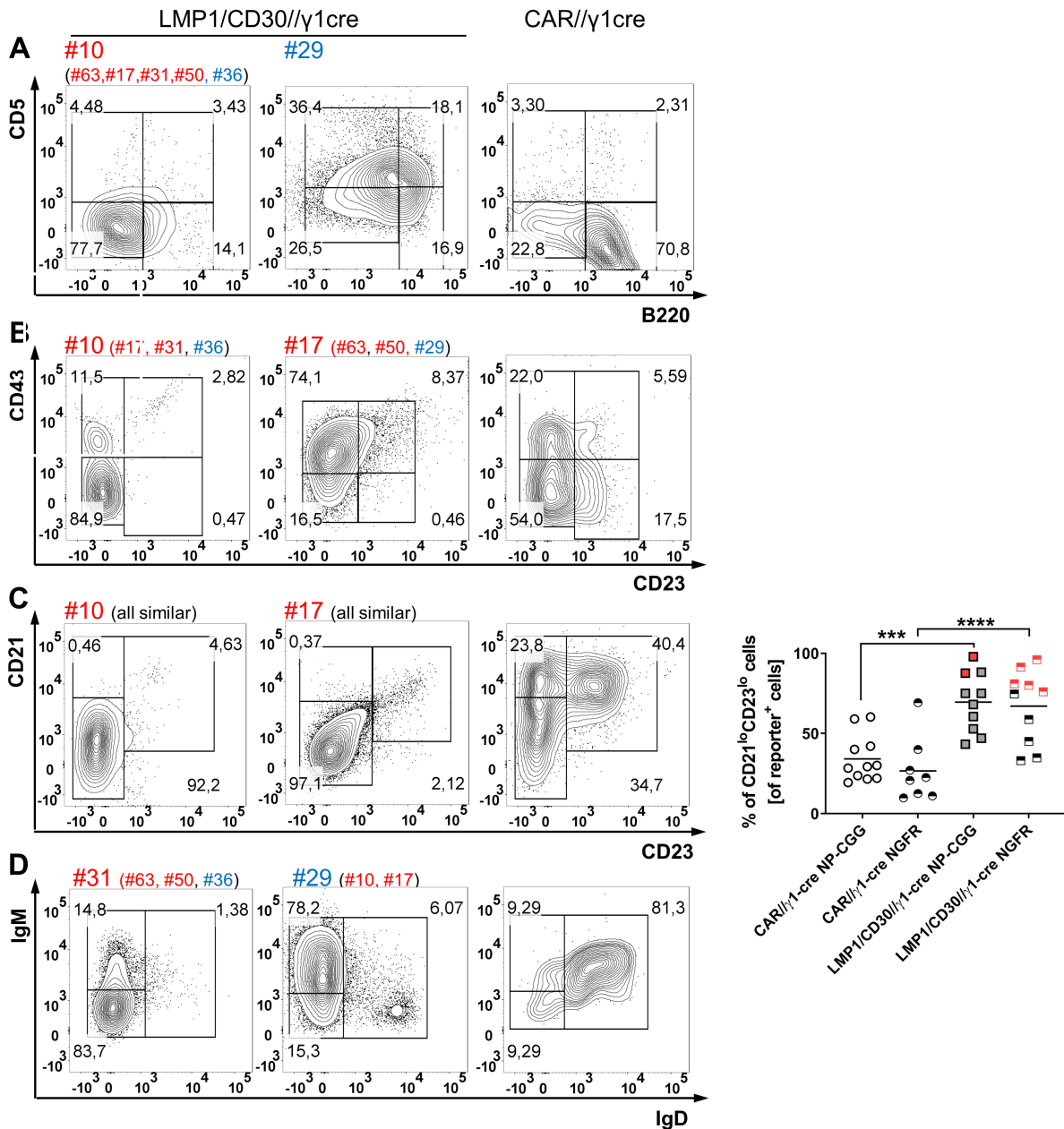


**Figure 47:** The FACS plots display different B cell sub-populations in the SP of two different lymphoma samples and a CAR control, cells were pregated for CD19<sup>+</sup> and reporter<sup>+</sup> (A): The cells were analyzed for B1a (CD5<sup>+</sup>, B220<sup>lo</sup>), B1b (CD5<sup>lo</sup>, B220<sup>lo</sup>) and B2 (CD5<sup>lo</sup>, B220<sup>+</sup>) cells; (B): The cells were analyzed for CD43<sup>+</sup>/CD23<sup>lo</sup>, CD43<sup>lo</sup>/CD23<sup>lo</sup>, CD43<sup>lo</sup>/CD23<sup>+</sup>; (C): The splenic cells were analyzed for CD21<sup>lo</sup>/CD23<sup>lo</sup>, CD21<sup>+</sup>/CD23<sup>lo</sup>, CD23<sup>+</sup>/CD21<sup>+</sup>, the diagram on the right side shows the percentages of CD21<sup>lo</sup>, CD23<sup>lo</sup> cells of reporter<sup>+</sup> CD19<sup>+</sup> cells in aged mice in the SP; (D): The cells were analyzed for IgM<sup>+</sup>, IgM<sup>+</sup>/IgD<sup>+</sup>, and IgM<sup>lo</sup>/IgD<sup>lo</sup>, the numbers above refer to the mouse number the FACS plot was taken from, the numbers in brackets refer to mice which looked similar to the depicted plot, blue for NP-CGG, red for MHV-68-NGFR infected mice.

Some reporter expressing cells were negative for the IgM expression. HL expresses high levels of CD30, are associated with EBV infection and are characterized by a loss of B cell specific gene expression profile, including the BCR [Schwering et al., 2003,

Aldinucci et al., 2010]. To discriminate whether in  $IgM^-$  cells the BCR components are downregulated like in HL or whether the cells have switched to another isotype we stained for the BCR-signaling domain  $CD79\beta$  ( $Ig\beta$ ) which is associated with the BCR independent of the switched isotype [Murphy et al., 2012]. The mice detected with a lymphoma revealed a high expressed  $CD79\beta$  (Figure 48A), indicating that they express an isotype switched BCR on their cell surface. The cell size of the LMP1/CD30 expressing B cells in mice with a tumor was clearly increased in comparison to controls which was detected by the forward scatter (FSC) of these cells in comparison to control B cells (Figure 48B).

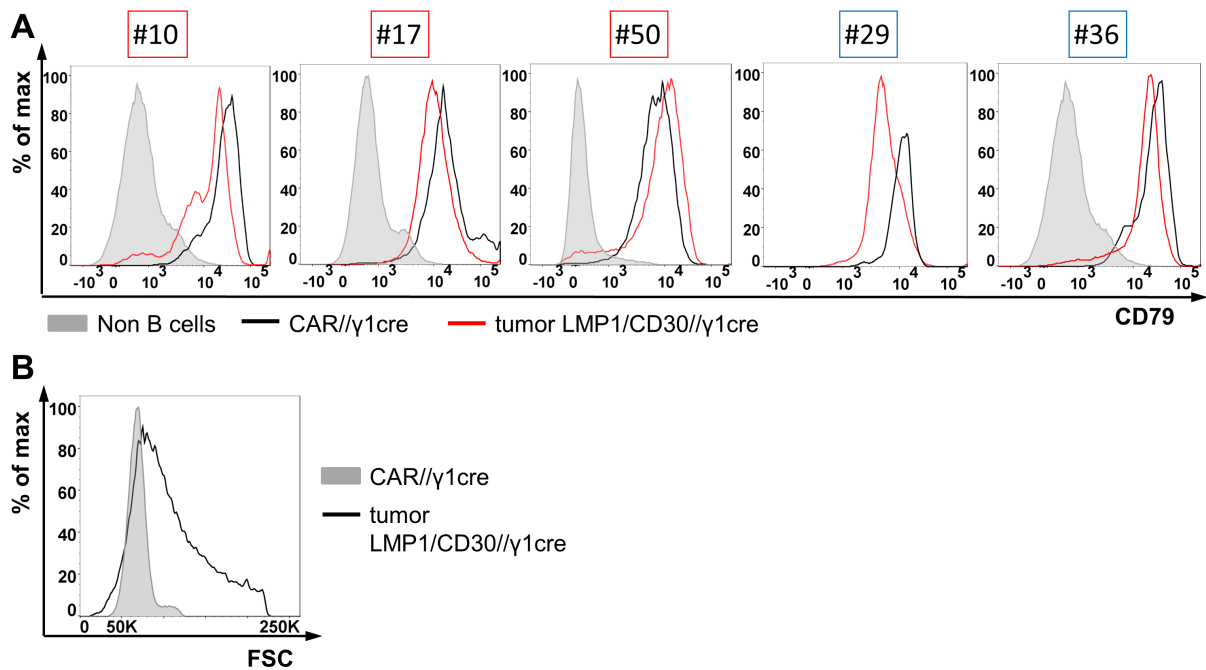


**Figure 48:** (A): The histograms show an overlay of  $CD79\beta$  expression of non B cells, reporter<sup>+</sup> cells of a CAR// $C\gamma 1$ -cre mouse, and the different LMP1/CD30// $C\gamma 1$ -cre tumor samples as indicated, the numbers in the red boxes are infected mice, numbers in the blue boxes indicate immunized mice; (B): The histogram shows one representative example of the FSC of reporter<sup>+</sup> cells of one LMP1/CD30// $C\gamma 1$ -cre tumor sample (black line) and one control (grey).

The increased cell size of degenerated reporter<sup>+</sup> cells characterizes activated cells. Therefore, we tested CD95 as activation marker. Here, we compared CD95 expression of the reporter positive versus negative B cells. In aged LMP1/CD30// $C\gamma 1$ -cre mice without a mono- or oligoclonal cell expansion, CD95 was upregulated in LMP1/CD30 expressing cells in comparison to control CAR expressing cells. In burdened mice, CD95 was further upregulated in both  $hCD2^+$  and negative B cells. In some cases, the reporter<sup>-</sup> B cells even demonstrated a similar upregulation of CD95 like the reporter expressing B cells (Figure 49A). This hints to an activation of normal cells by the tumor cells. Furthermore, among the analyzed mice, the burdened mice exposed the highest percentage of CD95<sup>+</sup> reporter<sup>+</sup> B cells (Figure 49B).

In order to examine whether the lymphoma cells infiltrate the BM, the percentages of reporter<sup>+</sup> B cells in the BM were determined. All mice with a lymphoma displayed higher percentages of LMP1/CD30 expressing B cells compared to the tumor-free samples. Especially, in lymphomas of infected LMP1/CD30//C $\gamma$ 1-cre mice, up to 75% B cells were reporter<sup>+</sup> indicating that the lymphoma cells infiltrated the BM (Figure 49C).

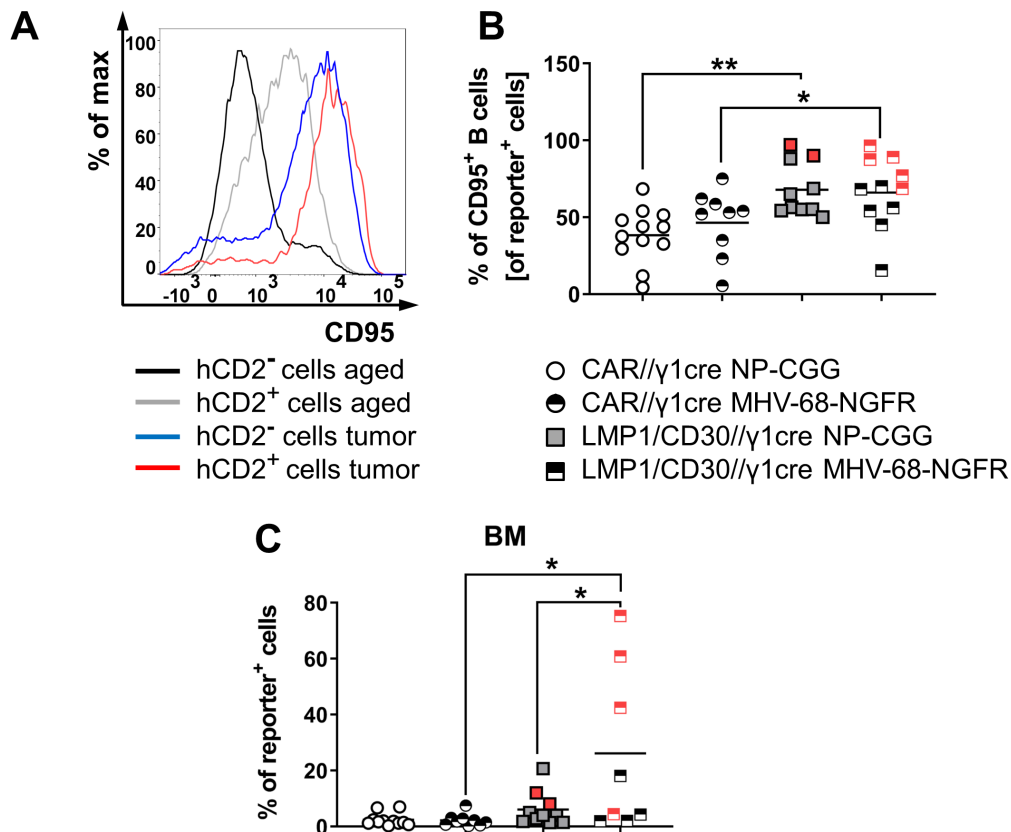


**Figure 49:** (A): The histogram shows an overlay of CD95 expression of hCD2<sup>+</sup> and hCD2<sup>-</sup> B (CD19<sup>+</sup>) cells of an aged mouse (grey+black) and a tumor mouse (blue+red); (B): The diagram shows the percentages of CD95<sup>+</sup> reporter<sup>+</sup> B cells in the SP; (C): The graph shows the percentages of reporter<sup>+</sup> cells in the BM. Cells were pregated for lymphocytes and CD19<sup>+</sup> cells. Every dot represents the value obtained from one mouse, the bar represents the mean of the percentages.

In order to assess the lymphomas further, histology was performed on frozen and paraffin embedded spleen sections. The staining on the paraffin embedded sections was performed in cooperation with Dr. Feuchtinger and Dr. Parzefall from the Core Facility Analytical Pathology. Generally, the splenic sections of the analyzed LMP1/CD30//C $\gamma$ 1-cre mice displayed similar alterations (Figure 50). The Hematoxylin/Eosin staining revealed a disrupted splenic structure. This was caused by a large infiltration of neoplastic cells in the white pulp, provoking a compression of the red pulp. The expanded cell population was composed of heterogeneous cells. In the HE staining, large, often blastic

B cells were intermingled with small lymphocytes, monocytes, macrophages, mesenchymal spindle cells, few granulocytes, extramedullary erythrohemopoietic cells and various numbers of multinucleated giant cells. The B220 staining was greatly diminished in the lymphoma samples. This was already visible in the FACS analysis (see Figure 47). Also, no clear location of the B cells in the B cell zone was visible. The CD3 expressing T cells remained comparable in number but lost their localization in the T cell zone in some cases (Figure 50).

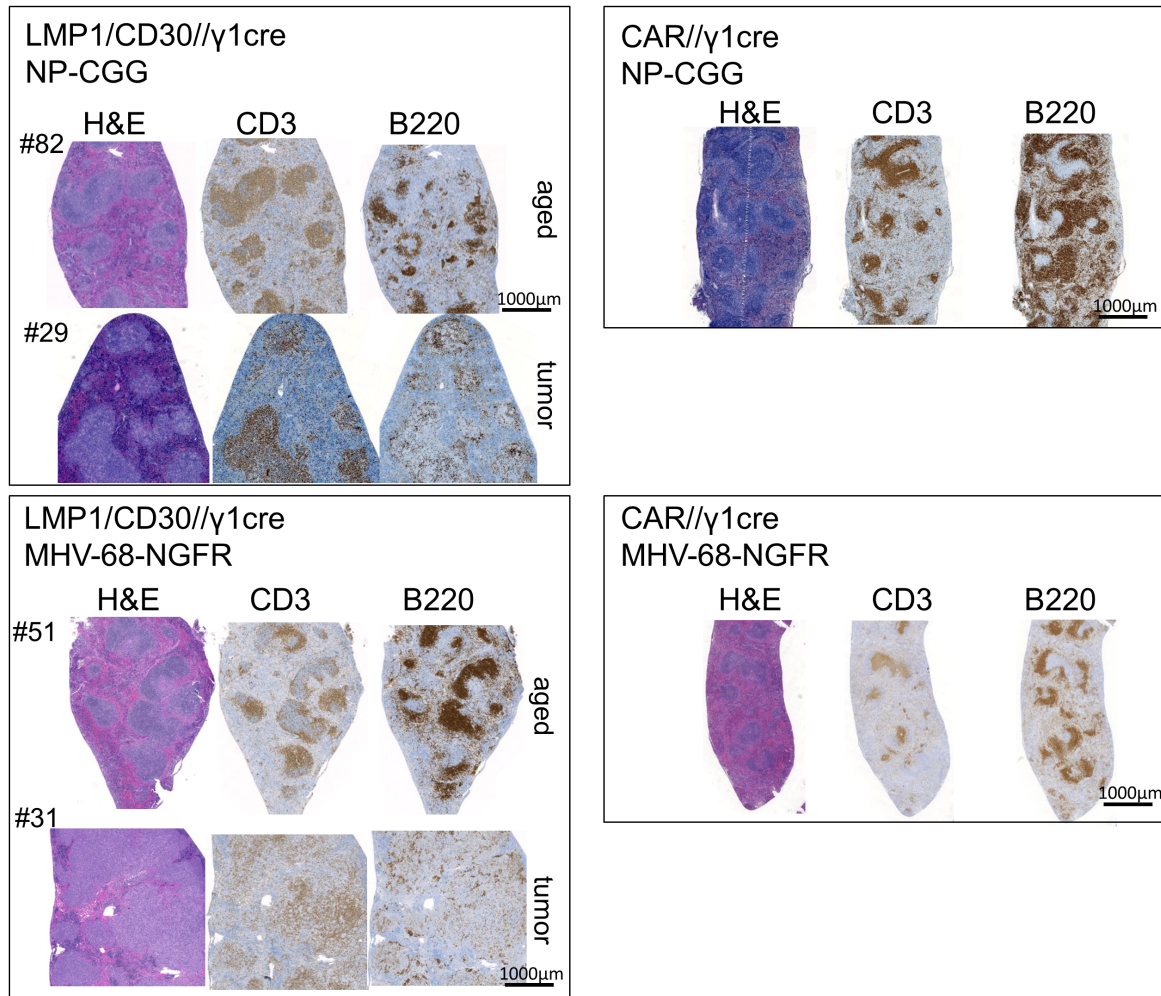


**Figure 50:** The histology images show staining of paraffin embedded SP samples. The tissue was stained with Hematoxylin/Eosin, anti-CD3 (T cells), and anti-B220 (B cells). In both LMP1/CD30//C $\gamma$ 1-cre groups, one aged without lymphoma and one tumor sample is shown, respectively. On the right side, one control mouse from each group is depicted.

Some multinucleated giant cells which were visible in the white pulp resembled the phenotype of the Reed-Sternberg cells in HL. Therefore, we asked if the developed lymphoma resemble HL. Further staining was performed to characterize these large cells (Arrows, Figure 51A). These cells were partially positive for CD79 $\alpha$  but negative for CD19, CD30 and CD45R (Figure 51A). Following, these cells were stained for the von Willebrand

factor (vWF). The positive staining for this factor characterized them as megakaryocytes rather than Reed-Sternberg cells [Chuang et al., 2000]. To add on this, an increased CD30 expression, distributed throughout the expanded cell population, was observed (Figure 51B). Thus, we wanted to typify the CD30<sup>+</sup> cells further.

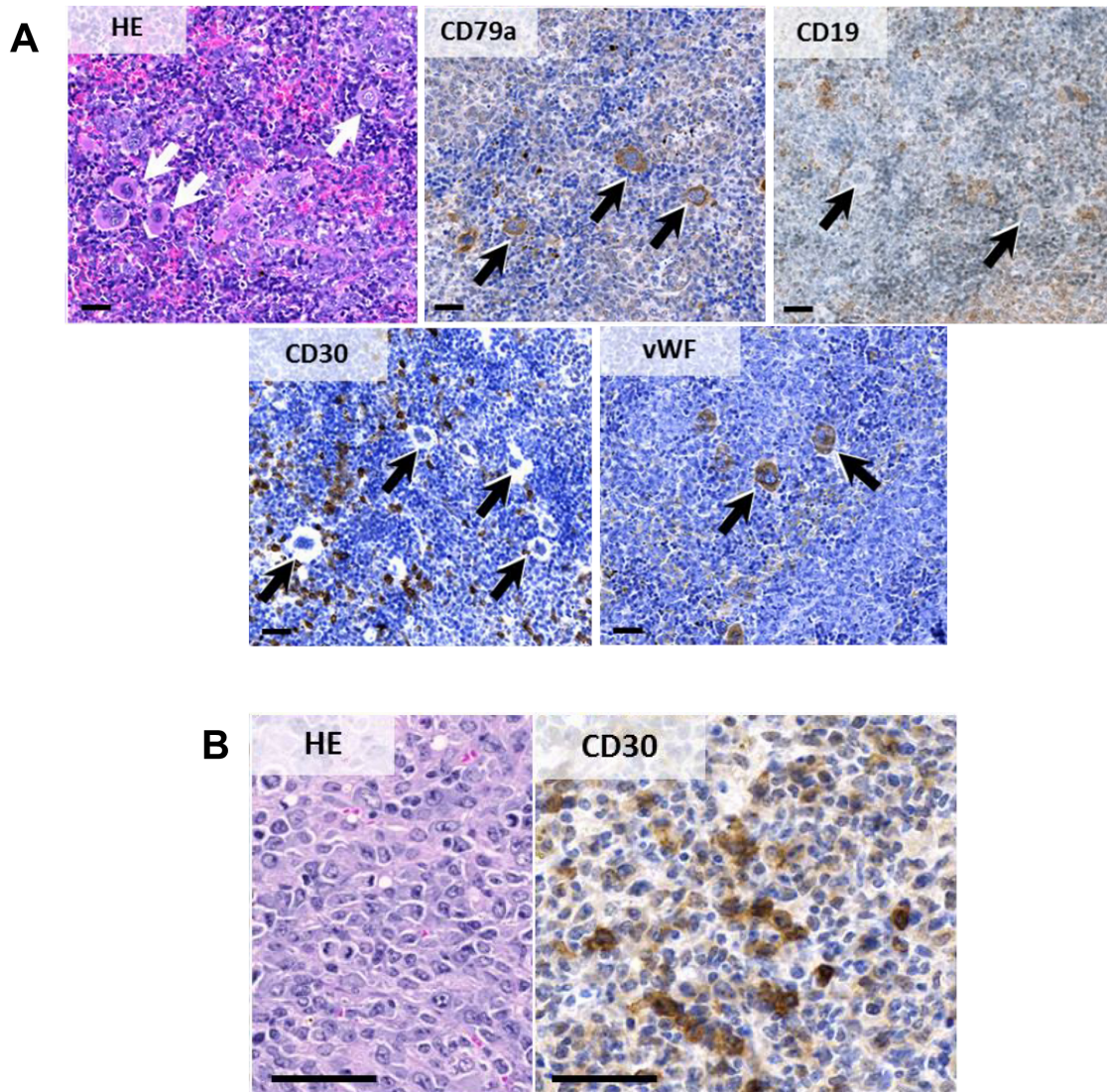


**Figure 51:** (A+B): Representative histology of spleens of one LMP1/CD30//C $\gamma$ 1-cre mice which was detected with a mono- or oligoclonal expansion. Tissue was stained with CD19, CD79 $\alpha$ , HE, CD45R, CD30, and vWF. Bars = 50  $\mu$ m.

The staining for CD30 in the paraffin embedded splenic sections was run by Dr. Parze-fall from the Core Facility Analytical Pathology. Figure 52A compares a wt spleen section with a tumor (#29) spleen section. In both staining, no co-stained CD3 and CD30 cells were visible. Therefore, the effects which were examined in the LMP1/CD30//C $\gamma$ 1-cre mice can probably be attributed to the CD30 expression of B cells. The detection of reporter<sup>+</sup> cells was carried out on the splenic sections embedded in OCT. CD30 expres-

sion was monitored by staining for hCD2 (Figure 52B). First, we examined the aged mice without a tumor burden. Here, the hCD2 expressing B cells were mainly found within the follicle or at the border of it assuming a pre-plasmablast phenotype. The mouse of the left picture revealed 7% hCD2<sup>+</sup> cells in the FACS analysis and the mouse from the right picture 19% proofing the correctness of the staining. The expression pattern seemed unequal among the cells. There were also clusters differing in size and location with a higher hCD2 expression compared to the remaining reporter positive cells. In the lymphoma samples on the other hand, only big clusters of hCD2 expressing B cells, scattered throughout the splenic tissue, were visible. There was no clear follicle structure discernible in order to characterize the location of the degenerated B cells within the spleen. But also clusters expressing higher levels of hCD2 were distributed among this population.

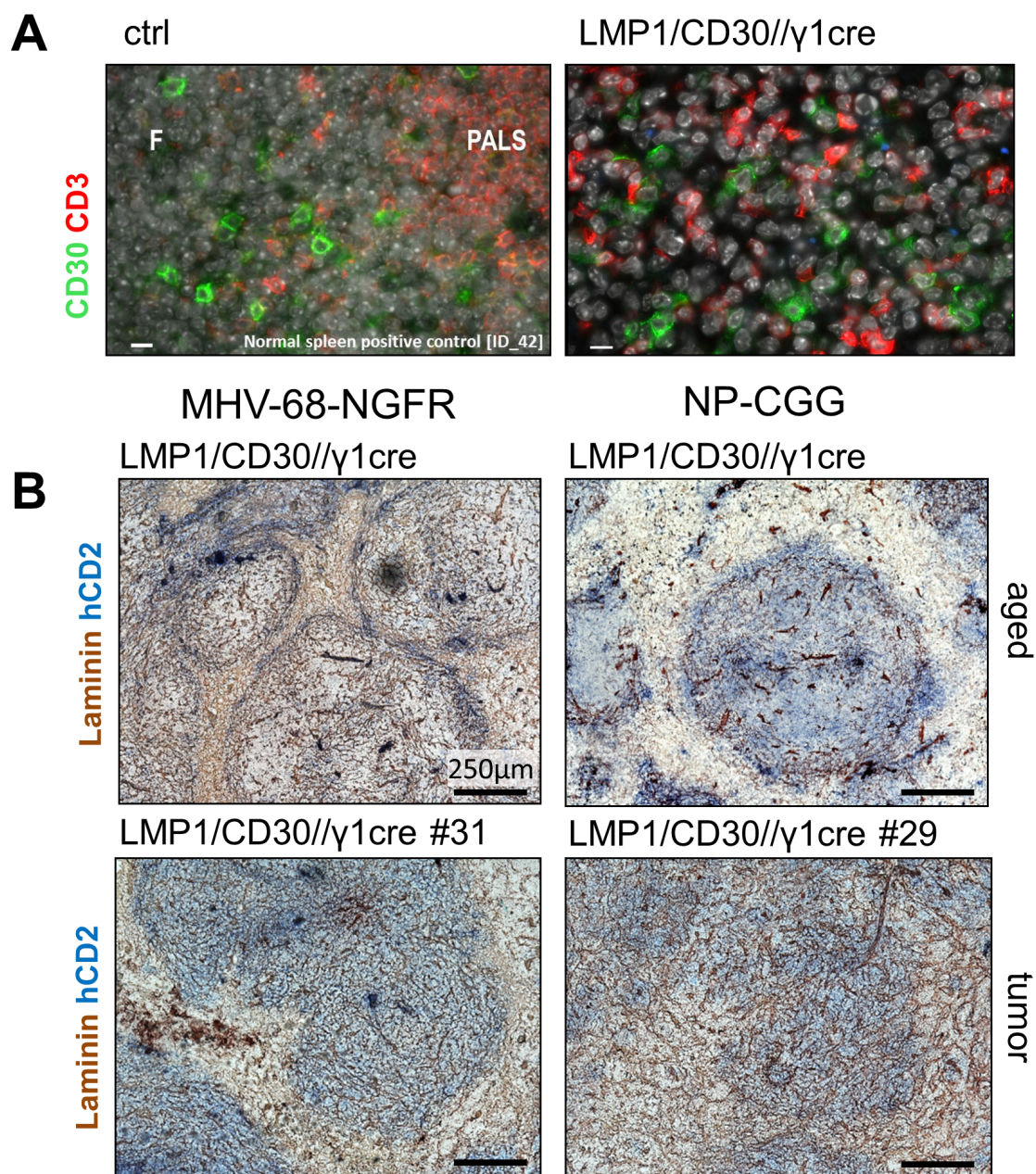


**Figure 52:** (A): Paraffin embedded splenic tissue was stained for CD3 (red) and CD30 (green), shown is one ctrl section and one tumor sample (#29); (B): OCT embedded splenic tissue was stained with anti-hCD2 and anti-Laminin. From the LMP1/CD30// $\gamma$ 1-cre groups one representative example of an aged and a tumor mouse is depicted.

#### 5.4 Infection of mice with MHV-68-LMP1wt virus leads to its elimination

EBV is the first described lymphoma associated virus [Palmer et al., 1964]. In several B cell lymphomas, NK-, and T- non HL as well as epithelial derived malignancies, EBV

occurrence could be identified [Thorley-Lawson and Gross, 2004]. LMP1 is expressed in most of these malignancies and is considered to contribute to the malignant transformation. LMP1 is known to be the key factor in driving cell proliferation and promoting metastasis, apoptotic resistance, and immune modulation. Until now, the effect of LMP1 could only be analyzed through transgenic expression in B cells of mice, in LCLs *in vitro*, or by infecting humanized immunodeficient mice [Middeldorp and Pegtel, 2008]. The cloning of LMP1 in a recombinant MHV-68, and the subsequent infection of mice with this virus, appears to be a model mimicking much more the physiological condition found in EBV associated lymphomas. Therefore, a recombinant MHV-68 expressing LMP1 was constructed by BAC technology which was performed by Wei Zhang in H. Adlers laboratory. The virus is named MHV-68-LMP1wt thereafter (Figure 53A). Additionally, another recombinant MHV-68 containing the LMP1 sequence with mutations in both signaling domains was used as control, named MHV-68-LMP1mut hereafter. Both, LMP1wt and LMP1mut are expressed under the control of the CMV promoter. First, we analyzed the lytic replication of the constructed viruses *in vitro*. Both LMP1 variants attained similar titers as the parental virus at the different time points (Figure 53B). Therefore, the replication of the MHV-68-LMP1wt and -LMP1mut viruses seemed not affected by the insertion of the LMP1 sequence. The expression of LMP1 induced through viral infection was shown by western blot analysis of infected NIH3T3. The LMP1wt protein run at 63 kDa whereas the LMP1mut was slightly underneath located due to the shortened amino acid sequence (Figure 53C).

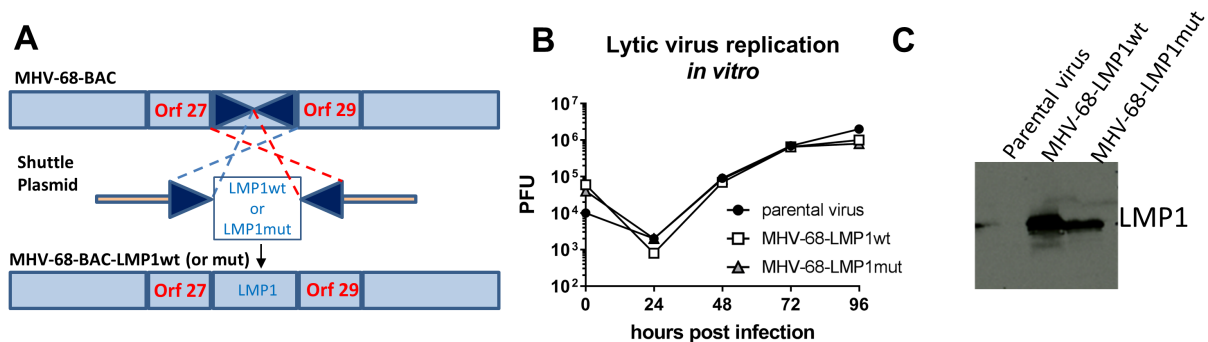


**Figure 53:** (A): The LMP1wt or the LMP1mut, with a mutated signaling domain, were expressed under the control of the CMV promoter and inserted between Orf27 and 29 in the MHV-68 BAC by homologous recombination; (B): NIH3T3 were infected with the indicated viruses at a multiplicity of infection (MOI) of 0.1. At the different time points after infection, cells and supernatants were harvested. The virus titers were detected by plaque assay on BHK-21 cells; (C): NIH3T3 were infected with either MHV-68-LMP1wt or MHV-68-LMP1mut virus. 3 d p.i., protein was isolated and analyzed for LMP1 expression by western blot.

#### 5.4.1 MHV-68-LMP1wt infection leads to a terminated splenic GC reaction in mice

LMP1 mimics the CD40 receptor of B cells but needs no ligand for an active signaling [Rastelli et al., 2008, Uchida et al., 1999]. On the other hand, chronic CD40 as well as chronic LMP1 expression in B cells leads to a block in the GC reaction [Hömig-Hölzel et al., 2008, Uchida et al., 1999]. However, there are some GC B cells with active CD40 signaling due to the initiation of positive selection through CD40L expressing T cells. Also LMP1<sup>+</sup> B cells are found in the GC [Tsai et al., 2018, Thorley-Lawson, 2015]. Therefore, the question was if GC are developed in mice infected with MHV-68-LMP1wt. The infection with MHV-68 induces a GC reaction in C57BL/6 mice [Sunil-Chandra et al., 1992]. The GC formation was analyzed by FACS and histology. For this, C57BL/6 mice were infected with the parental virus, MHV-68-LMP1wt, or MHV-68-LMP1mut and analyzed after 14, 17, and 21 d (Figure 54A). At d 14, the percentages of GC B cells were comparable in the spleen in all three groups of mice. However, at d 17 and 21, the percentages of GC B cells were strongly decreased in the spleen of mice infected with MHV-68-LMP1wt (Figure 54A+C). MHV-68-LMP1mut infected mice displayed a similar percentage of GC B cells as parental virus infected mice at d 17 p.i.. However, at d 21 p.i., the percentage of GC B cells was reduced when compared to mice infected with parental virus. In contrast, at all analyzed time points, the GC formation, investigated in the LN, was increased in the MHV-68-LMP1wt infected mice in comparison to the groups infected either with the parental virus or MHV-68-LMP1mut (Figure 54B). The peak was reached at d 21 p.i., the percentage of GC B cell in the MHV-68-LMP1wt infected mice was almost fourfold higher than in the two other groups. This could hint to a stronger persistence in the LN rather than in the spleen of the MHV-68-LMP1mut virus in comparison to the control viruses.

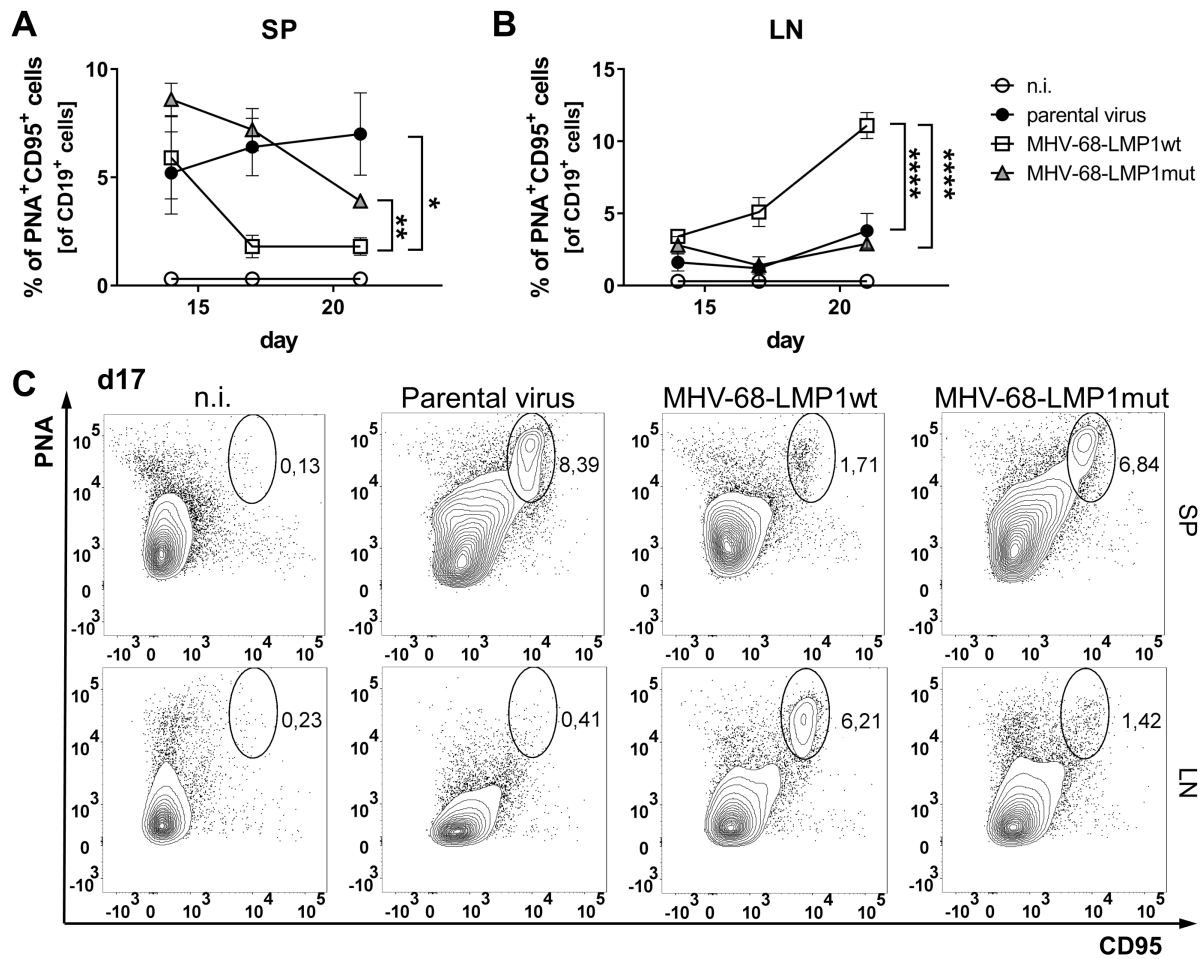


**Figure 54:** Mice were infected with parental virus, MHV-68-LMP1wt and MHV-68-LMP1mut intranasally (i.n.) and analyzed at d 14, 17, and 21 p.i. (A): The splenocytes of mice infected with the indicated viruses or n.i. were stained for GC B cells (PNA<sup>+</sup>, CD95<sup>+</sup>); (B): The LN cells of mice infected with the indicated viruses or n.i. were stained for GC B cells (PNA<sup>+</sup>, CD95<sup>+</sup>); (C) The FACS plots show one representative example of the gated GC B cells at d 17 p.i. of SP and LN, numbers indicate the percentages,  $n \geq 3$ .

The development of the GC in the spleen could be confirmed by histology at d 17 p.i.. Staining with PNA proved the reduction of GC in the spleens of MHV-68-LMP1wt infected mice in comparison to the parental virus and the MHV-68-LMP1mut (Figure 55A). Furthermore, the staining of LMP1 revealed positive stained cells in the center of the follicle and at the border between B and T cell zone (Figure 55B). Summing up, the infection of mice with MHV-68-LMP1wt induced a GC reaction but displayed a fast decline in the spleen at d 17. However, the percentage of GC B cells in the LN was increased in these mice at d 17 and expanded further until d 21. Further, we found evidence for LMP1 expressing B cells in the splenic follicle. In contrast, the infection with MHV-68-LMP1mut displayed a faster decline of GC B cells in comparison to the parental virus.

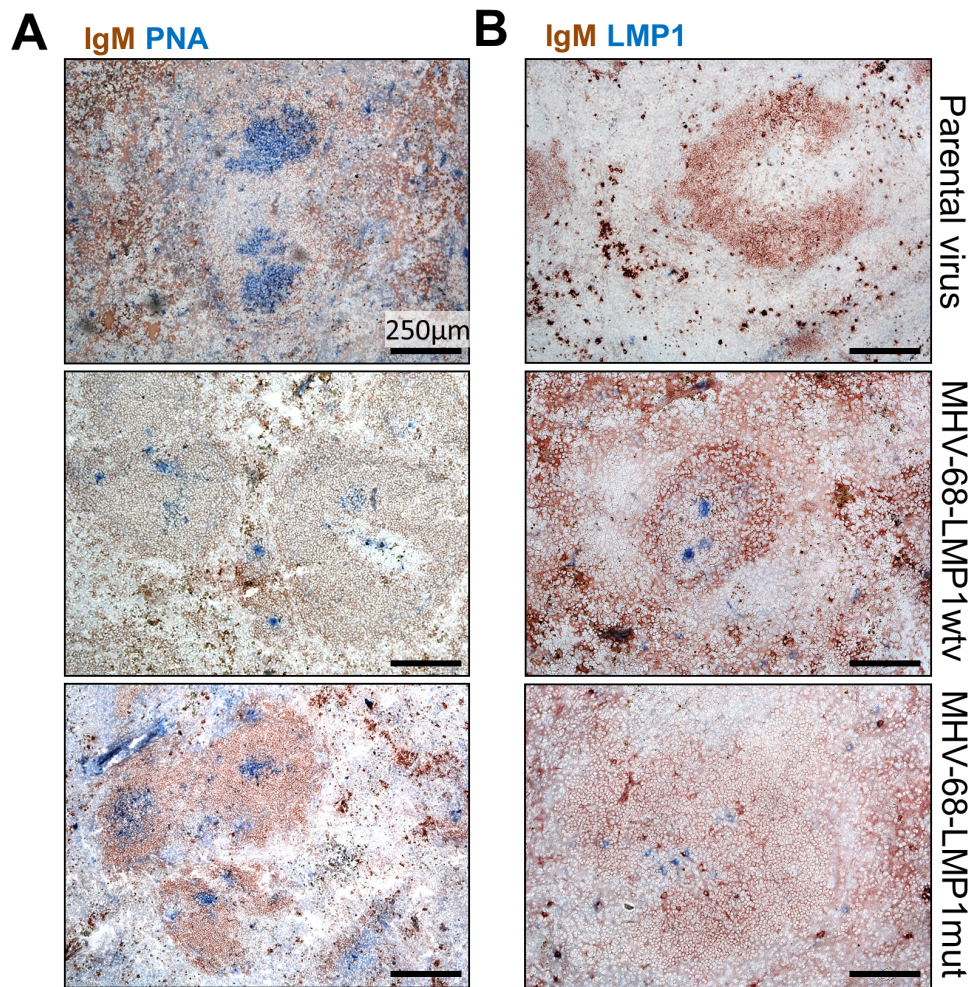


**Figure 55:** At d 17 p.i., splenic sections of parental virus, MHV-68-LMP1wt and MHV-68-LMP1mut infected mice were embedded. (A): Splenic sections were stained with anti-PNA (blue) and anti-IgM (brown); (B): Splenic sections were stained with anti-IgM (brown) and anti-LMP1 (blue), shown is one representative example.

#### 5.4.2 MHV-68-LMP1wt showed impaired lytic replication in the lungs of infected mice and no reactivation *ex vivo*

After intranasal inoculation, MHV-68 replicates lytically in the lung [Sunil-Chandra et al., 1992]. After the peak of the lytic replication at d 7, the virus infection spreads towards the other organs like the spleen and the LN. The splenic weight represents a strong indicator for lymphoproliferation which occurs during MHV-68 infection and peaks around d 17 [Sunil-Chandra et al., 1992]. Therefore, we monitored the splenic weight over three weeks starting at d 7 p.i. (Figure 56A). Interestingly, the splenic weight in the LMP1wt infected mice remained equal compared to the mice infected with both control viruses until d 10. However, at d 17, no further increase of the splenic weight was detectable, displaying almost similar values as in uninfected control mice. This was in strong contrast to the parental virus and MHV-68-LMP1mut infected mice. Thus, the

splenic weight as well as the percentages of GC B cells followed an analogous trend in MHV-68-LMP1wt infected mice. The splenic weight of the mice infected with MHV-68-LMP1mut was similar compared to parental virus infected mice until d 14 p.i.. At d 17 p.i., the splenic weight was slightly reduced. In order to further investigate the performance of the different viruses in these mice, the reactivation capacity was determined at d 17 p.i.. The *ex vivo* reactivation assay of splenic cells isolated from the three analyzed groups revealed an almost similar reactivation capacity of the MHV-68-LMP1mut virus compared to the parental virus (Figure 56B). In contrast, MHV-68-LMP1wt displayed no reactivation. This means that there was probably no reactivation-competent virus present in the spleen of MHV-68-LMP1wt infected mice. To answer the question if there was virus present at any time in the spleen, the genomic load was determined. Comparably to the results obtained before, the genomic load was decreased in MHV-68-LMP1wt infected mice at d 10 and 17 in the spleen (Figure 56C). However, at d 21 p.i., the levels were similar between all three groups in the spleen. In the LN, the genomic load of MHV-68-LMP1wt was comparable with the control viruses at d 10 p.i., but decreased dramatically at d 17 p.i.. At d 21 p.i., the genomic load was similarly decreased in MHV-68-LMP1wt and LMP1mut in comparison to the mice infected with the parental virus (Figure 56D). Therefore, the MHV-68-LMP1wt virus did not undergo latency establishment and was already cleared at d 17 p.i.. Finally, the virus titers of the lytic phase in the lung were determined by plaque assay. The MHV-68-LMP1wt revealed reduced lytic replication in the lung compared to the control viruses (Figure 56E).

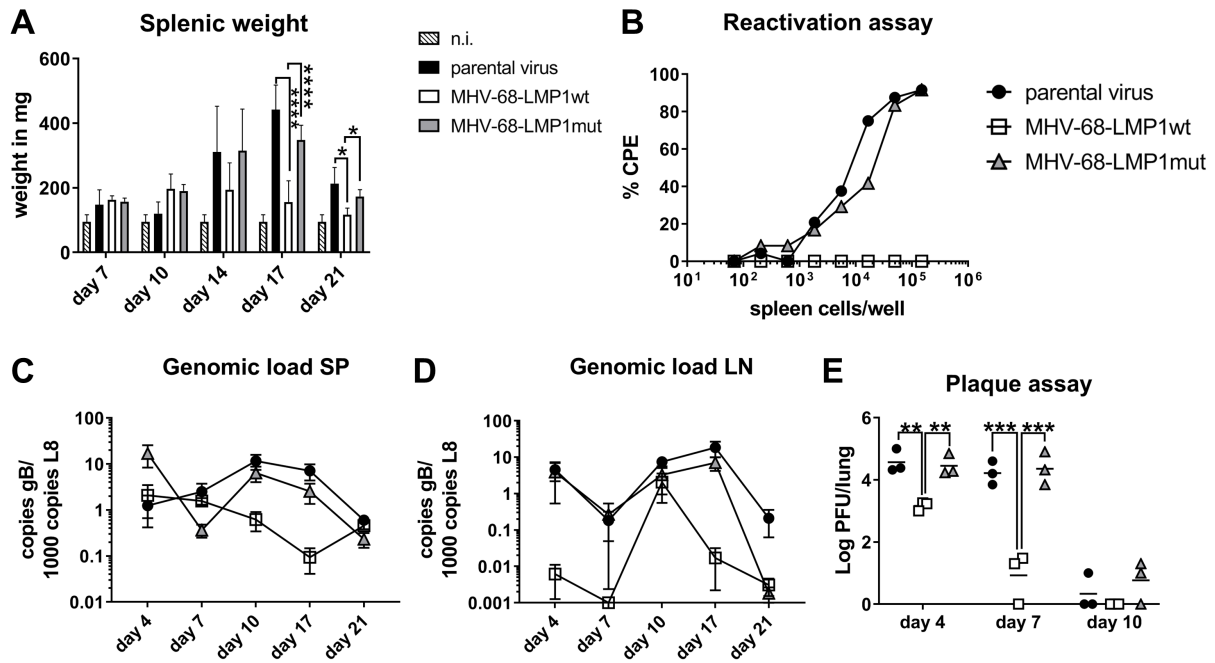


**Figure 56:** (A): The graph shows the splenic weight of n.i. mice or mice infected with the indicated viruses at different time points,  $n \geq 3$ ; (B): At d 17, splenocytes of mice infected with the indicated viruses were isolated and analyzed in an *ex vivo* reactivation assay. The splenocytes of three mice were pooled; (C+D): The genomic load of splenic and LN cells was determined by real time PCR upon isolation of DNA, the viral copies were quantified by amplifying viral copies (gB) and cellular copies (L8); (E): The lungs of infected mice were harvested at the indicated time points p.i., the virus titers of the homogenized lungs were determined by plaque assay,  $n \geq 3$ .

The genomic load was reduced in MHV-68-LMP1wt infected mice in the spleen and the LN. This was presumably triggered due to clearance of virus infected cell mediated by immune cells. Therefore, the PerC, another side of latency establishment of MHV-68, was examined. In the B cells of the PerC, the levels of the viral DNA were similar in all three groups at d 16 p.i. (Figure 57A). These levels were as high as detected in the spleen of parental virus infected mice at d 17. Also, the non B cells isolated from the PerC carried similar amounts of viral DNA in all three groups (Figure 57B). Therefore, despite the clear reduction of MHV-68-LMP1wt in the spleen and the LN, the virus was still detectable with even similar amounts as the control viruses in the PerC (Figure 57).

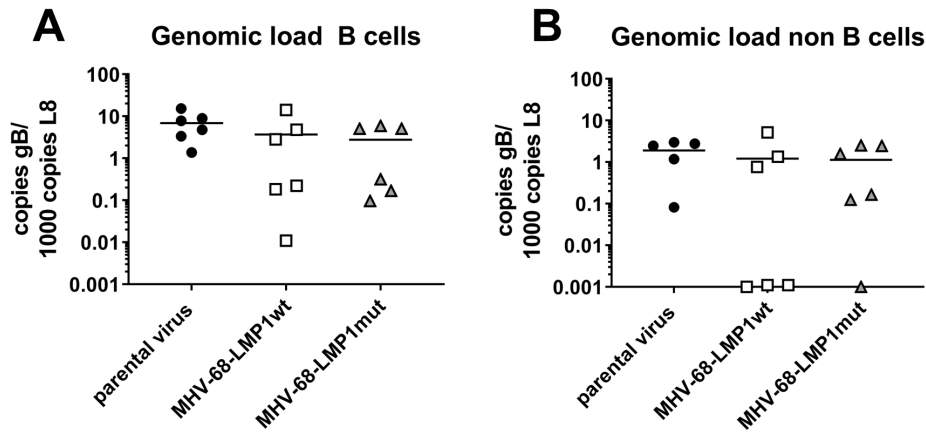


**Figure 57:** The genomic load of the cells isolated from the PerC was determined by real time PCR, the viral copies were quantified by amplifying gB and cellular copies by amplifying L8. B cells were isolated with the Pan B cell kit at d 16 p.i.. The genomic load was also determined from the non B cell fraction.

In summary, the expression of LMP1 in virus infected B cells caused a reduction of these cells starting between d 10 and d 14. Hereby, the LMP1 signaling can be ascribed as responsible due to the use of LMP1mut as control. The vanishing of the virus resulted in a total lack of reactivation capacity, reduced genomic load, and a reduced splenomegaly at d 17. Further, the reduced GC B cells in the MHV-68-LMP1wt infected B cells can probably be attributed to the low amounts of the virus in the spleen of these mice. However, cells carrying MHV-68-LMP1wt DNA to the same extent as the control viruses were detectable in the PerC.

#### 5.4.3 LMP1wt infected B cells obtain survival signals *in vitro*

LMP1 activates, similar to active CD40 signaling, NF- $\kappa$ B transcription factors and inhibits apoptosis [Rastelli et al., 2008, Uchida et al., 1999, Cahir-McFarland et al., 2004]. Thus, cells expressing LMP1 should receive an enhanced survival signal. The reason for the fast disappearance of cells infected with the MHV-68-LMP1wt is therefore difficult to understand. To study the survival of MHV-68-LMP1wt infected B cells without the influence of other immune cells, we infected naive splenic B lymphocytes with MHV-68-NGFR, MHV-68-LMP1wt, or MHV-68-LMP1mut *in vitro*. This was realized with a co-culture of murine fibroblasts supporting lytic replication of the viruses. Due to the infection with MHV-68-LMP1wt, the B cells express LMP1wt with active signaling. The infection with MHV-68-LMP1mut induces expression of LMP1 in the infected B cells with silenced signaling. The cell numbers of splenic B lymphocytes were monitored for 7 d. The cell numbers were higher in the MHV-68-LMP1wt infected B cells with the greatest difference at d 7 p.i. (Figure 58A). The cell numbers of MHV-68-LMP1wt infected splenocytes remained almost stable between d 1 and d 7 whereas the cell numbers of B cells infected with either MHV-68-NGFR or MHV-68-LMP1mut decreased over time. The staining

for LMP1 revealed 16% LMP1<sup>+</sup> B cells at d 3 and 34% LMP1<sup>+</sup> B cells at d 5 (Figure 58A, lower panel). The analysis of living cells showed only a difference at d 7 between the analyzed viruses (Figure 58B). Here, the percentage of living cells remained stable between d 4 and 7 p.i.. In contrast the cells infected with the control viruses revealed a drop in the percentage of living cells in this period of time. This means that infection of B lymphocytes with MHV-68-LMP1wt evoked a proliferation and survival advantage.

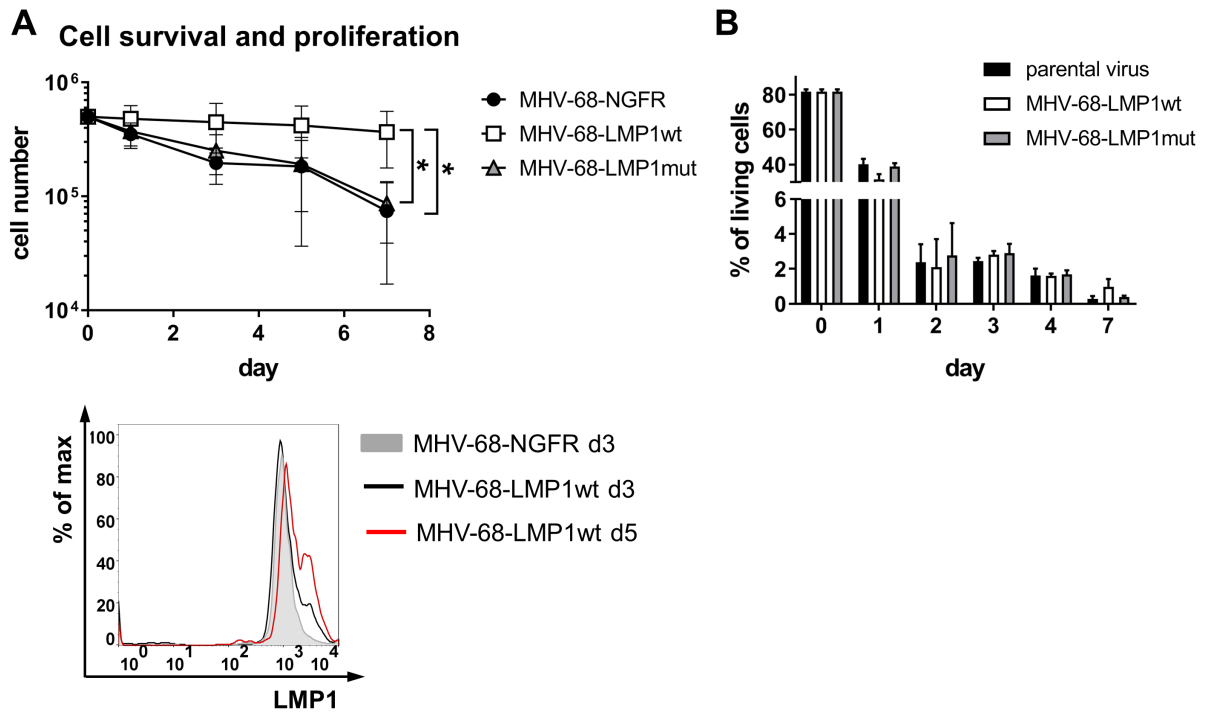


**Figure 58:** (A): Cell survival and proliferation was determined by counting cells with trypan blue at the indicated d p.i. with the indicated viruses. B cells were obtained by magnetic cell separation (MACS) sorting with the Pan B cell kit from splenocytes of wt mice and incubated in co-culture on a monolayer of NIH3T3, the lower histogram displays an overlay of LMP1 staining of the B cells infected with the indicated viruses n=3; (B): The graph shows the percentages of the living cells (TO-PRO3<sup>-</sup>) upon infection with the indicated viruses at the indicated time points.

#### 5.4.4 T cells reveal a stronger response to LMP1wt infected B cells

There was no negative selection of MHV-68-LMP1wt infected cells *in vitro*. We asked now whether the infected cells are eliminated by T cells. Another question was if T cells respond stronger upon MHV-68-LMP1wt infection than towards MHV-68-LMP1mut infection. Here, we used an Enzyme Linked Immuno Spot Assay (ELISpot) to determine the frequency of IFN $\gamma$  producing T cells isolated from the spleens of infected mice upon *in vitro* restimulation with epitope specific peptides. The secretion of IFN $\gamma$  can be used as a marker for T cell responsiveness towards a specific antigen [Halminen et al., 1997]. Orf6 and Orf61 were chosen due to their different expression patterns during MHV-68 infection. Orf6 is mainly expressed in the lytic phase, and Orf61 during establishment

of latency [Woodland et al., 2001]. Orf6 elicited a comparable IFN $\gamma$  response from the analyzed T cells (Figure 59A). However, the T cell response of MHV-68-LMP1wt infected mice towards Orf61 was dramatically reduced in comparison to both control groups. This means only a small number of T cells was primed against the antigen which is mainly expressed in later stages of MHV-68 infection. This is consistent with the finding that the viral genomic load after infection with MHV-68-LMP1wt was reduced at d 17 p.i. (see Figure 56D+E).

In order to discover and compare the direct response of T cells with regard to B cells harboring MHV-68-LMP1wt, these cells were used as target in the ELISpot. For this, T cells from mice infected with parental virus or MHV-68-LMP1wt were isolated and co-cultured with B cells which were infected with one of the three viruses *in vitro*. Afterwards, the T cell response was measured by the frequency of IFN $\gamma$  secreting T cells. The reaction towards the three different types of B cells was determined for every mouse. A clear stronger answer towards the MHV-68-LMP1wt infected B cells in comparison to the two other types of B cells was detectable in all analyzed mice (Figure 59B+C). This was true for the T cells isolated from parental virus infected (Figure 59B) and from MHV-68-LMP1wt infected mice (Figure 59C). As control, the reaction towards naive B cells was measured. Neither the T cells from mice infected with parental virus nor the T cells from mice infected with MHV-68-LMP1wt responded with IFN $\gamma$  secretion to these B cells (data not shown). Therefore, the LMP1 signaling seemed to induce a mechanism in the B cells which triggers a stronger immunogenic response of the T cells.

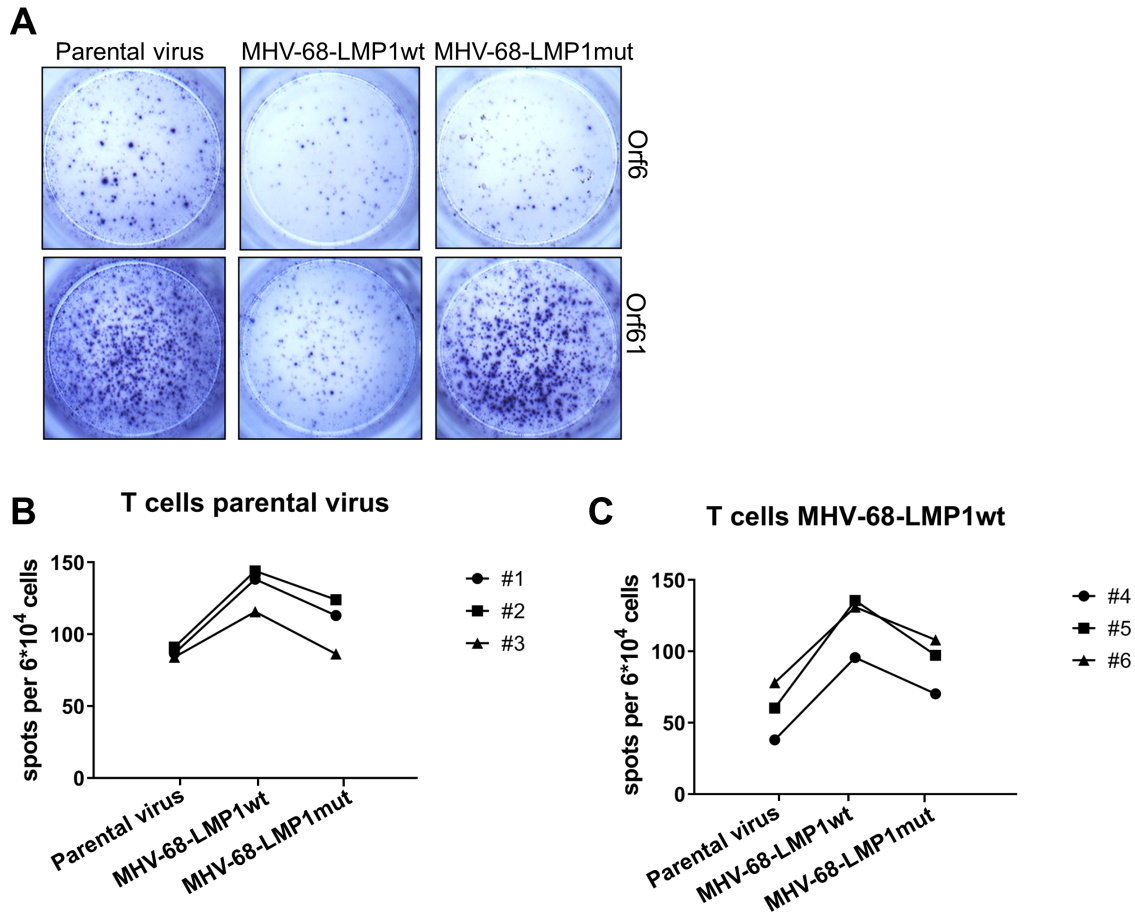


**Figure 59:** (A): Splenic T cells were isolated from wt mice which were infected with the indicated viruses and plated onto ELISpot plates at d 17 p.i.. The plates were coated with either Orf6 or Orf61. IFN $\gamma$  producing T cells were detected after 18 h incubation. The pictures show one representative example of two independent experiments. n=6; (B+C): T cells were isolated from the SP of parental virus or MHV-68-LMP1wt infected mice and were plated together with B cells which were infected 4 d before with either parental virus, MHV-68-LMP1wt, or MHV-68-LMP1mut in a ratio of 2:1 onto ELISpot plates. Plates were coated with IFN $\gamma$  capturing antibody (AN18). IFN $\gamma$  secreting T cells were detected after 18 h, every line represents the number of IFN $\gamma$  secreting T cells of one mouse, the experiment was performed in two independent experiments.

#### 5.4.5 MHV-68-LMP1wt infected B cells cannot be rescued in TCR $\beta\delta$ KO mice

Due to the stronger response of T cells towards MHV-68-LMP1wt infected B cells and their important role during the latency establishment of MHV-68, we wanted to test whether a hyper-activated T cell response is responsible for the reduced numbers of MHV-68-LMP1wt infected B cells *in vivo*. We used TCR $\beta\delta$  KO mice lacking all T cells and infected them with parental virus, MHV-68-LMP1wt, and MHV-68-LMP1mut. After i.n. viral inoculation of wt mice, the virus establishes latency predominantly in the spleen. This coincides with a transient splenomegaly, caused by a massive expansion of B and T cells [Nash et al., 2001]. First, we determined the splenic weight 17 p.i.. The spleens of

the MHV-68-LMP1wt infected mice revealed the highest splenic weight in comparison to the two other groups due to higher B cell numbers in these mice (Figure 60A+B). The splenic weight of the mice infected with the parental virus was indicative for a splenic atrophy. The splenomegaly which is found upon MHV-68 infection in laboratory mice is probably driven by CD4<sup>+</sup> cells. Additionally, B cells as well as CD4<sup>+</sup> T cells are necessary for the evolution of the splenomegaly upon infection [Usherwood et al., 1996, Nash et al., 2001]. Mice lacking CD4<sup>+</sup> T cells displayed no splenomegaly upon MHV-68 infection [Ehtisham et al., 1993]. Also, IFN $\gamma$ R KO mice display a splenic atrophy which correlates with the severity of the infection [Ebrahimi et al., 2001]. This means the stronger the viral load the stronger the reduction of the cell number in the spleen. Our findings upon infection of the TCR $\beta\delta$  KO mice could hint to a similar mechanism due to the observed splenic atrophy upon infection with the parental virus. Therefore, the viral genomic load was determined to analyze the amount of virus which persists in the splenocytes. There was nearly no viral DNA detectable in the splenocytes isolated from mice infected with MHV-68-LMP1wt (Figure 60C). In contrast, the viral load in the two other groups was 50 to 100 times higher than usually detected in infected wt mice, confirming the important role of T cells in controlling the infection. As expected there was no reactivation detectable upon infection of wt mice with MHV-68-LMP1wt. In contrast the reactivation capacity of MHV-68-LMP1wt could be partly restored upon infection of TCR $\beta\delta$  KO mice (Figure 60D). Thus, the T cells appeared to play a role in the clearance of MHV-68-LMP1wt infected cells. However, there seemed to be additional cells which contribute to the elimination of MHV-68-LMP1wt infected cells.

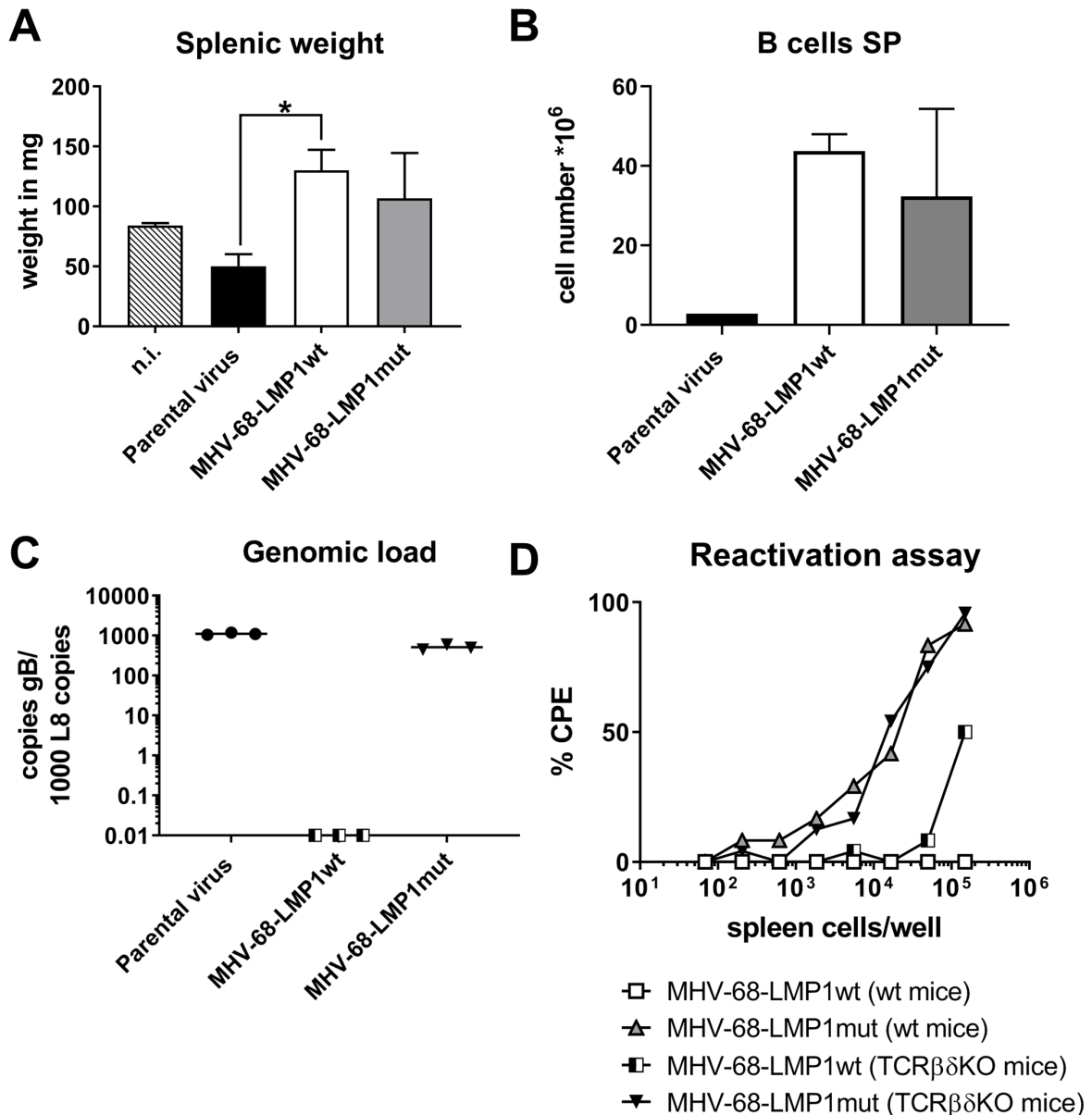


**Figure 60:** (A): The graph indicates the splenic weight of n.i. and infected TCR $\beta\delta$  KO mice with the indicated viruses at d 17 p.i., n=3; (B): The graph displays the B cell number (CD19<sup>+</sup>) from the SP isolated from mice infected with the indicated viruses at d 17 p.i.; (C): DNA was isolated from splenocytes. Real-time PCR was performed to detect the genomic load at d 17 p.i.; (D): At d 17 p.i., splenocytes of mice infected with the indicated viruses were isolated and applied on NIH3T3 in a serial dilution. 24 wells per dilution were plated in 96 well plates. The splenocytes of three mice were pooled. The reactivation was determined by analyzing the cytopathic effect in every well.

#### 5.4.6 NK cells contribute to the clearance of MHV-68-LMP1wt infected B cells

The control of MHV-68 infection seems to be independent of NK cells [Adler et al., 2014]. However, LMP1 expression may result in the upregulation of surface molecules leading to the activation of NK cells. These cells could be responsible for the early and stronger

clearance of MHV-68-LMP1wt infected B cells. Therefore, we stained the NK cells of the infected TCR $\beta\delta$  KO mice for activation markers 17 d p.i.. CD69 is upregulated on activated NK cells. Induced signaling of CD69 leads to cytotoxic activity and proliferation of NK cells [Borrego et al., 1999]. The expression of CD69 was upregulated on NK cells of infected mice in comparison to uninfected mice but similar between MHV-68-LMP1wt and MHV-68-LMP1mut infected TCR $\beta\delta$  KO mice (Figure 61A). NK1.1<sup>-</sup> cells were used as negative control. However, the percentage of NK cells expressing CD107 was increased in MHV-68-LMP1wt infected mice (Figure 61B). CD107 surface expression correlates with cytokine secretion and targeted cell lysis [Alter et al., 2004]. Thus, the NK cells seemed to display a stronger activity in MHV-68-LMP1wt infected mice.

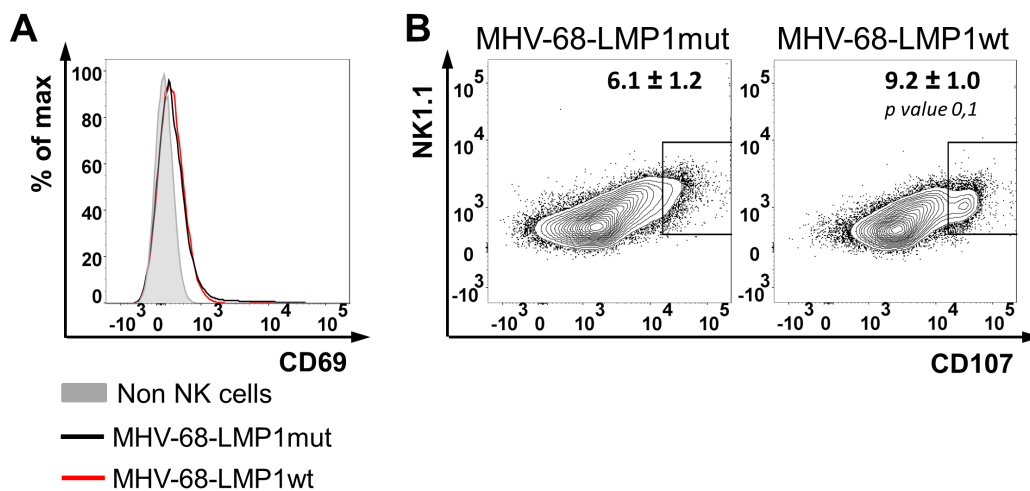


**Figure 61:** TCR $\beta\delta$  KO mice were infected with either MHV-68-LMP1wt or MHV-68-LMP1mut and analyzed at d 16 p.i., (A): Splenic NK cells (NK1.1<sup>+</sup>) of LMP1wt (red) and LMP1mut (black) were stained for CD69 and compared to NK1.1<sup>-</sup> cells (negative control); (B): Splenocytes were stained with anti-NK1.1 and anti-CD107, numbers indicate the mean and the SD of the percentages of granulated NK cells (NK1.1<sup>+</sup>, CD107<sup>+</sup>), n=3.

In order to identify the NK cells as possible cause for the elimination of MHV-68-LMP1wt infected cells, we depleted NK cells in TCR $\beta\delta$  KO mice by injecting an anti-NK1.1 antibody twice a week starting one d before viral infection. As control, an isotype control antibody was injected. Mice were analyzed at d 14 p.i.. The comparison of the percentages of NK cells in the analyzed mouse groups revealed a reduction of NK cells of 63% in the antibody depleted mice (Figure 62A). This means that despite the depletion, around 2.2% of NK cells were still present in these mice. The NK cell depleted MHV-68-LMP1wt infected mice showed slightly higher splenic weights compared to the isotype treated mice (Figure 62B). Further, the splenic weight was significantly higher in the NK cell depleted MHV-68-LMP1wt infected mice in comparison to the MHV-68-LMP1mut infected mice. Additionally, the percentage of splenic B cells was significantly higher in

the NK cell depleted MHV-68-LMP1wt infected mice in comparison to the two other groups (Figure 62C). To answer the question if the presence of the MHV-68-LMP1wt might be responsible for this effect, the reactivation assay was conducted at d 17 p.i.. The reactivation increased considerably after depletion of NK cells when compared to the MHV-68-LMP1wt infected mice treated with the isotype control (Figure 62D). The detected CPE was almost similar at the highest splenic cell concentration in the two mouse groups. Further, the depletion of NK cells evoked a tendentious increased genomic load when compared to the isotype treated groups (Figure 62E). We concluded from this data that both NK and T cells contributed to the elimination of the MHV-68-LMP1wt infected B cells in mice. Nevertheless, there were further unknown mechanisms which played a role in this phenomenon.

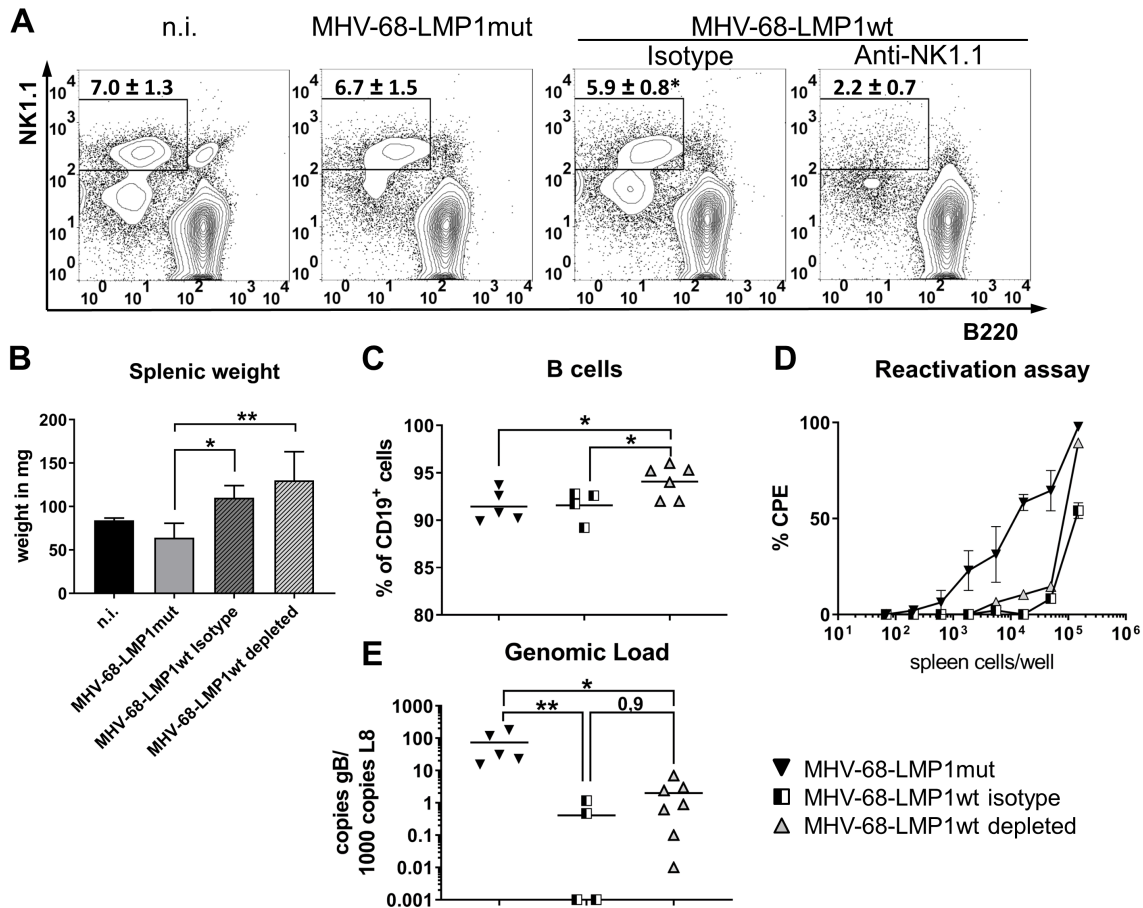


**Figure 62:** TCR $\beta\delta$  KO mice were infected with either MHV-68-LMP1wt or MHV-68-LMP1mut and analyzed at d 14 p.i.. MHV-68-LMP1wt infected mice were either depleted with anti-NK1.1 antibody or the isotype control twice per week starting one d before infection, (A): The FACS plots show the mean and the SD of the percentage of NK cells NK1.1<sup>+</sup>, B220<sup>lo</sup> of the indicated groups; (B): Splenic weight of the three mouse groups; (C): The graph shows the percentages of B cells (CD19<sup>+</sup>) among all lymphocytes of the infected mice; (D): Splenocytes of mice infected with the indicated viruses were isolated and applied on NIH3T3 in a serial dilution. 24 wells per dilution were plated in 96 well plates. The splenocytes of three mice were pooled. The reactivation was determined by analyzing the cytopathic effect in every well, data are from two independent experiments; (E): DNA of splenocytes was isolated and used in real-time PCR to determine the genomic load at d 14 p.i..

## 6 Discussion

High CD30 expression of a large B cell population is patho-physiological and related to several B cell lymphomas. Despite this, the physiological regulation and expression of CD30 in B cells is still mainly unknown. The use of CD30 KO mice did not lead to conclusive results, and the low amount of CD30 expressing B and T cells *in vivo* restricts the possibilities of investigation in wt mice. The generation of a mouse model with a constitutively active CD30 signaling in B cells enabled us to study CD30 from another point of view. In this work, the role of CD30 in B cells in general and especially in the GC B cells could be illuminated. Additionally, the influence of chronic, in GC B cells

induced, CD30 signaling on lymphoma development was examined. Finally, the additional effect of a herpesviral infection on B cell lymphoma development was investigated. This knowledge is not only relevant from the biological and diagnostic perspective but could also be helpful for the ongoing studies using CD30 as treatment target. Currently, an anti-CD30 antibody coupled to a microtubule inhibitor (brentuximab vedotin) is part of several studies analyzing the degree of applicability in different B cell lymphomas [Küppers, 2005].

## 6.1 LMP1/CD30 expressing cells are encouraged to plasma cell differentiation

Petra Fiedler showed that the chronic LMP1/CD30 expression in B cells induces an expansion of B1 cells and PC, accompanied by higher serum titers of IgM, IgA, and IgG3 [Sperling et al., 2019]. In this work, we demonstrate that the expanded B1 cell population is intermixed with higher percentages of PB when compared to control mice. Further, this population can differentiate towards PB *in vitro* without stimulation and partly without proliferation. Moreover, LPS stimulation of LMP1/CD30 expressing B cells induces the expansion of PB *in vitro*. Similar effects were also observable *in vivo*. The TI immunization drove the enlargement of the B1 cell and the PC population in LMP1/CD30 mice. This appeared together with higher IgM and IgG3 titers (see Figure 9). Recently, it was shown that also splenic control B1 cells contain a fraction of PB [Yang et al., 2007]. The authors could also provide evidence that a part of B1 cells differentiate towards ASC without proliferation *in vitro*. Additionally, also human B1 cells seem to display some features of pre-PB [Covens et al., 2013].

The pre-activated status of B1 cells seems to be further promoted due to the LMP1/CD30 expression and favors the fast differentiation towards PB and PC. This is also supported by the higher expression of TACI, a known marker of PC differentiation, of the B1 cell population of LMP1/CD30 mice [Pracht et al., 2017].

Besides B1 cells, also B2 cells were affected by the chronic CD30 signaling. CD40 stimulation of LMP1/CD30 B2 cells yielded more PB and CD43<sup>+</sup>, CD23<sup>lo</sup> B cells compared to control cells *in vitro*. This population was lower in CD22 and higher in CXCR4 in both LMP1/CD30 and control mice in comparison to FoB cell population. This is in accord with pre-PB or activated B1 cell phenotype [Minnich et al., 2016, Moon et al., 2012]. Further, the possibility of the trans-differentiation from B2 into B1 cells was recently shown by Graf et al. [Graf et al., 2019]. Together, this data supports the theory that LMP1/CD30 expressing B2 cells reveal an enhanced differentiation towards a B1 or pre-PB population upon CD40 stimulation. Afterwards, we wanted to elucidate the responsible signaling pathway leading to the higher number of PB in LMP1/CD30 mice. Here, we found higher levels of pSTAT3 and pSTAT6 in the nucleus of LMP1/CD30 expressing B2 cells

when compared to controls upon short term CD40 stimulation. Further, stronger nuclear translocation of p65 and IRF4 were detected in these cells in comparison to control cells. Therefore, we concluded that the chronic CD30 signaling in B2 cells seems to cooperate with the CD40 signaling in driving PB differentiation by a higher activation of pSTAT3 which upregulates BLIMP-1 which in turn induces PC differentiation in the GC reaction. The activation of the NF $\kappa$ B pathway induces the IRF4 expression which was demonstrated previously [Diehl et al., 2008, Reljic et al., 2000, Grumont and Gerondakis, 2000]. Also during class switching, the LMP1/CD30 expression appeared to have a small additive effect with CD40 signaling in combination with IL4. This was revealed by a higher differentiation towards IgG1<sup>+</sup> B cells upon CD40/IL4 stimulation *in vitro*. The effect might be mediated due to the higher pSTAT6 expression upon CD40 stimulation in LMP1/CD30 expressing B cells. As STAT6 is an important factor during IL4 induced class switch recombination [Linehan et al., 1998]. Additionally, recently was shown that IL4 induces CD30 expression in a STAT6 mediated manner [Mokada-Gopal et al., 2017]. This might trigger a positive feedback loop in LMP1/CD30 expressing cells upon CD40/IL4 stimulation and result in the enhanced differentiation towards IgG1 positive B cells *in vitro*. Regarding class switch towards IgG1, CD30 signaling seemed to be able to substitute the CD40 signaling, at least partly.

The TD immunization of LMP1/CD30 mice revealed a block in the GC which was shown by Petra Fiedler [Sperling et al., 2019]. Also, the steady GC reaction of the PP displayed a clear counter-selection of LMP1/CD30 expressing cells in this side. This led us to the assumption that CD30<sup>+</sup> B cells are hampered in entering the GC reaction. Therefore, we crossed the LMP1/CD30 mice with a C $\gamma$ 1-cre mice in order to induce the chronic CD30 signaling directly in the GC B cells. Thereby, we could provide prove that GC reaction was developed upon TD immunization in this mouse model. LMP1/CD30 expressing GC B cells adopted to a higher extent a CD43<sup>+</sup>, CD23<sup>lo</sup> phenotype when compared to controls. This population was again intermixed with PB and PC. Both populations were expanded in the LMP1/CD30//C $\gamma$ 1-cre mice in comparison to CAR//C $\gamma$ 1-cre mice. Therefore, also the induction of chronic CD30 signaling in GC B cells drives them towards the same phenotype as found in the LMP1/CD30//CD19cre mice. The PC differentiation in GC cells is mediated by IRF4. Therefore, we analyzed the expression of IRF4 in the GC by histology. Higher percentages of IRF4<sup>+</sup> B cells were detected in the DZ and the LZ but also at the border of the GC of the immunized LMP1/CD30//C $\gamma$ 1-cre mice in comparison to control mice. The CD40L expressing T cells in the GC reaction might induce, together with the active CD30 signaling, the IRF4 expression during positive selection of GC B cells. This could lead, through the upregulation of BLIMP-1, mediated by IRF4, to the escape from the GC reaction. Thus, BLIMP-1 could downregulate *BCL6* and *PAX5* which could then result in more PC in the LMP1/CD30//C $\gamma$ 1-cre mice. Under physiological conditions, IRF4<sup>+</sup> cells are mainly found among the centrocyte population and to

a lesser extent among the centroblasts [Falini et al., 2013]. It is assumed that PC derive from the IRF4<sup>+</sup> centrocytes [Cattoretti et al., 2006]. Recently, the CD30<sup>+</sup> cells in the GC were characterized as positively selected centrocytes receiving signals from CD40L expressing T cells [Weniger et al., 2018]. Upon migrating into the DZ, they might switch off CD30 signaling, due to the contact loss towards T cells, and undergo further rounds of hypermutation and proliferation. In contrast, LMP1/CD30 expressing B cells are not able to turn off the chronic CD30 signaling. Due to the expression of PC fate inducing TF, the CD30 signaling might negatively influence the fate decision towards memory B cells which are reduced in LMP1/CD30//C $\gamma$ 1-cre mice. The use of the newly identified memory B cell precursor marker CCR6 could further elucidate the origin and the localization of memory B cells emerging in LMP1/CD30//C $\gamma$ 1-cre mice [Suan et al., 2017].

## 6.2 Herpesviral infection amplifies the lymphoma development in LMP1/CD30//C $\gamma$ 1-cre mice

A high percentage of CD30<sup>+</sup> B cell lymphomas originating from GC B cells are associated with EBV or KSHV infection. The question was if a herpesviral infection, together with the deregulated CD30 signaling, have a synergistic effect in driving B cell lymphoma development. Therefore, we combined a herpesviral infection with a chronic CD30 signaling triggered in GC B cells. EBV does not infect murine B cells therefore we used MHV-68 instead. MHV-68 is a murine  $\gamma$ -herpesvirus with a similar infection route and latency establishment like EBV and KSHV. The detection of viral infected B cells was realized by cloning a reporter MHV-68 which expressed NGFR (MHV-68-NGFR). First, we proved that the infection of LMP1/CD30//C $\gamma$ 1-cre mice induces the deletion of the STOP-cassette and leads to a GC reaction which was a precondition to answer this question. Mice were either immunized with NP-CGG or infected with the MHV-68-NGFR virus and analyzed after 2 weeks, 2 months, or when mice were diseased. The question was which influence has the GC induced chronic CD30 signaling on the lymphoma development and if a additional infection acts synergistically in driving lymphomagenesis. Therefore, both groups were analyzed in parallel. The CAR//C $\gamma$ 1-cre mice served as control in both groups. The virus infection induced a stronger GC reaction in both analyzed genotypes in comparison to the immunization. However, only a third of the GC cells expressed the CAR or hCD2 reporter in the infected mice. Besides, both LMP1/CD30//C $\gamma$ 1-cre mice revealed a significantly higher percentage of cre-recombinase induced reporter expression than their control mice. The MHV-68 infection results in secretion of high amounts of IFN $\gamma$  by T cells which is necessary to restrict the latent infection [Canny et al., 2014]. In the C $\gamma$ 1cre mouse strain, the cre-recombinase is under the control of the endogenous IgG1 promoter. Yet, IFN $\gamma$  impedes the induction of IgG1 expression [Kawano et al., 1994]. Therefore, also the expression of the sterile transcripts of the IgG1 locus could be affected

and prevent the expression of the cre-recombinase leading to reduced percentages of reporter expressing B cells in the GC population. As the percentage of reporter expressing B cells was still comparable with the immunized mice and NGFR<sup>+</sup> reporter expressing B cells were detectable, we did not assume a disadvantage by this mechanism. Additionally, during infectious mononucleosis between 0.5-2% of the B cell compartment is positive for EBV [Klein et al., 1976]. This is similar to the percentage of NGFR<sup>+</sup> cells. We detected, around 1.5% NGFR<sup>+</sup> in the CAR//C $\gamma$ 1-cre mice and around 1.1% NGFR<sup>+</sup> among the splenic B cells in the LMP1/CD30//C $\gamma$ 1-cre mice.

In addition to the GC cells, NGFR expressing B cells were also found in the progenitor cells of PC and in GC B cells. This was in contrast to the findings of Collins et al. obtained with a YFP-MHV-68 [Collins and Speck, 2012]. Here, the most prominent amount of virus positive cells was found in the GC B cells (PNA<sup>+</sup>, CD95<sup>+</sup>) and the PC (CD138<sup>+</sup>, B220<sup>lo</sup>). However, these results were obtained at d 17 p.i., we analyzed the mice at d 14 p.i.. The CD38<sup>+</sup>, CD95<sup>+</sup> population as well as CD138<sup>+</sup>, B220<sup>+</sup> population might differentiate towards GC and PC, respectively. Therefore, an analysis conducted at d 17 p.i. might probably lead to similar results. Additionally, we stained for GC (CD38<sup>lo</sup>, CD95<sup>+</sup>) cells using CD38 and CD95 instead of PNA and CD95 which could also lead to different results. The percentage of NGFR<sup>+</sup> cells was similar between the infected CAR//C $\gamma$ 1-cre and the LMP1/CD30//C $\gamma$ 1-cre mice at all analyzed time points. This means either the constitutive CD30 signaling had no additive effect on the virus expansion or the spontaneous differentiation towards PC, driven by active CD30 signaling and a following switch towards the lytic cycle of the virus, could be the reason. However, due to the stronger expansion of reporter expressing cells in the LMP1/CD30//C $\gamma$ 1-cre mice, the total number of NGFR<sup>+</sup> cells was clearly enhanced in this mice.

In humans, it could be shown that the differentiation of an EBV infected memory B cell towards PC triggers the switch towards lytic replication of EBV [Laichalk and Thorley-Lawson, 2005]. The detection of NGFR positivity might not include all virus bearing cells. Although, a magnetic cell separation (MACS) enrichment of NGFR expressing cells, followed by a quantitative PCR, proofed a higher genomic load in NGFR<sup>+</sup> cells (data not shown). But still some NGFR<sup>-</sup> cells could contain the virus. A further validation of the B cells of infected mice needs to be performed in order to rule out possible counter regulation of the NGFR expression.

The expression rate of NGFR ranged around 4% in the aged cohort of LMP1/CD30//C $\gamma$ 1-cre mice and was only slightly higher than in control mice in the spleen. In the PerC, the percentage was lower in the LMP1/CD30//C $\gamma$ 1-cre mice than in controls. Despite that, the expansion of hCD2 expressing cells yielded an expansion in total numbers of infected cells in these mice. This could have several reasons. The LMP1/CD30 expressing cells displayed a significantly reduced percentage of GC B cells compared to control mice two months after infection. The reason might be the defective entry into the GC reaction

as observed in the LMP1/CD30//CD19cre mice [Sperling et al., 2019]. Therefore, also the re-entry of LMP1/CD30 expressing cells in the LMP1/CD30//C $\gamma$ 1-cre mice might be hampered. The virus infection seemed not to intervene with the process. Also, the differentiation towards memory B cells was reduced in the LMP1/CD30//C $\gamma$ 1-cre mice in comparison to the control mice 2 weeks and 2 months p.i.. All together, these processes might have interfered with the latency establishment of MHV-68-NGFR in LMP1/CD30//C $\gamma$ 1-cre mice and hampered the spread of the virus, as MHV-68 predominantly survives in GC and memory B cells [Flaño et al., 2002]. This could have also reduced the influence of the virus towards lymphoma development.

The NGFR expression within the hCD2<sup>+</sup> cells ranged around 3% in the LMP1/CD30//C $\gamma$ 1-cre mice detected with a tumor. However, it seemed that not all reporter expressing cells are malignant in these mice. As the phenotype of the hCD2<sup>+</sup> cells is not completely homogeneous in these mice. Therefore, the percentage of malignant cells bearing MHV-68-NGFR might be higher and reach similar levels like EBV positive B cell lymphoma in human. Previous analysis of EBV positive DLBCL revealed in 5-40% of the malignant cells a positive EBER nuclear staining [Ziarkiewicz et al., 2016]. EBER are expressed in all EBV infected cells [Rezk and Weiss, 2007]. Also, in non HL, different patterns of EBV positive cells was detected. In some lymphomas over 50% of tumor cells bear EBV in other cases only 1-20% of the cells reacted positive for EBER staining. The reasons for the reduced infection rate might be either the loss of the viral episome which might during tumor progression lost the survival and proliferation advantage [Quintanilla-Martínez et al., 1997]. This process could be accelerated due to the expression of NGFR in MHV-68-NGFR infected cells. Another reason could be the occurrence of the infection after the clonal expansion [Quintanilla-Martínez et al., 1997]. This was also reported for cytotoxic aggressive T cell lymphoma. The secondary infection with EBV was assumed to result in a more aggressive behavior [Langer et al., 2010]. The chronic CD30 signaling promotes the expansion of the B1 cell population not only when expressed in all B cells but also if it is induced in GC B cells. Infection resulted in a stronger expansion of LMP1/CD30 expressing B1 cells than upon immunization. Thus, the B1a sub-population was more than threefold increased in the infected LMP1/CD30//C $\gamma$ 1-cre in comparison to the immunized ones. The increase might be accompanied by the increase of PC in the spleen of these mice. Higher percentages of PC in this side result in higher numbers of cells with a B1a cell phenotype.

Despite the enlarged PC population in young unimmunized LMP1/CD30//CD19cre mice, PC were not increased anymore in LMP1/CD30//CD19cre mice which had developed a lymphoma. However, the lymphoma population revealed a pre-PB or PB phenotype suggesting that the PC differentiation might be impaired in aged LMP1/CD30//CD19cre mice [Sperling et al., 2019]. The reason might be a further mutation resulting in inhibition of PC differentiation and therefore accumulation of a pre-plasmablastic stage. Also

LMP1/CD30 signaling, induced in the GC reaction, led to an intensified differentiation towards PC which emerged stronger upon virus infection than upon NP-CGG immunization. However, also in aged cohorts of these mice, the PC compartment was again comparable with the control mice. Therefore, independent of the used transgenic mouse model, a disrupted PC differentiation seems to develop in aged mice. And cells which were unable to differentiate towards PC might have become tumor cells. The additional virus infection appears not to intervene with this process but rather promoted it and resulted in higher numbers of burdened mice. Of note, besides one exception, all lymphomas of the infected LMP1/CD30//C $\gamma$ 1-cre mice revealed significantly reduced levels of Blimp-1 expression. Blimp-1 is a known tumor suppressor [Boi et al., 2015]. Around a quarter of human DLBCL reveal alterations in the *Blimp-1* locus leading to reduced expression levels and a block in the PC differentiation. Other DLBCL display a lack of BLIMP-1 protein without genetic alteration, hinting to other changed mechanisms affecting *PRDM1* expression. Interestingly, this *PRDM1* repression is only found in the ABC-DLBCL cases and is independent of IRF4 expression [Boi et al., 2015]. This is similar to our cases which revealed a strong downregulation of BLIMP-1 in mice with lymphomas in comparison to the other mice of the cohort but unchanged IRF4 levels. Further the active NF $\kappa$ B pathway in this lymphoma, which is also present in this model detected by higher CD95 expression, seems to synergize with the lack of the Blimp-1 protein contributing to the pathogenesis [Calado et al., 2010]. Anyway, it is assumed that the alteration of the *Blimp-1* expression alone is not sufficient to encourage the lymphoma pathogenesis. Therefore, the active NF $\kappa$ B pathway and the adjustment of the Blimp-1 expression might be contributing to the lymphomas detected in both immunized and infected LMP1/CD30//C $\gamma$ 1-cre mice. The LMP1/CD30//C $\gamma$ 1-cre mice displayed a decreased differentiation towards memory B cells upon NP-CGG immunization. The percentage of memory B cells remained decreased over the observed time period in comparison to the control mice. The infected LMP1/CD30//C $\gamma$ 1-cre displayed similar percentages of memory B cells in the aged cohorts as the control mice and even significantly higher percentages than the immunized LMP1/CD30//C $\gamma$ 1-cre. MHV-68 establishes latency mainly in memory B cells [Flaño et al., 2002]. If the memory B cells are triggered again, they differentiate towards PC which might be promoted through the chronic CD30 signaling. Due to reduced PC differentiation in the aged LMP1/CD30//C $\gamma$ 1-cre mice, the memory B cell population might be increasing induced through proliferation upon antigen encounter. Further investigation of virus infection and analyzing the proliferation of the memory B cell compartment over time could clarify this issue and might elucidate the underlying mechanism. An active NF $\kappa$ B pathway is an important hallmark for several B cell lymphomas. CD95 is a direct target of this pathway [Ouaaz et al., 1999]. CD40 stimulation of LMP1/CD30 B cells induces higher NF $\kappa$ b activation than in control B cells. Besides, both aged cohorts of LMP1/CD30//C $\gamma$ 1-cre mice displayed significantly increased CD95 expression

with the lymphoma samples being the highest. This hints to an active NF $\kappa$ B signaling also in the aged mice. Further, in the burdened mice, the LMP1/CD30 expressing cells seem also to induce the activation in the surrounding non-malignant reporter<sup>-</sup> B cells. This is similar to what is found in the microenvironment of some lymphomas like the cHL [Liu et al., 2014]. Some B cell lymphomas display deleterious mutations in the CD95 gene which are favorable due to its role as tumor suppressor. Most of them are found in the lymphomas with a (post-) GC phenotype. It is assumed that these mutations occur during somatic hypermutations [Müschen et al., 2002]. However, there are other cancer cells displaying high expression of CD95 but are resistant towards CD95 mediated apoptosis like found in the multiple myeloma and non HL [Müschen et al., 2000]. In contrast, they profit from higher proliferation, increased survival and higher invasiveness mediated by active CD95 signaling. Besides, T cells use CD95L-CD95 interaction to control the spread of viral infections like EBV and MHV-68. In apoptosis resistant B cell lymphoma cells, CD95 signaling inhibits the lytic replication of  $\gamma$ -herpesviruses [Tan et al., 2016]. Also, it is reported that an active NF $\kappa$ B pathway contributes towards latency establishment rather than virus reactivation [Krug et al., 2007, Grossmann and Ganem, 2008]. Therefore, the higher expression of CD95 in the infected LMP1/CD30//C $\gamma$ 1-cre mice might have hampered the spread of the MHV-68-NGFR due to a reduced lytic replication of the virus. But it also secures the survival of the infected cell. This would be similar to the processes in human. LMP1 is assumed to suppress the switch towards the lytic cycle during EBV infection [Shannon-Lowe et al., 2017]. How the NF $\kappa$ B and CD95 signaling influence the viral infection in our model needs further investigation. Also, the presence of CD95L expressing T cells should be examined, considering previous results which displayed a downregulation of CD95 surface expression of tumor cells as escape mechanism [French and Tschopp, 2002].

All mice which were diagnosed with a mono- or oligoclonal B cell expansion displayed to a minor extent a subset of B cells without LMP1/CD30 expression. But also within the fraction of LMP1/CD30 expressing B cells, phenotypic variances were present. Besides the downregulated surface expression CD21 and CD23, the expression pattern of other markers was not completely similar within the reporter<sup>+</sup> B cells. Thus, the cell size and the CD79 $\beta$  expression varied, assuming that the reporter<sup>+</sup> cells contain a malignant and nonmalignant population. The expression level of CD79 $\beta$  varied between the different subgroups of B cell lymphoma but was not downregulated. This was in contrast to HL. HRS cells are characterized by complete downregulation of CD79 $\beta$  [Küppers, 2012].

Histology on splenic section was used to determine the location of hCD2 expressing B cells within the splenic follicle. In the aged mice which were not detected with a tumor, hCD2<sup>+</sup> cells were mainly localized at the border of the follicle and partly within the follicle regardless of immunization or infection. This hints to a PB phenotype [Pereira et al., 2010]. Aged LMP1/CD30//C $\gamma$ 1-cre mice detected with a tumor, revealed large compact popula-

tions of hCD2<sup>+</sup> cells appearing like a follicle. These mice revealed a disrupted B and T cell zone within the spleen. Therefore, no clear conclusion can be drawn about the positioning of the malignant cells. Of note, small areas of cells with stronger anti-hcd2 staining were detected which were found in burdened and aged mice independent of infection and immunization. These cells might be PC which show stronger hCD2 expression (data not shown). To test whether LMP1/CD30 expression resulted in the upregulation of CD30, we also stained for CD30<sup>+</sup> cells in histology. The number of CD30<sup>+</sup> B cells was clearly increased in the burdened LMP1/CD30//C $\gamma$ 1-cre mice in comparison to wt mice. Also in GC B cells, a stronger upregulation of CD30 expression could be demonstrated in FACS analysis of LMP1/CD30//C $\gamma$ 1-cre mice in comparison to control mice [Sperling et al., 2019]. A co-staining of extracellular CD30 and hCD2 could provide insight into the relation of their expression patterns on the B cells. However, the staining has to be repeated with an antibody recognizing the extracellular tail of CD30. Therefore, LMP1/CD30 as well as cells expressing endogenous CD30 were detected. The stronger CD30 expression is in accord with a recently reported autocrine expression loop of CD30 which seems to be induced by LMP1/CD30 expression as well [Watanabe et al., 2005]. Wt mice displayed single CD30<sup>+</sup> cells scattered throughout the follicle. LMP1/CD30//C $\gamma$ 1-cre revealed small compact populations of CD30 expressing cells. Besides, the staining of CD30 of spleen sections of burdened mice was localized in the cytoplasm and the endoplasmic reticulum. This was similar to wt mice. It is also in line with other CD30<sup>+</sup> B cell lymphomas like ALCL and DLBCL [Stein et al., 2000, Gardner et al., 2001, Burger and Kipps, 2006]. Also in the human lymphoma, CD30 is localized in the cytoplasm and the endoplasmic reticulum. Therefore, independent of endogenous CD30 signaling or LMP1/CD30 expression, the LMP1/CD30//C $\gamma$ 1-cre mice revealed similar localization patterns as wt mice and malignant cells in human lymphoma.

Both groups displayed increased CD4<sup>+</sup> and CD8<sup>+</sup> cell numbers in the aged cohorts. Thereby, the CD8<sup>+</sup> cells of the immunized LMP1/CD30//C $\gamma$ 1-cre mice revealed to a significant extent an effector phenotype, the CD8<sup>+</sup> of the infected LMP1/CD30//C $\gamma$ 1-cre mice a memory phenotype. Nishimura et al. showed that the differentiation of memory T cells depends on CD30/CD30L signaling during a *Listeria monocytogenes* infection [Nishimura et al., 2005]. Further, CD30 as part of the TNFR superfamily was shown to provide crucial signals for the differentiation towards effector T cells [Croft, 2003]. Here, we show expanded memory T cells in mice with chronic CD30 expression in B cells upon virus infection. In contrast, immunized LMP1/CD30//C $\gamma$ 1-cre mice revealed expanded effector T cells in the spleen. This might mean that the differentiation towards memory T cells needs not only the CD30 signaling but also an additional trigger provided by the infection. We have shown that the LMP1/CD30 expression also induces the endogenous CD30 expression [Sperling et al., 2019]. Thus, histology of lymphoma samples displayed no co-expression of CD30 and CD3. Besides, CD30L expressing T cells could

receive reverse signaling from CD30 expressing B cells which might lead to similar results [Kennedy et al., 2006]. Also, secondary effects of CD30 expression on B cells might also influence the differentiation of T cells. This matter would need further investigation in order to draw a conclusion from this information.

Besides this, we analyzed T cells in the aged cohorts for exhaustion markers. Exhausted T cells were found during chronic infections but also in cancer patients [Jiang et al., 2015]. Due to overexpressed inhibitory receptors, decreased effector cytokine production, and cytolytic activity, their capacity to eliminate cancer cells is strongly impaired [Jiang et al., 2015]. The percentage of CD8<sup>+</sup> T cells which were positive for TIM3 and KLRG1 was increased in both aged cohorts of LMP1/CD30//C $\gamma$ 1-cre mice in comparison to the CAR//C $\gamma$ 1-cre control mice without a visible effect through the infection. The burdened mice did not display a further expansion of exhausted CD8<sup>+</sup> T cell populations. Still, the chronic LMP1/CD30 expression could favor an inflammatory environment promoting the development of exhausted T cells. Thus, the chronic CD30 signaling in B cells could promote the lymphoma development due to impaired T cell function similar to reduced T cell numbers. The most prominent example are patients with HIV. Besides the non HL which are classified as AIDS related, also the cHL emerges 10-20 times more often in combination with AIDS [Shannon-Lowe et al., 2017]. The higher incidence of lymphoma development is associated with the decreased number of functioning T cells. Therefore, the chronic LMP1/CD30 signaling might promote the lymphomagenesis by affecting the surrounding T cells in a negative manner.

Aged LMP1/CD30 mice displayed with an incidence of 80% a mono- or oligoclonal lymphoma [Sperling et al., 2019]. The immunized LMP1/CD30//C $\gamma$ 1-cre mice revealed in 15% of the analyzed cases a lymphoma, the infected mice with an incidence of 42%. The virus infection had a significant impact in the lymphoma development of LMP1/CD30//C $\gamma$ 1-cre. All detected tumors consisted of a mono- or oligoclonal cell expansion which was also similar to the lymphomas in the aged LMP1/CD30//CD19cre mice. This means that also the chronic CD30 signaling induced in the GC reaction is not competent to induce lymphomagenesis alone. A second mutation is needed to drive this process. Also, the virus infection was not sufficient. However, the virus infection seemed to enhance the lymphomagenesis indicated by the higher incidence of lymphomas in the infected LMP1/CD30//C $\gamma$ 1-cre mouse cohort. The virus could substitute mutations leading to deregulated signaling pathways as assumed for the role of EBV [Shannon-Lowe et al., 2017]. The sequencing of the malignant cells of the LMP1/CD30//C $\gamma$ 1-cre mice would be necessary to draw this conclusion. Besides the higher incidence of lymphomas in the infected group, further phenotypic differences were not visible in these two groups in FACS or histology. The virus seems to synergize with the effect of the chronic CD30 signaling in this process. In summary, the tested mouse model appears to be suitable to analyze the pathogenesis of EBV in the devel-

opment of CD30 positive lymphomas. CD30 is overexpressed in cHL and ALCL. It is assumed that overexpression induces the self-activation of CD30 expression which leads to a ligand-independent, constitutively active signaling. A self-association of the extracellular and intracellular domain of CD30 was demonstrated assuming a high density of CD30 on the cells surface as condition [Horie et al., 2003]. This reported mechanism was shown by *in vitro* experiments of isolated HRS cells and HEK293 cells overexpressing CD30 [Horie et al., 2002b]. Also, cytoplasmic aggregation of TRAF proteins appears to reflect constitutive CD30 signaling in HRS cells which was revealed by HRS derived cell lines [Horie et al., 2002a]. The use of the LMP1/CD30//C $\gamma$ 1-cre mouse model leads to a chronic CD30 expression in a subset of activated B cells. Further, the similar pattern of infection and latency establishment of MHV-68, EBV, and KSHV makes the MHV-68 infection of LMP1/CD30//C $\gamma$ 1-cre mice a good tool to resemble the physiological processes found in EBV or KSHV GC derived CD30<sup>+</sup> B cell lymphoma. Further, the signaling pathways NF $\kappa$ B and the JAK/STAT pathway are also active in the HL lymphoma similar to our mouse model [Küppers, 2012]. Also, the Blimp-1 expression might be regulated in EBV<sup>+</sup> GC derived lymphoma [Vrzalikova et al., 2011]. But in order to finalize this project, especially sequencing data of the lymphomas are necessary. These are necessary to confirm that the lymphoma cells underwent the GC reaction and to confirm active signaling pathways like NF $\kappa$ B and JAK/STAT. Also, a bigger mouse cohort would be necessary to assure this observed effect of the infection in this environment. Additionally, other, more sensitive methods besides the southern blot might be necessary to detect a mono- or oligoclonal cell expansion, as especially the B cell compartment makes up only a small part in the whole splenic tissue in some mice detected with a tumor.

Due to the optimized treatment therapy of chemotherapy and radiotherapy, alone and in combination, HL are highly curable. However, still 10% of the diseased patients suffer relapse making a new innovative treatment necessary. Bretuximab vedotin, a novel antibody drug conjugate, is the first promising approach targeting CD30. The drug binds to CD30 which leads endocytosis of the drug bound to the receptor. The contact of the drug conjugate with the intracellular lysozyme induces the release of the antimetabolic agent mono-methylauristatin E. This causes the inhibition of the tubulin formation and induces cell apoptosis [van der Weyden et al., 2017]. It leads to an overall response rate of over 75% in HL [Lambert Charles Q Morris, 2017]. However, the side effects which are mainly neutropenia and neuropathy limit the success of this approach [Schirrmann et al., 2014]. Further, direct apoptosis of CD30 expressing cells seems not to be the only capacity of Bretuximab vedotin. T cell activation and priming and maturation of dendritic cells are reported effects of this treatment in mouse models [van der Weyden et al., 2017]. Additionally, the levels of CD30 expression cannot be used as indicator for the treatment success of the coupled antibody therapy, as shown in different studies [van der Weyden et al., 2017]. Therefore, more information about the

different underlying signaling and regulating processes in CD30<sup>+</sup> lymphomas are necessary, especially to broaden the application spectrum and to individualize the therapy depending on the specific needs. The here introduced approach could deliver some of this information.

### 6.3 Active LMP1 signaling hampers the latency establishment in mice

EBV is a B cell lymphoma associated virus [Shannon-Lowe et al., 2017]. The expression of LMP1 seems to play an important role by inducing lymphomagenesis in human. Thereby, LMP1 and LMP2A are shown to cooperate in order to promote lymphomagenesis but are not essential [Ma et al., 2017]. LMP1 resembles a constitutively active CD40 receptor and activates several downstream pathways which result into B cells proliferation and resistance towards apoptosis [Rastelli et al., 2008]. Besides, if EBV is deficient in LMP1 expression, T cell help is required for malignant expansion [Ma et al., 2015]. Until now, the function of LMP1 *in vivo* was only examined by using transgenic mouse models which induced expression of LMP1 in murine B cells [Wirtz et al., 2016, Zhang et al., 2012, Kulwichit et al., 1998]. In order to mimic more the physiological situation a MHV-68 expressing LMP1wt (MHV-68-LMP1wt) was constructed. Additionally, the cloning of the MHV-68-LMP1mut, characterized by a lack of active LMP1-signaling, enabled the direct comparison of the effect of the protein itself and with an active signaling. Therefore, the two viruses should be a good tool to provide new information on the effect of LMP1 during virus infection and its contribution towards lymphomagenesis. MHV-68 infection alone leads not to lymphomagenesis in wt mice. Surprisingly, infection of wt mice with MHV-68-LMP1wt resulted in a complete loss of virus infected cells 17 d p.i., characterized by a lack of reactivation and no detectable genomic load in the spleen or in the LN. In contrast, this effect was not visible upon infection with MHV-68-LMP1mut. The results obtained with this virus were rather similar to the parental virus. Therefore, the elimination of the virus was probably triggered by active LMP1 signaling. Surprisingly, the genomic load of the B cells in the PerC was similar in mice infected with MHV-68-LMP1wt, MHV-68-LMP1mut, and parental virus. Also, in the LN, the viral clearance was delayed compared to the course found in the spleen. Thus, the depletion of the infected cells might be caused by the specific micro-environment. The LN and the PerC could provide a protective niche which secured at least temporarily the survival of the virus. For example, HIV persists in the LN which are used as major anatomical reservoir even upon combined anti-retroviral therapies [Huot et al., 2018]. The prolonged persistence of LMP1 expressing cells might induce activation of surrounding cells. This could have resulted in the longer maintenance of the GC reaction in mice infected with MHV-68-LMP1wt.

In order to analyze the effect of LMP1 expression, a survival curve of infected B cells was generated *in vitro*. The expression of active LMP1 in B cells during infection resulted in a significantly increased proliferation or rather survival of the B cells compared to the B cells infected with MHV-68-LMP1mut or MHV-68-NGFR. This was in line with the observed effects in human B cells, where LMP1 activates similar pathways as CD40 signaling and provides survival signals [Klein et al., 1999]. Therefore, the expression of LMP1 probably induces processes which lead to the elimination by extrinsic and not intrinsic factors. This hypothesis was corroborated by the stronger IFN $\gamma$  release of T cells upon encounter of MHV-68-LMP1wt infected B cells in comparison to the two control viruses. The elimination of LMP1 expressing B cells was also reported by Zhang et al. using a conditional transgenic LMP1 mouse model [Zhang et al., 2012]. They demonstrated that the clearance was mainly mediated by T cells. But, it was recently shown, that in comparison to EBNA1 and EBNA3C, the immunogenic response of CD4<sup>+</sup> helper cells towards LMP1 is much lower [Leen et al., 2001]. Therefore, the T cell response towards LMP1 might be activated by secondary effects of LMP1 which are normally modulated by miRNAs during EBV infection [Albanese et al., 2017]. In order to elucidate if T cells are responsible for the elimination of MHV-68-LMP1wt infected cells, we infected TCR $\beta\delta$  KO mice. Due to the lack of T cells, a reactivation capacity of 50% was reached with the highest tested cell concentration *in vitro* from mice infected with MHV-68-LMP1wt in comparison to MHV-68-LMP1mut. However, the genomic load was still not detectable in T cell lacking mice upon infection with MHV-68-LMP1wt. On that account, T cells seem to play a role in eliminating the LMP1 expressing cells. However, T cells are not the major reason for it. NK cells are increasing in number upon MHV-68 infection but have no function regarding clearing or controlling MHV-68 infected cells [Barton et al., 2011]. But, the NK cells of the MHV-68-LMP1wt infected mice displayed a higher proportion of degranulated NK cells hinting to a participation at the elimination. Indeed, depletion of NK cells in the TCR $\beta\delta$  mice resulted in a further increased reactivation of infected splenocytes when compared to the non NK cell depleted MHV-68-LMP1wt infected mice. Also, the genomic load was higher in these mice but still significantly reduced when compared to MHV-68-LMP1mut infected mice implying still reduced levels of MHV-68-LMP1wt. Most of the NK cells were successful depleted upon anti-NK1.1 antibody treatment. But the depletion efficiency reached only 63%. The remaining NK cells might be still sufficient to result in the elimination of the MHV-68-LMP1wt infected cells. The mechanism behind the NK cell activation through LMP1wt infected cells remained still elusive. In contrast to MHV-68, other herpesviruses infections like EBV are controlled by NK cells [Biron, 1997]. Also, Zhang et al. reported that NK cells provide important immune protection against lymphomas derived from LMP1 expressing B cells [Zhang et al., 2012]. They further revealed the expression of NKG2D on the LMP1 expressing B cells which mediated partially the killing by NK cells. Besides, they were unable to elucidate the

driving factor leading to the elimination of LMP1 expressing B cells by T and NK cells. Adler et al. determined the MHV-68 mediated upregulation of CEACAM 1 as driving factor for the immune evasion from NK cells [Adler et al., 2014]. They further demonstrated the inhibition of the cytotoxicity but not the degranulation of NK cells through the expression of CEACAM1 of infected cells. Following, they suggested that the FAS/FASL or the TNF-TNFR pathway mediate the killing of MHV-68 infected cells through NK cells. LMP1 expression induces upregulation of Fas/CD95 which might result in an optimized killing by NK cells. The use of a Fas-Fc fusion protein has shown that also in the transgenic mouse model with LMP1 expressing B cells NK cells are partly responsible for the killing of the LMP1 expressing B cells [Zhang et al., 2012]. Preliminary results displayed a reduced CEACAM1 expression of B cells infected with MHV-68-LMP1wt. Taken together, the LMP1 expression in infected B cells might lead to reduced upregulation of CEACAM1 and to a higher expression of CD95. This might hamper the immune escape from NK cells and might support the killing mediated by NK cells. Therefore, another NK cell depletion protocol might be worthwhile to implement in order to study this hypothesis. A mouse model expressing LMP1 under the control of the Ig heavy chain promoter and enhancer developed LMP1<sup>+</sup> lymphomas. In young mice, the LMP1 expression was almost not detectable [Kulwichit et al., 1998]. This could hint to the need of a more restricted LMP1 expression rather than a steady one to allow a LMP1 driven lymphomagenesis without curtailing the immune system in such strong way. This means also that this model is unsuitable to mimic the effect of LMP1 expression during viral infection in mice.

## 7 Material

### 7.1 Mouse strains

#### CD19cre BALB/c

The cre-recombinase was placed under the control of the B cell specific CD19 promoter [Rickert et al., 1997]. If crossed with mice bearing a STOP-cassette flanked by the loxP sites, a deletion efficiency of 75-80% in the BM and up to 95% in the periphery in B cells is reached. In this work, CD19cre mice were either crossed to LMP1/CD30<sup>flSTOP</sup> mice or used alone as control mice.

#### LMP1/CD30<sup>flSTOP</sup> BALB/c

The targeting construct was inserted into the Rosa26 locus under the control of the endogenous Rosa26 promoter. The construct precedes a loxP site flanked STOP-cassette ensuring a cre-dependent expression of LMP1/CD30. An IRES-hCD2 cassette was inserted downstream of LMP1/CD30. This leads to the parallel expression

of LMP1/CD30 and hCD2 [Sperling et al., 2019]. The fusion gene LMP1/CD30 consists of the transmembrane domain of the viral protein LMP1 and the cytoplasmic domain of murine CD30. Due to the self-oligomerization of LMP1 in the plasma membrane, the CD30 ligand is not needed to induce CD30 signaling. Instead, a chronic signaling is established in the respective cell in which the fusion gene is expressed.

### $\gamma$ 1-cre BALB/c

This mouse strain has an insertion of an IRES cassette followed by the cre-coding sequence behind the last membrane-coding exon of the Ig $\gamma$  constant region gene segment (C $\gamma$ 1) locus [Casola et al., 2006]. Thereby a GC specific expression of genes with a loxP site flanked STOP-cassette is reached. These mice were either crossed with the R26CAR mice or with the LMP1/CD30<sup>flSTOP</sup> mice.

### R26/CAG-CAR $\Delta$ 1<sup>StopF</sup> BALB/c

The sequence of CAR under the control of the CAG promoter with a precedent loxP flanked STOP-cassette was inserted into the rosa26 locus [Schmidt-Supprian and Rajewsky, 2007]. This strain allows to monitor cells which underwent Cre dependent recombination by staining for the receptor CAR. These mice were crossed to the  $\gamma$ 1-cre and served as control for the LMP1/CD30<sup>flSTOP</sup>// $\gamma$ 1-cre mice.

### TCR $\beta\delta$ KO C57BL/6

This mouse strain was purchased from the Jackson Laboratory with the stock number 002121. Mice homozygous for the targeted mutation in the *TCR $\beta$ <sup>tm1Mom</sup>* and *TCR $\delta$ <sup>tm1Mom</sup>* gene do not express the  $\alpha\beta$  T-cell receptor nor any  $\gamma\delta$  T-cell receptor.

### C57BL/6

These mice were purchased from Charles River.

## 8 Methods

### 8.1 Molecular biology

#### 8.1.1 DNA isolation

##### 8.1.1.1 Genomic DNA isolation from tissue

In order to perform genotyping from the transgenic mice, the DNA of ear or tail clippings was isolated. The tissue was incubated over night at 56°C while shaking with 500  $\mu$ l lysis buffer (100 mM Tris/HCl pH = 8, 5 mM EDTA, 0,2% SDS, 200 nM NaCl, 100  $\mu$ g/ml Proteinase K). At the next day, 170  $\mu$ l of saturated NaCl (at least 5 M) was added to

precipitate the protein. The samples were centrifuged for 10 min at 20.000xg at 4°C. Then, the supernatant was transferred into a new tube containing 500 µl of 100% (v/v) isopropyl alcohol. After inverting the tube several times, tubes were centrifuged again. Afterwards, the pelleted DNA was washed with 70% (v/v) ethanol and centrifuged another time. The DNA was dried at 37°C and dissolved in 100 µl TE (10 mM Tris pH = 7,9; 1 mM EDTA) buffer at 37°C while shaking for 2-3 h.

#### **8.1.1.2 Genomic DNA isolation from whole splenocyte pellets**

For the Southern Blot analysis, the genomic DNA of whole splenocyte pellets was isolated in the following way. The pellets were digested as described in section 8.1.1.1. Afterwards, 50 µl of 3 M NaAc and 1.25 ml of 100% ethanol were added. The tube was then carefully panned until the DNA was visible as silver ball. With the help of a bend glass cuvette, the DNA was removed from the tube. The DNA was washed for 10 min in 70% ethanol and then air dried. DNA was dissolved in 100 µl TE buffer while shaking at 37°C.

#### **8.1.2 Mouse genotyping**

Depending on the transgenic mice, different genes needed to be amplified in a PCR reaction in order to detect the specific genotype. The following tables show the primers used (Table 1), the PCR mixtures (Table 2) and the programs (Table 3) which were run in the thermal cyclers (Biometra) for all used mice. The primers were purchased from metabion, DMSO from Carl Roth and the residual components from Thermo Fisher.

#### **8.1.3 Agarose gel electrophoresis of DNA**

Agarose gel electrophoresis was performed to detect amplified DNA products from a PCR. The gels which were loaded with the DNA contained 1x TAE (40 mM Tris/HCl, 20 mM acetic acid, 1 mM EDTA pH 8.5), 5 µg/ml ethidium bromide, and 1.5 - 2% (w/v) agarose (Biozym). The electrophoresis was performed in gel chambers (PEQLAB Biotechnologie GmbH) containing 1x TAE buffer at 80 to 100 V for up to 1.5 h. The ethidium bromide intercalated with the nucleic acids which could than be visualized under a UV luminescence screen (Quantum ST-4).

#### **8.1.4 Southern Blot**

For the Southern blot analysis, the DNA was isolated as described in section 8.1.1.2. 25 µl DNA were digested with 3.5 µl enzyme buffer (NEB, 10x), 0.35 µl Bovine serum albumin (BSA) (NEB, 100x), 0.35 µl spermidin (0.1 M, Sigma Aldrich), 0.35 µl DTT (0.1 M, Promega), 0.15 µl RNase (10 mg/ml, Thermo Fisher), 3.3 µl water, and 2 µl EcoRI (NEB, 100 Units/µl) for 16 h at 37°C. DNA was applied on an agarose gel (0.8%) and gel electrophoresis was performed at 50 V overnight. The DNA was depurinated

**Table 1:** The table displays the used primer for every PCR reaction

PCR	Oligonucleotide	Sequence 5'-3' direction
CD19	Cre7 CD19c CD19d	tca gct aca cca gag acg g aac cag tca aca ccc ttc c cca gac tag ata cag acc ag
TCR $\beta$	TCR-mut for-12834 TCR-2-15243 TCR-wt-for-15242	gct act tcc att tgt cac gtc c cct aac cca gaa tga tct tg ccc cac cca gta tag gac ag
TCR $\delta$	TcRd 6916 TCRd 6917 TCRd wt 8744 TCRd wt 8745	cct ggg tgg aga ggc tat tc agg tga gat gac agg aga tc caa atg ttg ctt gtc tgg tg gtc agt cga gtg cac agt tt
CAR	CAR for CAR rev	cag cca ctc gat gat gta cag cgg cag gag cga gag ccg cct ac
$\gamma$ 1-cre	IgG1 KPN1 Cre13 IgG1 rev3	tgt tgg gac aaa cga gca ggg ggc tgg acc aat gta aat a gtc atg gca atg cca agg teg cta g
CD30	hCD2 rev CD30c	gga gac tgc acc ttt gga ag cag tga tcg tgg gct ctc tgt a
rosa	hCD2 rev CD30c	gga gac tgc acc ttt gga ag cag tga tcg tgg gct ctc tgt a

**Table 2:** The table displays the volume of the ingredients per one PCR reaction

Componer	CAR	CD30	CD19	$\gamma$ 1-cre	TCR $_{\beta\delta}$ KO	rosa
dH <sub>2</sub> O	18.85 $\mu$ l	16.65 $\mu$ l	18.55 $\mu$ l	19 $\mu$ l	17.65 $\mu$ l	18.4 $\mu$ l
Taq buffer (10x)	2.5 $\mu$ l	2.5 $\mu$ l	2.5 $\mu$ l	2.5 $\mu$ l	2.5 $\mu$ l	2.5 $\mu$ l
MgCL <sub>2</sub> (50mM)	0.5 $\mu$ l	1 $\mu$ l	1 $\mu$ l	1 $\mu$ l	1.3 $\mu$ l	1.5 $\mu$ l
dNTP (10mM)	0.5 $\mu$ l	0.5 $\mu$ l	0.5 $\mu$ l	0.5 $\mu$ l	0.5 $\mu$ l	0.5 $\mu$ l
Primer (100 $\mu$ M)	0.25 $\mu$ l	0.1 $\mu$ l	0.1 $\mu$ l	0.1 $\mu$ l	0.1 $\mu$ l	0.1 $\mu$ l
Taq polymerase (5U/ $\mu$ l)	0.15 $\mu$ l	0.15 $\mu$ l	0.15 $\mu$ l	0.15 $\mu$ l	0.15 $\mu$ l	0.15 $\mu$ l
DMSO (100%)	-	0.5 $\mu$ l	-	-	0.5 $\mu$ l	0.25 $\mu$ l
DNA (5-10 ng)	2 $\mu$ l	1 $\mu$ l	2 $\mu$ l	1 $\mu$ l	1 $\mu$ l	1.5 $\mu$ l

**Table 3:** The table displays the different PCR cycles

Phases	CAR	CD30	CD19	$\gamma$ 1-cre	TCR $_{\beta\delta}$ KO	rosa
Initial.	3' 95°C	5' 95°C	5' 95°C	2.30' 95°C	2' 94°C	5' 95°C
Denat.	15'' 95°C	45'' 95°C	45'' 95°C	40'' 94°C	20'' 94°C/ 15'' 94°C	45'' 95°C
Hybrid.	30'' 62°C	45'' 56°C	45'' 57°C	40'' 58°C	15'' 65°C/ 15'' 60°C	45'' 58°C
Elongation	1' 72°C	1' 72°C	1.15' 72°C	40'' 72°C	10'' 68°C/ 10' 72°C	1' 72°C
Final elongation	10' 72°C	10' 72°C	10'' 72°C	10' 72°C	2' 72°C/ 2' 94°C	10' 72°C
No. of cycles	32	33	30	30	10/28	33

by tossing the gel for 20 min in 0.25 M HCl. The gel was then passed on for 60 min in transfer buffer (0.4 M NaOH, 0.6 M NaCl) to denature the DNA. The DNA was blotted on a nylon membrane (Immobilon TM Ny+ membrane, Millipore) by applying capillary pressure with the transfer buffer overnight. To neutralize the membrane, it was rinsed twice with 2x SSC (0.3 M NaCl, 0.03 M Na Citrate, pH 6.5). Then, the membrane was baked at 80°C for 1 h to crosslink the DNA to the membrane. The membrane was incubated at 65°C overnight with the pre-hybridization buffer (1M NaCl, 50 mM Tris (pH 7.6), 10% (w/v) Dextranulfat, 1% (w/v) SDS, 250 µg salmon sperm DNA/ml (Sigma Aldrich) incubated for 10 min at 100°C and cooled down on ice for 1 min). Afterwards, the probe was prepared. 200 ng of probe DNA (isolated from a Bluescript vector, isolated with restriction enzymes NaeI and EcoRI by digest from the region between JH4 and Eµ of the murine IgH locus) was filled up with water to 50 µl. Then, probe DNA was denaturated for 5 min at 95°C and cooled down on ice for 2 min. The probe DNA solution was mixed with a Amersham ready-to-go DNA labeling bead (GE Healthcare) and 50 µCi <sup>32</sup>P dCTP (Hartmann Analytic) and incubated for 45 min at 37°C. The labeled probe was separated from the non incorporated nucleotides by using Sephadex G-50 columns (GE Healthcare). The efficiency of the incorporation of <sup>32</sup>P dCTP in the probe was measured with the bioscan QC 4000 XER. Probes with values starting from 35.000.000 dpm were used. Afterwards, the probe was incubated at 99°C for denaturation and cooled down on ice for 5 min. Then, the probe was added to the membrane with the hybridization buffer and incubated again over night at 65°C. The membrane was washed with 0.5x SSC and 0.5% SDS at 60°C to remove unbound DNA. The washing was performed until the membrane had a radioactivity of around 70 counts. The labeled DNA was visualized by applying a radio-sensitive film (Biomax MS PE Applied Biosystems 35x43 cm, KODAK) for 2 d at -80°C in a Biomax cassette.

## 8.2 Mouse related assays

### 8.2.1 Preparation of murine lymphocytes

The mice which were used for analysis were euthanized with CO<sub>2</sub> or killed by cervical dislocation. After preparation, the spleen and the LN were kept in 1% B cell medium (BCM) (1x RPMI 1640 containing 1% (v/v) heat-inactivated fetal calf serum (FCS) (PAA Cell culture Company), 100 U/ml penicillin, 100 µg/ml streptomycin, 1 mM sodium pyruvate, 2 mM L-glutamine, 1x non-essential amino acids, and 52 µM β-mercaptoethanol (all purchased from Gibco)) on ice. BM cells were isolated by flushing the tight bone with 1% BCM medium using a cannula. The B cells from the PerC were isolated by filling the peritoneum with 1% BCM with a cannula, slight shaking, followed by sucking up the medium with a cannula. The blood was prepared directly from the opened heart with a Pasteur pipette. Then the blood was either stored directly on ice for serum preparation or

mixed with 10x of volume of PBS with 5 nM EDTA for FACS analysis. The spleen and the LN were pushed through a 70  $\mu\text{m}$  sieve to achieve a single cell suspension. Splenic and BM cell suspension were lysed for 3 min with 1 ml of lysis buffer (1x RBC buffer, eBioscience) to reduce the erythrocytes from the cell suspension. The reaction was stopped by adding 10 ml of 1% BCM and centrifuging at 1200 rounds per minute (rpm) for 10 min at 4°C (Rotanta 460-R, Hettich centrifuge). The cell suspension from the blood was lysed at least 2 times with 3 ml of lysis buffer.

### 8.2.2 Isolation of B cells, T cells and B cell sub-populations

The isolation of B and T cells was either performed with MACS kits (Miltenyi Biotec) or by cell sorting (FACS Aria III, Beckton Dickinson). For the MACS, the Pan B cell kit, the CD43 depletion kit, or the Pan T cell kit were used. Cells were purified according to the instructions of the manufacturer.

In order to reduce the time of cell sorting, first, B cells were enriched with the Pan B cell kit and then stained with the necessary antibodies to separate the desired population by sorting in the second step. The applied sorting strategy is explained under the according figures.

### 8.2.3 Preparation of serum

For the determination of the antibody titers in the serum. Blood was kept on ice for at least 3 h after isolation. Afterwards, the blood was centrifuged for 15 min with 14000 rpm at 4°C. Then, the supernatant (serum) was transferred into a clean tube and centrifuged again. The supernatant was again transferred into a new tube. Finally, the serum was stored at  $-80^{\circ}\text{C}$ .

### 8.2.4 ELISA (enzyme-linked immunosorbent assay)

For the detection of NP specific antibodies, NUNC<sup>TM</sup> plates (Nunc) were coated with either NP3-BSA (10 mg/l in carbonate buffer, Biosearch technologies) or NP13-BSA (10 mg/ml) diluted 1:2000 in carbonate buffer (0.1 M  $\text{NaHCO}_3$ , pH 9.5) over night at 4°C. At the next day, plates were washed three times with 200  $\mu\text{l}$  of PBS/well and blocked for 1 h with 50  $\mu\text{l}$ /well blocking buffer (1% low-fat milk powder in PBS). Afterwards, serum of immunized and unimmunized mice was diluted 1:10 in blocking buffer. In the first row of the plate, 50  $\mu\text{l}$  of diluted serum was pipetted and, with a 1:2 serial dilution, distributed over 8 wells. After 1 h incubation and washing of the plate three times with PBS, 1  $\mu\text{g}/\text{ml}$  diluted in blocking buffer of the biotinylated antibody specific for the to detecting isotype (anti-IgM R6-60.2, anti-IgG1 A85-1, anti-IgG3 R40-82, BD Biosciences) was added and incubated for 30 min. The plate was washed again three time with PBS and incubated for 1 h with 2.5  $\mu\text{g}/\text{ml}$  streptavidin horseradish peroxidase Avidin D (Vector,

A-2004) which was diluted in blocking buffer. Then, bound streptavidin was detected with o-Phenylenediamine (Sigma, P-7288) in substrate buffer (0.1 M citric acid, 0.1 M Tris (Sigma)) with 0.015% H<sub>2</sub>O<sub>2</sub>. The plate was slightly shaken and measured with the ELISA reader (Photometer Sunrise RC, Tecan) with of OD 405 nm and a reference wavelength of 620 nm. In order to compare different assays between each other, internal standards consisting of serum pools from NP-CGG immunized mice were used.

For the detection of antibodies in the supernatant of cultivated cells, the NUNC<sup>TM</sup> plates were coated with 5 µg/ml Ig-specific rat anti-mouse IgM antibody (II/41, BD Bioscience) diluted in carbonate buffer (0.1 M NaHCO<sub>3</sub> pH 9.5). The supernatant of cultivated cells was diluted 1:1 with blocking buffer before distributed on the plates. Despite this exceptions, the detection followed the same procedure as described above.

### 8.2.5 ELISpot (enzyme-linked immunospot assay)

#### ELISpot of NP-specific ASC

In order to detect the number of ASC, an ELISpot was performed. Membrane plates (Millipore) were coated with 50 µl of either 25 µg/ml NP3-BSA or NP13-BSA, in carbonate buffer at 4°C overnight. After washing the plate three times with PBS, plates were blocked with BCM (containing 10% FCS (10% BCM)) for 2 h at 37°C. 5x10<sup>5</sup> splenocytes per well in 10% FCS BCM, were plated and incubated for 48 h at 37°C. Afterwards, plates were washed six times with PBS-T (PBS, 0,025% Tween 20). Then, a biotinylated antibody (anti-IgM, anti-IgG1, anti-IgG3) was diluted 1:500 in PBS/1% BSA and incubated for 2 h at 37°C. After washing again with PBS-T, streptavidin horseradish peroxidase Avidin D was diluted 1:2000 in PBS/1% BSA and incubated for 45 min at RT. Following, the plate was washed three times with PBS-T and three times with PBS. In 5 ml distilled water, one tablet of each 3,3'-Diaminobenzidin peroxidase-substrate (0.7 mg/ml, Sigma-Aldrich) and UREA H<sub>2</sub>O<sub>2</sub> (2.0 mg/ml, Sigma-Aldrich) were solved. 50 µl of this solution was pipetted in each well and incubated until spots were visible. Finally, the plate was washed with water and left to dry. The spots were measured and counted with the ELISpot reader AID Elispot3.2 and the appropriate software (Autoimmune Diagnostika GmbH).

#### IFN $\gamma$ ELISpot

The IFN $\gamma$  ELISpot was performed with the Mabtech #3321-2AW Plus kit according to the instruction manual. To analyze the reaction towards MHV-68 specific peptides, Orf6 or Orf61 in DMSO were added to the ELISpot plate with a final concentration of 10 µg/ml, together with the splenocyte suspension. The percentage of T cells in the splenocyte suspension was detected by FACS staining against CD3<sup>+</sup> cells. Afterwards, 60.000 T cells per well were seeded. Spots were detected 18 h after cell seeding.

In order to analyze the IFN $\gamma$  secreting T cells in response to infected B cells, B cells were infected with MHV-68 in a co-culture with NIH3T3 at 0.5 MOI for 4 d before the

ELISpot assay (see section 8.7.5). MOI is the ratio of virus (pfu) to cells in the culture. T cells were isolated with a Pan T cell isolation kit (Miltenyi). T and B cells were seeded together on the coated ELISpot plate with a ratio of 1:2 (60.000:120.000 cells/well). Cells were seeded in triplicates.

### 8.2.6 Flow cytometry

The flow cytometry analysis were performed with the FACS Calibur, the LSR Fortessa or the FACSCanto all from Beckton Dickinson. The evaluation was done with the FlowJo 10 software. Per staining,  $5 \times 10^5$ - $1 \times 10^6$  cells were distributed into one well of a FACS plate (Greiner Bio One) and washed with MACS buffer by centrifuging for 5 min with 1200 rpm (Rotanta 460-R, Hettich centrifuge). Then, the cells were stained with 25  $\mu$ l of antibody mix diluted in MACS buffer (BD) and incubated for 20 min in the dark on ice. The antibodies were coupled to following fluorochromes: FITC, PE, PerCP, APC, Alexa Fluor 700, Horizon V450, Brilliant Violet 421, Pe-Vio 770 (Miltenyi), APC-Vio770 (Miltenyi). The antibodies were specific for B220, Blimp-1, CD2 (human), CD19, CD21, CD23, CD25, CD38, CD86, CD138, IgD, IgM, Irf4, Thy1.2-Bio, CD62L, CD44, CD79b, CD5, CD95 and were purchased from BD Biosciences. The antibody against CAR was purchased from Santa Cruz and the antibody against LMP1 came from the antibody facility of the Helmholtz Center. Afterwards, cells were washed again, diluted with MACS buffer, and transferred into FACS tubes. If needed, cells were stained with TOP-RO3 (1:40000, Molecular Probes) directly before measuring. The staining of intracellular molecules was performed on fixed cells. Cells were washed with PBS and fixed with 2% PFA for 10 min at RT. Then, cells were washed with PBS and centrifuged again. Afterwards, the cells were resuspended in ice cold methanol (stored at  $-20^\circ\text{C}$ ) and either stored in the freezer covered with adhesive foil or directly used for staining. The cells were washed twice with PBS and then stained for 1 h at RT.

### 8.3 Cell culture

Cell culture was performed under the sterile workbench (Bio Flow technique) with sterile pipettes (Gilson/Eppendorf) and expendable materials. For the cultivation,  $5 \times 10^5$ - $1 \times 10^6$  cells were plated per well in a round or flat bottom plate (Nunc). The cultivation was carried out at  $37^\circ\text{C}$ , with 5%  $\text{CO}_2$ , and 95% humidity in an incubator (Binder). The cells were kept in 10% BCM with and without different kind of stimuli. Depending on the assay, the following stimuli were added: anti-CD40 antibody (2,5  $\mu\text{g}/\text{ml}$ , HM40-3, eBioscience), IL4 (Interleukin-4, 10  $\text{ng}/\text{ml}$ , Sigma-Aldrich), IgM (15  $\mu\text{g}/\text{ml}$ , 115-006-020 Jackson Immunology Research), LPS (Lipopolysacharid, 50  $\mu\text{g}/\text{ml}$ , Sigma-Aldrich). The cells were incubated for up to 5 d. The proliferation of the cells was tracked by CFSE (2,5  $\mu\text{mol}$ , Molecular Probes) labeling. After entering the cell, the two acetate groups of

CFSE are removed by intracellular esterase. As a result, CFSE becomes highly fluorescent. After each cell division, the fluorescence intensity is halved in each daughter cell. The staining was performed after Parrish et al. [Quah and Parish, 2010].

## 8.4 Immunohistochemistry and immunofluorescence

Parts of the spleen were embedded into tissue tek (VWR Chemicals), frozen on dry ice, and stored at  $-80^{\circ}\text{C}$ . The splenic sections were cut into 7-8  $\mu\text{m}$  thick slices with a cryostat (Leica) and air dried for 15 min. Afterwards, sections were either stored at  $-80^{\circ}\text{C}$  or fixed for 10 min with ice cold acetone and air dried for another 15 min. The tissue sections were re-hydrated for 5 min in PBS and blocked for 20 min with 5% goat serum in PBS with 1% BSA. After washing again with PBS, the sections were blocked with the Avidin-Biotin blocking kit (SP-2001, Vector) if biotin coupled antibodies were used. The sections were washed three times with PBS and the 1<sup>st</sup> antibody diluted into PBS with 1% BSA was applied over night at  $4^{\circ}\text{C}$  or for 1 h at RT. After incubation of all necessary antibodies, sections were developed with the AEC substrate Kit (Vector Laboratories SK-4200) and the Alkaline Phosphatase Kit (Vector Laboratories SK-5300). Finally, the tissue sections were air dried and embedded in Kaiser's Gelatine (Merck KGaA). The following antibodies were used: PNA-Bio (B-1075, Vector) with Streptavidin-Alkaline Phosphatase (S-2890, Sigma-Aldrich), goat anti-mouse IgM POX (A-8786, Sigma-Aldrich), mouse anti-human CD2-Bio (RPA-2.10, BD), rabbit anti-mouse Laminin (L9393, Sigma), goat anti-rabbit POX (A5795, Sigma), and rat anti-LMP1 (1G6, IgG2a, Antibody facility, Helmholtz Center Munich).

For immunofluorescence, tissue sections embedded in OCT were air dried and fixed with 3% PFA for 10 min and rinsed with PBS for 5 min. The rehydration was performed for 5 min with PBS+ (PBS and 50 mM  $\text{NH}_4\text{Cl}$ ). Then, slices were permeabilized and blocked with 0.3% Triton X, 1% BSA, 2% goat serum in PBS for 20 min. The 1<sup>st</sup> antibody, diluted in PBS with 1% BSA, was incubated for 1 h at RT, after rinsing with PBS. 3 x 5 min washing with PBS was followed by incubation of the 2<sup>nd</sup> antibody for 1 h at RT. After washing, slices were embedded in SlowFade Gold (Thermo Fisher). The following 1<sup>st</sup> antibodies were applied: anti-B220-APC (RA3-6B2, BD), anti-GL7-FITC (GL7, BD), anti-IRF4 (3E4, eBioscience). Anti-rat Alexa Fluor 594 (A-11007, Thermo Scientific), and anti-FITC Alexa Fluor 488 (A-11094, Thermo Scientific) were used as secondary antibodies. All staining combinations are shown in table 4.

Immunohistochemically stained splenic sections were evaluated with an Axioskop (Zeiss) with a Zeiss Plan NEOFLUAR objective 10x/0.3. The images were obtained with an AxioCam MRc5 digital camera in combination with AxioVision rel.4.6.3.0 software (Carl Zeiss MicroImaging GmbH, Jena, Germany). The slices stained with immunofluorescences were obtained with the Leica TCS SP5 II with an 8 kHz resonant scanner and a HCX PL

APO CS 20x objective and the LAS AF software.

The staining of the paraffin embedded tissue were performed by the Research Unit Analytical Pathology of the Helmholtz Center Munich.

**Table 4:** The table displays the used combination of antibodies.

Primary antibody	Secondary antibody	Detection kit
PNA-Bio	Streptavidin-Alkaline Phosphatase	Alkaline Phosphatase Kit
goat anti-mouse IgM POX	/	AEC substrate Kit
mouse anti-human CD2-Bio	Streptavidin-Alkaline Phosphatase	Alkaline Phosphatase Kit
rabbit anti-mouse Laminin	goat anti-rabbit POX	AEC substrate Kit
rat anti-LMP1	anti-rat Bio	Alkaline Phosphatase Kit
anti-B220-APC	/	/
anti-IRF4	Anti-rat Alexa Fluor 594	/
anti-GL7-FITC	anti-FITC Alexa Fluor 488	/

## 8.5 Western Blot

About  $3-7 \times 10^6$  isolated B cells were washed twice with PBS by centrifuging at 2400 rpm at 4°C for 5 min. For the nucleus cytoplasmic fractioning the NE-PER kit (Thermo Scientific) was used according to the manufactures instructions. The protein concentration was determined by nanodrop at 280 nm. The protein detection was performed with the WES system, a fully automated western blot system (Protein Simple). The analysis and the quantification was performed with the Compass Software (Protein Simple). Cytoplasmic protein was standardized to  $\alpha\beta$ -tubulin and nuclear extracts with lamin B2. As basis for the protein quantification, the area under the curve at the respective size was used for the calculations. The area under the curve was calculated by the software. For the normalization, area under the curve of protein of interest was divided by its respective loading control. In order to secure a correct quantification of the protein of interest, the concentration of the protein lysate needed to be adapted to the used antibody. First, the protein lysate was tested in a dilution experiment to determine the optimal concentration of the lysate which needed to be within the dynamically range on Wes. This means, an increase or decrease of the protein lysate leads to an increase or decrease of bound material in the capillary on the WES. Thereby, protein lysate dilutions ranged from 0.12-3  $\mu\text{g}/\mu\text{l}$  in 5 steps and an antibody dilution of 1:50 for the dilution experiment. Linear regression analysis of chemiluminescence signal (peak area of protein of interest) and lysate concentration was used to pick the concentration of the protein within the linear increase. Afterwards, the antibody concentration was titrated from 1:10-1:200 in five

steps. This was necessary to ensure that the used antibody concentration can saturate the protein bound to the capillary in the Wes machine. Again, linear regression analysis of chemiluminescence signal (peak area of protein of interest) to antibody dilution was used. With increasing antibody concentration, the signal (chemiluminescence) increases until saturation. For optimal quantification an antibody concentration near the saturation level was chosen. The used antibodies dilutions are displayed with their corresponding concentration of lysate in table 5.

**Table 5:** The table displays the used antibodies and the used lysate concentrations in western blot

Antibody	Antibody concentration	Lysate concentration
anti- $\alpha\beta$ -tubulin	1:20	0.3 $\mu\text{g}/\mu\text{l}$ cytoplasmic extract
anti-LaminB2	1:50	0.3-0.4 $\mu\text{g}/\mu\text{l}$ nuclear extract
anti-pSTAT3	1:50	0.3 $\mu\text{g}/\mu\text{l}$ nuclear extract
anti-pSTAT6	1:50	0.3 $\mu\text{g}/\mu\text{l}$ nuclear extract
Irf4	1:50	0.4 $\mu\text{g}/\mu\text{l}$ nuclear extract
Irf4	1:50	4 $\mu\text{g}/\mu\text{l}$ cytoplasmic extract
p65	1:50	0.4 $\mu\text{g}/\mu\text{l}$ nuclear extract
p65	1:50	4 $\mu\text{g}/\mu\text{l}$ cytoplasmic extract

## 8.6 Immunization, infection and depletion

### NP-Ficoll immunization

For the T-cell independent immunization, NP-Ficoll (Biosearch Technologies) was used. NP<sub>(33)</sub>-Ficoll was diluted to a concentration of 250  $\mu\text{g}/\text{ml}$  in sterile Dulbecco's Phosphate-Buffered Saline (DPBS) (GIBCO). 50  $\mu\text{g}$  in 200  $\mu\text{l}$  DPBS were injected i.p..

### NP-CGG immunization

The T-dependent antigen NP-CGG (> 40, Biosearch Technologies) was diluted to a concentration of 1  $\text{mg}/\text{ml}$  in DPBS. Before each immunization experiment, the pH value of NP-CGG was adjusted. Here, 100  $\mu\text{g}$  of NP-CGG per mouse was mixed with the same volume of 0.4 M  $\text{KAl}(\text{SO}_4)_2$  in  $\text{H}_2\text{O}$ . The pH value was adjusted to 6.5 with 1 N NaOH and kept on ice for 30 min. Afterwards, the antigen was centrifuged with 5000 rpm at

4°C for 10 min. The supernatant was discarded and the yellow pellet was washed with 1 ml of DPBS. This step was repeated twice. Afterwards, the NP-CGG was adjusted to 500 µg/ml with sterile PBS. 100 µg of NP-CGG in 200 µl DPBS were injected i.p. per mouse.

### **Intranasal infection**

The frozen virus stock was thawed and diluted in sterile PBS to obtain  $5 \times 10^4$  pfu/30  $\mu$ l. Mice were anesthetized by i.p. injection of MMF (medetomidine 0.2 mg/kg, midazolam 1.0 mg/kg, fentanyl 0.025 mg/kg). After the mouse showed a deep anesthesia which was confirmed by the absence of reflexes on a footpath, the mouse was held in the scruff and 30  $\mu$ l of the virus suspension was gradually released in one nostril. The mouse was held in this position until normal breathing rhythm was achieved. Again anesthesia was antagonized by subcutaneous injection of naloxone (1.2 mg/kg), flumazenil (0.5 mg/kg) and atipamezole (2.5 mg/kg).

### **Intraperitoneal infection**

The frozen virus stock was thawed and diluted in sterile PBS to obtain  $25 \times 10^5$  pfu/ml. 200  $\mu$ l of virus suspension was applied by i.p. injection.

### **NK cell depletion**

NK cells from mice were depleted by injecting 250  $\mu$ g anti-NK1.1 antibody (PK136, Bio X cell) in 200  $\mu$ l DPBS i.p.. As control, the isotype antibody IgG2a (C1.18.4, Bio X Cell) was used. Mice were injected one day before infection and afterwards twice per week until analysis.

## **8.7 Virological assays**

### **8.7.1 Virus stock production**

Virus stocks were produced in baby hamster kidney (BHK-21) cells which were cultivated in Glasgow modified eagle medium (Pan Biotech) supplemented with 5% FCS, 2 mM L-glutamine, 5% tryptose phosphate broth (TBP), penicillin (100 U/ml) and streptomycin (100 mg/ml) (BHK-21 medium). MHV-68 was added at a MOI of 0.1 to the BHK-21 cells and incubated at 37°C until cytopathic effect (CPE) was visible in almost all cells. The cells were frozen and thawed twice to destroy the cell membrane and release the virus. The supernatant was cleared of cell debris by centrifuging 1300xg for 20 min at 4°C. The virus was pelleted at 26000xg for 2 h at 4°C. The virus was resuspended in 1 ml of BHK-21 cell culture medium, aliquoted in 50  $\mu$ l and stored at  $-80^\circ\text{C}$ .

### **8.7.2 Plaque assay**

The concentration of the virus stock was determined by plaque assay on BHK-21. Cells were plated at a concentration of  $5 \times 10^4$  per well in a 24 well plate and incubated for 24 h. Afterwards, the virus was diluted 10-fold with BHK-21 medium from  $10^{-1}$  to  $10^{-8}$ , transferred onto the BHK-21 cells, and incubated for 90 min at 37°C. The medium with the virus was removed and each well was covered with BHK-21 medium containing 1.5% carboxymethylcellulose (Carl Roth). After 5 d at 37°C, cells were stained with 0.1%

cristal violet solution (containing 1% formaldehyde in PBS (Carl Roth)) by applying to the plate after the BHK-21 medium was removed. The cristal violet solution was incubated for 10 min, removed with several washing steps with water, and plaques were counted. The virus titer was calculated with following equation:

$$\text{Titer (pfu/ml)} = n \text{ (plaque count per well)} / 0.9 * \text{viral dilution}$$

The viruses which were used together in one experiment were titrated in parallel.

Virus titers were as follows:

Parental virus:  $1.7 \times 10^7$  pfu/ml

MHV-68-NGFR:  $1.8 \times 10^7$  pfu/ml

MHV-68-LMP1wt:  $1.1 \times 10^7$  pfu/ml

MHV-68-LMP1mut:  $3.3 \times 10^7$  pfu/ml

For the *ex vivo* plaque assay, the left lung was extracted from the infected mice and frozen at  $-80^\circ\text{C}$ . The tissue was thawed and homogenized for 30 s in a tissue homogenizer (MP biomedical). The cell suspension was filled up to 500  $\mu\text{l}$  with BHK-21 medium and again frozen at  $-80^\circ\text{C}$ . The following steps were the same as described above.

### 8.7.3 Generation of recombinant virus

#### MHV-68-NGFR

MHV-68-NGFR was constructed by inserting a SFFV-NGFR cassette between ORF 27 and 29. The SFFV-NGFR cassette was extracted with restriction enzymes from the plasmid pCDH-SFFV-hspCas9-T2A-NGFR which was kindly provided by the group of Prof. I. Jeremias. The map is shown in supplementary 4. First, the hspCas9-T2A was excised by enzymatic digest with EcoRI and NsiI. Then, SFFV-NGFR was removed by using ClaI and SalI. After generating blunt ends on both sites with the help of the Klenow enzyme, the 1.15 kb SFFV-NGFR cassette was inserted into the PmlI site (nucleotide position 46347 of the MHV-68 genome) of the plasmid pST76K-SR (shuttle vector for BAC mutagenesis). This plasmid contained already a 4 kb SphI-SacI fragment of the MHV-68 genome (nucleotides 44301 to 48346). As a result, the SFFV-NGFR cassette is flanked on both sides by homologous sequences which enables the insertion of the cassette into the MHV-68-BAC by homologous recombination. The MHV-68-NGFR virus was then produced by the two-step mutagenesis procedure as described earlier [Fields et al., 2007, Wang et al., 2008].

#### MHV-68-LMP1wt/mut

MHV-68-LMP1wt and LMP1mut were constructed in the same way as described above. Here, a LMP1wt and a LMP1mut cassette were inserted which were kindly provided by Prof. A. Kieser as published in 2008 [Schneider et al., 2008]. Both genes are under the control of the HCMV promoter. The LMP1mut cassette has mutations in both signaling domains. CTAR1 carries an inactivating P(204)xQxT to AxAxA mutation and CTAR2 carries a deletion of 16 C-terminal amino acids. Both viruses were generated by Wei

Zhang in the laboratory from Prof. H. Adler.

#### 8.7.4 *Ex vivo* reactivation assay

For every group of infected mice, two 96 well plates were seeded with 6000 NIH3T3 cells/well in 200  $\mu$ l of medium. The cells were incubated in DMEM (GIBCO) supplemented with 10% fetal calf serum (FCS), 2 mM L-glutamine, penicillin (100 U/ml) and streptomycin (100 mg/ml). Plates were incubated for 24 h at 37°C. Spleens of infected mice were isolated and a cell suspension was generated as described in section 8.2.1. The splenocytes from mice, infected with the same virus, were pooled.  $13.5 \times 10^6$  Cells were adjusted to a concentration of  $1.5 \times 10^6$  cells with NIH3T3 medium. 3-fold serial dilutions with overall 7 dilutions were generated. For every dilution, 24 wells were used starting with  $5 \times 10^4$  splenocytes per 0.1 ml/culture well. The remaining cell suspension of every dilution was frozen at  $-80^\circ\text{C}$  for the detection of virus in the lytic phase. NIH3T3 were incubated for 14 d at 37°C. After 7 and 14 d, the cells were analyzed with the microscope and wells containing cells showing CPE were counted. The percentage of wells which were positive for CPE was calculated. To detect virus in the lytic phase, the remaining splenocyte suspension was frozen and thawed twice. Afterwards, cell suspension was handled as described before. Wells positive for CPE were subtracted from the wells calculated above to obtain the value % CPE of the virus in the latent phase.

#### 8.7.5 Viral infection of B cells *in vitro*

Murine B cells were infected in a co-culture with NIH3T3 cells. 7500 NIH3T3 cells per well of a 96 well plate were seeded and incubated for 24 h or until attached to the culturing surface. B cells from wt mice were isolated from the spleen with the Pan B cell isolation kit (Miltenyi). The medium of the NIH3T3 cells was removed.  $5 \times 10^5$  B cells per well in 10% BCM was applied. 100  $\mu$ l of virus suspension in 10% BCM was added to every well resulting in a MOI of 0.5. Cells were incubated at 37°C.

### 8.8 Statistics

The two-tailed Student's t-test was performed to calculate the significance of splenic weight values, percentages of cell populations and absolute cell numbers. In case that three or more groups were compared the ANOVA test was used. Immunoglobulin titers were logarithmized prior to the determination of significance. In case the respective values showed no gaussian distribution, which was calculated with the normalization analysis in Prism, the Mann-Whitney test was used to determine the significance.  $*P \leq 0.05$ ,  $**P \leq 0.01$ ,  $***P \leq 0.001$ , and  $****P \leq 0.0001$ . The statistical calculations were performed with Prism 9 (GraphPad Software).

## References

- [Adler et al., 2014] Adler, H., Steer, B., Juskewitz, E., and Kammerer, R. (2014). To the Editor Murine gammaherpesvirus 68 (MHV-68) escapes from NK-cell-mediated immune surveillance by a CEACAM1-mediated immune evasion mechanism. *European Journal of Immunology*, 44(8):2521–2522.
- [Albanese et al., 2017] Albanese, M., Tagawa, T., Buschle, A., and Hammerschmidt, W. (2017). MicroRNAs of Epstein-Barr Virus Control Innate and Adaptive Antiviral Immunity.
- [Aldinucci et al., 2010] Aldinucci, D., Gloghini, A., Pinto, A., Filippi, R. D., and Carbone, A. (2010). The classical Hodgkin ' s lymphoma microenvironment and its role. (April):248–263.
- [Alizadeh et al., 2000] Alizadeh, A. A., Eisen, M. B., Davis, R. E., Ma, C., Lossos, I. S., Rosenwald, A., Boldrick, J. C., Sabet, H., Tran, T., Yu, X., Powell, J. I., Yang, L., Marti, G. E., Moore, T., Hudson, J., Lu, L., Lewis, D. B., Tibshirani, R., Sherlock, G., Chan, W. C., Greiner, T. C., Weisenburger, D. D., Armitage, J. O., Warnke, R., Levy, R., Wilson, W., Grever, M. R., Byrd, J. C., Botstein, D., Brown, P. O., and Staudt, L. M. (2000). Distinct types of diffuse large B-cell lymphoma identified by gene expression profiling. *Nature*, 403(6769):503–511.
- [Alter et al., 2004] Alter, G., Malenfant, J. M., and Altfeld, M. (2004). CD107a as a functional marker for the identification of natural killer cell activity. *Journal of Immunological Methods*, 294(1-2):15–22.
- [Amakawa et al., 1996] Amakawa, R., Hakem, A., Kundig, T. M., Matsuyama, T., Simard, J. J. L., Timms, E., Wakeham, A., Mittrucker, H.-w., Griesser, H., Takimoto, H., Schmits, R., Shahinian, A., Ohashi, P. S., Penninger, J. M., and Mak, T. W. (1996). Impaired Negative Selection of T Cells in Hodgkin ' s Disease Antigen CD30 – Deficient Mice. *Cell*, 84:551–562.
- [Balázs et al., 2002] Balázs, M., Martin, F., Zhou, T., and Kearney, J. (2002). Blood dendritic cells interact with splenic marginal zone B cells to initiate T-independent immune responses. *Immunity*, 17(3):341–52.
- [Barton et al., 2011] Barton, E., Mandal, P., and Speck, S. H. (2011). Pathogenesis and Host Control of Gammaherpesviruses: Lessons from the Mouse. *Annual Review of Immunology*, 29(1):351–397.
- [Baumgarth, 2016] Baumgarth, N. (2016). B-1 Cell Heterogeneity and the Regulation of Natural and Antigen-Induced IgM Production. *Frontiers in immunology*, 7:324.
- [Bhatt et al., 2013] Bhatt, S., Ashlock, B. M., Natkunam, Y., Sujoy, V., Chapman, J. R., Ramos, J. C., Mesri, E. A., and Lossos, I. S. (2013). CD30 targeting with brentuximab vedotin: A novel therapeutic approach to primary effusion lymphoma. *Blood*, 122(7):1233–1242.
- [Biron, 1997] Biron, C. A. (1997). Activation and function of natural killer cell responses during viral infections. *Current opinion in immunology*, 9(1):24–34.
- [Bishop et al., 1995] Bishop, G. A., Warren, W. D., and Berton, M. T. (1995). Signaling via major histocompatibility complex class II molecules and antigen receptors enhances the B cell response to gp39/CD40 ligand. *European Journal of Immunology*, 25(5):1230–1238.
- [Blaskovic et al., 1980] Blaskovic, D., Stanceková, M., Svobodová, J., and Mistríková, J. (1980). Isolation of five strains of herpesviruses from two species of free living small rodents. *Acta virologica*, 24(6):468.
- [Boi et al., 2015] Boi, M., Zucca, E., Inghirami, G., and Bertoni, F. (2015). PRDM1 /BLIMP1: a tumor suppressor gene in B and T cell lymphomas. *Leukemia & Lymphoma*, 56(5):1223–1228.

- [Borrego et al., 1999] Borrego, F., Robertson, M. J., Ritz, J., Peña, J., and Solana, R. (1999). CD69 is a stimulatory receptor for natural killer cell and its cytotoxic effect is blocked by CD94 inhibitory receptor. *Immunology*, 97(1):159–65.
- [Boucher et al., 1997] Boucher, L. M., Marengère, L. E., Lu, Y., Thukral, S., and Mak, T. W. (1997). Binding sites of cytoplasmic effectors TRAF1, 2, and 3 on CD30 and other members of the TNF receptor superfamily. *Biochemical and Biophysical Research Communications*, 233(3):592–600.
- [Brynjolfsson et al., 2018] Brynjolfsson, S. F., Persson Berg, L., Olsen Ekerhult, T., Rimkute, I., Wick, M.-J., Mårtensson, I.-L., and Grimsholm, O. (2018). Long-Lived Plasma Cells in Mice and Men. *Frontiers in Immunology*, 9:2673.
- [Buchan and Al-Shamkhani, 2012] Buchan, S. L. and Al-Shamkhani, A. (2012). Distinct Motifs in the Intracellular Domain of Human CD30 Differentially Activate Canonical and Alternative Transcription Factor NF- $\kappa$ B Signaling. *PLoS ONE*, 7(9).
- [Bunker et al., 2015] Bunker, J., Flynn, T., Koval, J., Shaw, D., Meisel, M., McDonald, B., Ishizuka, I., Dent, A., Wilson, P., Jabri, B., Antonopoulos, D., and Bendelac, A. (2015). Innate and Adaptive Humoral Responses Coat Distinct Commensal Bacteria with Immunoglobulin A. *Immunity*, 43(3):541–553.
- [Bunker and Bendelac, 2018] Bunker, J. J. and Bendelac, A. (2018). IgA Responses to Microbiota. *Immunity*, 49(2):211–224.
- [Burger and Kipps, 2006] Burger, J. A. and Kipps, T. J. (2006). CXCR4: a key receptor in the crosstalk between tumor cells and their microenvironment. *Blood*, 107(5):1761–1767.
- [Cahir-McFarland et al., 2004] Cahir-McFarland, E. D., Carter, K., Rosenwald, A., Giltneane, J. M., Henrickson, S. E., Staudt, L. M., and Kieff, E. (2004). Role of NF-kappa B in cell survival and transcription of latent membrane protein 1-expressing or Epstein-Barr virus latency III-infected cells. *Journal of virology*, 78(8):4108–19.
- [Calado et al., 2010] Calado, D. P., Zhang, B., Srinivasan, L., Sasaki, Y., Seagal, J., Unitt, C., Rodig, S., Kutok, J., Tarakhovsky, A., Schmidt-Suppran, M., and Rajewsky, K. (2010). Constitutive Canonical NF- $\kappa$ B Activation Cooperates with Disruption of BLIMP1 in the Pathogenesis of Activated B Cell-like Diffuse Large Cell Lymphoma. *Cancer Cell*, 18(6):580–589.
- [Campo et al., 2011] Campo, E., Swerdlow, S. H., Harris, N. L., Pileri, S., Stein, H., and Jaffe, E. S. (2011). The 2008 WHO classification of lymphoid neoplasms and beyond: evolving concepts and practical applications. *Blood*, 117(19):5019–32.
- [Canny et al., 2014] Canny, S. P., Goel, G., Reese, T. A., Zhang, X., Xavier, R., and Virgin, H. W. (2014). Latent Gammaherpesvirus 68 Infection Induces Distinct Transcriptional Changes in Different Organs. *Journal of Virology*, 88(1):730–738.
- [Casola et al., 2006] Casola, S., Cattoretti, G., Uyttersprot, N., Koralov, S. B., Seagal, J., Segal, J., Hao, Z., Waisman, A., Egert, A., Ghitza, D., and Rajewsky, K. (2006). Tracking germinal center B cells expressing germ-line immunoglobulin gamma1 transcripts by conditional gene targeting. *Proceedings of the National Academy of Sciences of the United States of America*, 103(19):7396–401.
- [Cattoretti et al., 2006] Cattoretti, G., Shaknovich, R., Smith, P. M., Jäck, H.-M., Murty, V. V., and Alobeid, B. (2006). Stages of germinal center transit are defined by B cell transcription factor co-expression and relative abundance. *Journal of immunology (Baltimore, Md. : 1950)*, 177(10):6930–9.

- [Cerutti et al., 1998] Cerutti, A., Zan, H., Schaffer, A., Bergsagel, L., Harindranath, N., Max, E. E., and Casali, P. (1998). CD40 ligand and appropriate cytokines induce switching to IgG, IgA, and IgE and coordinated germinal center and plasmacytoid phenotypic differentiation in a human monoclonal IgM+IgD+ B cell line. *Journal of immunology (Baltimore, Md. : 1950)*, 160(5):2145–57.
- [Chesi, 1996] Chesi, M. (1996). Dysregulation of cyclin D1 by translocation into an IGH gamma switch region in two multiple myeloma cell lines. *Blood*.
- [Chiarle et al., 1999] Chiarle, R., Podda, A., Prolla, G., Podack, E. R., Thorbecke, G. J., and Inghirami, G. (1999). CD30 overexpression enhances negative selection in the thymus and mediates programmed cell death via a Bcl-2-sensitive pathway. *Journal of immunology (Baltimore, Md. : 1950)*, 163(1):194–205.
- [Choi et al., 2012] Choi, Y. S., Dieter, J. A., Rothausler, K., Luo, Z., and Baumgarth, N. (2012). B-1 cells in the bone marrow are a significant source of natural IgM. *European journal of immunology*, 42(1):120–9.
- [Chuang et al., 2000] Chuang, S.-S., Yung, Y.-C., and Li, C.-Y. (2000). von Willebrand Factor Is the Most Reliable Immunohistochemical Marker for Megakaryocytes of Myelodysplastic Syndrome and Chronic Myeloproliferative Disorders. Technical report.
- [Collins et al., 2009] Collins, C. M., Boss, J. M., and Speck, S. H. (2009). Identification of infected B-cell populations by using a recombinant murine gammaherpesvirus 68 expressing a fluorescent protein. *Journal of virology*, 83(13):6484–93.
- [Collins and Speck, 2012] Collins, C. M. and Speck, S. H. (2012). Tracking murine gammaherpesvirus 68 infection of germinal center B cells in vivo. *PLoS one*, 7(3):e33230.
- [Covens et al., 2013] Covens, K., Verbinnen, B., Geukens, N., Meyts, I., Schuit, F., Van Lommel, L., Jacquemin, M., and Bossuyt, X. (2013). Characterization of proposed human B-1 cells reveals pre-plasmablast phenotype. *Blood*, 121(6):5176–5183.
- [Croft, 2003] Croft, M. (2003). Co-stimulatory members of the TNFR family: keys to effective T-cell immunity? *Nature Reviews Immunology*, 3(8):609–620.
- [Dalloul, 2009] Dalloul, A. (2009). CD5: A safeguard against autoimmunity and a shield for cancer cells. *Autoimmunity Reviews*, 8(4):349–353.
- [Damania et al., 2000] Damania, B., Choi, J. K., and Jung, J. U. (2000). Signaling activities of gamma-herpesvirus membrane proteins. *Journal of virology*, 74(4):1593–601.
- [De Silva et al., 2016] De Silva, N. S., Anderson, M. M., Carette, A., Silva, K., Heise, N., Bhagat, G., and Klein, U. (2016). Transcription factors of the alternative NF- $\kappa$ B pathway are required for germinal center B-cell development. *Proceedings of the National Academy of Sciences*, 113(32):9063–9068.
- [Del Prete et al., 1995] Del Prete, G., De Carli, M., D’Elios, M. M., Daniel, K. C., Almerigogna, F., Alderson, M., Smith, C. A., Thomas, E., and Romagnani, S. (1995). CD30-mediated signaling promotes the development of human T helper type 2-like T cells. *The Journal of experimental medicine*, 182(6):1655–61.
- [Diehl et al., 2008] Diehl, S. A., Schmidlin, H., Nagasawa, M., van Haren, S. D., Kwakkenbos, M. J., Yasuda, E., Beaumont, T., Scheeren, F. A., and Spits, H. (2008). STAT3-Mediated Up-Regulation of BLIMP1 Is Coordinated with BCL6 Down-Regulation to Control Human Plasma Cell Differentiation. *The Journal of Immunology*, 180(7):4805–4815.

- [Dürkop et al., 1997] Dürkop, H., Anagnostopoulos, I., Bulfone-Paus, S., and Stein, H. (1997). Expression of several members of the TNF-ligand and receptor family on tonsillar lymphoid B cells. *British journal of haematology*, 98(4):863–8.
- [Ebrahimi et al., 2001] Ebrahimi, B., Dutia, B. M., Brownstein, D. G., and Nash, A. A. (2001). Murine gammaherpesvirus-68 infection causes multi-organ fibrosis and alters leukocyte trafficking in interferon-gamma receptor knockout mice. *The American journal of pathology*, 158(6):2117–25.
- [Ehtisham et al., 1993] Ehtisham, S., Sunil-Chandra, N. P., and Nash, A. A. (1993). Pathogenesis of Murine Gammaherpesvirus Infection in Mice Deficient in CD4 and CD8 T Cells. Technical report.
- [Falini et al., 2013] Falini, B., Fizzotti, M., Pucciarini, A., Bigerna, B., Marafioti, T., Pacini, R., Alunni, C., Tanci, L. N., Ugolini, B., Sebastiani, C., Cattoretti, G., Pileri, S., Dalla-favera, R., Stein, H., and Gambacorta, M. (2013). A monoclonal antibody ( MUM1p ) detects expression of the MUM1 / IRF4 protein in a subset of germinal center B cells , plasma cells , and activated T cells A monoclonal antibody ( MUM1p ) detects expression of the MUM1 / IRF4 protein in a subset of germin. 95(6):2084–2092.
- [Fields et al., 2007] Fields, B. N., Knipe, D. M. D. M., and Howley, P. M. (2007). *Fields virology*. Wolters Kluwer Health/Lippincott Williams & Wilkins.
- [Flaño et al., 2002] Flaño, E., Kim, I.-J., Woodland, D. L., and Blackman, M. A. (2002). Gamma-herpesvirus latency is preferentially maintained in splenic germinal center and memory B cells. *The Journal of experimental medicine*, 196(10):1363–72.
- [Förster and Rajewsky, 1987] Förster, I. and Rajewsky, K. (1987). Expansion and functional activity of Ly-1+ B cells upon transfer of peritoneal cells into allotype-congenic, newborn mice. *European Journal of Immunology*, 17(4):521–528.
- [French and Tschopp, 2002] French, L. E. and Tschopp, J. (2002). Defective death receptor signaling as a cause of tumor immune escape. *Seminars in Cancer Biology*, 12(1):51–55.
- [Froese et al., 1987] Froese, P., Lemke, H., Gerdes, J., Havsteen, B., Schwarting, R., Hansen, H., and Stein, H. (1987). Biochemical characterization and biosynthesis of the Ki-1 antigen in Hodgkin-derived and virus-transformed human B and T lymphoid cell lines. *Journal of immunology (Baltimore, Md. : 1950)*, 139(6):2081–7.
- [Gardner et al., 2001] Gardner, L. J., Polski, J. M., Evans, H. L., Perkkins, S. L., and Dunphy, C. H. (2001). CD30 expression in follicular lymphoma. *Archives of Pathology and Laboratory Medicine*, 125(8):1036–1041.
- [Gaspal et al., 2005] Gaspal, F. M. C., Kim, M.-Y., McConnell, F. M., Raykundalia, C., Bekiaris, V., and Lane, P. J. L. (2005). Mice deficient in OX40 and CD30 signals lack memory antibody responses because of deficient CD4 T cell memory. *Journal of immunology (Baltimore, Md. : 1950)*, 174(7):3891–6.
- [Gauld et al., 2013] Gauld, S. B., De Santis, J. L., Kulinski, J. M., McGraw, J. A., Leonardo, S. M., Ruder, E. A., Maier, W., and Tarakanova, V. L. (2013). Modulation of B-cell tolerance by murine gammaherpesvirus 68 infection: requirement for Orf73 viral gene expression and follicular helper T cells. *Immunology*, 139(2):197–204.
- [Gilfillan et al., 1998] Gilfillan, M. C., Noel, P. J., Podack, E. R., Reiner, S. L., and Thompson, C. B. (1998). Expression of the costimulatory receptor CD30 is regulated by both CD28 and cytokines. *Journal of immunology (Baltimore, Md. : 1950)*, 160(5):2180–7.

- [Gostissa et al., 2009] Gostissa, M., Yan, C. T., Bianco, J. M., Cogné, M., Pinaud, E., and Alt, F. W. (2009). Long-range oncogenic activation of Igh-c-myc translocations by the Igh 3' regulatory region. *Nature*, 462(7274):803–7.
- [Graf et al., 2019] Graf, R., Seagal, J., Otipoby, K. L., Lam, K.-P., Ayoub, S., Zhang, B., Sander, S., Chu, V. T., and Rajewsky, K. (2019). BCR-dependent lineage plasticity in mature B cells. *Science (New York, N.Y.)*, 363(6428):748–753.
- [Grossmann and Ganem, 2008] Grossmann, C. and Ganem, D. (2008). Effects of NFkappaB activation on KSHV latency and lytic reactivation are complex and context-dependent. *Virology*, 375(1):94–102.
- [Grumont and Gerondakis, 2000] Grumont, R. J. and Gerondakis, S. (2000). Rel induces interferon regulatory factor 4 (IRF-4) expression in lymphocytes: modulation of interferon-regulated gene expression by rel/nuclear factor kappaB. *The Journal of experimental medicine*, 191(8):1281–92.
- [Haas et al., 2005] Haas, K. M., Poe, J. C., Steeber, D. A., and Tedder, T. F. (2005). B-1a and B-1b Cells Exhibit Distinct Developmental Requirements and Have Unique Functional Roles in Innate and Adaptive Immunity to *S. pneumoniae*. *Immunity*, 23(1):7–18.
- [Halminen et al., 1997] Halminen, M., Klemetti, P., Vaarala, O., Hurme, M., and Ilonen, J. (1997). Interferon-gamma production in antigen specific T cell response: quantitation of specific mRNA and secreted protein. *Scandinavian journal of immunology*, 46(4):388–92.
- [Hamoudi et al., 2004] Hamoudi, R., Diss, T. C., Oksenhendler, E., Pan, L., Carbone, A., Ascoli, V., Boshoff, C., Isaacson, P., and Du, M.-Q. (2004). Distinct cellular origins of primary effusion lymphoma with and without EBV infection. *Leukemia research*, 28(4):333–8.
- [Hansen et al., 2000] Hansen, H. P., Dietrich, S., Kisseleva, T., Mokros, T., Mentlein, R., Lange, H. H., Murphy, G., and Lemke, H. (2000). CD30 shedding from Karpas 299 lymphoma cells is mediated by TNF-alpha-converting enzyme. *Journal of immunology (Baltimore, Md. : 1950)*, 165(12):6703–9.
- [Hao et al., 2015] Hao, X., Wei, X., Huang, F., Wei, Y., Zeng, H., Xu, L., Zhou, Q., and Feng, R. (2015). The expression of CD30 based on immunohistochemistry predicts inferior outcome in patients with diffuse large B-cell lymphoma. *PLoS ONE*, 10(5):1–11.
- [Hasbold et al., 1998] Hasbold, J., Lyons, A. B., Kehry, M. R., and Hodgkin, P. D. (1998). Cell division number regulates IgG1 and IgE switching of B cells following stimulation by CD40 ligand and IL-4. *European Journal of Immunology*, 28(3):1040–1051.
- [Haxhinasto et al., 2002] Haxhinasto, S. A., Hostager, B. S., and Bishop, G. A. (2002). Cutting edge: molecular mechanisms of synergy between CD40 and the B cell antigen receptor: role for TNF receptor-associated factor 2 in receptor interaction. *Journal of immunology (Baltimore, Md. : 1950)*, 169(3):1145–9.
- [Hayakawa et al., 1986] Hayakawa, K., Hardy, R. R., and Herzenberg, L. A. (1986). Peritoneal Ly-1 B cells: Genetic control, autoantibody production, increased lambda light chain expression. *European Journal of Immunology*, 16(4):450–456.
- [Heger et al., 2015] Heger, K., Kober, M., Rieß, D., Drees, C., de Vries, I., Bertossi, A., Roers, A., Sixt, M., and Schmidt-Supprian, M. (2015). A novel Cre recombinase reporter mouse strain facilitates selective and efficient infection of primary immune cells with adenoviral vectors. *European Journal of Immunology*, 45(6):1614–1620.
- [Hendrickson et al., 2007] Hendrickson, J. E., Chadwick, T. E., Roback, J. D., Hillyer, C. D., and Zimring, J. C. (2007). Inflammation enhances consumption and presentation of transfused RBC antigens by dendritic cells.

- [Herzenberg and Herzenberg, 1989] Herzenberg, L. A. and Herzenberg, L. A. (1989). Toward a Layered Immune System. Technical report.
- [Hirsch et al., 2008] Hirsch, B., Hummel, M., Bentink, S., Fouladi, F., Spang, R., Zollinger, R., Stein, H., and Dürkop, H. (2008). CD30-induced signaling is absent in Hodgkin’s cells but present in anaplastic large cell lymphoma cells. *American Journal of Pathology*, 172(2):510–520.
- [Hömig-Hölzel et al., 2008] Hömig-Hölzel, C., Hojer, C., Rastelli, J., Casola, S., Strobl, L. J., Müller, W., Quintanilla-Martinez, L., Gewies, A., Ruland, J., Rajewsky, K., and Zimmer-Strobl, U. (2008). Constitutive CD40 signaling in B cells selectively activates the noncanonical NF-kappaB pathway and promotes lymphomagenesis. *The Journal of experimental medicine*, 205(6):1317–29.
- [Horie et al., 2003] Horie, R., Higashihara, M., and Watanabe, T. (2003). Hodgkin’s lymphoma and CD30 signal transduction. *International journal of hematology*, 77(1):37–47.
- [Horie et al., 2002a] Horie, R., Watanabe, T., Ito, K., Morisita, Y., Watanabe, M., Ishida, T., Higashihara, M., Kadin, M., and Watanabe, T. (2002a). Cytoplasmic aggregation of TRAF2 and TRAF5 proteins in the Hodgkin-Reed-Sternberg cells. *American Journal of Pathology*, 160(5):1647–1654.
- [Horie et al., 2002b] Horie, R., Watanabe, T., Morishita, Y., Ito, K., Ishida, T., Kanegae, Y., Saito, I., Higashihara, M., Mori, S., Kadin, M. E., and Watanabe, T. (2002b). Ligand-independent signaling by overexpressed CD30 drives NF- $\kappa$ B activation in Hodgkin-Reed-Sternberg cells. *Oncogene*, 21(16):2493–2503.
- [Hsu and Hsu, 2000] Hsu, P. L. and Hsu, S. M. (2000). Autocrine growth regulation of CD30 ligand in CD30-expressing Reed-Sternberg cells: distinction between Hodgkin’s disease and anaplastic large cell lymphoma. *Laboratory investigation; a journal of technical methods and pathology*, 80(7):1111–9.
- [Hu et al., 2013] Hu, S., Xu-Monette, Z. Y., Balasubramanyam, A., Manyam, G. C., Visco, C., Tzankov, A., Liu, W. M., Miranda, R. N., Zhang, L., Montes-Moreno, S., Dybkær, K., Chiu, A., Orazi, A., Zu, Y., Bhagat, G., Richards, K. L., Hsi, E. D., Choi, W. W., Van Krieken, J. H., Huang, Q., Huh, J., Ai, W., Ponzoni, M., Ferreri, A. J., Zhao, X., Winter, J. N., Zhang, M., Li, L., Møller, M. B., Piris, M. A., Li, Y., Go, R. S., Wu, L., Jeffrey Medeiros, L., and Young, K. H. (2013). CD30 expression defines a novel subgroup of diffuse large B-cell lymphoma with favorable prognosis and distinct gene expression signature: A report from the International DLBCL Rituximab-CHOP Consortium Program Study. *Blood*, 121(14):2715–2724.
- [Huot et al., 2018] Huot, N., Bosinger, S. E., Paiardini, M., Reeves, R. K., and Müller-Trutwin, M. (2018). Lymph Node Cellular and Viral Dynamics in Natural Hosts and Impact for HIV Cure Strategies. *Frontiers in Immunology*, 9:780.
- [Jiang et al., 2015] Jiang, Y., Li, Y., and Zhu, B. (2015). T-cell exhaustion in the tumor microenvironment. *Cell Death & Disease*, 6(6):e1792–e1792.
- [Johnson et al., 2009] Johnson, N. A., Savage, K. J., Ludkovski, O., Ben-Neriah, S., Woods, R., Steidl, C., Dyer, M. J. S., Siebert, R., Kuruvilla, J., Klasa, R., Connors, J. M., Gascoyne, R. D., and Horsman, D. E. (2009). Lymphomas with concurrent BCL2 and MYC translocations: the critical factors associated with survival. *Blood*, 114(11):2273.
- [Josimovic-Alasevic et al., 1989] Josimovic-Alasevic, O., Dürkop, H., Schwarting, R., Backé, E., Stein, H., and Diamantstein, T. (1989). Ki-1 (CD30) antigen is released by Ki-1-positive tumor cells in vitro and in vivo. I. Partial characterization of soluble Ki-1 antigen and detection of the antigen in cell culture supernatants and in serum by an enzyme-linked immunosorbent assay. *European Journal of Immunology*, 19(1):157–162.

- [Jourdan et al., 2011] Jourdan, M., Caraux, A., Caron, G., Robert, N., Fiol, G., Rème, T., Bolloré, K., Vendrell, J.-P., Le Gallou, S., Mourcin, F., De Vos, J., Kassambara, A., Duperray, C., Hose, D., Fest, T., Tarte, K., and Klein, B. (2011). Characterization of a Transitional Preplasmablast Population in the Process of Human B Cell to Plasma Cell Differentiation. *The Journal of Immunology*, 187(8):3931–3941.
- [Kalia et al., 2013] Kalia, V., Sarkar, S., and Ahmed, R. (2013). CD8 T-Cell Memory Differentiation during Acute and Chronic Viral Infections.
- [Kawano et al., 1994] Kawano, Y., Noma, T., and Yata, J. (1994). Regulation of human IgG subclass production by cytokines. IFN-gamma and IL-6 act antagonistically in the induction of human IgG1 but additively in the induction of IgG2. *Journal of immunology (Baltimore, Md. : 1950)*, 153(11):4948–58.
- [Kennedy et al., 2006] Kennedy, M. K., Willis, C. R., and Armitage, R. J. (2006). Deciphering CD30 ligand biology and its role in humoral immunity. *Immunology*, 118(2):143–152.
- [Kieser and Sterz, 2015] Kieser, A. and Sterz, K. R. (2015). The Latent Membrane Protein 1 (LMP1). pages 119–149. Springer, Cham.
- [Kipps et al., 2017] Kipps, T. J., Stevenson, F. K., Wu, C. J., Croce, C. M., Packham, G., Wierda, W. G., O’Brien, S., Gribben, J., and Rai, K. (2017). Chronic lymphocytic leukaemia. *Nature Reviews Disease Primers*, 3:16096.
- [Klein et al., 1999] Klein, E., Teramoto, N., Gogolák, P., Nagy, N., and Björkholm, M. (1999). LMP-1, the Epstein-Barr virus-encoded oncogene with a B cell activating mechanism similar to CD40. *Immunology letters*, 68(1):147–54.
- [Klein et al., 1976] Klein, G., Svedmyr, E., Jondal, M., and Persson, P. O. (1976). EBV-determined nuclear antigen (EBNA)-positive cells in the peripheral blood of infectious mononucleosis patients. *International Journal of Cancer*, 17(1):21–26.
- [Klein et al., 2006] Klein, U., Casola, S., Cattoretti, G., Shen, Q., Lia, M., Mo, T., Ludwig, T., Rajewsky, K., and Dalla-Favera, R. (2006). Transcription factor IRF4 controls plasma cell differentiation and class-switch recombination. *Nature Immunology*, 7(7):773–782.
- [Klein et al., 2003] Klein, U., Gloghini, A., Gaidano, G., Chadburn, A., Cesarman, E., Dalla-Favera, R., and Carbone, A. (2003). Gene expression profile analysis of AIDS-related primary effusion lymphoma (PEL) suggests a plasmablastic derivation and identifies PEL-specific transcripts. *Blood*, 101(10):4115–4121.
- [Kräutler et al., 2017] Kräutler, N. J., Suan, D., Butt, D., Bourne, K., Hermes, J. R., Chan, T. D., Sundling, C., Kaplan, W., Schofield, P., Jackson, J., Basten, A., Christ, D., and Brink, R. (2017). Differentiation of germinal center B cells into plasma cells is initiated by high-affinity antigen and completed by Tfh cells. *The Journal of Experimental Medicine*, 214(5):1259–1267.
- [Kreslavsky et al., 2018] Kreslavsky, T., Wong, J. B., Fischer, M., Skok, J. A., and Busslinger, M. (2018). Control of B-1a cell development by instructive BCR signaling. *Current Opinion in Immunology*, 51:24–31.
- [Krug et al., 2007] Krug, L. T., Moser, J. M., Dickerson, S. M., and Speck, S. H. (2007). Inhibition of NF- $\kappa$ B Activation In Vivo Impairs Establishment of Gammaherpesvirus Latency. *PLoS Pathogens*, 3(1):e11.

- [Kulwichit et al., 1998] Kulwichit, W., Edwards, R. H., Davenport, E. M., Baskar, J. F., Godfrey, V., and Raab-Traub, N. (1998). Expression of the Epstein-Barr virus latent membrane protein 1 induces B cell lymphoma in transgenic mice. *Proceedings of the National Academy of Sciences of the United States of America*, 95(20):11963–8.
- [Küppers, 2005] Küppers, R. (2005). Mechanisms of B-cell lymphoma pathogenesis. *Nature Reviews Cancer*, 5(4):251–262.
- [Küppers, 2012] Küppers, R. (2012). New insights in the biology of Hodgkin lymphoma. *Hematology / the Education Program of the American Society of Hematology. American Society of Hematology. Education Program*, 2012:328–34.
- [Laichalk and Thorley-Lawson, 2005] Laichalk, L. L. and Thorley-Lawson, D. A. (2005). Terminal differentiation into plasma cells initiates the replicative cycle of Epstein-Barr virus in vivo. *Journal of virology*, 79(2):1296–307.
- [Lalor et al., 1989] Lalor, P. A., Herzenberg, L. A., Adams, S., and Stall, A. M. (1989). Feedback regulation of murine Ly-1 B cell development. *European Journal of Immunology*, 19(3):507–513.
- [Lambert Charles Q Morris, 2017] Lambert Charles Q Morris, J. M. (2017). Antibody-Drug Conjugates (ADCs) for Personalized Treatment of Solid Tumors: A Review.
- [Langer et al., 2010] Langer, R., Geissinger, E., Rüdiger, T., von Schilling, C., Ott, G., Mandl-Weber, S., Quintanilla-Martinez, L., and Fend, F. (2010). Peripheral T-cell Lymphoma With Progression to a Clonally Related, Epstein Barr Virus+, Cytotoxic Aggressive T-cell Lymphoma: Evidence for Secondary EBV Infection of an Established Malignant T-cell Clone. *The American Journal of Surgical Pathology*, 34(9):1382–1387.
- [Lee et al., 1996] Lee, S. Y., Lee, S. Y., Kandala, G., Liou, M. L., Liou, H. C., and Choi, Y. (1996). CD30/TNF receptor-associated factor interaction: NF-kappa B activation and binding specificity. *Proceedings of the National Academy of Sciences of the United States of America*, 93(18):9699–703.
- [Leen et al., 2001] Leen, A., Meij, P., Redchenko, I., Middeldorp, J., Bloemena, E., Rickinson, A., and Blake, N. (2001). Differential immunogenicity of Epstein-Barr virus latent-cycle proteins for human CD4(+) T-helper 1 responses. *Journal of virology*, 75(18):8649–59.
- [Linehan et al., 1998] Linehan, L. A., Warren, W. D., Thompson, P. A., Grusby, M. J., and Berton, M. T. (1998). STAT6 Is Required for IL-4-Induced Germline Ig Gene Transcription and Switch Recombination. *The Journal of Immunology*, 161(1).
- [Liu et al., 2014] Liu, Y., Sattarzadeh, A., Diepstra, A., Visser, L., and van den Berg, A. (2014). The microenvironment in classical Hodgkin lymphoma: An actively shaped and essential tumor component. *Seminars in Cancer Biology*, 24:15–22.
- [LORENZ and NEWBERRY, 2004] LORENZ, R. G. and NEWBERRY, R. D. (2004). Isolated Lymphoid Follicles Can Function as Sites for Induction of Mucosal Immune Responses. *Annals of the New York Academy of Sciences*, 1029(1):44–57.
- [Ma et al., 2017] Ma, S.-D., Tsai, M.-H., Romero-Masters, J. C., Ranheim, E. A., Huebner, S. M., Bristol, J. A., Delecluse, H.-J., and Kenney, S. C. (2017). Latent Membrane Protein 1 (LMP1) and LMP2A Collaborate To Promote Epstein-Barr Virus-Induced B Cell Lymphomas in a Cord Blood-Humanized Mouse Model but Are Not Essential. *Journal of virology*, 91(7).

- [Ma et al., 2015] Ma, S.-D., Xu, X., Plowshay, J., Ranheim, E. A., Burlingham, W. J., Jensen, J. L., Asimakopoulos, F., Tang, W., Gulley, M. L., Cesarman, E., Gumperz, J. E., and Kenney, S. C. (2015). LMP1-deficient Epstein-Barr virus mutant requires T cells for lymphomagenesis. *Journal of Clinical Investigation*, 125(1):304–315.
- [MacLennan, 1994] MacLennan, I. C. M. (1994). Germinal Centers. *Annual Review of Immunology*, 12(1):117–139.
- [Marín and García, 2017] Marín, N. D. and García, L. F. (2017). The role of CD30 and CD153 (CD30L) in the anti-mycobacterial immune response. *Tuberculosis*, 102:8–15.
- [Matsumoto et al., 1996] Matsumoto, M., Mariathasan, S., Nahm, M. H., Baranyay, F., Peschon, J. J., and Chaplin, D. D. (1996). Role of Lymphotoxin and the Type I TNF Receptor in the Formation of Germinal Centers. *Science*, 271(5253):1289–1291.
- [Middeldorp and Pegtel, 2008] Middeldorp, J. and Pegtel, D. (2008). Multiple roles of LMP1 in Epstein-Barr virus induced immune escape. *Seminars in Cancer Biology*, 18(6):388–396.
- [Minnich et al., 2016] Minnich, M., Tagoh, H., Bönelt, P., Axelsson, E., Fischer, M., Cebolla, B., Tarakhovskiy, A., Nutt, S. L., Jaritz, M., and Busslinger, M. (2016). Multifunctional role of the transcription factor Blimp-1 in coordinating plasma cell differentiation. *Nature immunology*, 17(3):331–43.
- [Mir et al., 2000] Mir, S. S., Richter, B. W., Duckett, C. S., Reiners, K., Borchmann, P., Rothe, A., Engert, A., and von Strandmann, E. P. (2000). Differential effects of CD30 activation in anaplastic large cell lymphoma and Hodgkin disease cells. *Blood*, 96(13):4307–12.
- [Mokada-Gopal et al., 2017] Mokada-Gopal, L., Boeser, A., Lehmann, C. H. K., Drepper, F., Dudziak, D., Warscheid, B., and Voehringer, D. (2017). Identification of Novel STAT6-Regulated Proteins in Mouse B Cells by Comparative Transcriptome and Proteome Analysis. *The Journal of Immunology*, page 1601838.
- [Montecino-Rodriguez and Dorshkind, 2011] Montecino-Rodriguez, E. and Dorshkind, K. (2011). Formation of B-1 B cells from neonatal B-1 transitional cells exhibits NF- $\kappa$ B redundancy. *Journal of immunology (Baltimore, Md. : 1950)*, 187(11):5712–9.
- [Montecino-Rodriguez and Dorshkind, 2012] Montecino-Rodriguez, E. and Dorshkind, K. (2012). B-1 B Cell Development in the Fetus and Adult. *Immunity*, 36(1):13–23.
- [Montes-Moreno et al., 2015] Montes-Moreno, S., Climent, F., González de Villambrosía, S., González Barca, E. M., Batlle, A., Insunza, A., Pané-Foix, M., Colorado, M., Martín-Sánchez, G., Espiga, C. R., Conde, E., and Piris, M. A. (2015). CD 30-positive transformed follicular lymphoma: Two case reports and literature review. *Histopathology*, 67(6):918–922.
- [Montes-Moreno et al., 2012] Montes-Moreno, S., Odqvist, L., Diaz-Perez, J. A., Lopez, A. B., de Villambrosía, S. G., Mazonra, F., Castillo, M. E., Lopez, M., Pajares, R., García, J. F., Mollejo, M., Camacho, F. I., Ruiz-Marcellán, C., Agrados, M., Ortiz, N., Franco, R., Ortiz-Hidalgo, C., Suarez-Gauthier, A., Young, K. H., and Piris, M. A. (2012). EBV-positive diffuse large B-cell lymphoma of the elderly is an aggressive post-germinal center B-cell neoplasm characterized by prominent nuclear factor- $\kappa$ B activation. *Modern Pathology*, 25(7):968–982.
- [Moon et al., 2012] Moon, H., Lee, J.-G., Shin, S. H., and Kim, T. J. (2012). LPS-Induced Migration of Peritoneal B-1 Cells is Associated with Upregulation of CXCR4 and Increased Migratory Sensitivity to CXCL12. *Journal of Korean Medical Science*, 27(1):27.
- [Mora and von Andrian, 2008] Mora, J. R. and von Andrian, U. H. (2008). Differentiation and homing of IgA-secreting cells. *Mucosal Immunology 2008 1:2*, 1(2):96.

- [Muramatsu et al., 2000] Muramatsu, M., Kinoshita, K., Fagarasan, S., Yamada, S., Shinkai, Y., and Honjo, T. (2000). Class Switch Recombination and Hypermutation Require Activation-Induced Cytidine Deaminase (AID), a Potential RNA Editing Enzyme. *Cell*, 102(5):553–563.
- [Murphy et al., 2012] Murphy, K. K. M., Travers, P., Walport, M., and Janeway, C. (2012). *Janeway's immunobiology*. New York : Garland Science, c2012., 8th ed. edition.
- [Müschen et al., 2002] Müschen, M., Rajewsky, K., Krönke, M., and Küppers, R. (2002). The origin of CD95-gene mutations in B-cell lymphoma. *Trends in immunology*, 23(2):75–80.
- [Müschen et al., 2000] Müschen, M., Warskulat, U., and Beckmann, M. (2000). Defining CD95 as a tumor suppressor gene. *Journal of Molecular Medicine*, 78(6):312–325.
- [Muta and Podack, 2013] Muta, H. and Podack, E. R. (2013). CD30: from basic research to cancer therapy. *Immunologic research*, 57(1-3):151–8.
- [Nagel et al., 2014] Nagel, D., Vincendeau, M., Eitelhuber, A. C., and Krappmann, D. (2014). Mechanisms and consequences of constitutive NF- $\kappa$ B activation in B-cell lymphoid malignancies. *Oncogene*, 33(50):5655–5665.
- [Nash et al., 2001] Nash, A. A., Dutia, B. M., Stewart, J. P., and Davison, A. J. (2001). Natural history of murine gamma-herpesvirus infection. *Philosophical transactions of the Royal Society of London. Series B, Biological sciences*, 356(1408):569–79.
- [Nawrocki et al., 1988] Nawrocki, J. F., Kirsten, E. S., and Fisher, R. I. (1988). Biochemical and structural properties of a Hodgkin's disease-related membrane protein. *Journal of immunology (Baltimore, Md. : 1950)*, 141(2):672–80.
- [Nera et al., 2006] Nera, K.-P., Kohonen, P., Narvi, E., Peippo, A., Mustonen, L., Terho, P., Koskela, K., Buerstedde, J.-M., and Lassila, O. (2006). Loss of Pax5 Promotes Plasma Cell Differentiation. *Immunity*, 24(3):283–293.
- [Nie et al., 2008] Nie, K., Gomez, M., Landgraf, P., Garcia, J.-F., Liu, Y., Tan, L. H. C., Chadburn, A., Tuschl, T., Knowles, D. M., and Tam, W. (2008). MicroRNA-mediated down-regulation of PRDM1/Blimp-1 in Hodgkin/Reed-Sternberg cells: a potential pathogenetic lesion in Hodgkin lymphomas. *The American journal of pathology*, 173(1):242–52.
- [Nishimura et al., 2005] Nishimura, H., Yajima, T., Muta, H., Podack, E. R., Tani, K., and Yoshikai, Y. (2005). A Novel Role of CD30/CD30 Ligand Signaling in the Generation of Long-Lived Memory CD8+ T Cells. *The Journal of Immunology*, 175(7):4627–4634.
- [Nutt et al., 2015] Nutt, S. L., Hodgkin, P. D., Tarlinton, D. M., and Corcoran, L. M. (2015). The generation of antibody-secreting plasma cells. *Nature Reviews Immunology*, 15(3):160–171.
- [Ouaaz et al., 1999] Ouaaz, F., Li, M., and Beg, A. A. (1999). A critical role for the RelA subunit of nuclear factor kappaB in regulation of multiple immune-response genes and in Fas-induced cell death. *The Journal of experimental medicine*, 189(6):999–1004.
- [Palmer et al., 1964] Palmer, R., Quinton, W., and Gray, J. (1964). Virus particles in cultured lymphoblasts from Burkitt's Lymphoma. *The Lancet*, 283(7335):702.
- [Pasqualucci et al., 2006] Pasqualucci, L., Compagno, M., Houldsworth, J., Monti, S., Grunn, A., Nandula, S. V., Aster, J. C., Murty, V. V., Shipp, M. A., and Dalla-Favera, R. (2006). Inactivation of the PRDM1/BLIMP1 gene in diffuse large B cell lymphoma. *The Journal of experimental medicine*, 203(2):311–7.

- [Pasqualucci et al., 2001] Pasqualucci, L., Neumeister, P., Goossens, T., Nanjangud, G., Chaganti, R. S. K., Küppers, R., and Dalla-Favera, R. (2001). Hypermutation of multiple proto-oncogenes in B-cell diffuse large-cell lymphomas. *Nature*, 412(6844):341–346.
- [Pereira et al., 2010] Pereira, J. P., Kelly, L. M., and Cyster, J. G. (2010). Editor’s Choice: Finding the right niche: B-cell migration in the early phases of T-dependent antibody responses. *International Immunology*, 22(6):413.
- [Phan et al., 2005] Phan, R. T., Saito, M., Basso, K., Niu, H., and Dalla-Favera, R. (2005). BCL6 interacts with the transcription factor Miz-1 to suppress the cyclin-dependent kinase inhibitor p21 and cell cycle arrest in germinal center B cells. *Nature Immunology*, 6(10):1054–1060.
- [Pillai and Cariappa, 2009] Pillai, S. and Cariappa, A. (2009). The follicular versus marginal zone B lymphocyte cell fate decision. *Nature Reviews Immunology*, 9(11):767–777.
- [PODACK et al., 2002] PODACK, E. R., STRBO, N., SOTOSEC, V., and MUTA, H. (2002). CD30-Governor of Memory T Cells? *Annals of the New York Academy of Sciences*, 975(1):101–113.
- [Pracht et al., 2017] Pracht, K., Meinzing, J., Daum, P., Schulz, S. R., Reimer, D., Hauke, M., Roth, E., Mielenz, D., Berek, C., Côte-Real, J., Jäck, H.-M., and Schuh, W. (2017). A new staining protocol for detection of murine antibody-secreting plasma cell subsets by flow cytometry. *European Journal of Immunology*, 47(8):1389–1392.
- [Quah and Parish, 2010] Quah, B. J. C. and Parish, C. R. (2010). The use of carboxyfluorescein diacetate succinimidyl ester (CFSE) to monitor lymphocyte proliferation. *Journal of visualized experiments : JoVE*, (44).
- [Quintanilla-Martínez et al., 1997] Quintanilla-Martínez, L., Lome-Maldonado, C., Ott, G., Gschwendtner, A., Gredler, E., Reyes, E., Angeles-Angeles, A., and Fend, F. (1997). Primary non-Hodgkin’s lymphoma of the intestine: high prevalence of Epstein-Barr virus in Mexican lymphomas as compared with European cases. *Blood*, 89(2):644–51.
- [Ramachandiran et al., 2015] Ramachandiran, S., Adon, A., Guo, X., Wang, Y., Wang, H., Chen, Z., Kowalski, J., Sunay, U. R., Young, A. N., Brown, T., Mar, J. C., Du, Y., Fu, H., Mann, K. P., Natkunam, Y., Boise, L. H., Saavedra, H. I., Lossos, I. S., and Bernal-Mizrachi, L. (2015). Chromosome instability in diffuse large B cell lymphomas is suppressed by activation of the noncanonical NF- $\kappa$ B pathway. *International Journal of Cancer*, 136(10):2341–2351.
- [Rastelli et al., 2008] Rastelli, J., Hömig-Hölzel, C., Seagal, J., Müller, W., Hermann, A. C., Rajewsky, K., and Zimmer-Strobl, U. (2008). LMP1 signaling can replace CD40 signaling in B cells in vivo and has unique features of inducing class-switch recombination to IgG1. *Blood*, 111(3):1448–55.
- [Reboldi and Cyster, 2016] Reboldi, A. and Cyster, J. G. (2016). Peyer’s patches: organizing B-cell responses at the intestinal frontier. *Immunological Reviews*, 271(1):230–245.
- [Reljic et al., 2000] Reljic, R., Wagner, S. D., Peakman, L. J., and Fearon, D. T. (2000). Suppression of signal transducer and activator of transcription 3-dependent B lymphocyte terminal differentiation by BCL-6. *J Exp Med*, 192(12):1841–1848.
- [Rezk and Weiss, 2007] Rezk, S. A. and Weiss, L. M. (2007). Epstein-Barr virus-associated lymphoproliferative disorders. *Human Pathology*, 38(9):1293–1304.
- [Rickert et al., 1997] Rickert, R. C., Roes, J., and Rajewsky, K. (1997). B lymphocyte-specific, Cre-mediated mutagenesis in mice. *Nucleic acids research*, 25(6):1317–8.

- [Saito et al., 2007] Saito, M., Gao, J., Basso, K., Kitagawa, Y., Smith, P. M., Bhagat, G., Pernis, A., Pasqualucci, L., and Dalla-Favera, R. (2007). A Signaling Pathway Mediating Downregulation of BCL6 in Germinal Center B Cells Is Blocked by BCL6 Gene Alterations in B Cell Lymphoma. *Cancer Cell*, 12(3):280–292.
- [Savage et al., 2017] Savage, H. P., Yenson, V. M., Sawhney, S. S., Mousseau, B. J., Lund, F. E., and Baumgarth, N. (2017). Blimp-1-dependent and -independent natural antibody production by B-1 and B-1-derived plasma cells. *The Journal of experimental medicine*, 214(9):2777–2794.
- [Schirrmann et al., 2014] Schirrmann, T., Steinwand, M., Wezler, X., ten Haaf, A., Tur, M. K., and Barth, S. (2014). CD30 as a Therapeutic Target for Lymphoma. *BioDrugs*, 28(2):181–209.
- [Schmidt-Supprian and Rajewsky, 2007] Schmidt-Supprian, M. and Rajewsky, K. (2007). Vagaries of conditional gene targeting. *Nat Immunol*, 8(7):665–668.
- [Schneider and Hübinger, 2002] Schneider, C. and Hübinger, G. (2002). Pleiotropic signal transduction mediated by human CD30: A member of the tumor necrosis factor receptor (TNFR) family. *Leukemia and Lymphoma*, 43(7):1355–1366.
- [Schneider et al., 2008] Schneider, F., Neugebauer, J., Griese, J., Liefold, N., Kutz, H., Briseño, C., and Kieser, A. (2008). The Viral Oncoprotein LMP1 Exploits TRADD for Signaling by Masking Its Apoptotic Activity. *PLoS Biology*, 6(1):e8.
- [Schwab et al., 1982] Schwab, U., Stein, H., Gerdes, J., Lemke, H., Kirchner, H., Schaad, M., and Diehl, V. (1982). Production of a monoclonal antibody specific for Hodgkin and Sternberg-Reed cells of Hodgkin’s disease and a subset of normal lymphoid cells. *Nature*, 299(5878):65–7.
- [Schwering et al., 2003] Schwering, I., Bräuninger, A., Klein, U., Jungnickel, B., Tinguely, M., Diehl, V., Hansmann, M.-L., Dalla-Favera, R., Rajewsky, K., and Küppers, R. (2003). Loss of the B-lineage-specific gene expression program in Hodgkin and Reed-Sternberg cells of Hodgkin lymphoma. *Blood*, 101(4):1505–12.
- [Shaffer et al., 2012] Shaffer, A. L., Young, R. M., and Staudt, L. M. (2012). Pathogenesis of Human B Cell Lymphomas. *Annual Review of Immunology*, 30(1):565–610.
- [Shaffer et al., 2000] Shaffer, A. L., Yu, X., He, Y., Boldrick, J., Chan, E. P., and Staudt, L. M. (2000). BCL-6 represses genes that function in lymphocyte differentiation, inflammation, and cell cycle control. *Immunity*, 13(2):199–212.
- [Shanebeck et al., 1995] Shanebeck, K. D., Maliszewski, C. R., Kennedy, M. K., Picha, K. S., Smith, C. A., Goodwin, R. G., and Grabstein, K. H. (1995). Regulation of murine B cell growth and differentiation by CD30 ligand. *European Journal of Immunology*, 25(8):2147–2153.
- [Shannon-Lowe et al., 2017] Shannon-Lowe, C., Rickinson, A. B., and Bell, A. I. (2017). Epstein-Barr virus-associated lymphomas. *Philosophical transactions of the Royal Society of London. Series B, Biological sciences*, 372(1732).
- [Shi et al., 2015] Shi, W., Liao, Y., Willis, S. N., Taubenheim, N., Inouye, M., Tarlinton, D. M., Smyth, G. K., Hodgkin, P. D., Nutt, S. L., and Corcoran, L. M. (2015). Transcriptional profiling of mouse B cell terminal differentiation defines a signature for antibody-secreting plasma cells. *Nature Immunology*, 16(6):663–673.
- [Smith et al., 1994] Smith, C. A., Farrah, T., and Goodwin, R. G. (1994). The TNF receptor superfamily of cellular and viral proteins: activation, costimulation, and death. *Cell*, 76(6):959–62.

- [Smith et al., 1993] Smith, C. A., Gruss, H. J., Davis, T., Anderson, D., Farrah, T., Baker, E., Sutherland, G. R., Brannan, C. I., Copeland, N. G., Jenkins, N. A., Grabstein, K. H., Gliniak, B., McAlister, I. B., Fanslow, W., Alderson, M., Falk, B., Gimpel, S., Gillis, S., Din, W. S., Goodwin, R. G., and Armitage, R. J. (1993). CD30 antigen, a marker for Hodgkin's lymphoma, is a receptor whose ligand defines an emerging family of cytokines with homology to TNF. *Cell*, 73(7):1349–1360.
- [Sperling et al., 2019] Sperling, S. A., Fiedler, P., Lechner, M., Pollithy, A., Ehrenberg, S., Schiefer, A.-I., Kenner, L., Feuchtinger, A., Kühn, R., Swinerd, G., Schmidt-Supprian, M., Strobl, L. J., and Zimmer-Strobl, U. (2019). Chronic CD30-signaling in B cells results in lymphomagenesis by driving the expansion of plasmablasts and B1 cells. *Blood*, page blood.2018880138.
- [Stein et al., 2000] Stein, H., Foss, H.-d., Du, H., Marafioti, T., Delsol, G., Pulford, K., Pileri, S., and Falini, B. (2000). CD30 (+) anaplastic large cell lymphoma : a review of its histopathologic , genetic , and clinical features. 96(12):3681–3695.
- [Stoermann et al., 2007] Stoermann, B., Kretschmer, K., Düber, S., and Weiss, S. (2007). B-1a cells are imprinted by the microenvironment in spleen and peritoneum. *European Journal of Immunology*, 37(6):1613–1620.
- [Suan et al., 2017] Suan, D., Kräutler, N. J., Maag, J. L. V., Butt, D., Bourne, K., Hermes, J. R., Avery, D. T., Young, C., Statham, A., Elliott, M., Dinger, M. E., Basten, A., Tangye, S. G., and Brink, R. (2017). CCR6 Defines Memory B Cell Precursors in Mouse and Human Germinal Centers, Revealing Light-Zone Location and Predominant Low Antigen Affinity. *Immunity*, 47(6):1142–1153.e4.
- [Sunil-Chandra et al., 1992] Sunil-Chandra, N. P., Efstathiou, S., Arno, J., and Nash, A. A. (1992). Virological and pathological features of mice infected with murine gammaherpesvirus 68. Technical report.
- [Tan et al., 2016] Tan, L., Zhang, C., Dematos, J., Kuang, L., Jung, J. U., and Liang, X. (2016). CD95 Signaling Inhibits B Cell Receptor-Mediated Gammaherpesvirus Replication in Apoptosis-Resistant B Lymphoma Cells. *Journal of virology*, 90(21):9782–9796.
- [Tangye and Tarlinton, 2009] Tangye, S. G. and Tarlinton, D. M. (2009). Memory B cells: Effectors of long-lived immune responses. *European Journal of Immunology*.
- [Tarkowski, 2003] Tarkowski, M. (2003). Expression and a role of CD30 in regulation of T-cell activity. *Current opinion in hematology*, 10(4):267–71.
- [TARLINTON, 1995] TARLINTON, D. M. (1995). To affinity and beyond. pages 0–1.
- [Thorley-Lawson, 2015] Thorley-Lawson, D. A. (2015). EBV Persistence—Introducing the Virus. In *Current topics in microbiology and immunology*, volume 390, pages 151–209.
- [Thorley-Lawson and Gross, 2004] Thorley-Lawson, D. A. and Gross, A. (2004). Persistence of the Epstein-Barr Virus and the Origins of Associated Lymphomas. *New England Journal of Medicine*, 350(13):1328–1337.
- [Toplin et al., 1966] Toplin, I., Schidlovsky, G., Kohn, G., zur Hausen, H., and Henle, G. (1966). Partial purification and electron microscopy of virus in the EB-3 cell line derived from a Burkitt lymphoma. *Science (New York, N.Y.)*, 152(3725):1084–5.
- [Tsai et al., 2018] Tsai, C.-Y., Sakakibara, S., Yasui, T., Minamitani, T., Okuzaki, D., and Kikutani, H. (2018). Bystander inhibition of humoral immune responses by Epstein-Barr virus LMP1. *International Immunology*, 30(12):579–590.

- [Tsuneto et al., 2014] Tsuneto, M., Kajikhina, E., Seiler, K., Reimer, A., Tornack, J., Bouquet, C., Simmons, S., Knoll, M., Wolf, I., Tokoyoda, K., Hauser, A., Hara, T., Tani-ichi, S., Ikuta, K., Grün, J. R., Grützkau, A., Engels, N., Wienands, J., Yanagisawa, Y., Ohnishi, K., and Melchers, F. (2014). Environments of B cell development. *Immunology Letters*, 157(1-2):60–63.
- [Uchida et al., 1999] Uchida, J., Yasui, T., Takaoka-Shichijo, Y., Muraoka, M., Kulwichit, W., Raab-Traub, N., and Kikutani, H. (1999). Mimicry of CD40 signals by Epstein-Barr virus LMP1 in B lymphocyte responses. *Science (New York, N.Y.)*, 286(5438):300–3.
- [Usherwood et al., 1996] Usherwood, E. J., Stewart, J. P., Robertson, K., Allen, D. J., and Nash, A. A. (1996). Absence of splenic latency in murine gammaherpesvirus 68-infected B cell-deficient mice. *Journal of General Virology*, 77(11):2819–2825.
- [van der Weyden et al., 2017] van der Weyden, C. A., Pileri, S. A., Feldman, A. L., Whisstock, J., and Prince, H. M. (2017). Understanding CD30 biology and therapeutic targeting: a historical perspective providing insight into future directions. *Blood Cancer Journal*, 7(9):e603.
- [Victora and Nussenzweig, 2012] Victora, G. D. and Nussenzweig, M. C. (2012). Germinal Centers.
- [Virgin et al., 1997] Virgin, H. W., Latreille, P., Wamsley, P., Hallsworth, K., Weck, K. E., Dal Canto, A. J., and Speck, S. H. (1997). Complete sequence and genomic analysis of murine gammaherpesvirus 68. *Journal of virology*, 71(8):5894–904.
- [Vrzalikova et al., 2011] Vrzalikova, K., Vockerodt, M., Leonard, S., Bell, A., Wei, W., Schrader, A., Wright, K. L., Kube, D., Rowe, M., Woodman, C. B., and Murray, P. G. (2011). Down-regulation of BLIMP1 $\alpha$  by the EBV oncogene, LMP-1, disrupts the plasma cell differentiation program and prevents viral replication in B cells: implications for the pathogenesis of EBV-associated B-cell lymphomas. *Blood*, 117(22):5907–17.
- [Waffarn et al., 2015] Waffarn, E. E., Hastey, C. J., Dixit, N., Soo Choi, Y., Cherry, S., Kalinke, U., Simon, S. I., and Baumgarth, N. (2015). Infection-induced type I interferons activate CD11b on B-1 cells for subsequent lymph node accumulation. *Nature Communications*, 6(1):8991.
- [Wang et al., 2008] Wang, Y., Li, H., Tang, Q., Maul, G. G., and Yuan, Y. (2008). Kaposi’s sarcoma-associated herpesvirus ori-Lyt-dependent DNA replication: involvement of host cellular factors. *Journal of virology*, 82(6):2867–82.
- [Watanabe et al., 2005] Watanabe, M., Sasaki, M., Itoh, K., Higashihara, M., Umezawa, K., Kadin, M. E., Abraham, L. J., Watanabe, T., and Horie, R. (2005). JunB induced by constitutive CD30-extracellular signal-regulated kinase 1/2 mitogen-activated protein kinase signaling activates the CD30 promoter in anaplastic large cell lymphoma and Reed-Sternberg cells of Hodgkin lymphoma. *Cancer Research*, 65(17):7628–7634.
- [Weniger et al., 2018] Weniger, M. A., Tiacchi, E., Schneider, S., Arnolds, J., Rüschenbaum, S., Duppach, J., Seifert, M., Döring, C., Hansmann, M.-l., and Küppers, R. (2018). Human CD30 + B cells represent a unique subset related to Hodgkin lymphoma cells. *The Journal of Clinical Investigation*, pages 1–12.
- [Wirtz et al., 2016] Wirtz, T., Weber, T., Kracker, S., Sommermann, T., Rajewsky, K., and Yasuda, T. (2016). Mouse model for acute Epstein–Barr virus infection. *Proceedings of the National Academy of Sciences*, 113(48):13821–13826.
- [Woodland et al., 2001] Woodland, D. L., Usherwood, E. J., Liu, L., Flaño, E., Kim, I.-J., and Blackman, M. A. (2001). Vaccination Against Murine  $\gamma$ -Herpesvirus Infection. *Viral Immunology*, 14(3):217–226.

- [Yang et al., 2007] Yang, Y., Tung, J. W., Ghosn, E. E. B., Herzenberg, L. a., and Herzenberg, L. a. (2007). Division and differentiation of natural antibody-producing cells in mouse spleen. *Proceedings of the National Academy of Sciences of the United States of America*, 104(11):4542–4546.
- [Ye et al., 1993] Ye, B. H., Lista, F., Lo Coco, F., Knowles, D. M., Offit, K., Chaganti, R. S., and Dalla-Favera, R. (1993). Alterations of a zinc finger-encoding gene, BCL-6, in diffuse large-cell lymphoma. *Science (New York, N.Y.)*, 262(5134):747–50.
- [Younes and Aggarwall, 2003] Younes, A. and Aggarwall, B. B. (2003). Clinical implications of the tumor necrosis factor family in benign and malignant hematologic disorders. *Cancer*, 98(3):458–67.
- [Yuseff et al., 2013] Yuseff, M.-I., Pierobon, P., Reversat, A., and Lennon-Duménil, A.-M. (2013). How B cells capture, process and present antigens: a crucial role for cell polarity. *Nature Reviews Immunology*, 13(7):475–486.
- [Zhang et al., 2012] Zhang, B., Kracker, S., Yasuda, T., Casola, S., Vanneman, M., Hömig-Hölzel, C., Wang, Z., Derudder, E., Li, S., Chakraborty, T., Cotter, S. E., Koyama, S., Currie, T., Freeman, G. J., Kutok, J. L., Rodig, S. J., Dranoff, G., and Rajewsky, K. (2012). Immune surveillance and therapy of lymphomas driven by Epstein-Barr virus protein LMP1 in a mouse model. *Cell*, 148(4):739–751.
- [Zhang et al., 2018] Zhang, Y., Tech, L., George, L. A., Acs, A., Durrett, R. E., Hess, H., Walker, L. S. K., Tarlinton, D. M., Fletcher, A. L., Hauser, A. E., and Toellner, K.-M. (2018). Plasma cell output from germinal centers is regulated by signals from Tfh and stromal cells. *The Journal of experimental medicine*, 215(4):1227–1243.
- [Ziarkiewicz et al., 2016] Ziarkiewicz, M., Wołosz, D., Dzieciatkowski, T., Wilczek, E., Dwilewicz-Trojaczek, J., Jędrzejczak, W. W., Gierej, B., and Ziarkiewicz-Wróblewska, B. (2016). Epstein-Barr Virus-Positive Diffuse Large B cell Lymphoma in the Experience of a Tertiary Medical Center in Poland. *Archivum immunologiae et therapeuticae experimentalis*, 64(2):159–69.

## 9 Supplement

### 9.1 Supplement data

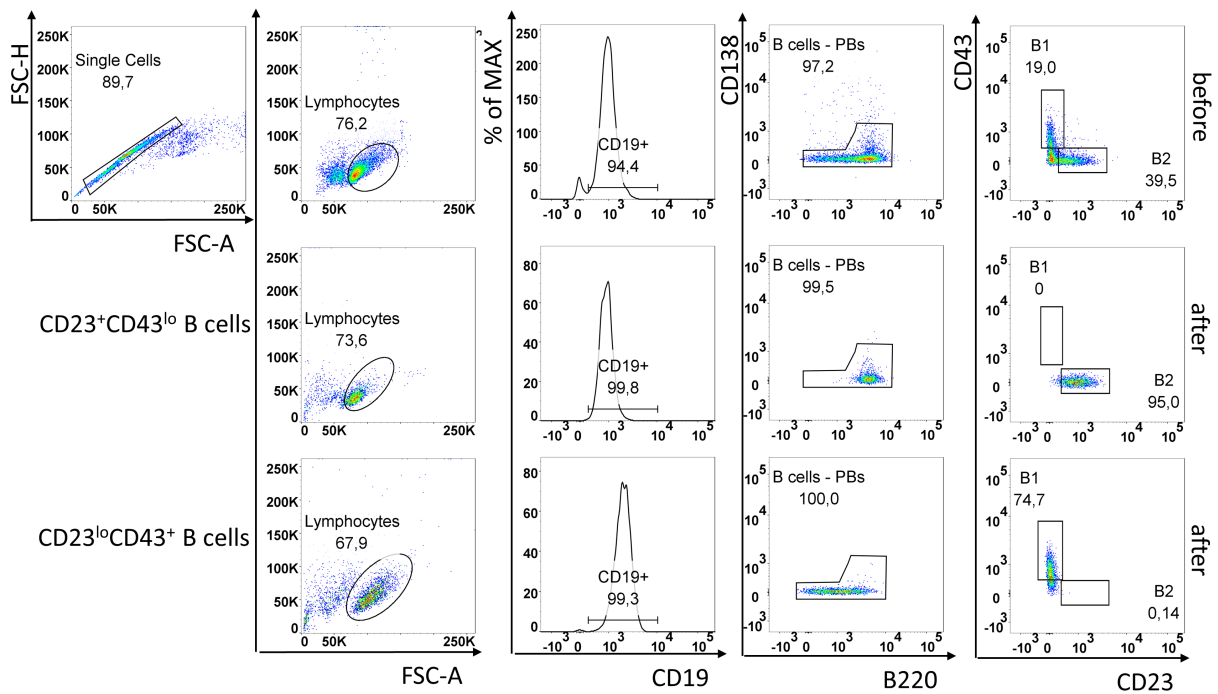


**Figure S1:** Splenic cells were sorted for single cells, lymphocytes, CD19<sup>+</sup> cells and CD138<sup>lo</sup> cells, and then either sorted for CD43<sup>+</sup>, CD23<sup>lo</sup> and the CD43<sup>-</sup>, CD23<sup>+</sup> population (before), both populations were resorted (after), and the lymphocytes were analyzed for CD19, CD23, and CD43 surface expression.

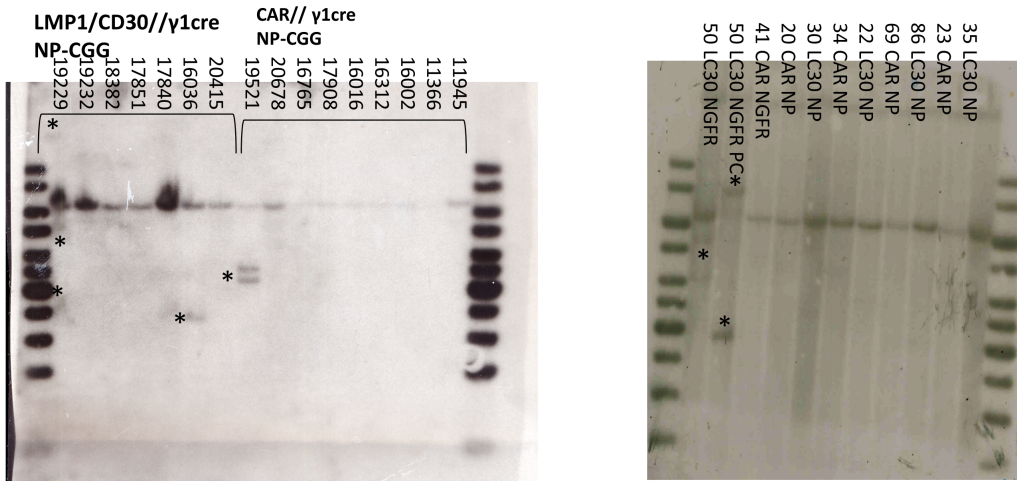


**Figure S2:** The lymphomas were detected by southern blot with a radioactive probe spanning the region between JH4 and E $\mu$  of the IgH locus,  $n \geq 11$ , the lower picture shows one example of a southern blot, the stars indicate additional band besides the germline band at 6 kB. The right picture uses following abbreviations LC30-LMP1/CD30//C $\gamma$ 1-cre, CAR-CAR//C $\gamma$ 1-cre, NP-NP-CGG, NGFR-MHV-68-NGFR

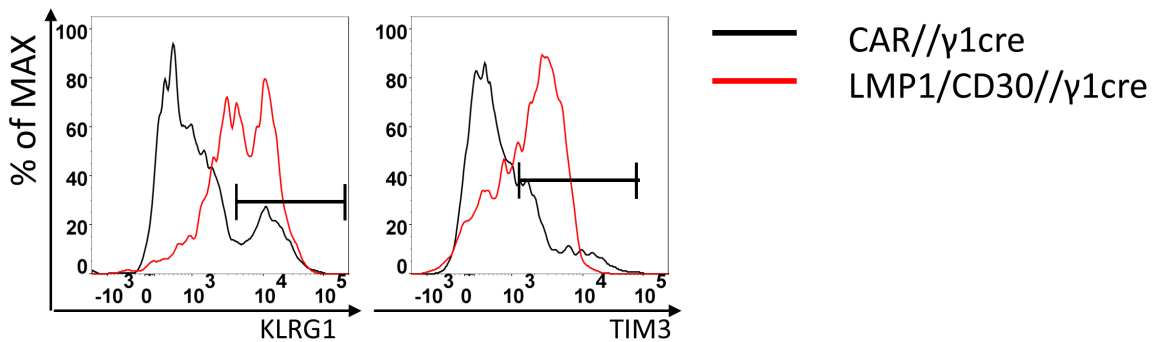


**Figure S3:** The histograms show an overlay of CD8<sup>+</sup> T cells stained for KLRG1 and TIM3 of one LMP1/CD30//C $\gamma$ 1-cre and one CAR//C $\gamma$ 1-cre mouse

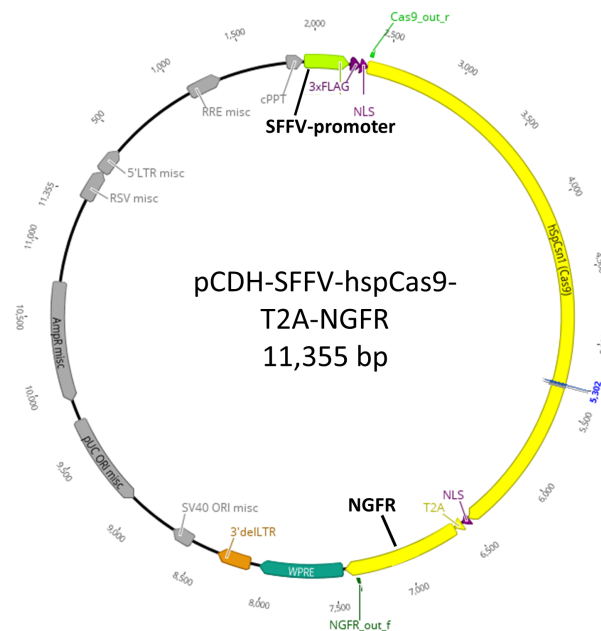


**Figure S4:** In order to isolate the SFFV NGFR cassette from the plasmid pCDH-SFFV-hspCas9-T2A-NGFR, hspCas9-T2A was removed with the enzymatic digest of EcoRI and NsiI. Then, SFFV-NGFR was removed by using ClaI and Sall. The plasmid was provided by the laboratory from Prof. I. Jeremias.

## 9.2 Curriculum Vitae

### Personal Data

Date of Birth: 02.04.1990  
 Place of Birth: Gera, Germany  
 Nationality: German  
 Contact: s-alexandra90@gmx.de

### Education

04/2015-04/2019: PhD, Helmholtz Zentrum München Research Unit Gene Vectors, Supervisor: PD Dr. Ursula Zimmer-Strobl  
 04/2012-03/2015: Master of Science, Molecular Biotechnology Technical University Munich  
 09/2008-09/2011: Bachelor of Science, Maritime Technologies University of Applied Sciences Bremerhaven  
 08/2000-06/2008: Abitur, Karl Theodor Liebe Gymnasium, Gera

## Practical Experience

- 04/2014 - 10/2014: Master Thesis, Helmholtz Zentrum München Institut for diabetes and regeneration research , Supervisor: Prof. Heiko Lickert
- 10/2013 - 04/2014: Intern, University of Otago Christchurch, New Zealand
- 03/2013 - 05/2013: Intern, Institute for experimental oncology and therapy research, Munich
- 11/2011 - 09/2012: Employee of quality control, HAC Biomed, Munich
- 09/2011 - 11/2011: Employee of quality control, HAC Biomed, Munich
- 03/2011 - 07/2011: Bachelor thesis, Helmholtz Centre for environmental research, Leipzig
- 11/2010 - 02/2011: Student Assistent, Alfred-Wegener-Institut, Bremerhaven

## Publications and Presentations

- 2019: Chronic CD30-signaling in B cells results in lymphomagenesis by driving the expansion of plasmablasts and B1 cells, Sperling S., Fiedler P., Lechner M., Pollithy A., Ehrenberg S., Strobl L., Zimmer-Strobl U., blood
- 2018: Poster presentation: Keystone Symposium, “B cells: Mechanisms in Immunity and Autoimmunity”, Dresden
- 2017: Poster presentation: 19th International Conference on lymphatic tissues and Germinal Centres in Immune reactions, Venice
- 2017: Oral presentation: 15th B cell forum, Mainz
- 2015: Positive and negative bioimprinted polymeric substrates: new platforms for cell culture, Mutreja, I.; Woodfield, T.; Sperling S; Evans J; Alkaisi M, 2015 Biofabrication
- 2012: Membrane Vesicle Formation as a Multiple-Stress Response Mechanism Enhances *Pseudomonas putida* DOT-T1E Cell Surface Hydrophobicity and Biofilm Formation, Baumgarten T, Sperling S, Seifert J, von Bergen M, Steiniger F, Wick LY, Heipieper HJ., 2012, AEM

### 9.3 Eidesstattliche Erklärung

Hiermit versichere ich an Eides Statt, dass die vorgelegte Dissertation von mir selbstständig angefertigt wurde. Ich habe nur die angegebenen Hilfsmittel verwendet und übernommene Erkenntnisse aus dem Schrifttum wurden gekennzeichnet und die Fundstelle wurde nachgewiesen.

München, den 27.05.2020

-----  
Stefanie Alexandra Sperling

### 9.4 Erklärung

Hiermit erkläre ich, dass die hier vorgelegte Dissertation nicht in dieser oder einer ähnlichen Form bei einer anderen Prüfungskommission eingereicht wurde. Außerdem versichere ich, dass die gebundene Ausgabe meiner Dissertation mit der elektronischen Fassung übereinstimmt.

München, den 27.05.2020

-----  
Stefanie Alexandra Sperling

## 9.5 Danksagung

Nachfolgend möchte ich allen Menschen danken, die dazu beigetragen haben, dass ich diese Arbeit zu einem erfolgreichem Abschluss bringen konnte.

Zuerst möchte ich PD Dr. Ursula Zimber-Strobl dafür danken, dass ich dieses interessante Thema in Ihrer Gruppe bearbeiten konnte. Ich danke Ihr für den steten fachlichen Input, die Unterstützung während meiner Arbeit und die Möglichkeit über mich hinauszuwachsen.

Außerdem möchte ich mich bei Prof. Heiko Adler bedanken, der mich in allen Fragen und Aufgaben jederzeit tatkräftig unterstützt hat. Vielen Dank auch für die "Taxi" Fahrten von Neuherberg und die tollen Zeichnungen, die das Verständnis für verschiedene Sachverhalte deutlich verbessert haben.

Weiterhin möchte ich meinen Thesis Committee Mitgliedern Prof. Olivier Gieres und Prof. Wolfgang Hammerschmidt für das Interesse an meiner Arbeit und die Ideen zur Verbesserung danken.

Natürlich möchte ich mich auch bei meinen Kollegen der Gruppe Strobl bedanken. Vielen Dank, dass ihr eine so angenehme Arbeitsatmosphäre geschaffen habt.

Besonders danke ich Laura Scheffler für Ihr offenes Ohr und Ihren Rat bei jeglichen fachlichen oder persönlichen Problemen und natürlich die Überlassung von Groot als sie selbst nicht zur Verfügung stand. Markus Lechner, danke ich für den unvergleichlichen Kaffee aber natürlich auch für die Unterstützung bei verschiedensten Experimenten. Danke Euch beiden, Ihr habt diese "Paperphase" erträglicher gemacht. Steffi E. danke ich für die ausführliche Einarbeitung in alle wichtigen Experimente und Geräte, dies hat mir den Einstieg deutlich vereinfacht.

Beatrix Steer möchte ich für die Einweisung in alle Experimente hinsichtlich der Virushandhabung und für die Mithilfe während verschiedener Experimente danken.

Bei den Mitarbeitern des Tierstalles, besonders Franziska Liebl, Michael Hagemann und Martina Möschter, möchte ich mich recht herzlich für die Betreuung meiner Tiere und für den beständigen Einsatz, alles Mögliche möglich zu machen, bedanken. Alina und Wiebe, danke für die schönen Kaffeepausen und die aufmunternden Worte in der anstrengenden Zeit.

Meiner Familie möchte ich für den fortwährenden Rückhalt danken. Ohne Euch hätte ich nicht so selbstbewusst an die Umsetzung und die Zielführung dieser Arbeit herangehen können. Felix, ich danke Dir für die Unterstützung während der gesamten Zeit, die Ablenkung wenn es nötig war und die ganzen Tipps während der Schreibphase. Durch Dich habe ich diese Phase leichter überstanden.